

INFORMATION TO USERS

This manuscript has been reproduced from the microfilm master. UMI films the text directly from the original or copy submitted. Thus, some thesis and dissertation copies are in typewriter face, while others may be from any type of computer printer.

The quality of this reproduction is dependent upon the quality of the copy submitted. Broken or indistinct print, colored or poor quality illustrations and photographs, print bleedthrough, substandard margins, and improper alignment can adversely affect reproduction.

In the unlikely event that the author did not send UMI a complete manuscript and there are missing pages, these will be noted. Also, if unauthorized copyright material had to be removed, a note will indicate the deletion.

Oversize materials (e.g., maps, drawings, charts) are reproduced by sectioning the original, beginning at the upper left-hand corner and continuing from left to right in equal sections with small overlaps. Each original is also photographed in one exposure and is included in reduced form at the back of the book.

Photographs included in the original manuscript have been reproduced xerographically in this copy. Higher quality 6" x 9" black and white photographic prints are available for any photographs or illustrations appearing in this copy for an additional charge. Contact UMI directly to order.

UMI

**A Bell & Howell Information Company
300 North Zeeb Road, Ann Arbor MI 48106-1346 USA
313/761-4700 800/521-0600**

UNIVERSITY OF ALBERTA

**SYNTHESIS, CHARACTERIZATION, AND COMPLEXATION OF
4-(PHOSPHINO)-2,5-DIMETHYL-2*H*-1,2,3σ²-DIAZAPHOSPHOLE
DERIVATIVES**

BY

MICHAEL DMITRI MIKOLUK



**A thesis submitted to the Faculty of Graduate Studies and Research in partial
fulfilment of the requirements for the degree of Doctor of Philosophy**

DEPARTMENT OF CHEMISTRY

EDMONTON, ALBERTA

FALL 1997



National Library
of Canada

Acquisitions and
Bibliographic Services

395 Wellington Street
Ottawa ON K1A 0N4
Canada

Bibliothèque nationale
du Canada

Acquisitions et
services bibliographiques

395, rue Wellington
Ottawa ON K1A 0N4
Canada

Your file Votre référence

Our file Notre référence

The author has granted a non-exclusive licence allowing the National Library of Canada to reproduce, loan, distribute or sell copies of this thesis in microform, paper or electronic formats.

The author retains ownership of the copyright in this thesis. Neither the thesis nor substantial extracts from it may be printed or otherwise reproduced without the author's permission.

L'auteur a accordé une licence non exclusive permettant à la Bibliothèque nationale du Canada de reproduire, prêter, distribuer ou vendre des copies de cette thèse sous la forme de microfiche/film, de reproduction sur papier ou sur format électronique.

L'auteur conserve la propriété du droit d'auteur qui protège cette thèse. Ni la thèse ni des extraits substantiels de celle-ci ne doivent être imprimés ou autrement reproduits sans son autorisation.

0-612-23037-6

UNIVERSITY OF ALBERTA

RELEASE FORM

NAME OF AUTHOR: MICHAEL DMITRI MIKOLUK

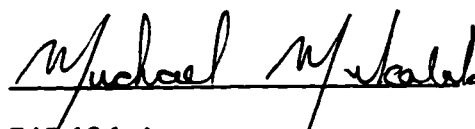
TITLE OF THESIS: SYNTHESIS, CHARACTERIZATION, AND
COMPLEXATION OF 4-(PHOSPHINO)-2,5-DIMETHYL-
2H-1,2,3σ²-DIAZAPHOSPHOLE DERIVATIVES

DEGREE: DOCTOR OF PHILOSOPHY

YEAR THIS DEGREE GRANTED: 1997

Permission is hereby granted to the University of Alberta Library to reproduce single copies of this thesis and to lend or sell such copies for private, scholarly or scientific research purposes only.

The author reserves all other publication and other rights in association with the copyright in the thesis, and except as hereinbefore provided neither the thesis nor any substantial portion thereof may be printed or otherwise reproduced in any material form whatever without the author's prior written permission.



745-13th Avenue
Lachine, Quebec.
Canada
H8S 3K4

Date: JUNE 23rd, 1997

UNIVERSITY OF ALBERTA

FACULTY OF GRADUATE STUDIES AND RESEARCH

The undersigned certify that they have read, and recommend to the Faculty of Graduate Studies and Research for acceptance, a thesis entitled Synthesis, Characterization, and Complexation of 4-(Phosphino)-2,5-dimethyl-2H-1,2,3 σ^2 -diazaphosphole Derivatives submitted by Michael Dmitri Mikoluk in partial fulfilment of the requirements for the degree of Doctor of Philosophy.



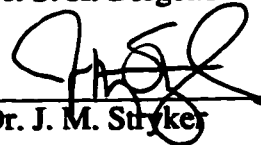
Dr. R. G. Cavell (supervisor)



Dr. M. Palcic



Dr. S. H. Bergens



Dr. J. M. Stryker



Dr. L. I. Wiebe



Dr. K. R. Dixon

Date: June 20th, 1997

"Imagination is more important than knowledge."

Albert Einstein

For those who believed in me.

Abstract

The substitution of the chlorines of the bisphosphine 4-(dichlorophosphino)-2,5-dimethyl-2*H*-1,2,3 σ^2 -diazaphosphole (1) with a variety of substituents such as fluorine (2), dimethylamino (3), and 2,2,2-trifluoroethoxy (11) has been accomplished in order to alter the chemical nature of the exo-phosphorus centre. Bulky secondary amines such as diisopropylamine allowed only one chlorine to be replaced and the resultant derivative was the asymmetric 4-(chlorodiisopropylaminophosphino)-2,5-dimethyl-2*H*-1,2,3 σ^2 -diazaphosphole (7). In this compound, the methyl and the methine groups in 7 were diastereotopic and showed fluxional behaviour at room temperature. Similarly, the methylene protons of the trifluoroethoxy group of 11 were also diastereotopic.

These bisphosphines were converted to their chalcogenato and imino derivatives in which only the exo-phosphorus centre was oxidized, thus creating a heterobifunctional ligand system. The reaction of 2 with *p*-cyanotetrafluorophenyl azide gave 4-(difluoro(*p*-cyanotetrafluorophenyl)iminophosphorano)-2,5-dimethyl-2*H*-1,2,3 σ^2 -diazaphosphole (18) which was characterized by spectroscopic methods and by x-ray crystallography. In all cases, large upfield shifts were observed in the $^{31}\text{P}\{^1\text{H}\}$ NMR spectrum upon oxidation of the exo-phosphorus centre. The reaction of 2 with 2,4,6-tri-*tert*-butylphenylamine in the presence of diethyl azodicarboxylate (DAD) resulted in the imino functionalized exo-phosphorus centre. The same reaction with *p*-toluidine, however, gave the four-membered 1,3,2,4-diazadiphosphetidine 20. The *gauche-trans* isomers of 20 were observed at low temperature in the ^{19}F NMR spectrum. The oxidation of the dimethylamino derivative 3 with trimethylsilyl azide placed a functional group on the imino moiety which can react further.

The diazaphosphole **2** easily replaced both carbon monoxide ligands on the complex $\text{CpRh}(\text{CO})_2$ to generate the disubstituted $\text{CpRh}(\mathbf{2})_2$ complex **31**. The $^{31}\text{P}\{^1\text{H}\}$ NMR spectrum showed a complex second order pattern for the *exo*-phosphorus centre. The one-bond phosphorus-rhodium coupling constant for this complex was 305 Hz. The solid-state structure of **31** showed a lengthening of the P-F bond, relative to the imino compound **18**, illustrating the electron density acceptor properties of the phosphorus-fluorine σ^* orbitals. The reducing ability of **2** was demonstrated by the reaction in which the palladium metal centre in the complex $\text{Pd}(\text{cod})\text{Cl}_2$ was reduced to give the complex $[\text{Pd}(\mathbf{2})_4]$ (**35**). The disubstituted platinum(II) complex was obtained with $\text{Pt}(\text{cod})\text{Cl}_2$ but the use of $\text{Pt}(\text{cod})\text{ClMe}$ resulted in the formation of the platinum(0) complex $[\text{Pt}(\mathbf{2})_4]$ (**36**). Unlike the chloro-bridged rhodium dimers, the metal-chloro bridges of $[\text{M}(\text{PEt}_3)\text{Cl}_2]_2$ ($\text{M} = \text{Pd}, \text{Pt}$) were cleaved and resulted in the *trans*-complexes $[\text{M}(\text{PEt}_3)(\mathbf{2})\text{Cl}_2]$ ($\text{M} = \text{Pd}$ (**37**), Pt (**38**)). A large $^1J_{\text{PPt}}$ of 5064 Hz was observed in the $^{31}\text{P}\{^1\text{H}\}$ NMR spectrum for the platinum complex **38**. The chiral complex $[\text{CpRuCl}(\text{PPh}_3)(\mathbf{2})]$ (**30**) showed complex coupling patterns in both the $^{31}\text{P}\{^1\text{H}\}$ and ^{19}F NMR spectra due to the diastereotopic fluorine substituents.

The dimethylamino derivative **3** gave the disubstituted complexes of the formula $[\text{M}(\mathbf{3})_2\text{Cl}_2]$ ($\text{M} = \text{Pd}$ (**41**), Pt (**42**)) and *trans*- $[\text{Rh}(\text{CO})(\mathbf{3})_2\text{Cl}]$ (**44**). Unlike the reaction with **2**, the $\text{Pt}(\mathbf{3})_2\text{ClMe}$ complex was obtained with $\text{Pt}(\text{cod})\text{ClMe}$. Similar results were obtained with palladium, platinum and rhodium with the trifluoroethoxy derivative **11**. The reaction of the trimethylsilylimino-bis(dimethylamino)phosphoranodiazaphosphole **23** with Cp^*TiCl_3 resulted in the formation of a nitrogen-metal sigma bond, *via* the elimination of chlorotrimethylsilane, to produce the metalated iminophosphorano diazaphosphole **48**, which was characterized spectroscopically and by x-ray crystallography.

ACKNOWLEDGEMENTS

I wish to express my gratitude to Professor R.G. Cavell for giving me the opportunity to explore the untamed area of phosphorus chemistry.

At the very least, I would like to thank the past and present group members for their friendship, inexhaustible help and experimental assistance: Dr. Richard Schutte, Dr. Roger Luo, Dr. Lucio Gelmini, Ernpeter Stüven, Dr. M.S. Balakrishna, Dr. Chih Y. Wong, Dr. Christo Angelov, Vivian J. Mozol, Dr. Robert W. Reed, and Dr. Kal Mahadev.

I would also like to acknowledge members of various analytical departments at the University of Alberta: Dr. Angelina Morales, Andrew Jodhan, Gerald Streefkerk, John Toonen, Darlene Mahlow, Andrea Dunn, Gerdy Aarts, Glen Bigham, Tom Brisbane Dr. Tom Nakashima, Lai Kong, Dr. Robert McDonald, and the many other people within the chemistry department.

I would like to thank the members of the chemistry hockey team, both past and present, for their patience during my rookie years between the pipes. A special thanks goes to V.M. for his urging. Finally, the unwavering support and encouragement of my parents throughout the years will always be remembered.

Table of Contents

Chapter 1

Introduction	1
1.1 Heterobifunctional Phosphine Based Ligands	1
1.2 Heterobifunctional Bisphosphine Ligand Systems	6
1.3 Ligand Systems Containing a Five-Membered Ring	10
1.3.1 Phospholanes	10
1.3.2 Phospholes	12
1.3.3 Heterophospholes	13
1.3.3.1 Synthesis of 2,5-Dimethyl-2<i>H</i>-1,2,3σ^2-diazaphosphole	14
1.3.4 Synthesis of 4-(Phosphino)-2,5-dimethyl-2<i>H</i>-1,2,3σ^2- diazaphosphole Derivatives	18
1.3.5 Synthesis of (2,5-Dimethyl-2<i>H</i>-1,2,3σ^2-diazaphosphol-4-yl)- aryliminophosphine	21
1.4 Metal Complexation	23
1.4.1 Metal Complexation Chemistry of the 2,5-dimethyl- 2<i>H</i>-1,2,3σ^2-diazaphosphole	23
1.4.2 Metal Complexation Chemistry of 4-(Phosphino)-2,5- dimethyl-2<i>H</i>-1,2,3σ^2-diazaphosphole Derivatives	25
1.4.3 Metal complexation Chemistry of (2,5-Dimethyl-2<i>H</i>- 1,2,3σ^2-diazaphosphol-4-yl)aryliminophosphine	29
1.4.4 Coordination Chemistry of the Two-Coordinate Phosphorus in Diazaphosphole Rings Systems	30
1.5 Scope of Present Work	32
1.6 References	35

Chapter 2

Syntheses of 4-(Phosphino)-2,5-dimethyl-2*H*-1,2,3 σ^2 diazaphosphole

Derivatives	39
2.1 Introduction.....	39
2.2 Modification of the Synthesis of 4-(dichlorophosphino)-2,5-dimethyl-2 <i>H</i> -1,2,3 σ^2 -diazaphosphole (1).....	41
2.3 Synthesis of 4-(dichlorophosphino)-2,5-dimethyl-2 <i>H</i> -1,2,3 σ^2 -diazaphosphole (2).....	42
2.3.1 Infrared Data for 4-(Difluorophosphino)-2,5-dimethyl-2 <i>H</i> -1,2,3 σ^2 -diazaphosphole (2).....	43
2.3.2 Multinuclear Magnetic Resonance Data for 4-(Difluorophosphino)-2,5-dimethyl-2 <i>H</i> -1,2,3 σ^2 -diazaphosphole (2).....	43
2.3.3 Attempted Quaternization of 2.....	48
2.4 Synthesis of 4-(Diaminophosphino)- and 4-(Aminochlorophosphino)-2,5-dimethyl-2 <i>H</i> -1,2,3 σ^2 -diazaphospholes.....	48
2.4.1 Infrared Data for 4-(Diaminophosphino)- and 4-(Aminochlorophosphino)-2,5-dimethyl-2 <i>H</i> -1,2,3 σ^2 -diazaphospholes.....	52
2.4.2 Multinuclear Magnetic Resonance Data for 4-(Diaminophosphino)- and 4-(Aminochlorophosphino)-2,5-dimethyl-2 <i>H</i> -1,2,3 σ^2 -diazaphospholes.....	52
2.5 Synthesis of 4-(Dialkoxy/aryloxyphosphino)-2,5-dimethyl-2 <i>H</i> -1,2,3 σ^2 -diazaphospholes.....	61
2.5.1 Infrared Data for (Dialkoxy/aryloxyphosphino)-2,5-dimethyl-2 <i>H</i> -1,2,3 σ^2 -diazaphospholes.....	61

2.5.2	Nuclear Magnetic Resonance Properties for the 4-(Dialkoxy/aryloxy-phosphino)-2,5-dimethyl-2 <i>H</i> -1,2,3σ ² -diazaphosphole Series.....	62
2.6	Attempts to Synthesize 4-(Dialkyl/arylphosphino)-2,5-dimethyl-2 <i>H</i> -1,2,3σ ² -diazaphospholes.....	64
2.7	Summary.....	66
2.8	References.....	76

Chapter 3

Oxidation of 4-(Phosphino)-2,5-dimethyl-2*H*-1,2,3σ²diazaphosphole

	Derivatives.....	78
3.1	Introduction.....	78
3.1.1	Oxidation with Chalcogens.....	80
3.1.2	Synthesis of Iminophosphoranes.....	83
3.2	Oxidation of 4-(Difluorophosphino)-2,5-dimethyl-2 <i>H</i> -1,2,3σ ² -diazaphosphole.....	87
3.2.1	Oxidation using Elemental Chalcogens.....	88
3.2.2	Spectroscopic Characterization of 16 and 17.....	89
3.2.3	Oxidation <i>via</i> the Staudinger Reaction; Formation of Iminophosphorane Derivatives.....	92
3.2.4	Spectroscopic Characterization of 18.....	92
3.2.5	Preparation of Iminophosphoranes: Redox-condensation with Diethyl Azodicarboxylate.....	100
3.3	Oxidation of 4-(Diaminophosphino)-2,5-dimethyl-2 <i>H</i> -1,2,3σ ² -diazaphospholes.....	104
3.3.1	Oxidation with Chalcogens.....	105

3.3.2	Iminophosphoranephosphole Derivatives: Oxidation with Azides.....	106
3.4	Oxidation of 4-(Di(2,2,2-trifluoroethoxy)phosphino)-2,5-dimethyl-2 <i>H</i> -1,2,3σ ² -diazaphosphole.....	108
3.4.1	Oxidation Using Elemental Selenium and <i>p</i> -Cyanotetrafluorophenyl Azide.....	108
3.5	Attempted Oxidation of 4-(Bis(dimethylaminothiophosphorano))-2,5-dimethyl-2 <i>H</i> -1,2,3σ ² -diazaphosphole, 21	110
3.6	Summary.....	110
3.7	References.....	120

Chapter 4

	Metal Complexation of 4-(Phosphino)-2,5-dimethyl-2<i>H</i>-1,2,3σ²-diazaphosphole Derivatives.....	123
4.1	Introduction.....	123
4.2	Metal Complexes of Phosphines.....	124
4.3	Complexation Chemistry of 4-(difluorophosphino)-2,5-dimethyl-2 <i>H</i> -1,2,3σ ² -diazaphosphole (2).....	126
4.3.1	Reactions with Metal Carbonyls.....	127
4.3.2	Reaction with the Prochiral Ruthenium Metal Complex CpRu(PPh ₃) ₂ Cl.....	137
4.3.3	Reactions with Rhodium Complexes.....	138
4.3.4	Formation of Complexes with Palladium and Platinum.....	155
4.4	Metal Complexation of 4-(Bis(dimethylamino)phosphino)-2,5-dimethyl-2 <i>H</i> -1,2,3σ ² -diazaphosphole.....	166
4.4.1	Reactions of 3 with Rhodium Complexes.....	166
4.4.2	Reactions of 3 with Palladium and Platinum Precursors.....	175

4.5	Metal Complexation of 4-((2,2,2-Trifluoroethoxy)phosphino)-2,5-dimethyl-2 <i>H</i> -1,2,3 σ^2 -diazaphosphole (11).....	177
4.6	Metal Complexation of Oxidized 4-(Phosphorano)-2,5-dimethyl-2 <i>H</i> -1,2,3 σ^2 -diazaphospholes.....	179
4.6.1	Metal Complexation of 4-(bis(dimethylamino)phosphorano)-2,5-dimethyl-2 <i>H</i> -1,2,3 σ^2 -diazaphospholes.....	179
4.6.2	Iminophosphorano Metal Complexes.....	180
4.7	Summary.....	188
4.8	References.....	196

Chapter 5

Experimental	201
5.1 Ligand Synthesis.....	204
5.2 Oxidation of 4-(Phosphino)-2,5-dimethyl-2 <i>H</i> -1,2,3 σ^2 -diazaphospholes.....	215
5.3 Metal Complexation.....	222
5.4 References.....	236

Chapter 6

Conclusion and Future Prospects	237
6.1 Conclusion.....	237
6.2 Coordination of the σ^2 P Centre.....	237
6.3 Bimetallic Complexes.....	238
6.4 Allyl-Type Metal Complexes.....	239
6.5 Coordination of the Imino Nitrogen.....	240
6.6 References.....	243

Appendices

A.1	Compounds and Complexes Synthesized.....	244
A.2	Analysis of an AA'XX' Spectrum.....	255
A.3	Solvents and Drying Agents.....	260
A.4	Crystallographic Data.....	261

List of Tables

Chapter 2

Table 2.1	$^{31}\text{P}\{^1\text{H}\}$ NMR Data for 4-(Phosphino)-2,5-dimethyl-2 <i>H</i> -1,2,3 σ^2 -diazaphospholes.....	68
Table 2.2	^1H NMR Data for Diazaphosphole Protons in 4-(Phosphino)-2,5-dimethyl-2 <i>H</i> -1,2,3 σ^2 -diazaphospholes.....	70
Table 2.3	$^{13}\text{C}\{^1\text{H}\}$ NMR Data for Diazaphosphole Carbons in 4-(phosphino)-2,5-dimethyl-2 <i>H</i> -1,2,3 σ^2 -diazaphospholes.....	72
Table 2.4	Infrared Data for 4-(Phosphino)-2,5-dimethyl-2 <i>H</i> -1,2,3 σ^2 -diazaphospholes.....	74

Chapter 3

Table 3.1	Structural Data for Some <i>N</i> -Substituted Imino-phosphoranes.....	95
Table 3.2	Selected Interatomic Distances (Å) for 4-(Difluoro- <i>p</i> -cyanotetrafluorophenyl)iminophosphorano)-2,5-dimethyl-1,2,3-diazaphosphole (18).....	98
Table 3.3	Selected Interatomic Angles (deg) for 4-(Difluoro- <i>p</i> -cyanotetrafluorophenyl)iminophosphorano)-2,5-dimethyl-2 <i>H</i> -1,2,3 σ^2 -diazaphosphole (18).....	99
Table 3.4	$^{31}\text{P}\{^1\text{H}\}$ NMR Data for Oxidized 4-(Phosphorano)-2,5-dimethyl-2 <i>H</i> -1,2,3 σ^2 -diazaphospholes.....	112
Table 3.5	$^{13}\text{C}\{^1\text{H}\}$ NMR Data for Diazaphosphole Carbons in 4-(Phosphorano)-2,5-dimethyl-2 <i>H</i> -1,2,3 σ^2 -diazaphospholes.....	114

Table 3.6	¹ H NMR Data for Diazaphosphole Protons in Oxidized 4-(Phosphorano)-2,5-dimethyl-2 <i>H</i> -1,2,3σ ² -diazaphospholes.....	116
Table 3.7	⁷⁷ Se NMR Data for 4-(Selenophosphorano)-2,5-dimethyl-2 <i>H</i> -1,2,3σ ² -diazaphospholes.....	118
Table 3.8	Infrared Data for Oxidized 4-(Phosphorano)-2,5-dimethyl-2 <i>H</i> -1,2,3σ ² -diazaphospholes.....	119
Chapter 4		
Table 4.1	ν(CO) Assignments in Cr(CO) ₅ L Complexes.....	128
Table 4.2	ν(CO) Assignments in <i>cis</i> -Mo(CO) ₄ L ₂ Complexes.....	134
Table 4.3	ν(CO) Assignments in <i>fac</i> -Mo(CO) ₃ L ₃ Complexes.....	135
Table 4.4	Selected Interatomic Distances (Å) for Cyclopentadienyl bis-(difluoro-{2,5-dimethyl-2 <i>H</i> -1,2,3σ ² -diazaphosphol-4-yl}phosphine)rhodium(I) (31).....	151
Table 4.5	Selected Interatomic Angles (deg) for Cyclopentadienyl bis(difluoro-{2,5-dimethyl-2 <i>H</i> -1,2,3σ ² -diazaphosphol-4-yl}phosphine)rhodium(I) (31).....	152
Table 4.6	Selected Interatomic Distances (Å) for tetrakis(difluoro-{2,5-dimethyl-2 <i>H</i> -1,2,3σ ² -diazaphosphol-4-yl}phosphine)-platinum(0) (36).....	165
Table 4.7	Selected Interatomic Angles (deg) for tetrakis(difluoro{2,5-dimethyl-2 <i>H</i> -1,2,3σ ² -diazaphosphol-4-yl}phosphine)-platinum(0) (36).....	165
Table 4.8	Infrared Data (Carbonyl) for <i>trans</i> -[RhCl(CO)(L) ₂] Complexes.....	169

Table 4.9	Selected Interatomic Distances (Å) for <i>trans</i> -Chlorocarbonyl-(bis(bis-(dimethylamino)-(2,5-dimethyl-2 <i>H</i> -1,2,3σ ² -diazaphosphol-4-yl)-phosphine))rhodium(I) (39).....	173
Table 4.10	Selected Interatomic Angles (deg) for <i>trans</i> -Chlorocarbonyl-(bis(bis-(dimethylamino)-(2,5-dimethyl-2 <i>H</i> -1,2,3σ ² -diazaphosphol-4-yl)phosphine))rhodium(I) (39).....	174
Table 4.11	Structural Data for Iminophosphorano Complexes of Titanium.....	184
Table 4.12	Selected Interatomic Distances (Å) for [(η ⁵ -C ₅ Me ₅)TiCl ₂ -(N=P(NMe ₂) ₂)(2,5-dimethyl-2 <i>H</i> -1,2,3σ ² -diazaphosphol-4-yl)] (46).....	186
Table 4.13	Selected Interatomic Angles (deg) for [(η ⁵ -C ₅ Me ₅)TiCl ₂ -(N=P(NMe ₂) ₂)(2,5-dimethyl-2 <i>H</i> -1,2,3σ ² -diazaphosphol-4-yl)] (46).....	187
Table 4.14	³¹ P{ ¹ H} and ¹⁹ F NMR Data for Metal Complexes with 4-(difluorophosphino)-2,5-dimethyl-2 <i>H</i> -1,2,3σ ² -diazaphospholes.....	190
Table 4.15	³¹ P{ ¹ H} NMR Data for Metal Complexes of 4-(Bis-(dimethylamino)phosphino)-2,5-dimethyl-2 <i>H</i> -1,2,3σ ² -diazaphospholes.....	193
Table 4.16	³¹ P{ ¹ H} NMR Data for Metal Complexes of 4-(Bis(2,2,2-trifluoroethoxy)phosphino)-2,5-dimethyl-2 <i>H</i> -1,2,3σ ² -diazaphospholes.....	194
Table 4.17	³¹ P{ ¹ H} NMR Data for Metal Complexes of 4-(Bis-(dimethylamino)iminophosphorano)-2,5-dimethyl-2 <i>H</i> -1,2,3σ ² -diazaphospholes.....	195

Chapter 4

Table 5.1	Starting Materials Prepared.....	203
------------------	---	------------

Appendix

Table A.1.1	Compounds and Complexes Synthesized.....	244
Table A.2.1	Transitions of AA"XX" System: Frequencies and Relative Intensities of the A Portion.....	256
Table A.4.1	Crystallographic Experimental Data for 18.....	261
Table A.4.2	Weighted Least-Squares Planes for 18.....	238
Table A.4.3	Selected Torsional Angles (deg) for 4-(difluoro(<i>p</i>-cyano-tetrafluoro-phenyl)iminophosphorano)-2,5-dimethyl-2<i>H</i>-1,2,3σ^2-diazaphosphole (18).....	239
Table A.4.4	Atomic Coordinates and Equivalent Isotropic Displacement Parameters for 18.....	240
Table A.4.5	Crystallographic Experimental Data for 31.....	241
Table A.4.6	Selected Torsional Angles (deg) for [CpRh(difluoro(2,5-dimethyl-2<i>H</i>-1,2,3σ^2-diazaphosphol-4-yl)phosphine)₂](31).....	244
Table A.4.7	Atomic Coordinates and Equivalent Isotropic Displacement Parameters for 31.....	246
Table A.4.8	Crystallographic Experimental Data for 36.....	247
Table A.4.9	Selected Torsional Angles (deg) for tetrakis(difluoro(2,5-dimethyl-2<i>H</i>-1,2,3σ^2-diazaphosphol-4-yl)phosphine)-platinum(0) dihydrate (36).....	250
Table A.4.10	Atomic Coordinates and Equivalent Isotropic Displacement Parameters for 36.....	251
Table A.4.11	Crystallographic Experimental Data for 39.....	252

Table A.4.12	Selected Torsional Angles (deg) for <i>trans</i> -[RhCl(CO)(bis- {dimethylamino} {2,5-dimethyl-2 <i>H</i> -1,2,3σ ² -diazaphosphol- 4-yl}phosphine) ₂] (39).....	255
Table A.4.13	Atomic Coordinates and Equivalent Isotropic Displacement Parameters of 39	259
Table A.4.14	Crystallographic Experimental Data for 46	261
Table A.4.15	Selected Torsional Angles (deg) for [(η ⁵ -C ₅ Me ₅)-TiCl ₂ - (N=P(NMe ₂) ₂)(2,5-dimethyl-2 <i>H</i> -1,2,3σ ² -diazaphosphol-4 -yl)] (46).....	264
Table A.4.16	Atomic Coordinates and Equivalent Isotropic Displacement Parameters of [(η ⁵ -C ₅ Me ₅)TiCl ₂ (N=P(NMe ₂) ₂)(2,5 -dimethyl-2 <i>H</i> --1,2,3σ ² -diazaphosphol-4-yl)] (46).....	266

List of Figures

Chapter 1

Figure 1.1	1-Methylphosphole.....	12
Figure 1.2	Examples of heterophospholes.....	14
Figure 1.3	Solid-state structure of 2,5-dimethyl-2 <i>H</i> -1,2,3σ ² - diazaphosphole·HCl, XX·HCl.....	16
Figure 1.4	Solid-state structure of 1,5-dimethyl-1 <i>H</i> -1,2,3σ ² - diazaphosphole, XXI.....	16
Figure 1.5	Solid-state structure of the intermediate aminophosphino- phosphine, XXIX.....	22
Figure 1.6	Solid-state structure of $\text{Cp}^*(\text{CO})_2\text{Fe}-\overline{\text{N}=\text{PC}(\text{NMe}_2)-\text{C}(\text{CO}_2^t\text{Bu})=\text{N}}$, XXXIII.....	25
Figure 1.7	Solid state structure of the complex XXXVI.....	28
Figure 1.8	Coordination of the phosphinodiazaphosphole on a monodentate and bridging fashion with metal centres.....	33
Figure 1.9	Coordination of the phosphoranodiazaphosphole in a monodentate and chelating fashion with metal centres.....	34

Chapter 2

Figure 2.1	³¹ P{ ¹ H} NMR spectrum of 4-(difluorophosphino)-2,5- dimethyl-2 <i>H</i> -1,2,3σ ² -diazaphosphole (2) in CDCl ₃	46
Figure 2.2	¹⁹ F NMR spectrum of 4-(difluorophosphino)-2,5-dimethyl- 2 <i>H</i> -1,2,3σ ² -diazaphosphole (2) in CDCl ₃	46

Figure 2.3	A stacked plot of $^{31}\text{P}\{^1\text{H}\}$ NMR spectra obtained at different delay intervals ($\tau = 0.1, 0.2, 0.4, 0.6, 10.0, 20.0$ sec.) to determine the T_1 values for 4-(difluorophosphino)-2,5-dimethyl-2 <i>H</i> -1,2,3 σ^2 -diazaphosphole (2) in CDCl_3	47
Figure 2.4	Possible coordination of the pyrazole rings and cyclic phosphorus centre with 9	52
Figure 2.5	^1H NMR spectra of compound 6 at temperatures between -20°C and 25°C in CDCl_3	57
Figure 2.6	Methyl region $^{13}\text{C}\{^1\text{H}\}$ NMR spectra of compound 6 at -20°C and 25°C in CDCl_3	58
Figure 2.7	Two dimensional C,H-correlation (HETCOR) spectrum for compound 6 at -20°C in CDCl_3	59
Figure 2.8	^1H NMR spectrum of the methylene protons of compound 11 in CDCl_3	65
 Chapter 3		
Figure 3.1	Formation of a π bond between phosphorus and oxygen using the oxygen p orbital and an antibonding orbital of e symmetry on phosphorus (the AH_3 moiety).....	81
Figure 3.2	Walsh diagram for the pyramidal AH_3 system.....	82
Figure 3.3	Resonance forms of the λ^5 -iminophosphorane system.....	86
Figure 3.4	Orbitals proposed for the π backbonding between the nitrogen and phosphorus.....	86
Figure 3.5	Description of the phosphorus-nitrogen double bond as two Ω bonds.....	87
Figure 3.6	Resonance forms for compound 18	93

Figure 3.7	Perspective view of 4-(difluoro(<i>p</i> -cyanotetrafluorophenyl)-iminophosphorano)-2,5-dimethyl-2 <i>H</i> -1,2,3σ ² -diazaphosphole (18). Non-hydrogen atoms are represented by Gaussian ellipsoids at the 20% probability level.....	97
Figure 3.8	<i>Gauche</i> and <i>trans</i> isomers of compound 20	103

Chapter 4

Figure 4.1	Monodentate coordination and bridging action of the phosphino-2,5-dimethyl-2 <i>H</i> -1,2,3σ ² -diazaphospholes with metal centres.....	123
Figure 4.2	Monodentate and and chelating coordination of the phosphorano-2,5-dimethyl-2 <i>H</i> -1,2,3σ ² -diazaphosphole with metal centres.....	124
Figure 4.3	Molecular orbital picture of transition metal carbonyls.....	125
Figure 4.4	Molecular orbital picture of transition metal phosphine complexes showing back donation into the σ* orbital of the P-R bond.....	125
Figure 4.5	(a) ³¹ P{ ¹ H} spectrum at 81.015 MHz and (b) ¹⁹ F NMR spectrum at 188.313 MHz of 27 in CDCl ₃ at room temperature.....	129
Figure 4.6	(a) ³¹ P{ ¹ H} spectrum at 161.977 MHz and (b) ¹⁹ F NMR spectrum at 376.503 MHz of 27 in CDCl ₃ at room temperature.....	130
Figure 4.7	(a) ³¹ P{ ¹ H} spectrum at 202.392 MHz and (b) ¹⁹ F NMR spectrum at 470.304 MHz of 27 in CDCl ₃ at room temperature.....	131

Figure 4.8	(a) $^{31}\text{P}\{^1\text{H}\}$ NMR (161.977 MHz) spectrum for the exo-phosphorus region and (b) ^{19}F NMR (376.503 MHz) spectrum in CDCl_3 of complex 29	136
Figure 4.9	Newman projection along the P-Ru bond of compound 30 ...	138
Figure 4.10	The $^{31}\text{P}\{^1\text{H}\}$ NMR (81.015 MHz) of complex 30 in CDCl_3	139
Figure 4.11	(a) $^{31}\text{P}\{^1\text{H}\}$ NMR (81.015 MHz) spectrum in CDCl_3 and (b) simulated spectrum of the exo-phosphorus region for the complex 30	140
Figure 4.12	(a) ^{19}F NMR (188.313 MHz) spectrum in CDCl_3 and (b) simulated ^{19}F NMR spectrum for complex 30	141
Figure 4.13	The $^{31}\text{P}\{^1\text{H}\}$ NMR (81.015 MHz) spectrum of $\text{CpRh}(\mathbf{2})_2$ in CDCl_3	145
Figure 4.14	The ^{19}F NMR (188.015 MHz) spectrum of $\text{CpRh}(\mathbf{2})_2$ in CDCl_3	146
Figure 4.15	The $^{31}\text{P}\{^{19}\text{F}\}$ NMR (81.015 MHz) spectrum of $\text{CpRh}(\mathbf{2})_2$ in CDCl_3	147
Figure 4.16	The $^{19}\text{F}\{^{31}\text{P}$ at 260 ppm) NMR (188.015 MHz) spectrum of $\text{CpRh}(\mathbf{2})_2$ in CDCl_3	148
Figure 4.17	The solid-state structure of cyclopentadienylbis(difluoro- {2,5-dimethyl-2 <i>H</i> -1,2,3 σ^2 -diazaphosphol-4-yl} phosphine)- rhodium(I) (31). Non-hydrogen atoms are represented by Gaussian ellipsoids at the 20% probability level. Hydrogen atoms are shown with arbitrarily small thermal parameters.....	150
Figure 4.18	The $^{31}\text{P}\{^1\text{H}\}$ NMR (81.015 MHz) spectrum of the exo-phosphorus portion of $\text{Pt}(\mathbf{2})_2\text{ClMe}$ (36-b) in CDCl_3	163

- Figure 4.19** The solid-state structure of tetrakis(difluoro{2,5-dimethyl-2*H*-1,2,3σ²-diazaphosphol-4-yl}phosphine)platinum(0) (**36**). Non-hydrogen atoms are represented by Gaussian ellipsoids at the 20% probability level. Hydrogen atoms are shown with arbitrarily small thermal parameters.....164
- Figure 4.20** The ³¹P {¹H}NMR (81.015 MHz) spectrum of ((bis(bis(dimethylamino){2,5-dimethyl-2*H*-1,2,3σ²-diazaphosphol-4-yl}phosphine) rhodium(I) (**39**) in CDCl₃.....168
- Figure 4.21** Perspective view of the major (75%) isomer of *trans*-chloro-carbonyl((bis(bis(dimethylamino){2,5-dimethyl-2*H*-1,2,3σ²-diazaphosphol-4-yl}phosphine) rhodium(I) (**39**). Non-hydrogen atoms are represented by Gaussian ellipsoids at 20% probability level. Hydrogen atoms have been omitted for clarity170
- Figure 4.22** View of minor (25%) isomer of **39**. Compared to the major isomer, the positions of the chloro and carbonyl ligands have been exchanged, while the dispositions of the phosphine ligands are unchanged.....172
- Figure 4.23** The ¹⁹⁵Pt NMR (21.40 MHz) spectrum of Pt(3)₂MeCl (**42**) in CDCl₃.....176
- Figure 4.24** Possible metallacycles formed using the phosphino- and phosphoranodiazaphospholes.....179
- Figure 4.25** Possible structure for the product of the reaction of **21** with Mo(cht)(CO)₃.....180
- Figure 4.26** Resonance structures of the iminophosphorano metal complexes with a non-linear M-N-P moiety.....181

Figure 4.27	End-on titanium-nitrogen multiple bonding in a phosphinimate.....	183
Figure 4.28	Perspective view of the $[(\eta^5\text{-C}_5\text{Me}_5)\text{TiCl}_2(\text{N}=\text{P}(\text{NMe}_2)_2\text{-}(2,5\text{-dimethyl-}2H\text{-}1,2,3\sigma^2\text{-diazaphosphol-4-yl}))]$ (47) showing the atom labelling scheme. Non-hydrogen atoms are represented by Gaussian ellipsoids at the 20% probability level. Hydrogen atoms have been omitted.....	185
 Chapter 6		
Figure 6.1	Possible coordination modes of the phosphorano-2,5-dimethyl-2 <i>H</i> -1,2,3σ ² -diazaphospholes.....	240
Figure 6.2	Formation of metallacycles <i>via</i> coordination of nitrogens on the exo-phosphorus centre.....	241
Figure 6.3	Possible reaction product of 18 with $\text{Re}(\text{CO})_4(\text{THF})\text{Br}$	242
 Appendix		
Figure A.2.1	The effect on one portion of the AA'XX' spectrum due to varying the coupling constant values.....	258

List of Schemes

Chapter 1

- Scheme 1.1** Comparison of the reactions of the iridium (I) cod complex with (2-dimethylaminoethyl)diisopropylphosphine and (2-methoxyethyl)-diisopropylphosphine.....4
- Scheme 1.2** Synthesis of "head-to-tail" and "head-to-head" bimetallic complexes with pyridylphosphines.....5
- Scheme 1.3** Equilibrium between the chelated and monodentate bisphosphine on a rhodium-bisphosphine complex system in the presence of carbon monoxide.....9
- Scheme 1.4** The equilibrium between XI and XII in the presence of ethylene.....9
- Scheme 1.5** Synthesis of the titanium-palladium bimetallic complex, XIV.....10
- Scheme 1.6** Equilibrium between the σ^2 phosphorus and the σ^3 phosphorus in 1,2,5-triphenylphosphole, XVII.....12
- Scheme 1.7** Transformation of the 1*H*-phosphole tungsten complex to the 2*H*-phosphole complex XIX.....13
- Scheme 1.8** Preparation of 2,5-dimethyl-2*H*-1,2,3 σ^2 -diazaphosphole, XX.....14
- Scheme 1.9** Synthesis of 2*H*-1,2,3 σ^2 -diazaphospholes *via* benzothiadiphosphole (XXIII) and an azaoalkene.....17
- Scheme 1.10** Preparation of 4-(dichlorophosphino)-2,5-dimethyl-2*H*-1,2,3 σ^2 -diazaphosphole, 1, from the reaction of phosphorus trichloride with XX or acetone methylhydrazone.....18

Scheme 1.11	The preparation of 4-(dimethoxy)phosphino-2,5-dimethyl-2 <i>H</i> -1,2,3σ ² -diazaphosphole, XXIV.....	19
Scheme 1.12	Preparation of the methyl and phenyl derivatives of 4-phosphino-2,5-dimethyl-2 <i>H</i> -1,2,3σ ² -diazaphosphole.....	19
Scheme 1.13	Reaction of 2,5-dimethyl-2 <i>H</i> -1,2,3σ ² -diazaphosphole, XX, with <i>tert</i> -butyllithium.....	20
Scheme 1.14	Reaction of the 2,5-dimethyl-2 <i>H</i> -1,2,3σ ² -diazaphosphole XX with methyllithium.....	21
Scheme 1.15	Synthesis of <i>P</i> -(2,5-dimethyl-2 <i>H</i> -1,2,3σ ² -diazaphosphol-4-yl)aryliminophosphine, XXVIII.....	22
Scheme 1.16	Reaction of XX with [MCl ₂ (PEt ₃) ₂] (M = Pd, Pt).....	24
Scheme 1.17	Synthesis of Cp [*] (CO) ₂ Fe- $\overline{\text{N=PC(NMe}_2\text{)-C(CO}_2\text{ }^t\text{Bu)=N}}$, XXXII.....	24
Scheme 1.18	Selected reactions of 4-(dichlorophosphino)-2,5-dimethyl-2 <i>H</i> -1,2,3σ ² -diazaphosphole (1) with metallic species.....	27
Chapter 2		
Scheme 2.1	The Arbuzov reaction of a phosphite with an alkyl halide.....	40
Scheme 2.2	Alcohol exchange of with triaryl phosphites.....	41
Scheme 2.3	Synthesis of 4-(difluorophosphino)-2,5-dimethyl-2 <i>H</i> -1,2,3σ ² -diazaphosphole (2).....	42
Scheme 2.4	Reaction of 1 with aminosilanes.....	48
Scheme 2.5	Reaction of 1 with secondary amines in the presence of a base.....	49
Scheme 2.6	The reaction of 4-(dichlorophosphino)2,5-dimethyl-2 <i>H</i> -1,2,3σ ² -diazaphosphole (1) with diisopropylamine.....	50

Scheme 2.7	Preparation of 4-(dialkoxy/aryloxyphosphino)-2,5-dimethyl-2 <i>H</i> -1,2,3σ ² -diazaphospholes.....	61
-------------------	---	----

Chapter 3

Scheme 3.1	Oxidation of a phosphine with an elemental chalcogen.....	80
Scheme 3.2	Oxidation of a phosphine with hydrogen peroxide or trimethylamine oxide.....	80
Scheme 3.3	Oxidation of a phosphine <i>via</i> the Staudinger reaction.....	83
Scheme 3.4	Formation of a phosphinimine <i>via</i> the Kirsanov reaction.....	83
Scheme 3.5	Redox-condensation of a phosphine with a primary amine using diethyl azodicarboxylate.....	83
Scheme 3.6	Deprotonation of an aminophosphinium salt and its conversion to an iminophosphorane.....	84
Scheme 3.7	Proposed structures for the phosphazide intermediate.....	85
Scheme 3.8	Mechanism for the Staudinger reaction.....	85
Scheme 3.9	Oxidation of 2 with elemental sulfur or elemental selenium.....	88
Scheme 3.10	Previously reported synthesis of 16 using zinc fluoride as the fluorinating reagent.....	89
Scheme 3.11	Reaction of 2 with <i>p</i> -tetrafluorobenzonitrile azide.....	92
Scheme 3.12	Synthesis of iminophosphoranes <i>via</i> redox-condensation.....	100
Scheme 3.13	Formation of the monomeric compounds 19 and 20 and the possible route to the dimeric difluorophosphorano-diazaphospholes (R = <i>mes</i> [*] , <i>p</i> -MePh).....	101
Scheme 3.14	Dimerization of the iminophosphorane to a phosphetidine...	104

Chapter 4

Scheme 4.1	Formation of the <i>cis</i> -Mo(CO) ₄ (2) ₂ (28) and <i>fac</i> -Mo(CO) ₃ (2) ₃ (29) complexes.....	133
Scheme 4.2	Reaction of coordinating ligands with [M(cod)Cl] ₂ (M = Rh, Ir).....	142
Scheme 4.3	Reaction of 2 with [Rh(cod)Cl] ₂ , [Rh(CO) ₂ Cl] ₂ , and CpRh(CO) ₂	143
Scheme 4.4	Formation of the rhodium complex 32 with 2	154
Scheme 4.5	Reaction of 2 with Pt(cod)Cl ₂	157
Scheme 4.6	Reaction of 2 with Pd(cod)Cl ₂	158
Scheme 4.7	Reductive elimination of Pt(cod)ClMe with 2	161
Scheme 4.8	Proposed mechanism for the formation of the <i>trans</i> -[Rh(CO)Cl(L)] from the reaction of [Rh(CO) ₂ Cl] ₂ and a tertiary phosphine.....	167
Scheme 4.9	Synthesis of the titanium complex 46	182

Chapter 6

Scheme 6.1	Possible coordination of the σ ² P centre with niobium.....	238
Scheme 6.2	Synthesis of an A-frame bimetallic from the rhodium complex 39	238
Scheme 6.3	Formation of molybdenum bimetallics from the phosphinodiazaphosphole 3	239

List of Abbreviations and Symbols

anal.	analysis
B.P.	boiling point
br	broad (IR and NMR)
Bu	butyl, C₄H₉-
°C	degrees celcius
calcd.	calculated
cht	cycloheptatriene
cod	1,5-cyclooctadiene
Cp	cyclopentadiene
Cp*	pentamethylcyclopentadiene
15-crown-5	1,4,7,10,13-pentaoxacyclopentadecane
δ	chemical shift
d	doublet (NMR)
dba	dibenzylideneacetone
dppm	bis(diphenylphosphino)methane
ether	diethyl ether (C₄H₁₀O)
Et	ethyl, C₂H₅-
g	grams
Hz	hertz
I	nuclear spin (units of $h/2\pi$)
IR	infrared
J	NMR coupling constant in hertz
L	ligand
<i>m</i>-	meta

m	medium (IR), multiplet (NMR)
Me	methyl, CH₃-
mg	milligram
mL	millilitres
mmol	millimoles
mol	mole
M.P.	melting point
MS	mass spectrometry
NMR	nuclear magnetic resonance
<i>o</i>-	ortho
<i>p</i>-	para
Ph	phenyl, C₆H₅-
ppm	parts per million
R	alkyl
s	strong (IR), singlet (NMR)
sat.	satellites (NMR)
t	triplet (NMR)
THF	tetrahydrofuran (C₄H₈O)
TMS	tetramethylsilane
ν	frequency, cm⁻¹ in IR, hertz in NMR
vs	very strong (IR)
w	weak (IR)

CHAPTER 1

INTRODUCTION

1.1 Heterobifunctional Phosphine Based Ligands

Heterobifunctional phosphine ligands play an important and by no means fully developed role in coordination chemistry. The nature of the substituents contained within these ligands confer unique properties on the system and define the behaviour of the system. Beyond the intrinsic interest in the chemistry of the various kinds of phosphine systems which can be accessed, phosphines have found widespread applications in a large number of areas, not the least of which is their use as supporting ligands for transition metals as participants in homogeneous catalytic systems. Much of the chemistry of phosphines themselves is directed toward the provision of compounds and ultimately metal-phosphine complexes with special properties of reactivity, stability, or selectivity for these applications. Our interest in the area is focussed on heterobifunctional phosphine ligands, that is ligands which provide actions or properties beyond the behaviour of simple phosphines. This allows the possibility of controlling reactivity and other properties of the ligand and the complexes of this ligand by means of modification or shaping of the chemical properties of phosphine-based systems. We seek to introduce additional reactivity beyond that of a simple phosphine and to control the behaviour of the new ligands through modification of the chemical substituents and structure of the phosphorus based ligand. We focus herein on a system of heterobifunctional, phosphorus based ligands as part of an overall effort on the establishment of heterobifunctional bisphosphine ligands. Our strategy is to take a compound which contains two phosphorus centers of different character and further shape the reaction properties of the system with various substituents which alter the character and structure of the

ligand. Although the outcome of the preparative pathways follows established principles, the effect of the various structural modifications on the complexation and reactive properties of these ligands is not and will only be established by experimentation.

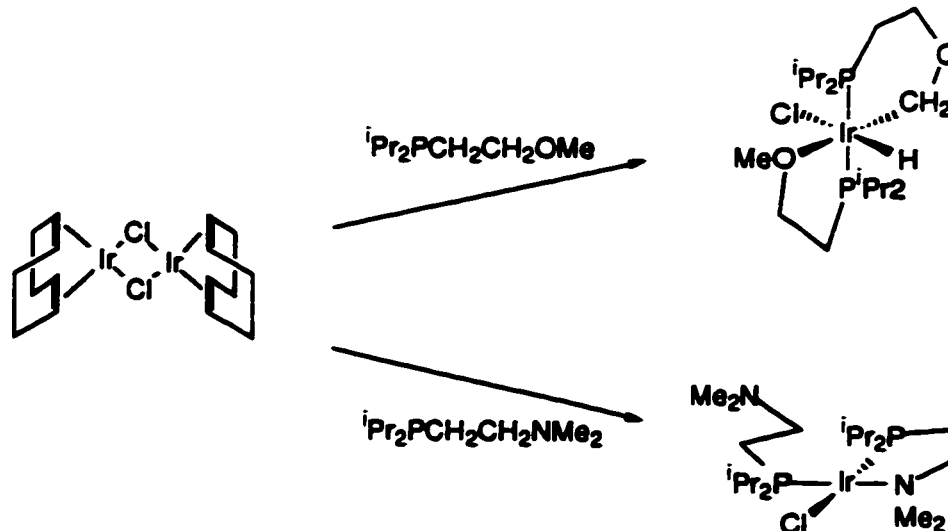
Heterobifunctional phosphine ligands are of interest because they offer the ability of uniting two contrasting, or dissimilar, characteristics within the interaction of one ligand with a metal. The basic metal-ligand interactions, which are globally Lewis acid-base interactions, can be described in terms of the "hardness" and "softness" of the coordinating atoms offered to the metal by the ligand.^{1,2} Metals are similarly classified in "hard" and "soft" terms. A "soft" donor site preferentially binds to a "soft" metal and a "hard" donor site to a "hard" metal. In general, highly oxidized metals and those from the early part of the transition metal block are classified as "hard" and metals in low oxidation states and those which occur in the later part of the transition metal block are classed as "soft". Phosphorus and sulfur provide "soft" donor centers whereas nitrogen and oxygen typically act as "hard" donors. These classifications are by no means rigid and the relative characteristics of each of the donor sites can be subtly controlled by the remainder of the molecular structure. For this important reason extensive exploration of ligand chemistry can be rewarded by the production of unique ligand systems which can in turn control the chemistry of the metal center to which the ligand is attached. This strategy has been beneficially applied in the development of many homogeneous catalytic systems which are based on selected combinations of metals and ligands. The specific process of designing appropriate ligand systems is often called "tailoring".

The idea of building phosphine ligand systems with different coordinating sites is well established, and is exemplified by ligands such as pyridylphosphines which have been known for many years.^{3,4} Substantial applications of this ligand system have been recently reviewed.⁴ In contrast, ligands containing non-aromatic

nitrogen such as (2-*N,N*-diethylaminoethyl)-diphenylphosphine are less well explored. This ligand type was first synthesized in 1965,⁵ and the coordination chemistry of the *N,N*-dimethylamino derivative was not explored until 1984.⁶ A number of other functionalized monophosphines have also been synthesized but, overall, the use of such "tailored" phosphines as ligands has not been exhaustively explored.

Recent work illustrating the contrasting coordination chemistry which can result from different ligand structures is provided by the chemistry of (2-ethylamino)diisopropylphosphine *versus* its ether analogue, (2-methoxyethyl)diisopropylphosphine.⁷ This system provides a dramatic example of the influence of subtle changes in the nature of the components of a heterobifunctional ligand system. Attempted preparation of iridium complexes containing (2-methoxyethyl)diisopropylphosphine resulted in an intramolecular C-H activation (i.e. oxidative addition) of a C-H bond in the methoxy moiety of the ligand to ultimately form the iridium(III) octahedral complex.⁸ In contrast, the (2-ethylamino)diisopropylphosphine gave only the square planar iridium(I) complex with one monodentate ligand and one chelating ligand (Scheme 1.1).⁹ The observed differences in behaviour of the two related ligands could not have been predicted.

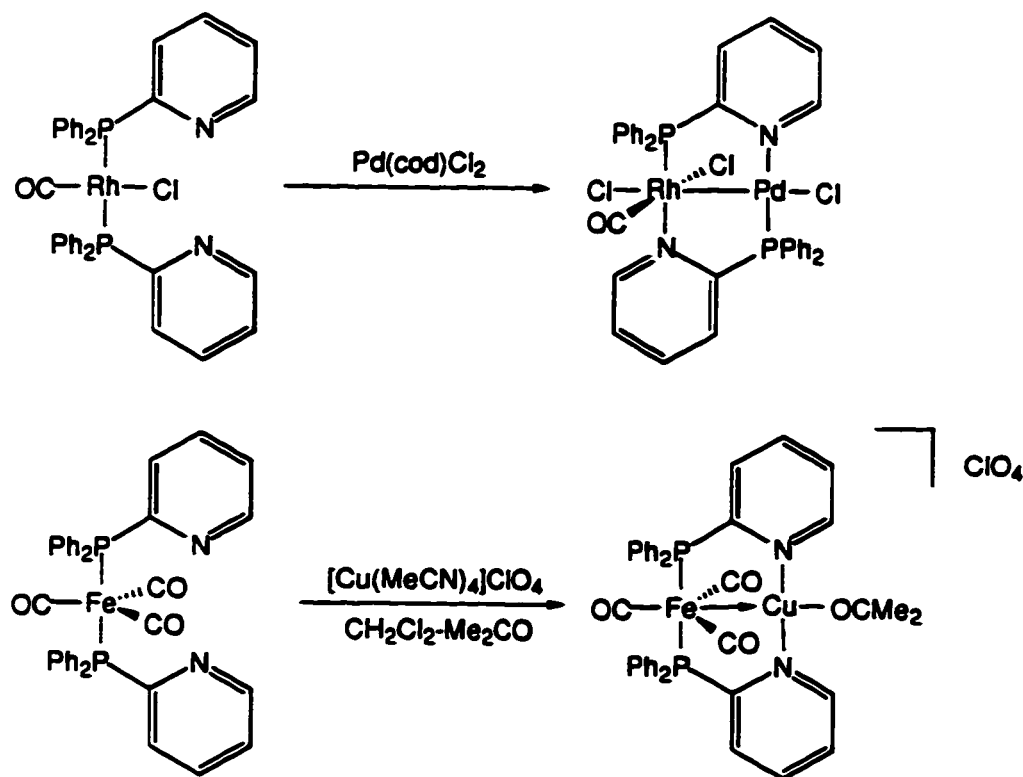
Pyridyl phosphines comprise an extensively investigated set of ligands.⁴ Many variations have been synthesized but only a few of them are of the bisphosphine type. In the case of the pyridyl monophosphines, it is possible to form complexes wherein only the phosphorus is coordinated to the metal centre. For example, the reaction of a rhodium bis(pyridylphosphine) complex with an equivalent of either $[\text{Rh}(\text{CO})_2\text{Cl}]_2$ or $\text{Pd}(\text{cod})\text{Cl}_2$ gave a bimetallic complex which rearranged ultimately to form a "head-to-tail" coordination arrangement (Scheme 1.2).¹⁰ The reaction of bis(pyridylphosphino)platinum dichloride with (norbornadiene)-molybdenum tetracarbonyl however proceeded without rearrangement of the



Scheme 1.1 Comparison of the reactions of the iridium (I) dimer complex with (2-dimethylaminoethyl)diisopropylphosphine and (2-methoxyethyl)-diisopropylphosphine.

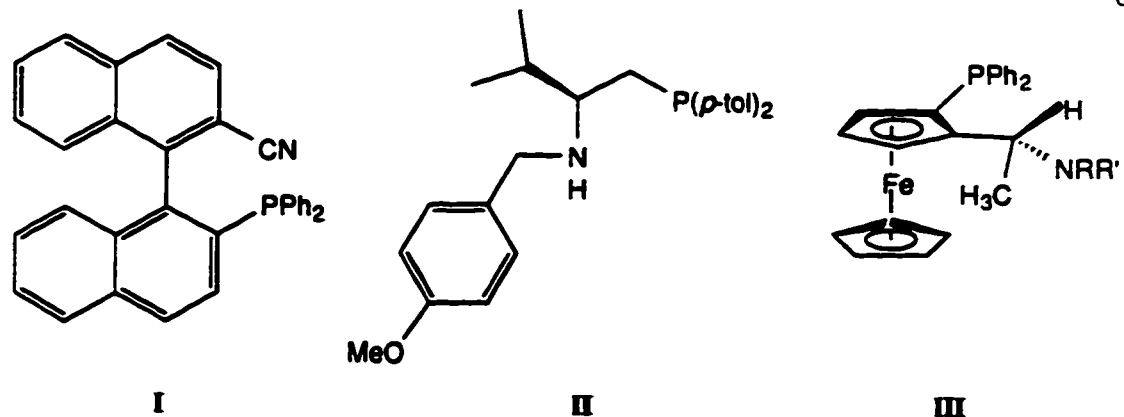
coordination on the primary metal and ultimately a "head-to-head" complex was obtained.¹¹ Li *et al.*¹² recently reported the synthesis of pyridylphosphine bridged iron-copper heterobimetallic complexes wherein the transformation of the ligand arrangement was also not observed (Scheme 1.2).

It has often been suggested that metallic complexes with two different transition metals in proximity could display chemical properties which are different from those of the separated, individual fragments.¹³ Particular interest has been focused on bimetallics containing both an electron-deficient and an electron-rich transition metal and such structured combinations could offer reactivity patterns which would be different from bimetallics containing identical or closely related transition metals. The synergistic interactions which develop between electron-deficient and electron rich metal centres in bimetallic systems may be useful in catalysis.¹³



Scheme 1.2 Synthesis of "head-to-tail" and "head-to-head" bimetallic complexes with pyridylphosphines.

As an extension of the heterobifunctional phosphine systems, many monophosphines with stereogenic centres have also been synthesized. Examples include the binaphthylmonophosphine **I**,^{14,15} the aminophosphine **II**,¹⁶ and the aminophosphinoferrocene complex **III**.¹⁷ In the case of **III**, good optical yields have been obtained in cross-coupling reactions catalyzed by palladium complexes. Other examples of catalytic applications of chiral complexes with mixed coordination spheres are known. The role that each of the ligand atoms plays is not completely understood.¹⁸⁻²⁵

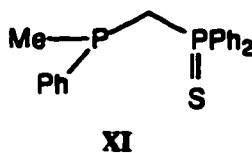
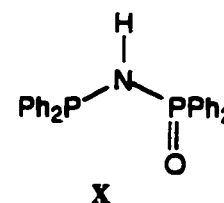
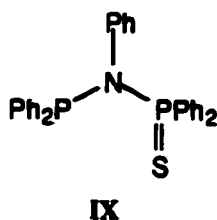
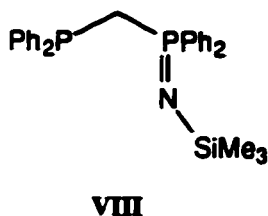


While many bifunctional monophosphine ligands have been synthesized and have shown promising results when applied to the establishment of metal complexes with catalytic behaviour, one particular complication remains inherent to the design of these ligand systems and that is the establishment of communication between the two coordinating centres. The use of ^{31}P NMR spectroscopy to analyze such systems can provide some limited information however significant changes to the ligand system may not impart sufficiently notable chemical shift differences to be deemed meaningful. In any case ^{31}P NMR spectroscopy is a useful diagnostic and monitoring analytical tool supporting the study of phosphine ligands and their complexes.

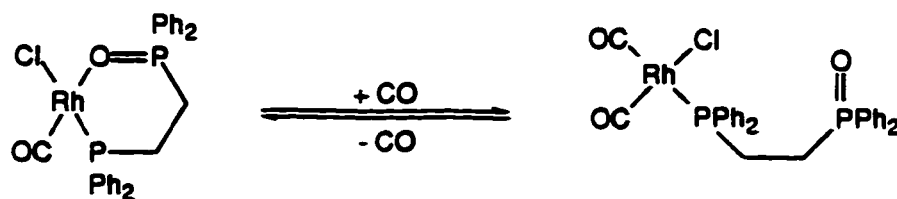
1.2 Heterobifunctional Bisphosphine Ligand Systems

Incorporation of two distinct phosphorus centres in either an asymmetric or a heterobifunctional ligand system will show phosphorus-phosphorus coupling between the two centres which can be observed in the $^{31}\text{P}\{^1\text{H}\}$ NMR spectrum. Changes in the relative orientation or the coordination of one phosphorus moiety is often reflected by a change in the coupling constant between the two phosphorus centres. Such diagnostic features are useful, however it is not always clear how the parameters can be correlated with the nature of the phosphorus centres.

moieties to a metal centre, a phosphorus and a different terminal atom. Several diphosphine ligand systems of this class have been synthesized; examples are **VIII**,³² **IX**,³³ **X**,³⁴ and **XI**.³⁵ A variety of multi-faceted, mixed "hard"/"soft" ligand systems can be created in this way.

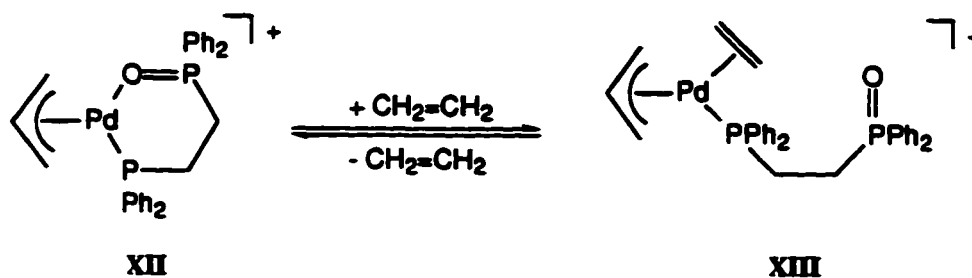


The potential versatility of diphosphines, especially those which belong to the mixed oxidation state systems, is of some interest in building catalytic systems. "Tuning" the reactivity with different substituents may allow for "tailoring" of the behaviour of the bisphosphine to suit specific requirements of a catalytic cycle. In general, metal complexes formed from such difunctional chelate ligands offer the potential for establishing dissociative equilibria where one of the substituents, which is more loosely bound than the other, is easily displaced by other ligands. This property has been termed hemilability.³⁶ For example, the system depicted in Scheme 1.3 has been found to be extremely active towards the carbonylation of methanol under mild conditions.³⁷ The equilibrium established in this system demonstrates such a concept. One of the donors, presumably the more weakly bound, dissociates and is replaced with carbon monoxide. The diphosphine remains attached so if the CO is either displaced or transformed, the tethered ligand can easily coordinate and stabilize the system.



Scheme 1.3 Equilibrium between the chelated and monodentate bisphosphine on a rhodium-bisphosphine complex system in the presence of carbon monoxide.

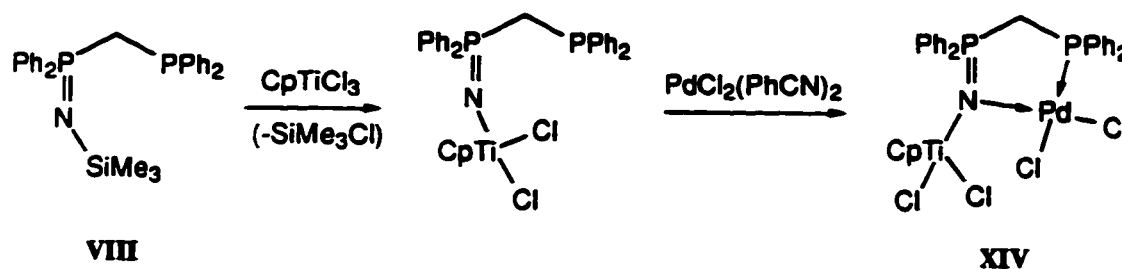
Another recent example³⁸ of the use of this pendant-arm interaction is provided by the same ligand system in the cationic palladium η^3 -allyl complex XII. In the presence of ethylene, the phosphine oxide donor of the ligand was displaced and at -80°C , the ethylene complex XIII was the major species in solution (Scheme 1.4).



Scheme 1.4 The equilibrium between XI and XII in the presence of ethylene.

These heterobifunctional bisphosphines can also be used to synthesize heterobimetallics. The stepwise fashion described above for the pyridylphosphines provides one such example. Another example from this laboratory uses the bisphosphine VIII to bridge titanium and palladium metal centres (Scheme 1.5). For the free bisphosphine, the chemical shifts for the phosphorus centres were found at -28.2 ppm for the P(III) and -1.4 ppm for the P(V) with an observed two-bond phosphorus-phosphorus coupling constant of 58 Hz. Replacement of the silyl group by the CpTiCl_2 moiety gave a downfield shift for the resonance of the P(V) centre (to

38.6 ppm) whereas the chemical shift for the P(III) was essentially unaffected.³⁹ Subsequent reaction of the titanium complex with $\text{PdCl}_2(\text{PhCN})_2$ resulted in the bimetallic complex **XIV**. The formation of the bimetallic complex resulted in a downfield shift of the P(III) signal (to 16.2 ppm) while the P(V) signal shifted upfield to 33.4 ppm. There was also a decrease in the $^2J_{\text{PP}}$ coupling constant (to 7 Hz).⁴⁰ All parameters thus indicated a significant perturbation of the chemical environment of the phosphorus centres and the interaction between them.



Scheme 1.5 Synthesis of a titanium-palladium bimetallic complex, **XIV**.

Controlling the reactivities of transition metals by the formation of heteroatomic chelate complexes has sparked interest in the synthesis of different types of heterofunctional ligands. The construction and design of chemo- and stereoselective heterofunctional ligands ultimately provides access to a variety of complexes with metal having potentially useful catalytic properties.

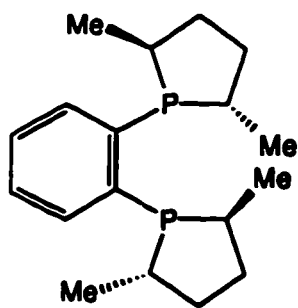
1.3 Ligand Systems Containing a Five-Membered Ring

1.3.1 Phospholanes

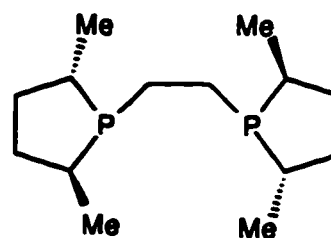
One attractive form of a diphosphine ligand incorporates at least one of the phosphorus centres into a saturated ring system. This class of cyclic phosphines are known as phospholanes. Most bisphosphines which have been synthesized contain unfettered substituents which tend to be extremely limber when attached to the phosphorus centre. Such flexibility of the substituents may interfere in the catalytic

cycle by creating a phosphorus centre that may either be too congested or insufficiently rigid and this may in turn create a complex which may not have a discrete chiral pocket⁴¹ that is needed to discriminate between two diastereomers. The degree of flexibility of phospholanes can be altered by changing the ring size. Three- or four-membered ring systems tend to be very rigid and may be prone to nucleophilic attack to relieve the ring strain. Six-membered phospholane ring systems tend to be very flexible. The five-membered ring systems may provide a suitable configuration and conformational rigidity needed to modify the metals atoms so that the desired stereochemistry is achieved. Such systems should provide some intriguing chemistry.

Burk has synthesized a series of diphosphines wherein the phosphorus centre is part of a five-membered ring system. Examples of these bisphosphines are 1,2-bis((2*S*,5*S*)-2,5-dimethylphospholano)benzene ((*S,S*)-Me-DuPHOS), XV,⁴² and 1,2-bis((2*S*,5*S*)-2,5-dimethylphospholano)ethane ((*S,S*)-Me-BPE), XVI.⁴³ These bisphosphines have shown much promise in enantioselective hydrogenation.^{44,45}



XV



XVI

Related C_2 -symmetric bisphosphines have also been synthesized with a variety of substituents on the five-membered ring such as methyl, ethyl, propyl, and benzyl groups. As well as altering the substituents on the five-membered ring, a number of backbones such as benzene, ethane, and propane have been utilized. The

ability to alter both the substituents and the backbones makes this ligand system extremely versatile.

1.3.2 Phospholes

Adding unsaturation to the five-membered ring system, creates a rigid ring structure. Such five-membered ring systems are known as phospholes. These systems contain a three-coordinate phosphorus atom in the +3 oxidation state. An example of a phosphole is shown in Figure 1.1.

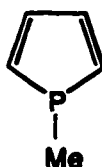
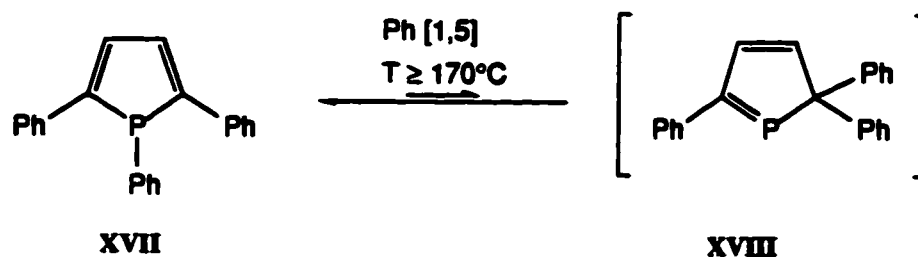


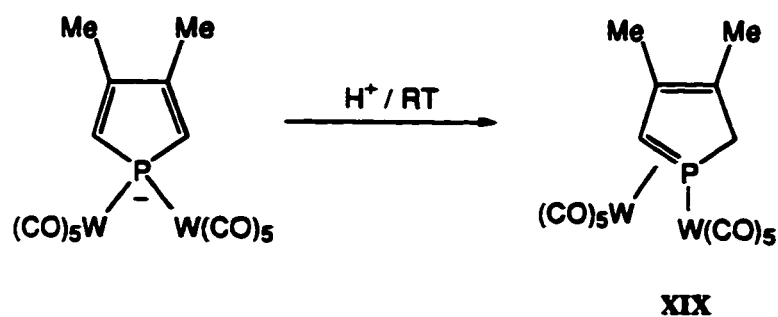
Figure 1.1 1-Methylphosphole.

In some phenyl substituted systems, it was discovered that a [1,5] sigmatropic shift occurred creating an equilibrium between the two-coordinate phosphorus species and the three-coordinate phosphorus species.⁴⁶ Scheme 1.6 shows the equilibrium observed for 1,2,5-triphenylphosphole at elevated temperatures. This reduction of the coordination number is contrary to the normal tendency of phosphorus(III) to maintain its tricoordinate state and this rearrangement also suppresses the weak aromatic stabilization of the phosphole ring.



Scheme 1.6 Equilibrium between the σ^2 -phosphorus and the σ^3 -phosphorus in 1,2,5-triphenylphosphole, XVII.

In a related system, the tungsten complex, XIX, trapped the two-coordinate phosphorus compound which resulted from the protonation of the phosphole (Scheme 1.7).⁴⁷



Scheme 1.7 Transformation of the 1*H*-phosphole tungsten complex to the 2*H*-phosphole complex XIX.

1.3.3 Heterophospholes

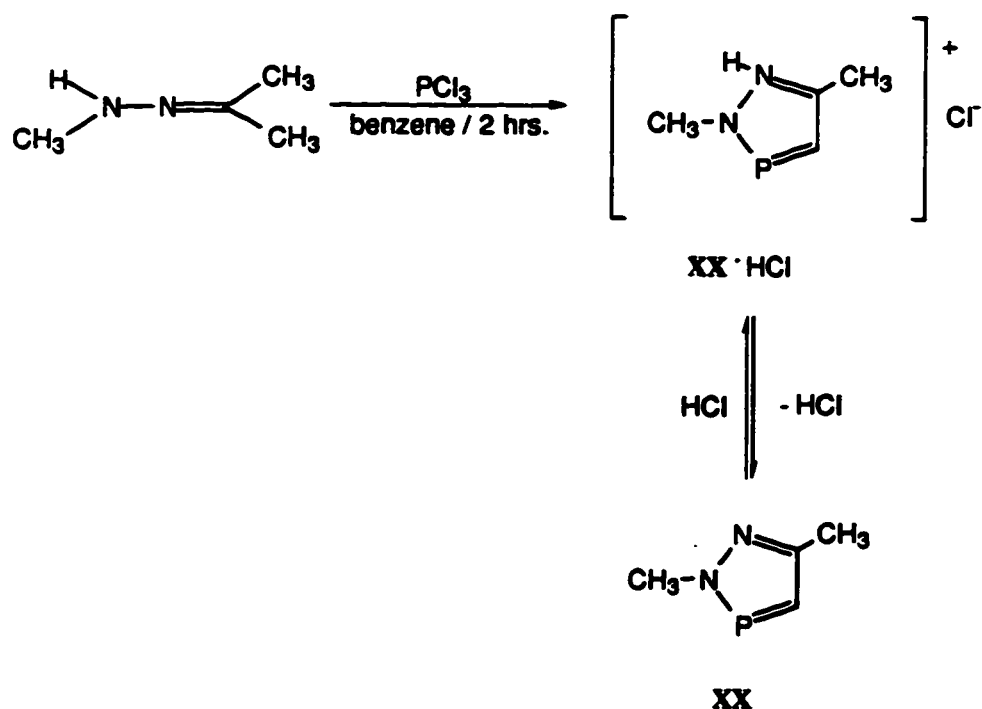
Introducing a heteroatom such as nitrogen into the five-membered phosphole ring allows the isolation of small heterocyclic ring systems with a two-coordinate phosphorus atom in the +3 oxidation state. These heterophospholes are five-membered, 6π , ring systems. The phosphorus atom in the ring has a formal pair of electrons exocyclic to the ring and contributes one π electron to the ring. The ring also contains one other group, such as N-R, O, or S, which provides an exocyclic pair of electrons and contributes two π electrons to the π -system. The heteroatoms are therefore formally capable of acting as electron pair donors in the usual Lewis base sense and, in addition, the structure is stabilized by the aromaticity of the ring. These systems may also be assembled with more than one two-coordinate nitrogen atom in the ring. All the potentially allowed combinations of these units gives a total of 48 possible ring systems but only 21 have been synthesized so far.⁴⁸ Examples of the different types of heterophospholes are given in Figure 1.2. The chemical shifts of the phosphorus centre in such rings ranges from 400 ppm to 0 ppm.⁴⁹



Figure 1.2 Examples of heterophospholes.

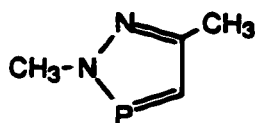
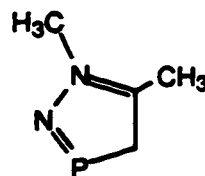
1.3.3.1 Synthesis of 2,5-Dimethyl-2*H*-1,2,3 σ^2 -diazaphosphole

One heterophosphole which is of interest is 2,5-dimethyl-2*H*-1,2,3 σ^2 -diazaphosphole, **XX**. It can be prepared by the reaction of acetone methylhydrazone with an equimolar amount of phosphorus trichloride in benzene at elevated temperatures in a yield of 58%. The hydrochloric acid adduct is isolated from the reaction mixture as a crystalline product (Scheme 1.8).⁵⁰ The phosphorus chemical shift of **XX**·HCl occurs at 230.7 ppm. The acid-free phosphole can be isolated by the addition of a base, such as triethylamine, to remove the acid. In the neutral compound, the signal for the phosphorus centre has a chemical shift of 204.4 ppm.



Scheme 1.8 Preparation of 2,5-dimethyl-2*H*-1,2,3 σ^2 -diazaphosphole, **XX**.

The condensation reaction between acetone methylhydrazone and phosphorus trichloride gives two structural isomers of the diazaphosphole, the methylene-phosphane, 2,5-dimethyl-2*H*-1,2,3 σ^2 -diazaphosphole, **XX**, and the iminophosphane, 1,5-dimethyl-1*H*-1,2,3 σ^2 -diazaphosphole, **XXI**, in yields of 50% and 12%, respectively.⁵¹ The chemical shift of the phosphorus in **XXI**, lies upfield (223.0 ppm) of **XX**.

**XX****XXI**

The major product, 2,5-dimethyl-2*H*-1,2,3 σ^2 -diazaphosphole, **XX**, can be separated from the mixture by distillation. Interconversion from one isomer to the other was not observed under these conditions.

The solid-state structures of both the hydrogen chloride adduct of 2,5-dimethyl-2*H*-1,2,3 σ^2 -diazaphosphole, **XX**·HCl,⁵⁰ (Figure 1.3), and the 1,5-dimethyl-1*H*-1,2,3 σ^2 -diazaphosphole, **XXI**,⁵¹ (Figure 1.4) have been determined by single crystal x-ray diffraction. Both structures show a planar phosphole ring system. The angle about the phosphorus atom (C-P-N) is 90.4° for **XX**·HCl whereas the corresponding angle in **XXI** increased to 92.9°. For **XX**·HCl, the N(3)-Cl(1) distance is 2.999(2)Å, with the N(3)-H(11) distance being 0.89(3) Å. The N(3)-H(31)-Cl(1) angle is almost linear at 173°. All bond distances within the ring of **XX**·HCl are consistent with a 6 π delocalized aromatic structure described above.

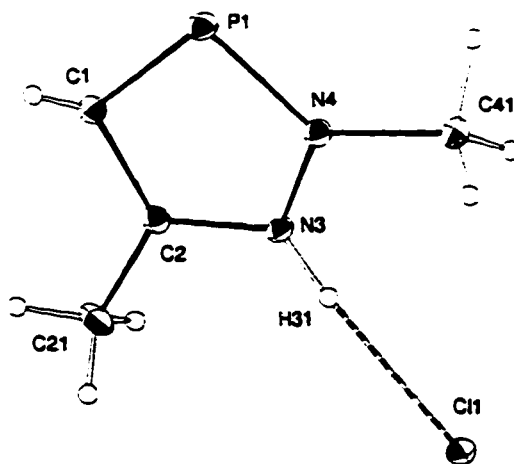


Figure 1.3 Solid-state structure of 2,5-dimethyl-2*H*-1,2,3 σ^2 -diazaphosphole-HCl, XX-HCl. [Reference 50]

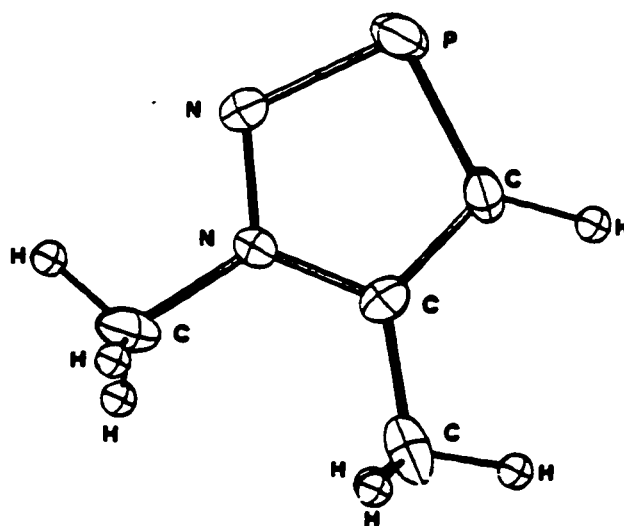
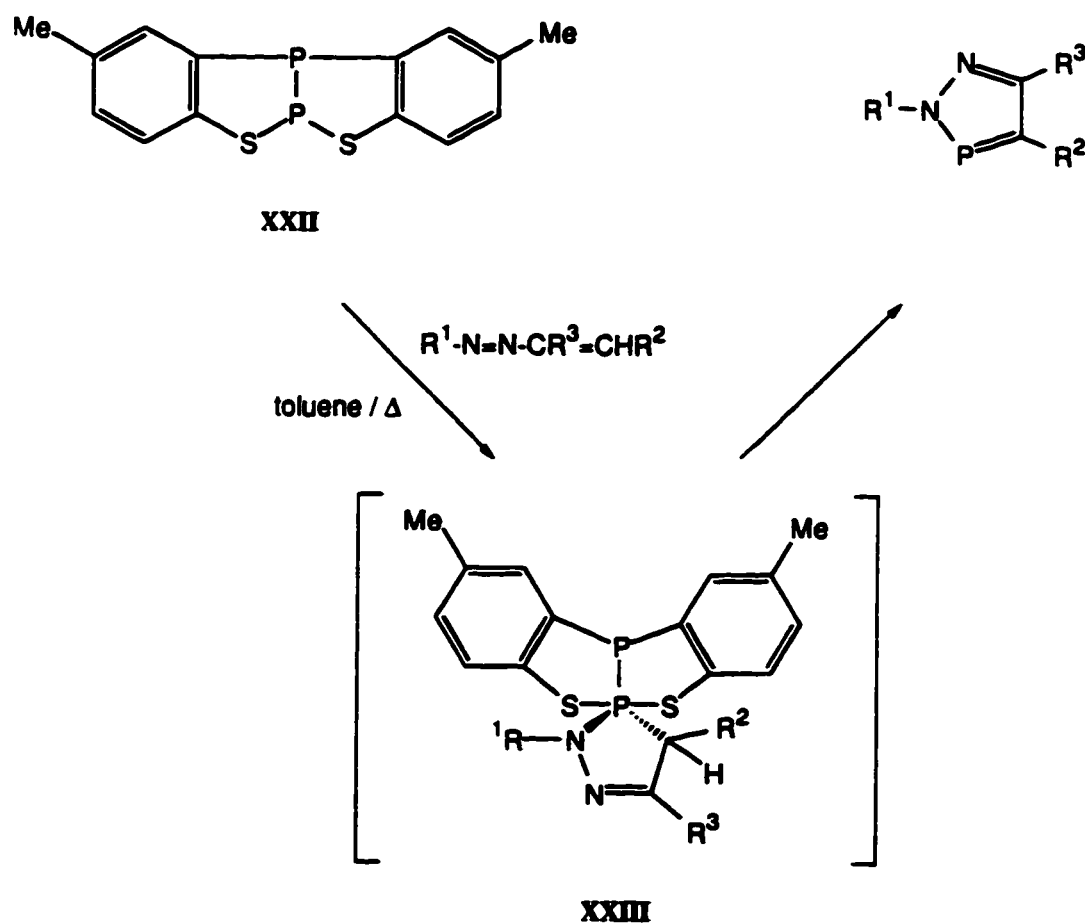


Figure 1.4 Solid-state structure of 1,5-dimethyl-1*H*-1,2,3 σ^2 -diazaphosphole, XXI. [Reference 51]

Recently, another route which involves the reaction of benzothiadiphosphole, **XXII**, with an azaoalkene has been used to synthesize a variety of 4,5-dimethyl-2*H*-1,2,3 σ^2 -diazaphospholes (Scheme 1.9).⁵² This reaction is thought to proceed through the establishment of a spirocyclic pentacoordinate **XXIII** intermediate which then transforms *via* a reductive elimination process to give the substituted diazaphosphole.

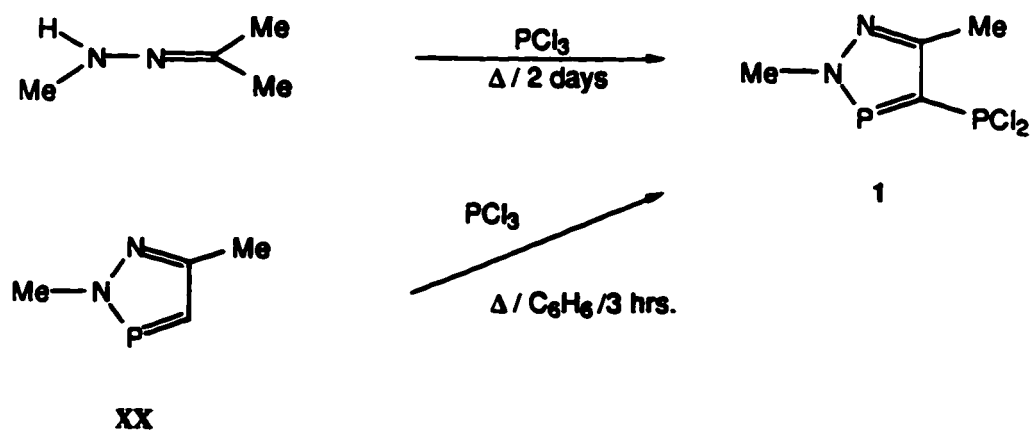


Scheme 1.9 Synthesis of 2*H*-1,2,3 σ^2 -diazaphospholes *via* benzothiadiphosphole (**XXII**) and an azaoalkene.

1.3.4 Synthesis of 4-(Phosphino)-2,5-dimethyl-2*H*-1,2,3σ²-diazaphosphole

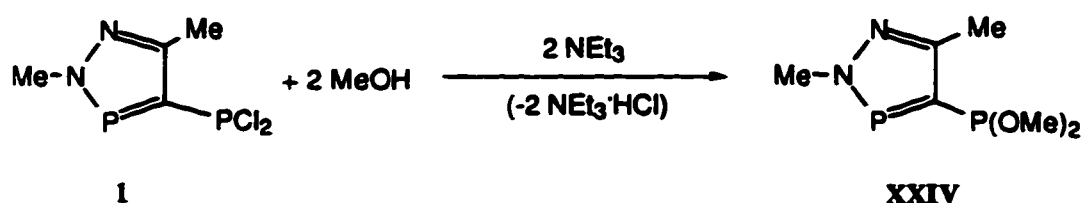
Derivatives

The 2,5-dimethyl-2*H*-1,2,3σ²-diazaphosphole, **XX**, readily provides access to the 4-phosphino substituted 2*H*-1,2,3σ²-diazaphosphole series. These derivatives are interesting members of the bisphosphine series because the ligand contains two distinct phosphorus centres which should have different reactivities. The 4-(dichlorophosphino)-2,5-dimethyl-2*H*-1,2,3σ²-diazaphosphole, **1**, is easily obtained by condensation of acetone methylhydrazone with an excess of phosphorus trichloride.⁵³ Another route to this bisphosphine is provided by the reaction of 2,5-dimethyl-2*H*-1,2,3σ²-diazaphosphole with phosphorus trichloride. Both synthetic routes are shown in Scheme 1.10. The ³¹P{¹H} NMR shows a downfield signal at δ 249.0 ppm for the cyclic σ²P centre and a signal at a higher field, δ 157.6 ppm, for the exo-cyclic σ³P centre. The observed two-bond phosphorus-phosphorus coupling is 79 Hz.



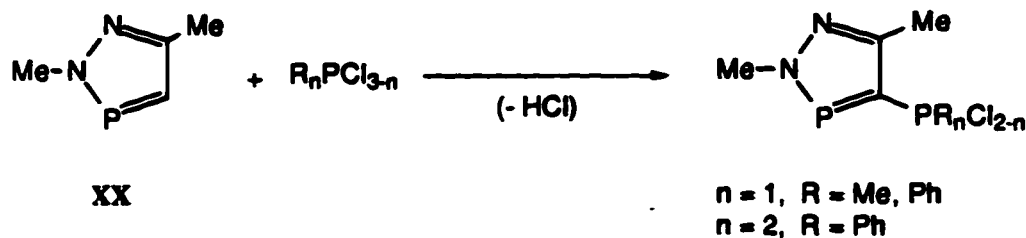
Scheme 1.10 Preparation of 4-(dichlorophosphino)-2,5-dimethyl-2*H*-1,2,3σ²-diazaphosphole, **1**, from the reaction of phosphorus trichloride with **XX** or acetone methylhydrazone.

Previously known substituents on the exo-phosphorus are methoxy, methyl, and phenyl.⁵⁴ 4-(Dimethoxyphosphino)-2,5-dimethyl-2*H*-1,2,3σ²-diazaphosphole, XXIV, was obtained from the reaction of the dichlorophosphinophosphole (1) with methanol in the presence of triethylamine (Scheme 1.11). The phosphorus chemical shifts for the σ²P and σ³P centres are 240.0 ppm and 157.2 ppm, respectively, and ²J_{PP} is 21 Hz.



Scheme 1.11 The preparation of 4-(dimethoxy)phosphino-2,5-dimethyl-2*H*-1,2,3σ²-diazaphosphole, XXIV.

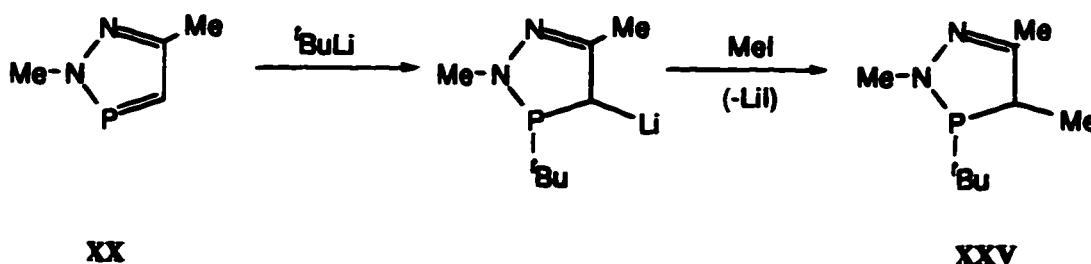
The methyl and phenyl derivatives were synthesized by the reaction of the diazaphosphole with the corresponding chlorophosphines (Scheme 1.12).⁵⁴ The yields for these reactions tend to be low (6% to 36%).



Scheme 1.12 Preparation of the methyl and phenyl derivatives of 4-phosphino-2,5-dimethyl-2*H*-1,2,3σ²-diazaphosphole.

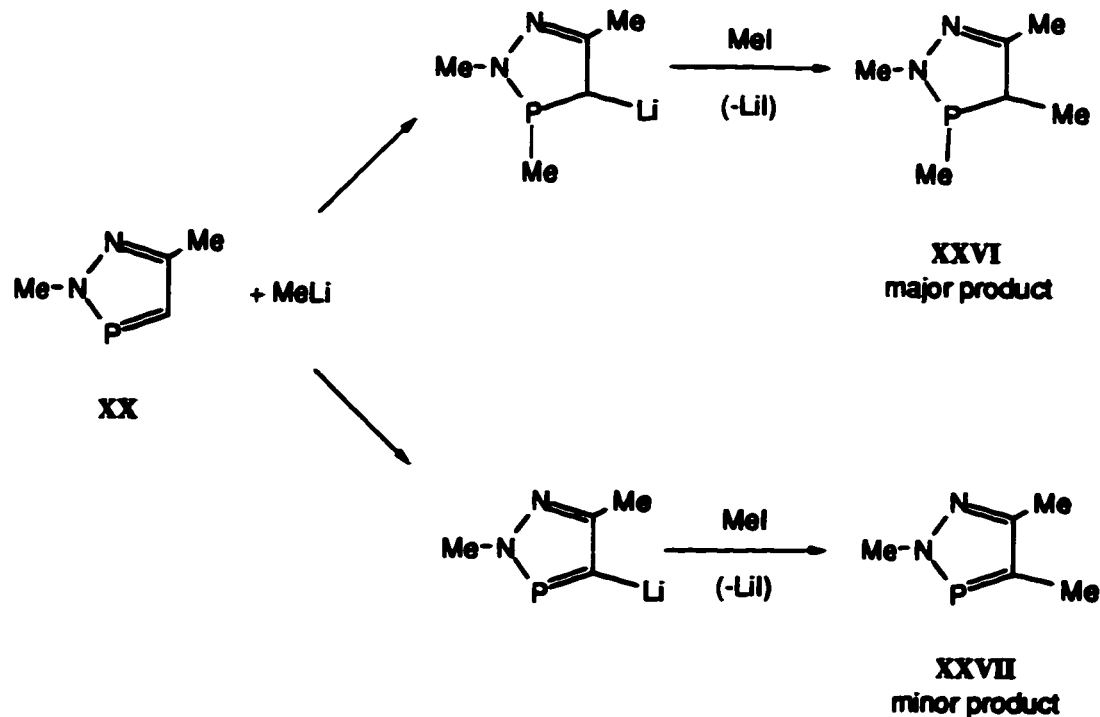
In an effort to improve the yields for the methyl and phenyl derivatives beyond that given by these direct transformations other routes were explored.^{55,56}

The reaction of *tert*-butyllithium with the diazaphosphole XX resulted in a 1,2-addition across the phosphorus-carbon double bond to produce a three-coordinate phosphorus diazaphosphole.⁵⁵ Subsequent addition of iodomethane gave the cyclic compound XXV. This transformation is signalled by a marked upfield shift for the phosphorus signal from δ 204.4 ppm, for diazaphosphole, to δ 55 ppm. This shift in the NMR signal for the phosphorus centre is the result of the change in the coordination of the phosphorus centre from a $\sigma^2\text{P}$ to a $\sigma^3\text{P}$ center and the resultant change in the hybridization from sp^2 to sp^3 .



Scheme 1.13 Reaction of 2,5-dimethyl-2H-1,2,3σ²-diazaphosphole, XX, with *tert*-butyllithium. [Reference 55]

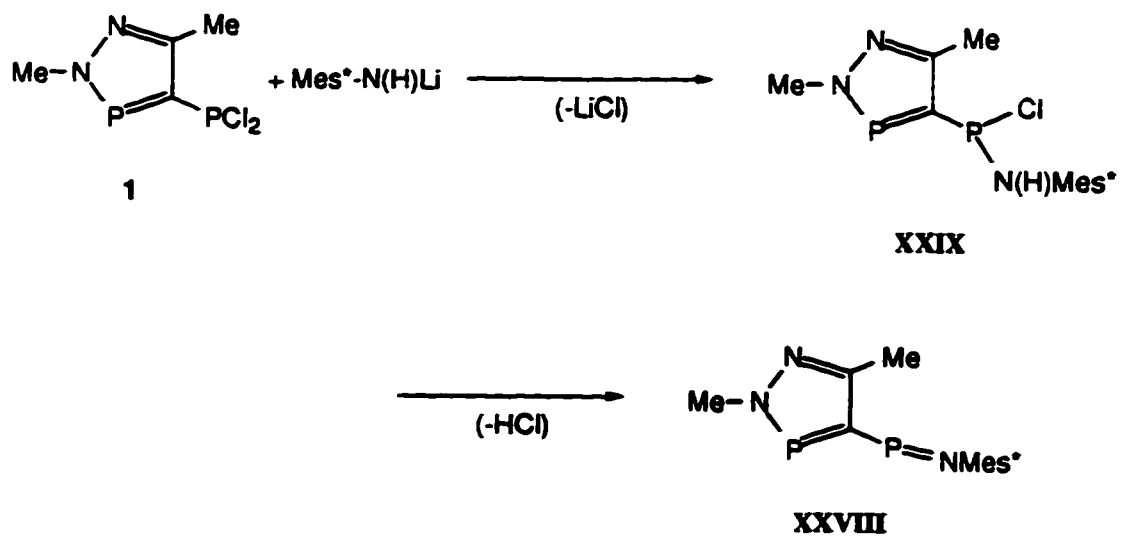
The reaction of XX with the less sterically hindered methyllithium gave two products (Scheme 1.14).⁵⁶ Following the subsequent addition of iodomethane, the major product of the reaction was found to be the three-coordinate phosphorus diazaphosphole, XXVI, and only a minor amount of the $\sigma^2\text{P}$ compound 2,4,5-trimethyl-2H-1,2,3σ²-diazaphosphole, XXVII, was produced. Once again there is a large shift for the phosphorus centre signal (63.2 ppm) in the ³¹P NMR spectrum for the major product which is due to an increase in the coordination number of the phosphorus atom.



Scheme 1.14 Reaction of the 2,5-dimethyl-2*H*-1,2,3 σ^2 -diazaphosphole XX with methyllithium. [Reference 56]

1.3.5 Synthesis of (2,5-Dimethyl-2*H*-1,2,3 σ^2 -diazaphosphol-4-yl)aryliminophosphine

Also derived from 4-(dichlorophosphino)-2,5-dimethyl-2*H*-1,2,3 σ^2 -diazaphosphole is *P*-(2,5-dimethyl-2*H*-1,2,3 σ^2 -diazaphosphol-4-yl)aryliminophosphine, XXVIII.⁵⁷ Both phosphorus centres are two-coordinate in this system. The synthesis is shown in Scheme 1.15. An intermediate XXIX was isolated and its solid-state structure is shown in Figure 1.5. The $^{31}\text{P}\{^1\text{H}\}$ NMR spectrum of XXVIII showed the chemical shift for the endocyclic $\sigma^2\text{P}$ centre at 246.3 ppm while the exocyclic imino $\sigma^2\text{P}$ centre resonated at a lower field of 363.1 ppm. The two-bond phosphorus-phosphorus coupling was not observed in this system due to the broadening of the signals.



Scheme 1.15 Synthesis of *P*-(2,5-dimethyl-2*H*-1,2,3 σ^2 -diazaphosphol-4-yl)aryliminophosphine, **XXVIII**.

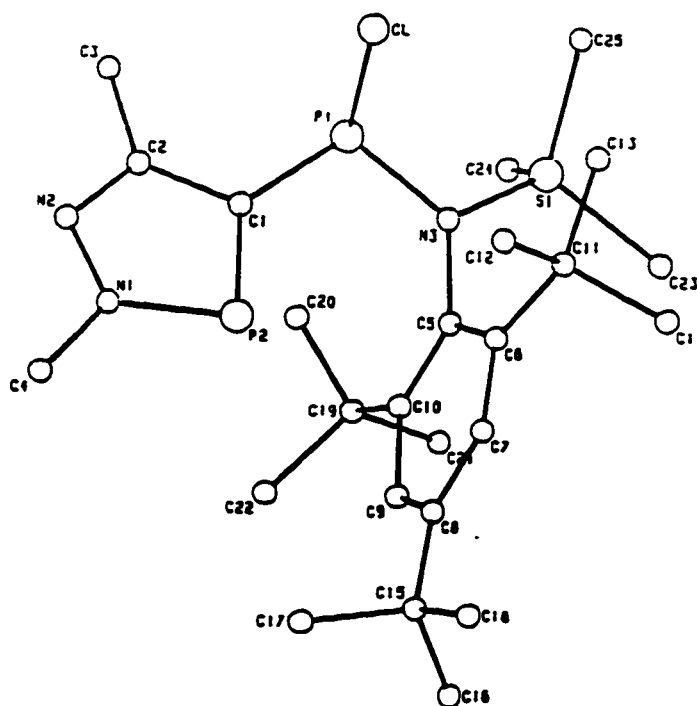


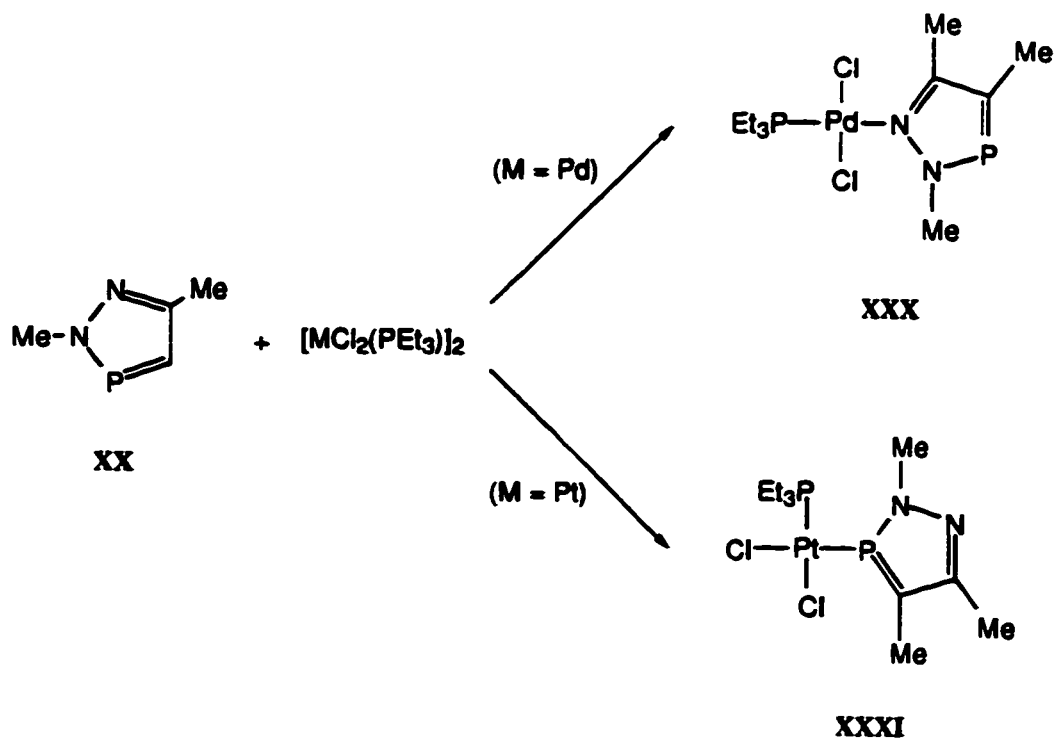
Figure 1.5 Solid-state structure of the intermediate aminophosphinophosphine, **XXIX** (hydrogen atoms have been omitted for clarity). [Reference 57]

1.4 Metal Complexation

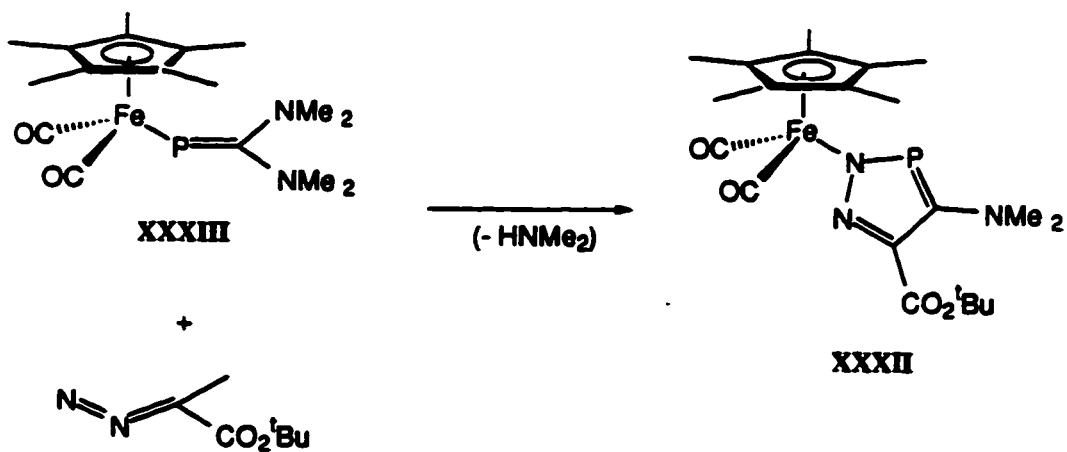
1.4.1 Metal Complexation Chemistry of the 2,5-dimethyl-2*H*-1,2,3σ²-diazaphosphole

Only limited exploration of the coordination chemistry of the 2,5-dimethyl-2*H*-1,2,3σ²-diazaphosphole, **XX**, has been reported. The reaction of **XX** with [PdCl₂(PEt₃)]₂ gave the *trans* complex **XXX**, wherein the nitrogen is coordinated to the palladium metal centre.⁵⁸ A small change in the phosphorus chemical shift of 8 ppm downfield (236.5 ppm) accompanied coordination. In contrast, the platinum analogue gave the *cis* complex, **XXXI**, wherein the phosphorus is coordinated to the metal. In this case the phosphorus chemical shift moves upfield (166.1 ppm) and the signal is accompanied by a ¹J_{PPt} value of 4676 Hz, clearly indicating platinum-phosphorus bonding. The reaction with [Me₂AuCl]₂ was similar to that of the palladium complex giving a nitrogen coordinated gold complex wherein a downfield shift for the phosphorus was observed (228.5 ppm).⁵⁹

The example of the iron complex **XXXII** reveals a final product in which the diazaphosphole ring is attached to the metal centre through the nitrogen *via* a cycloaddition to the phosphorus-carbon double bond.⁶⁰ This reaction is a polar [3+2] cycloaddition of *tert*-butyl diazoacetate to the iron phosphalkene **XXXIII**, followed by the elimination of dimethylamine with a sigmatropic 1,5-shift of the CpFe(CO)₂ fragment from the phosphorus to the nitrogen (Scheme 1.17). Interestingly, the chemical shift for the phosphorus signal in **XXXII** was 228.8 ppm which is comparable to that shown by related metal-free phospholes (225 ppm to 230 ppm). The coordination of the iron centre to the ring has thus had very little effect on the chemical shift of the cyclic phosphorus. The solid-state structure of the final product is shown in Figure 1.6.⁶⁰



Scheme 1.16 Reaction of **XX** with $[\text{MCl}_2(\text{PEt}_3)_2]$ ($\text{M} = \text{Pd}, \text{Pt}$).



Scheme 1.17 Synthesis of $\text{Cp}^*(\text{CO})_2\text{Fe}-\text{N}=\text{PC}(\text{NMe}_2)-\text{C}(\text{CO}_2^t\text{Bu})=\text{N}$, **XXXII**.

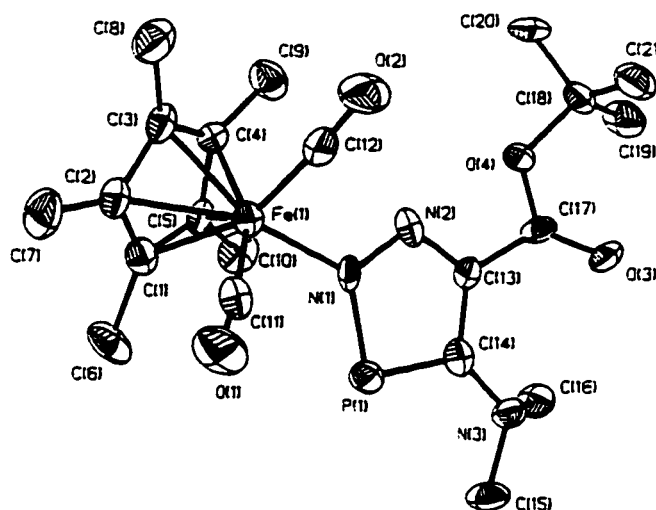


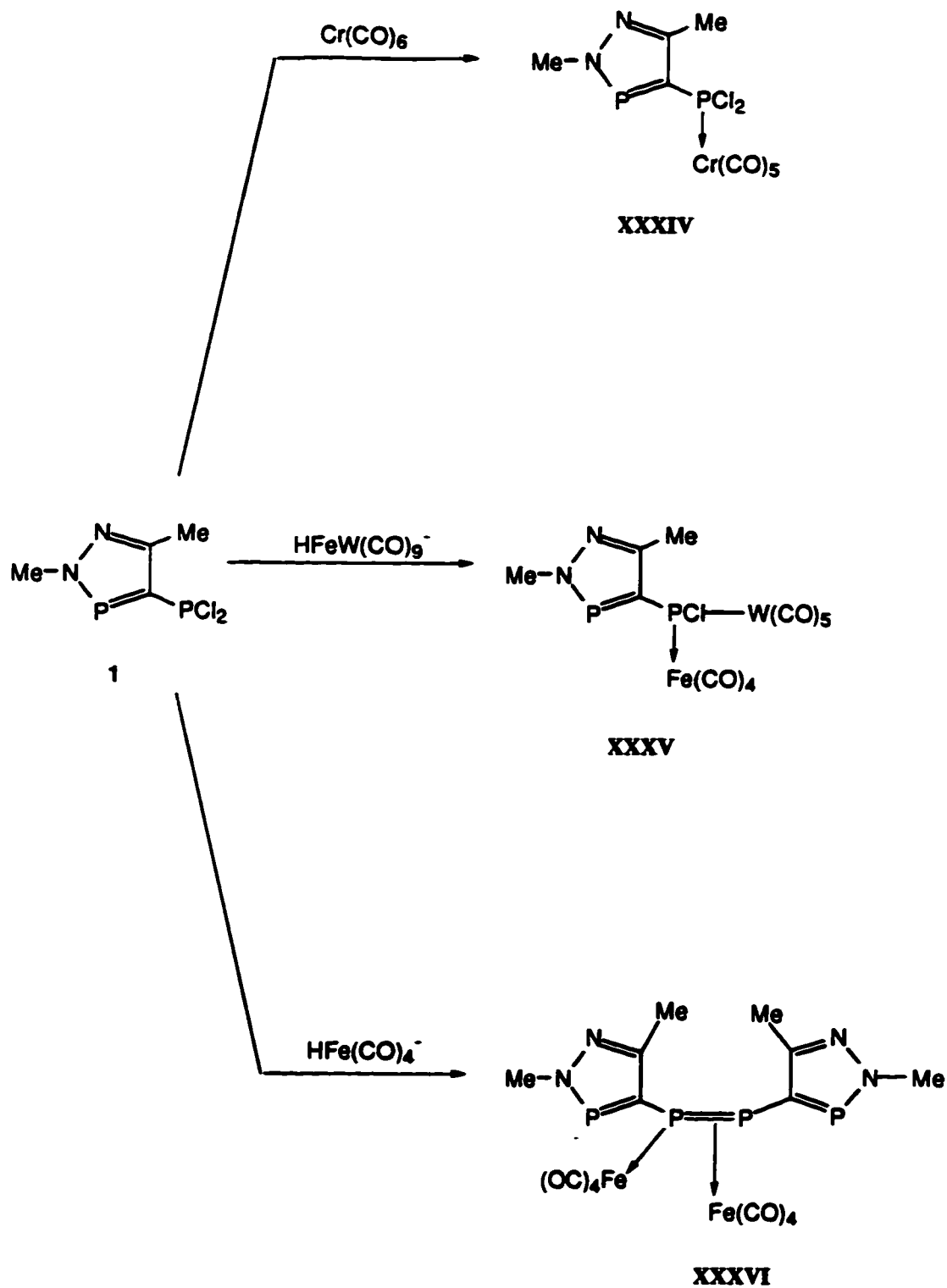
Figure 1.6 Solid-state structure of $\text{Cp}^*(\text{CO})_2\text{Fe-N}=\text{PC}(\text{NMe}_2)\text{-C}(\text{CO}_2^t\text{Bu})=\text{N}$, XXXIII. [Reference 60]

The solid-state structure in Figure 1.6 shows an Fe-N(1) bond length of 1.95 Å. The phosphole ring is planar, with the Fe atom located in the plane of the ring. The bond angle for N(1)-P(1)-C(14) is 91°. All bond lengths and other bond angles compare well with those of similar diazaphospholes.

1.4.2 Metal Complexation Chemistry of 4-(Phosphino)-2,5-dimethyl-2H-1,2,3σ²-diazaphosphole Derivatives

Some metal complexation chemistry of these systems has been reported. In the cases of the reactions involving the dichlorophosphino-diazaphosphole (1), the site of reaction was the σ³P centre, as shown in Scheme 1.18. This reaction of 1 with either Cr(CO)₆ or Cr(CO)₅(MeCN) gave the complex in which the exo-phosphorus was coordinated to the chromium metal centre (complex XXXIV).⁵⁴ A downfield shift in the ³¹P{¹H} NMR signal for the coordinated exocyclic phosphorus (186.4

ppm) was observed while the σ^{2P} experienced a slight upfield shift of 9 ppm (240.1 ppm). There was also a slight decrease in the ${}^2J_{PP}$ value (74 Hz). Westermann⁶¹ reported that $HFeW(CO)_9^-$ reacted with the diazaphosphole **1** with the cleavage of iron-tungsten bond and the elimination of HCl to form the complex **XXXV** as a species containing both a phosphorus-tungsten bond to the exocyclic phosphorus which now only has one chloride substituent. The same exocyclic phosphorus centre is coordinated to the $Fe(CO)_4$ moiety. No NMR data was provided in support of this interpretation. In contrast, reaction of **1** with $HFe(CO)_4^-$ resulted in an unusual coupling of the exo-phosphorus groups of two phosphinodiazaphospholes.⁶² The product, **XXXVI**, has two $Fe(CO)_4$ groups coordinated to the coupled phosphinodiazaphosphole rings which are coupled by the formation of a phosphorus-phosphorus double bond. One of the exo-phosphorus atoms (which is now dicoordinate) is coordinated to one $Fe(CO)_4$ group with the usual two electron σ donor bond while the phosphorus-phosphorus double bond is coordinated in an η^2 fashion to the other $Fe(CO)_4$ group. The solid-state structure of this unusual complex is shown in Figure 1.7.



Scheme 1.18 Selected reactions of 4-(dichlorophosphino)-2,5-dimethyl-2H-1,2,3 σ^2 -diazaphosphole (**1**) with metallic species.

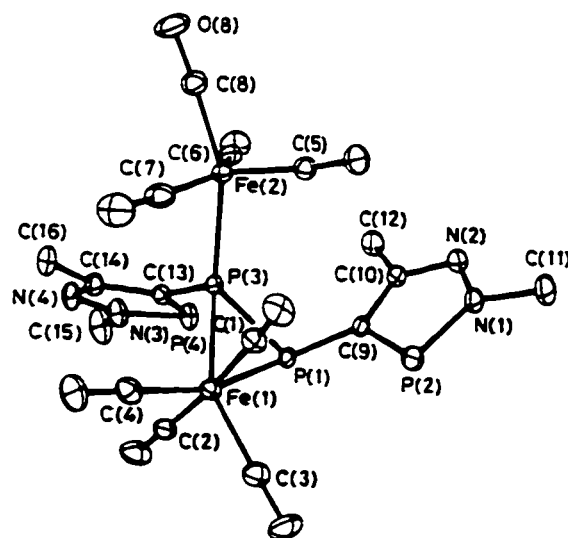


Figure 1.7 Solid-state structure of the complex XXXVI. [Reference 62]

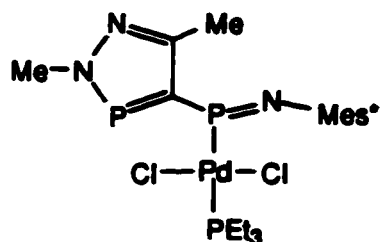
The solid-state structure of XXXVI revealed that both phosphole rings are planar with slightly different angles at the phosphorus centre in each of the rings. In one of the phosphole rings, the C(9)-P(2)-N(1) bond angle is 89.3° while in the other phosphole ring the related C(13)-P(4)-N(3), bond angle is 88.7° . The C(13)-P(3)-P(1) bond angle is 89.3° . The P(1)-P(3) bond length is 2.15 \AA , although considerably longer than that usually shown by normal phosphorus-phosphorus double bonds (2.034 \AA ⁶³), is typical for a diphosphene which is acting as both a side-on and an end-on bonding ligand (2.139 \AA ⁶⁴ and 2.184 \AA ⁶⁵).

The $^{31}\text{P}\{^1\text{H}\}$ NMR spectrum of XXXVI showed the pattern of an ABXY spin system consisting of the two σ^2 phosphole phosphorus atoms A and B (224.8 ppm (P(2)) and 244.3 ppm (P(4))), the σ^3 exo-phosphorus, P(1) ($\delta -52.4 \text{ ppm}$) and the σ^4 exo-phosphorus, P(3) ($\delta 8.2 \text{ ppm}$). The P(1) signal has large coupling constant

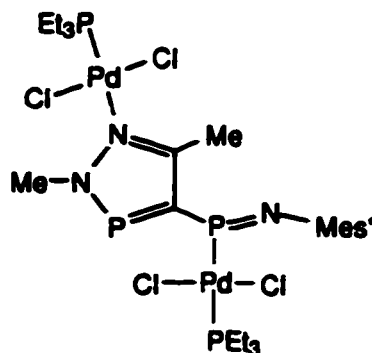
connecting it to the phosphole phosphorus P(2) (${}^2J_{P(1)P(2)} = 166$ Hz) and the $\sigma^4P(3)$ (${}^1J_{P(1)P(3)} = 384$ Hz). The P(3) couples to both the phosphole phosphorus centres but with much smaller coupling constants (${}^2J_{P(3)P(4)} = 36$ Hz, ${}^3J_{P(3)P(2)} = 19$ Hz).

1.4.3 Metal Complexation Chemistry of (2,5-Dimethyl-2*H*-1,2,3- σ^2 -diazaphosphol-4-yl)aryliminophosphine

The metal complexation chemistry of the iminophosphinodiazaphosphole was demonstrated by the coordination of the exocyclic σ^2P atom of the iminophosphine with either palladium or platinum.⁵⁷ The reaction of $[MCl_2(PEt_3)]_2$ ($M = Pd, Pt$) with two equivalents of the iminophosphino-diazaphosphole **XXIX** with the palladium dimer gave the complex **XXXVII**, in which only the exo-phosphorus site is coordinated to the metal. The ${}^{31}P\{^1H\}$ NMR spectrum of this palladium complex gave chemical shift signals for the σ^2P at 252.4 ppm and for the imino σ^3P at 80.1 ppm. The ${}^2J_{PP}$ was 107 Hz. The PEt_3 ligand gave a ${}^{31}P\{^1H\}$ NMR signal at 36.0 ppm and coupling to the imino σ^3P phosphine centre was large (${}^2J_{PP}$ 680 Hz). Reaction between one equivalent of the phosphinodiazaphosphole with the same palladium source gave the bimetallic complex **XXXVIII**, wherein both the unsubstituted nitrogen and the exo-phosphorus of the diazaphosphole are coordinated to two different palladium centres, similar to the behaviour that was previously observed with the diazaphosphole **XX**.⁵⁸ The reaction of two equivalents of the phosphinodiazaphosphole with the platinum dimer gave a monometallic complex similar in nature to **XXXVII**. The ${}^{31}P\{^1H\}$ NMR spectrum showed the σ^2P signal at δ 262.6 ppm and the imino σ^3P resonance at δ 214.0 ppm coupled (${}^2J_{PP}$) by 51 Hz. The ${}^1J_{PPt}$ coupling was 4452 Hz and that for the ${}^2J_{PPEt_3}$ was 17 Hz.



XXXVII



XXXVIII

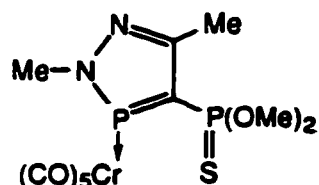
1.4.4 Coordination Chemistry of the Two-Coordinate Phosphorus in Diazaphosphole Rings Systems

The coordination chemistry of the two-coordinate phosphorus atom in the diazaphosphole ring is limited. This in part can be ascribed to hybridization (electron distribution about the two-coordinate phosphorus centre). Although these hetero atoms including the phosphorus atom in the aromatic diazaphosphole rings possess formal exocyclic lone pairs which might be thought suitable for formation of donor bonds, the solid-state structures reveal that the typical bond angle about the phosphorus is approximately 90° (i.e. Figures 1.3 and 1.4). Thus when the bonds between the phosphorus, the nitrogen and the carbon are formulated, the major participant in the bond formation could be described as principally constructed from the three unhybridized phosphorus p orbitals. The remaining pair of electrons then remains in an s orbital. This places the electron pair in a diffuse orbital which can only, without extensive rehybridization, provide weak overlap with the metal orbital. Of course the addition of the metal center, if the interactions are appropriate, can induce rehybridization at the phosphole center to generate more favourable

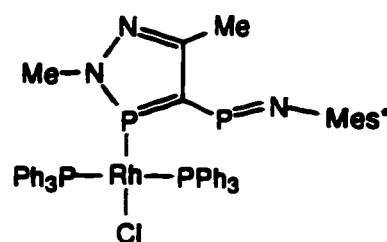
interactions, thus the initial electronic state of the dicoordinate phosphorus does not obviate in itself the ability of the phosphole to act as a base.

Two complexes with the phosphinodiazaphosphole system have been reported. A chromium(0) complex, **XXXIX**, wherein the exocyclic phosphorus has been oxidized with sulfur to provide a derivative of **XX** has been reported.⁵⁴ In this case the $^{31}\text{P}\{^1\text{H}\}$ NMR spectrum showed a downfield shift of 12 ppm to δ 265.9 ppm for the ring phosphorus signal while the signal for the exo-phosphorus showed a shift of 2.3 ppm to δ 79.7 ppm. There was also a small decrease of 6 Hz in the two-bond phosphorus-phosphorus coupling to 81 Hz. These $^{31}\text{P}\{^1\text{H}\}$ NMR parameters indicate that the interaction between the cyclic phosphorus and the chromium metal centre is relatively weak.

The other complex reported wherein the cyclic phosphorus is coordinated to a metal centre arises from the reaction of iminophosphinodiazaphosphole **XXIX** with $\text{Rh}(\text{PPh}_3)_3\text{Cl}$.⁵⁷ Upon complexation, the diazaphosphole phosphorus signal had shifted downfield by 36 ppm to δ 282.3 ppm and the exo-phosphorus centre also shifted downfield in this case by 24 ppm to δ 387.0 ppm. The observed phosphorus-phosphorus coupling constant for the coordinated iminophosphinodiazaphosphole was 191 Hz and a one-bond phosphorus-rhodium coupling constant of 238 Hz was observed, indicating direct phosphorus-rhodium bonding. These latter values are much larger and are suggestive of relatively strong interactions between the ligand and the metal.



XXXIX



XL

1.5 Scope of Present Work

The previous two metal complexes (XXXIX and XL) have shown that under the right conditions it is possible to create a phosphorus centre which can either weakly or strongly coordinate to a metal centre. The conditions that are involved revolve about the nature of the exocyclic phosphorus centre. Changing substituents or the coordination number of this phosphorus centre can strongly affect the endocyclic phosphorus atom. With such a precedent established, investigations of the interactions of the two phosphorus centres with one another becomes important.

To build on the development of heterobifunctional bisphosphine ligands previously synthesized in this laboratory (e.g. VIII and IX), the chemistry of this type of bisphosphine system which contains both a two- and a three-coordinate phosphorus centre was explored. This study focused on expanding the versatility of this system and the exploration of the potential of this system as a heterobisphosphine. The starting material was the bisphosphine ligand, 4-(dichlorophosphino)-2,5-dimethyl-2*H*-1,2,3σ²-diazaphosphole (1), which is easily prepared in good quantities. The chlorine groups on the exo-phosphorus(III) are readily substituted, allowing facile alterations of the exocyclic phosphorus centre to change the basicity and/or steric nature. Several derivatives such as the fluorides, amino, and alkoxy derivatives were thus synthesized. Substitution at the exocyclic phosphorus may also alter the character of the endocyclic phosphorus atom to enhance its reactivity.

The second facet of the study focussed on the evaluation of metal complexation behaviour of the $\sigma^2\text{P}-\sigma^3\text{P}$ phosphinodiazaphosphole system to augment the very limited existing metal complexation studies and garner further insight into the complexation behaviour of the system. Metals such as chromium, rhodium, palladium, and platinum have been explored. The rigid backbone structure of the ligand, arising from the constraints of the sp^2 hybridized bridging carbon connecting them, means that the bite angle is too large to allow chelation to most metal centres. As a result the ligand would then be expected to be restricted to monodentate coordination to a metal centre or, alternatively, it could build bridged dimers. The latter would be particularly of interest because of current activity in such systems.



Figure 1.8 Coordination of the phosphinodiazaphosphole on a monodentate and bridging fashion with metal centres.

This bisphosphine system which provides two distinctly different trivalent phosphorus centres may also be further transformed by preferential selective oxidation of one of the centres to create a heterobifunctional bisphosphine, such as has been done with many other trivalent phosphorus ligands. To this end, these bisphosphines have been oxidized with chalcogens, such as elemental sulfur and elemental selenium, and with various azides. The coordination chemistry of these differentially oxidized systems has also been explored.

The expansion of the bite angle geometry that results from the oxidation of the exocyclic phosphorus will enhance the possibility for the formation of chelated binding to metals in order to create a five-membered metallacycle. This factor could

also improve the prospects for enhancing the involvement of the dicoordinate phosphorus centre.



Figure 1.9 Coordination of the phosphoranodiazaphosphole in a monodentate and chelating fashion with metal centres.

In addition to simple coordination, the trimethylsilyl derivative of the iminophosphoranodiazaphosphole is readily accessible when Me_3SiN_3 is used as the oxidant. The resultant silyl-imine system can eliminate trimethylsilylchloride from a metal chloride to form a metal-nitrogen sigma bond. The ligand then acts as a monoanionic as well as a potential coordinating ligand. This chemistry has been extensively explored in this laboratory with the $\text{Ph}_2\text{PCH}_2\text{P}(=\text{NSiMe}_3)\text{Ph}_2$ and related ligand systems (e.g. Scheme 1.5).^{39,66,67}

1.6 References

- (1) Shriver, D. F.; Atkins, P. W.; Langford, C. H. *Inorganic Chemistry*; W.H. Freeman and Company: New York, 1990, pp 173.
- (2) Pearson, R. G. *Hard and Soft Acids and Bases*; Dowden, Hutchinson, and Ross: Stroudsburg, Pennsylvania, 1973.
- (3) Davies, W. C.; Mann, F. G. *J. Chem. Soc.* **1944**, 276.
- (4) Newkome, G. R. *Chem. Rev.* **1993**, *93*, 2067.
- (5) Issleib, K.; Rieschel, R. *Chem. Ber.* **1965**, *98*, 2086.
- (6) Anderson, G. K.; Kumar, R. *Inorg. Chem.* **1984**, *23*, 4064.
- (7) Werner, H.; Hampp, A.; Peters, K.; Peters, E. M.; von Schnering, H. G. *Z. Naturforsch.* **1990**, *45b*, 1548.
- (8) Schulz, M.; Werner, H. *Organometallics* **1992**, *11*, 2790.
- (9) Werner, H.; Schultz, M.; Windmüller, B. *Organometallics* **1995**, *14*, 3659.
- (10) Farr, J. P.; Olmstead, M. M.; Balch, A. L. *J. Am. Chem. Soc.* **1980**, *102*, 6654.
- (11) Farr, J. P.; Olmstead, M. M.; Rutherford, N. M.; Wood, F. E.; Balch, A. L. *Organometallics* **1983**, *2*, 1758.
- (12) Li, S.-L.; Mak, T. C. W.; Zhang, Z.-Z. *J. Chem. Soc. Dalton Trans.* **1996**, 3475.
- (13) Stephan, D. W. *Coord. Chem. Rev.* **1989**, *95*, 41.
- (14) Uozumi, Y.; Tanahashi, A.; Lee, S.-Y.; Hayashi, T. *J. Org. Chem.* **1993**, *58*, 1945.
- (15) Uozumi, Y.; Suzuki, N.; Ogiwara, A.; Haashi, T. *Tetrahedron* **1994**, *50*, 4293.
- (16) Berger, H.; Nesper, R.; Presgosin, P. S.; Rügger, H.; Würle, M. *Helv. Chim. Acta.* **1993**, *76*, 1520.
- (17) Hayashi, T.; Konishi, M.; Fukushima, M.; Kanehira, K.; Hioki, T.; Kumada, M. *J. Org. Chem.* **1983**, *48*, 2195.
- (18) Pastor, S. D.; Togni, A. *Helv. Chim. Acta* **1991**, *74*, 905.

- (19) Ito, Y.; Sawamura, M.; Shirakawa, E.; Hayashizaki, K.; Hayashi, T. *Tetrahedron Lett.* **1988**, *29*, 235.
- (20) Ito, L. N.; Johnson, B. J.; Mueting, A. M.; Pignolet, L. H. *Inorg. Chem.* **1989**, *28*, 2026.
- (21) Hayashi, T.; Sawamura, M.; Ito, Y. *Tetrahedron* **1992**, *48*, 1999.
- (22) Togni, A.; Pastor, S. D. *J. Org. Chem.* **1990**, *55*, 1649.
- (23) Sawamura, M.; Ito, Y.; Hayashi, T. *Tetrahedron Lett.* **1990**, *31*, 2723.
- (24) Schnyder, A.; Togni, A.; Wiesli, U. *Organometallics* **1997**, *16*, 255.
- (25) Burckhardt, U.; Gramlich, V.; P., H.; Nesper, R.; P.S., P.; Salzmann, E.; Togni, A. *Organomet.* **1996**, *15*, 3496.
- (26) Pietrusiewicz, K. M.; Zablocka, M. *Chem. Rev.* **1994**, *94*, 1375.
- (27) Noyori, R. *Asymmetric Catalysis in Organic Synthesis*; Wiley-Interscience Publication: New York, 1994.
- (28) Petit, M.; Mortreux, A.; Petit, F.; Buono, G.; Peiffer, G. *Nov. J. Chim.* **1983**, *7*, 593.
- (29) Heidel, H.; Huttner, G.; Helmchen, G. *Z. Naturforsch.* **1993**, *48b*, 1681.
- (30) Roberts, N. K.; Wild, S. B. *J. Am. Chem. Soc.* **1979**, *101*, 6254.
- (31) Mozol, V. J. M.Sc. Thesis, University of Alberta, 1993.
- (32) Katti, K. V.; Batchelor, R. J.; Einstein, F. W. B.; Cavell, R. G. *Inorg. Chem.* **1990**, *29*, 808.
- (33) Balakrishna, M. S.; Klein, R.; Uhlenbrock, S.; Pinkerton, A. A.; Cavell, R. G. *Inorg. Chem.* **1993**, *32*, 5676.
- (34) Bhattacharya, P.; Slawin, A. M. Z.; Smith, M. B.; Woollins, J. D. *Inorg. Chem.* **1996**, *35*, 3675.
- (35) Grim, S. O.; Mitchell, J. D. *Inorg. Chem.* **1977**, *16*, 1770.
- (36) Jeffrey, J. C.; Rauchfuss, T. B. *Inorg. Chem.* **1979**, *18*, 2658.

- (37) Wegman, R. W.; Abatjoglou, A. G.; Harrison, A. M. *J. Chem. Soc., Chem. Commun.* **1987**, 1891.
- (38) Mecking, S.; Keim, W. *Organometallics* **1996**, *15*, 2650.
- (39) Katti, K. V.; Cavell, R. G. *Inorg. Chem.* **1989**, *28*, 413.
- (40) Katti, K. V.; Cavell, R. G. *Organometallics* **1991**, *10*, 539.
- (41) Merrill, R. E. *Chemtech* **1981**, *11*, 118.
- (42) Burk, M. J. *J. Am. Chem. Soc.* **1991**, *113*, 8518.
- (43) Burk, M. J.; Feaster, J. E.; Harlow, R. L. *Tetrahedron: Asymmetry* **1991**, *2*, 569.
- (44) Burk, M. J.; Gross, M. F.; Harper, T. G. P.; Kalberg, C. S.; Lee, J. R.; Martinez, J. P. *Pure. & Appl. Chem.* **1996**, *68*, 37.
- (45) Nugent, W. A.; RajanBabu, T. V.; Burk, M. J. *Science* **1993**, *259*, 479.
- (46) Mathey, F.; Mercier, F.; Charrier, C. *J. Am. Chem. Soc.* **1981**, *103*, 4595.
- (47) Holand, S.; Charrier, C.; Mathey, F.; Fischer, J.; Mitschler, A. *J. Am. Chem. Soc.* **1984**, *106*, 826.
- (48) Schmidpeter, A.; Karaghiosoff, K. In *Multiple Bonds and Low Coordination in Phosphorus Chemistry.*; M. Regitz and O. J. Scherer, Ed.; Georg Thieme Verlag: New York, 1990; pp 258.
- (49) Karaghiosoff, K.; Schmidpeter, A. *phosphorus and Sulfur* **1988**, *36*, 217.
- (50) Lubert, J.; Schmidpeter, A. *Angew. Chem. Int. Ed. Eng.* **1976**, *15*, 111.
- (51) Weinmaier, J. H.; Lubert, J.; Schmidpeter, A.; Pohl, S. *Angew. Chem. Int. Ed. Eng.* **1979**, *18*, 412.
- (52) Baccolini, G.; Orsolan, G.; Mezzina, E. *Tetrahedron Lett.* **1995**, *36*, 447.
- (53) Lubert, J.; Schmidpeter, A. *J. Chem. Soc., Chem. Commun.* **1976**, 887.
- (54) Weinmaier, J. H.; Brunnhuber, G.; Schmidpeter, A. *Chem. Ber.* **1980**, *113*, 2278.
- (55) Rösch, W.; Regitz, M. *Synthesis* **1984**, 591.

- (56) Kersch, S.; Wrackmeyer, B.; Willhalm, A.; Schmidpeter, A. *J. Organomet. Chem.* **1987**, *319*, 49.
- (57) Romanenko, W. D.; Rudzevich, V. L.; Gudima, A. O.; Sanchez, M.; Rozhenko, A. B.; Chernega, A., N.; Mazières, M. R. *Bull. Soc. Chim. Fr.* **1993**, *130*, 726.
- (58) Kraaijkamp, J. G.; Grove, D. M.; van Koten, G.; Schmidpeter, A. *Inorg. Chem.* **1988**, *27*, 2612.
- (59) Dash, K. C.; Schmidbaur, H.; Schmidpeter, A. *Inorg. Chim. Acta* **1980**, *41*, 167.
- (60) Weber, L.; Kaminski, O.; Stammer, H.-G.; Neumann, B. *Organometallics* **1995**, *14*, 581.
- (61) Westermann, H.; Nieger, M.; Niecke, E.; Majoral, J.-P.; Caminade, A.-M.; Mathieu, R. *Organometallics* **1989**, *8*, 244.
- (62) Galindo del Pozo, A.; Caminade, A.-M.; Dahan, F.; Majoral, J.-P.; Mathieu, R. *J. Chem. Soc., Chem. Commun.* **1988**, 574.
- (63) Yoshifuji, K.; Shima, L.; Inamoto, N. *J. Am. Chem. Soc.* **1981**, *103*, 4587.
- (64) Mathieu, R.; Caminade, A.-M.; Majoral, J.-P.; Attali, S.; Sanchez, M. *Organometallics* **1986**, *5*, 1914.
- (65) Flynn, K. M.; Hope, H.; Murray, B. D.; Olmstead, M. M.; Power, P. P. *J. Am. Chem. Soc.* **1983**, *105*, 7750.
- (66) Katti, K. V.; Cavell, R. G. *Inorg. Chem.* **1989**, *28*, 3033.
- (67) Katti, K. V.; Cavell, R. G. *Organometallics* **1989**, *8*, 2147.

CHAPTER 2

SYNTHESES OF 4-(PHOSPHINO)-2,5-DIMETHYL-2*H*-1,2,3 σ^2 -DIAZAPHOSPHOLE DERIVATIVES

2.1 Introduction

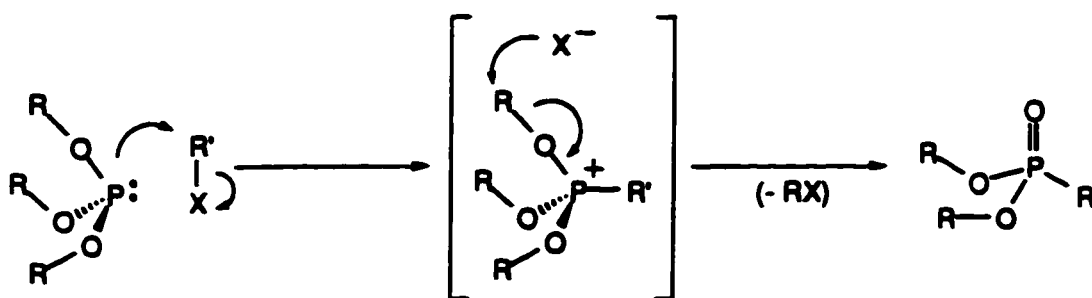
The basis for this study, 4-(dichlorophosphino)-2,5-dimethyl-2*H*-1,2,3 σ^2 -diazaphosphole (**1**), contains two trivalent phosphorus centres which are different in their chemical nature. The endocyclic phosphorus atom is two-coordinate (σ^2) while the exo-phosphorus atom is three-coordinate (σ^3). This difference in coordination number (and hence electronic character) provides the possibility that one of the phosphorus centres may be more reactive towards oxidizing reagents such as chalcogens (e.g. sulfur) or azides and may preferentially coordinate to metal centres.

The precursor (**1**) is easily synthesized. The chlorine substituents on the exo-phosphorus (σ^3 phosphorus) centre in **1** can be easily transformed to other systems by simple replacement reactions yielding the fluoro, amino, and alkoxo derivatives. Each substituent imparts its own character to the molecule and alters the nucleophilicity of the more basic phosphorus centre. With the introduction of the more electronegative fluorine on the exo-phosphorus, for example in **2**, this phosphorus centre becomes less basic. The fluorines also provide additional information about the phosphorus centre through the NMR active nucleus ^{19}F ($I = 1/2$, 100% natural abundance) which yields phosphorus-fluorine coupling interactions.

When the chlorine atoms of **1** are replaced by amino groups, two properties of the exo-phosphorus will change. The substitution increases the basicity of the $\sigma^3\text{P}$ centre, relative to the halide derivatives **1** and **2**. Less obvious but also important is the fact that the congestion about the exo-phosphorus will also be modified. The

steric bulk about the $\sigma^3\text{P}$ can be further controlled by using either branched or unbranched secondary amines in addition to varying the chain length of the alkyl group on the amine. With a wealth of secondary amines available, it becomes possible to tailor aminophosphines with highly specific characteristics.

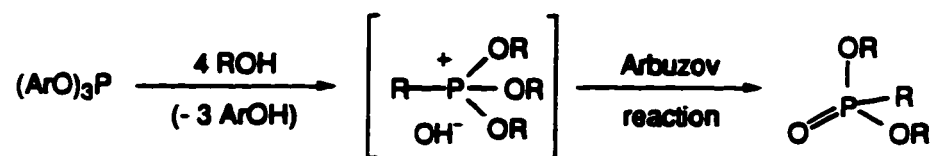
Similar to the aminophosphines, one can easily vary the substituents and the properties of phosphonites, $\text{RP}(\text{OR}')_2$, which can be obtained from the starting dichlorophosphino-diazaphosphole **1**. A drawback to this system however is that phosphites or phosphonites suffer the Arbuzov rearrangement (Scheme 2.1) which converts a P(III) centre into a pentavalent $\text{P}=\text{O}$ centre.¹



Scheme 2.1 The Arbuzov reaction of a phosphite with an alkyl halide.

The Arbuzov reaction is presumed to proceed through the attack of the electron lone pair of the phosphite on the alkyl group of the alkyl halide. The ionic intermediate, as illustrated in Scheme 2.1, is formed wherein the alkyl group is attached to the phosphorus. The next step involves the attack of the halide on the alkyl group of the alkoxy substituent, elimination of alkyl halide and the formation of the phosphorus-oxygen double bond. The reaction may appear catalytic if $\text{R} = \text{R}'$ or a stoichiometric transformation if $\text{R} \neq \text{R}'$. The overall important consequence of this reaction is the oxidation of the phosphorus from the trivalent to the pentavalent state. Conversion of the $\text{P}-\text{O}-\text{C}$ linkage into the $\text{P}(=\text{O})-\text{C}$ structure involves a net gain of between 32 to 64 kcal mole^{-1} in bond stabilization and provides the driving force for the rearrangement.²

Aryloxy groups, or other electron-withdrawing alcohols, retard the Arbuzov reaction by inhibiting the initial nucleophilic attack of the electron lone pair of the phosphorus on the alkyl halide by making the phosphorus less basic. When there are aryloxy groups on the phosphorus, the rearrangement does not take place as such, but in the presence of alkyl alcohols, an exchange occurs at elevated temperatures followed by the Arbuzov reaction as shown in Scheme 2.2.^{3,4}



Scheme 2.2 Alcohol exchange with triaryl phosphites.

The alkoxy compounds, in general, have physical properties which are intermediate between those of the halide and of the amino analogues.

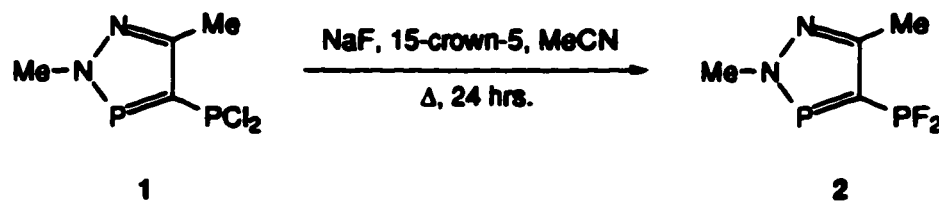
2.2 Modification of the Synthesis of 4-(dichlorophosphino)-2,5-dimethyl-2*H*-1,2,3σ²-diazaphosphole (1)

As mentioned above, the fluoride, the amino, and the alkoxy derivatives are synthesized from 4-(dichlorophosphino)-2,5-dimethyl-2*H*-1,2,3σ²-diazaphosphole (1). The synthesis of 1 can be achieved by two methods as shown in Scheme 1.11. The preparation of 1 from acetone methylhydrazone and phosphorus trichloride was only briefly described in the literature.⁵ The product is initially a hydrochloride salt which can be purified by sublimation. Though not mentioned in this paper, the diazaphosphole hydrochloride readily sublimed out of the reaction vessel into the condenser during the distillation of 1, resulting in the contamination of the phosphinodiazaphosphole with the hydrochloride salt. To minimize the contamination, a larger excess of phosphorus trichloride and longer reflux times were used. In addition, the intermediate hydrochloride compound was crystallized out of

the reaction mixture before the distillation step. These modifications substantially improved the yield.

2.3 Synthesis of 4-(difluorophosphino)-2,5-dimethyl-2*H*-1,2,3σ²-diazaphosphole (2)

Conversion of a chlorophosphine to a fluorophosphine can be achieved by the reaction of sodium fluoride,⁶ antimony trifluoride,⁷ or zinc fluoride⁸ with the chlorophosphine. With antimony trifluoride, there is also the possibility of oxidizing the phosphorus centre to a tetrafluorophosphorane⁹ hence this reagent is not often used unless the phosphorane is the desired product. The synthesis of 4-(difluorophosphino)-2,5-dimethyl-2*H*-1,2,3σ²-diazaphosphole (2) was achieved by halide exchange between sodium fluoride and 1 in acetonitrile in the presence of a small amount of 15-crown-5 at elevated temperatures for a period of 24 hours (Scheme 2.3). The yields for 2 ranged for 81% to 88%.



Scheme 2.3 Synthesis of 4-(difluorophosphino)-2,5-dimethyl-2*H*-1,2,3σ²-diazaphosphole (2).

The fluorinated phosphole, 2, is a volatile, colourless liquid which has a boiling point of 172°C under argon. Compound 2 was stored at -40°C under argon. Over a period of time, the phosphole slowly becomes yellow and must be repurified a by trap-to-trap vacuum distillation, which is done with the receiving flask cooled to -25°C.

2.3.1 Infrared Data for 4-(Difluorophosphino)-2,5-dimethyl-2*H*-1,2,3σ²-diazaphosphole (2)

The absorption region in the infrared that is characteristic for the phosphorus-fluorine stretching occurs between 990 to 710 cm⁻¹. For compound 2, the stretching frequencies are assigned to the bands at 805 cm⁻¹ and 780 cm⁻¹. As a comparison we find the P-F stretching frequencies in PF₃ at 890 cm⁻¹ and 864 cm⁻¹, while for PhPF₂, these frequencies are found at 974 cm⁻¹ and 865 cm⁻¹.¹⁰

2.3.2 Multinuclear Magnetic Resonance Data for 4-(Difluorophosphino)-2,5-dimethyl-2*H*-1,2,3σ²-diazaphosphole (2)

The ³¹P{¹H} NMR spectrum of compound 2 showed two sets of resonances as expected (Figure 2.1). The endocyclic diazaphosphole phosphorus, which is two coordinate (σ²), showed a broadened resonance downfield (255.0 ppm) while the resonance for the three coordinate (σ³) exocyclic phosphorus was sharp and occurred upfield (208.8 ppm). Interestingly, the chemical shift of the σ³P unit of compound 2 is similar to that of PPhF₂ (208.3 ppm). The chemical resonances of both of these compounds lie downfield from phosphorus trifluoride (98 ppm) by a large shift. In most cases, it is possible to make good estimates of the chemical shift of phosphorus compounds by the summation of increments that are characteristic for each ligand. There are a few exceptions to this rule, one of them being phosphorus centres carrying fluorine atoms.¹¹ This inconsistency is apparently due to enhanced bonding interactions which occur between phosphorus and fluorine atoms.

The phosphorus atoms in compound 2 are coupled to each other (²J_{PP} 107 Hz) and to both fluorine atoms on the σ³P. This results in a NMR splitting pattern of a doublet of triplets for each phosphorus signal (Figure 2.1). For the σ²P centre, the coupling to the fluorines was not well resolved as the signal was broadened by quadrupolar relaxation from the adjacent nitrogen centre in the phosphole ring. There

was an increase in the two-bond phosphorus-phosphorus coupling, relative to that of **1** ($^2J_{PP}$ 78 Hz), which may be due to an increase of the s character in the σ^3P bonding in contrast to σ^2P bonding induced by the greater electronegativity of fluorine, compared to that of chlorine.

The ^{19}F NMR spectrum was centred at -89.3 ppm and showed splitting by both phosphorus centres (Figure 2.2) to give a pattern of a doublet of doublets. Unlike the $^{31}P\{^1H\}$ NMR spectrum, the peaks were sharp and coupling of the fluorine to the σ^2P unit was clearly resolved ($^3J_{PF}$ 31 Hz). The $^1J_{PF}$ coupling was 1169 Hz, which is within the typical range observed for one-bond phosphorus-fluorine coupling.¹²

The 1H NMR spectrum of **2** showed a resonance for the methyl group of the nitrogen at the 2-position of the ring at δ 4.00, coupled only to the σ^2P centre ($^3J_{\sigma^2PH}$ 8.2 Hz). In comparison, the protons of the imino group of **1** were coupled to both phosphorus centres ($^3J_{\sigma^2PH}$ 8.0 Hz, $^5J_{\sigma^3PH}$ 0.9 Hz). The magnitudes of the three-bond phosphorus-proton coupling for both compounds were similar, as one might expect since the halide exchange does not affect the ring system directly. The resonance for the methyl group at the 5 position in the ring (2.50 ppm) of **2** did not show coupling to either of the phosphorus centres as was observed in the case of **1** ($^4J_{\sigma^2PH}$ 2.1 Hz, $^4J_{\sigma^3PH}$ 1.4 Hz).

The $^{13}C\{^1H\}$ NMR spectrum of **2** showed a signal for the resonance for the carbon of the methyl group at the 5-position (14.8 ppm) was coupled only to the σ^2P centre ($^3J_{\sigma^2PC}$ 7 Hz). The carbon of the methyl group on the nitrogen at the 2-position, (41.5 ppm) was also coupled only to the σ^2P centre ($^2J_{\sigma^2PC}$ 7 Hz). The carbon adjacent to both phosphorus centres (157.2 ppm) showed a larger coupling to the σ^2P centre ($^3J_{\sigma^2PC}$ 35 Hz) than the σ^3P centre ($^3J_{\sigma^3PC}$ 6 Hz). The carbon at the 5-position (135.2 ppm) was also coupled to both phosphorus centres ($^2J_{\sigma^2PC}$ 5 Hz, $^2J_{\sigma^3PC}$ 19 Hz), but in this case the coupling to the σ^2P centre was smaller than to the

${}^2J_{\sigma^3PC}$. The reason for this is that this spacing is the sum of both the ${}^2J_{\sigma^2PC}$ and the ${}^3J_{\sigma^2PC}$ coupling constants and the two coupling constants are of opposite signs.

The marked difference in the linewidths of the σ^2P and σ^3P units in **2** led us to consider the spin relaxation times (T_1) of the phosphorus nuclei because this factor can influence the observed linewidths. Although most values lie between 2 and 20 seconds,¹³ some cases can deviate substantially. To evaluate the different characteristics in **2**, T_1 NMR relaxation measurement for the phosphorus centres was carried out. The result (Figure 2.3) gave the respective relaxation times of 3.49 seconds for the σ^3P and 8.64 seconds for the σ^2P . The σ^3P relaxation time lies within the range of T_1 normally observed for PX_3 ($X = \text{halogen}$) environments, where a T_1 ranges from 3 to 6 seconds. For the σ^2P unit, one would expect the T_1 to be similar to a quaternary carbon in a phenyl ring. For example, the T_1 values for the aromatic carbons in ethylbenzene are ~18-23 s while the *ipso* carbon has a T_1 of ~72 s. The methyl group has a T_1 of ~7 s.¹⁴ Comparative literature values for T_1 for two-coordinate phosphorus atoms could not be found. The relatively short T_1 of the σ^2P unit in **2** can be attributed to quadrupolar relaxation arising from the adjacent nitrogen centre and this quadrupolar relaxation will also contribute to the broadening of the signal for the σ^2P unit.

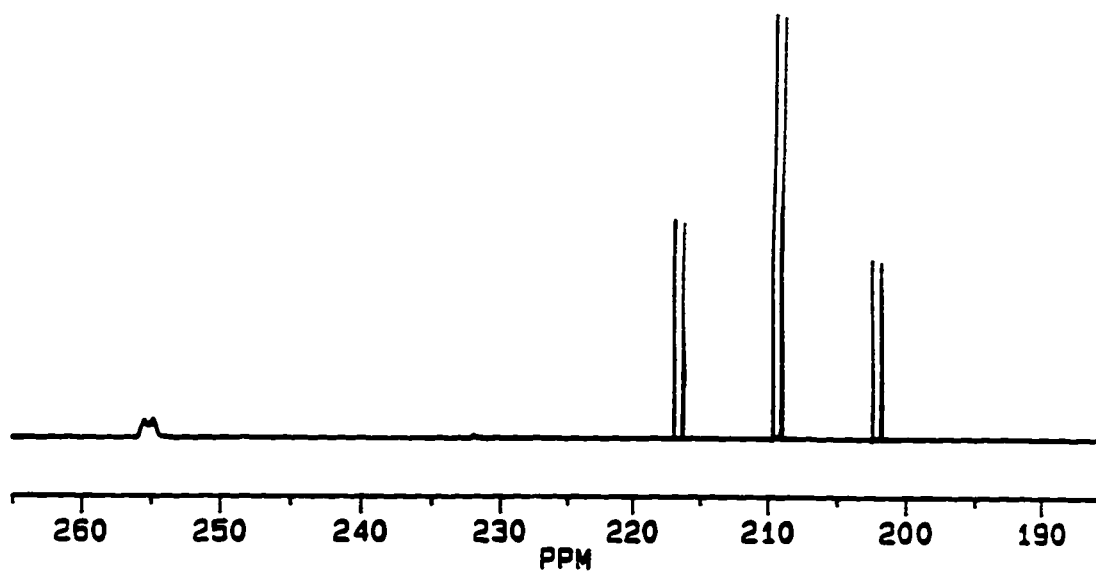


Figure 2.1 $^{31}\text{P}\{^1\text{H}\}$ NMR spectrum of 4-(difluorophosphino)-2,5-dimethyl-2H-1,2,3 σ^2 -diazaphosphole (2) in CDCl_3 .

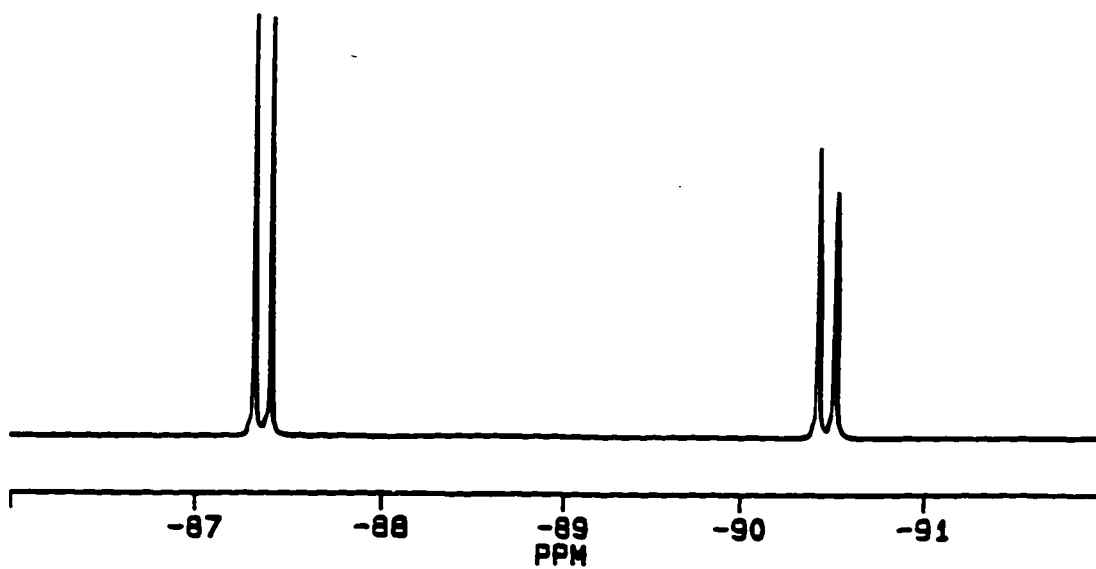


Figure 2.2 ^{19}F NMR spectrum of 4-(difluorophosphino)-2,5-dimethyl-2H-1,2,3 σ^2 -diazaphosphole (2) in CDCl_3 .

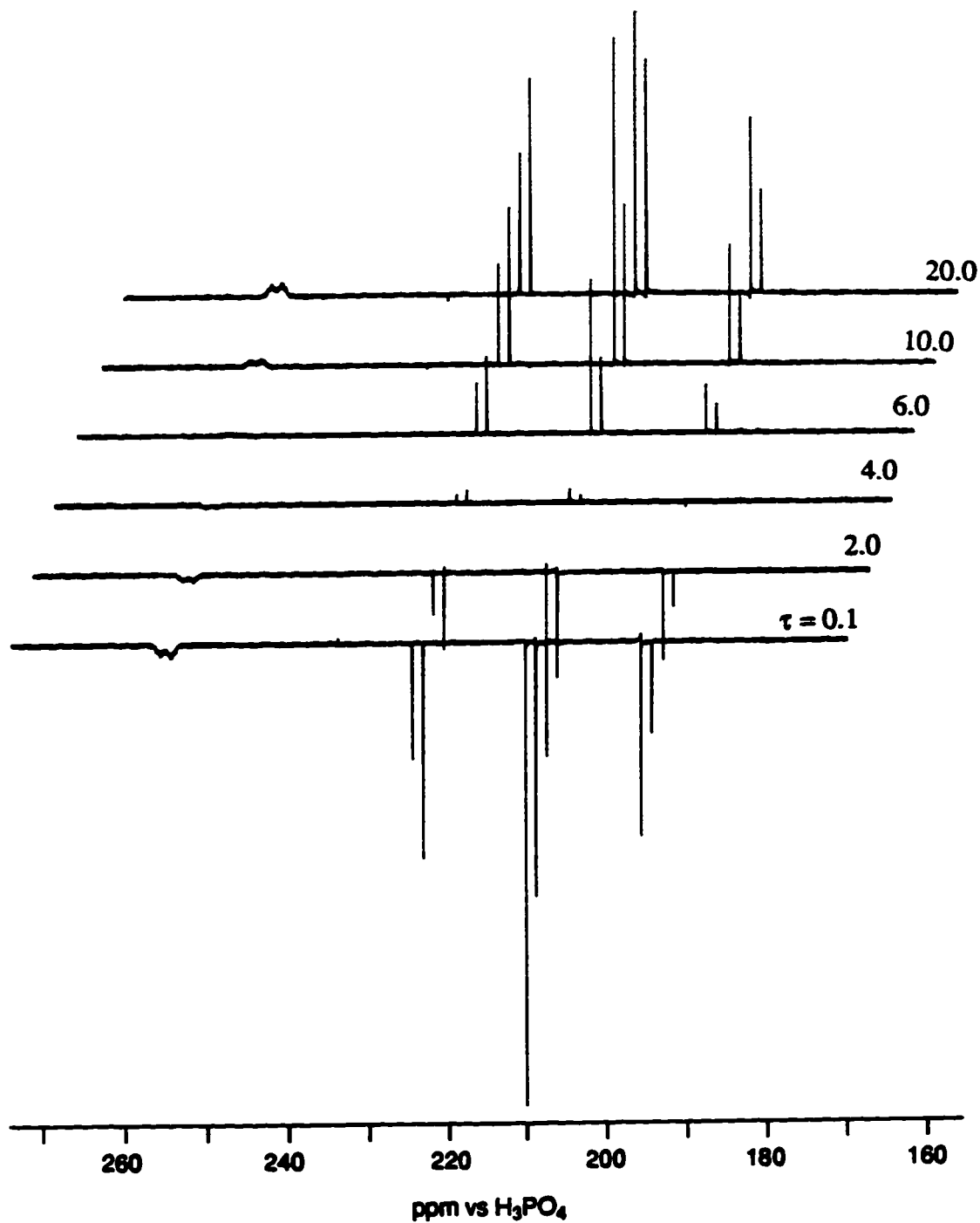


Figure 2.3 A stacked plot of $^{31}\text{P}\{^1\text{H}\}$ NMR spectra obtained at different delay intervals ($\tau = 0.1, 0.2, 0.4, 0.6, 10.0, 20.0$ sec.) to determine the T_1 values for 4-(difluorophosphino)-2,5-dimethyl-2*H*-1,2,3- σ^2 -diazaphosphole (2) in CDCl_3 .

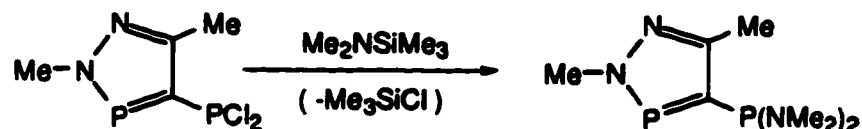
2.3.3 Attempted Quaternization of 2.

A major contribution to the reactivity of the trivalent phosphorus centre can be described in terms of the nucleophilicity of the centre.¹⁵ Introduction of electronegative fluorine atoms on the $\sigma^3\text{P}$ makes the phosphorus centre less basic and therefore less reactive in those processes dependent on inherent nucleophilicity. The reaction of iodomethane with 2 in an attempt to quaternize either phosphorus centres did not result in the formation of a phosphonium salt. Similar results were observed in cases which have CF_3 substituents on the phosphorus atom.¹⁶ Thus this fluorinated phosphorus centre is not markedly nucleophilic.

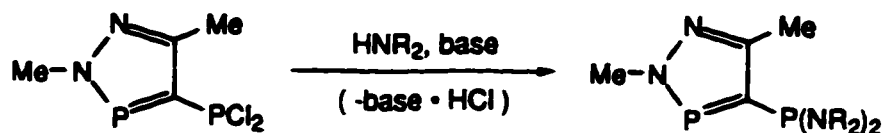
2.4 Synthesis of 4-(Diaminophosphino)- and 4-(Aminochlorophosphino)-2,5-dimethyl-2H-1,2,3 σ^2 -diazaphospholes

The introduction of amino groups on the exo-phosphorus centre should make it more basic than is the case for the exo-phosphorus centre in 1 or 2. Furthermore, the basicity of this phosphorus centre can be enhanced by the inductive effect of alkyl substituents on the nitrogen. In addition, these amino substituted derivatives, in comparison to 1 and 2, offer the possibility of introducing a variety of bulky amino groups which may influence the course of the reactions by protecting and stabilizing metal centres against nucleophilic attack through the control of steric shielding about the $\sigma^3\text{P}$ centre.

The 4-(diaminophosphino)-2,5-dimethyl-2H-1,2,3 σ^2 -diazaphospholes were synthesized by simple replacement reactions with either silylated amines (Scheme 2.4) or secondary amines in the presence of a base (Scheme 2.5).



Scheme 2.4 Reaction of 1 with aminosilanes.



Scheme 2.5 Reaction of **1** with secondary amines in the presence of a base.

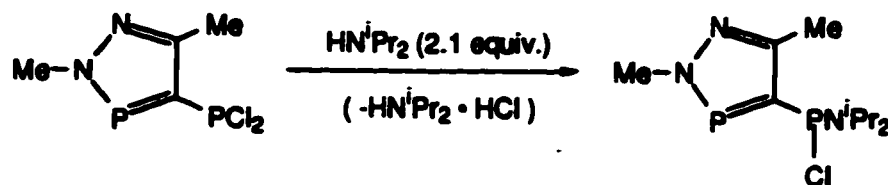
To synthesize the dimethylamino derivative (**3**), *N,N*-dimethylamino-trimethylsilane (b.p. 86°C) was used due to the relative ease of handling of this reagent in contrast to the more volatile dimethylamine (b.p. 7°C). The addition of the *N,N*-dimethylaminotrimethylsilane to **1** in dichloromethane was performed at 0°C after which the solution was allowed to warm to room temperature and stirred for a period of 12 hours. The excess dimethylaminotrimethylsilane and chlorotrimethylsilane by-product were then removed *in vacuo*. Compound **3** was distilled at 93-96°C at 0.6 torr. The yields for **3** ranged from 82% to 87%.

Compound **2** was also treated with *N,N*-dimethylaminotrimethylsilane in an attempt to provide an alternative route to the same aminophosphinodiazaphosphole. Interestingly enough, no reaction took place even though formation of the reaction products of aminophosphinodiazaphosphole and trimethylfluorosilane from the fluorophosphine and the aminotrimethylsilane should be favoured by at least 20 kJ mol⁻¹. The reasons for the lack of reaction are not clear as many examples are known in which the reaction proceeds as expected.¹⁷⁻¹⁹ Other cases are also known where the fluorophosphorane does not react with aminosilanes.¹⁹

The other amino derivatives such as diethylamino (**4**), dipropylamine (**5**), diisopropylamine (**6**), dibenzylamine (**7**), and iminodibenzyl (**8**), were prepared by the second synthetic route (Scheme 2.5). In some cases the base was an excess of the amine itself (e.g. diethylamine) especially when the amine was sufficiently volatile, otherwise triethylamine or 1,8-diazabicyclo[5.4.0]undec-7-ene (DBU) was employed. Complexation and removal of the hydrogen chloride produced by the reaction of the

amine with the chlorophosphine enhances the reaction and retards nucleophilic attack by the acid at the two-coordinate phosphorus centre. This secondary reaction transforms the $\sigma^2\text{P}$ centre to a $\sigma^3\text{P}$ centre and was observed in the case of the reaction of trichlorophosphine sulfide with the diazaphosphole.⁸ The resulting amine salt was insoluble in the diethyl ether solvent and was easily removed by filtration. These reactions were performed at 0°C with the addition of **1** to the solution containing the amine and then the solution was allowed to warm to room temperature and maintained with thorough stirring at this temperature for a period of 12 hours in order to ensure complete reaction. These diamminophosphinodiazaphosphole derivatives are liquids which were obtained in good yields (72% to 83%). They varied in colour from light yellow, in the case of the dimethyl derivative (**3**), to orange yellow for the dipropyl analogue (**5**).

When the reaction was carried out between diisopropylamine and **1**, only one of the chloride atoms was substituted giving the asymmetric aminochlorophosphinodiazaphosphole **6** (Scheme 2.6). The monosubstitution of **1** is the result of the increased bulk of the isopropyl groups on the nitrogen and opens the possibility that perhaps alternate substitution at the exocyclic phosphorus centre could be explored.



Scheme 2.6 The reaction of 4-(dichlorophosphino)2,5-dimethyl-2H-1,2,3 σ^2 -diazaphosphole (**1**) with diisopropylamine.

Several other bulky secondary amines, such as dibenzylamine and iminodibenzyl, gave the same result yielding **7** and **8**. This result suggests that there

may be some steric interaction between the amino group and the diazaphosphole ring. The reaction between dichlorophosphinophosphole (1) and the more bulky and less basic iminodibenzyl required a stronger base such as DBU to effect the transformation. This reaction, producing 8, resulted in a much lower yield (36%) than that which was achieved for either 6 (82%) or 7 (78%). The 4-(diisopropylaminochlorophosphino)diazaphosphole 6 was volatile enough to be purified by sublimation. The other aminochlorophosphino derivatives were precipitated with hexanes from a dichloromethane solution. These asymmetric 4-(aminochloro-phosphino)diazaphospholes were white to off-white solids which were very sensitive towards moisture.

In an attempt to mimic *tris*-pyrazolylborate chemistry and to evaluate the relative behaviour of the phosphole and the pyrazole nitrogen when the latter is present in an independent ring, the pyrazole- (9) and 3,5-dimethylpyrazole-phosphinodiazaphospholes (10) were synthesized. It was thought that the formation of tripodal $\sigma^3\text{P}$ might encourage the coordination of the two-coordinate diazaphosphole phosphorus once the initial chelation of the nitrogen of the pyrazole ring to the metal centre had occurred. (Figure 2.4) The second route (i.e., Scheme 2.5) was used to synthesize these particular pyrazolephosphinodiazaphospholes, and triethylamine was the choice of base. Substitution of both chlorines of 1 occurred with both pyrazole derivatives. Both pyrazole derivatives were white solids that were extremely moisture sensitive, with the 3,5-dimethylpyrazole being slightly less reactive towards moisture, as one might expect, due to the greater protective bulk provided by the methyl groups.

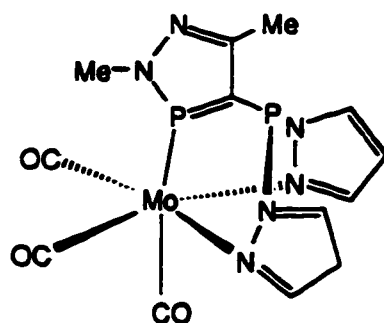


Figure 2.4 Possible coordination of the pyrazole rings and cyclic phosphorus centre with **9**.

2.4.1 Infrared Data for 4-(Diaminophosphino)- and 4-(Aminochlorophosphino)-2,5-dimethyl-2*H*-1,2,3σ²-diazaphospholes

The range of the stretching frequencies is 850-650 cm⁻¹ for the phosphorus-nitrogen single bond, while the nitrogen-carbon stretching frequencies occur at 750-680 cm⁻¹.¹⁰ The diaminophosphino derivatives showed P-N stretching frequencies at ~713 and ~680 cm⁻¹. The chloroamino derivatives gave P-N bands at 705 and 662 cm⁻¹ and a N-C band at 710 cm⁻¹. Full infrared data is given in Table 2.4.

2.4.2 Multinuclear Magnetic Resonance Data for 4-(Diaminophosphino)- and 4-(Aminochlorophosphino)-2,5-dimethyl-2*H*-1,2,3σ²-diazaphospholes

As previously stated, the NMR chemical shift of a phosphine can be estimated from a sum of contributions from each of the substituents on the phosphorus centre (except fluorine). This allows the use of ³¹P{¹H} NMR to evaluate the number of amino groups attached to the exo-phosphorus atom on compound **1**. The phosphorus chemical shifts for the disubstituted aminophosphine ranged from 77.9 ppm for **4** to 86.9 ppm for **3**. The phosphorus chemical signals for the σ³P of the monosubstituted aminophosphines were shifted far upfield from **1** as observed with the diaminophosphino analogues. The differences in the change in the chemical shift of the exo-phosphorus unit were only half as large, thus showing that only one chlorine

was substituted. Mass spectrometry and elemental analysis confirmed these results. The aminochlorophosphines ranged from 118.5 ppm for **8** to 127.5 ppm for **7**. For both the pyrazole (**9**) and 3,5-dimethylpyrazole (**10**) analogues, the phosphorus chemical shifts were further shifted to 59.2 ppm and 49.3 ppm, respectively.

Unlike the behaviour of **2** where $^2J_{PP}$ increased relative to **1**, the two-bond phosphorus-phosphorus coupling constants in the diamino derivatives decreased significantly relative to **1**. The disubstituted amino derivatives **3**, **4**, and **5**, showed a decrease in $^2J_{PP}$ with increasing chain length of the alkyl group contained within the amino group (33 Hz, 29 Hz, and 23 Hz, respectively for the methyl, ethyl, and propyl groups). For the corresponding aminochlorophosphines, a similar $^2J_{PP}$ trend was observed between **6** and **7** (29 Hz and 25 Hz, respectively). There was an additional marked decrease in $^2J_{PP}$ (6 Hz) in the case of **8** wherein a rigid iminodibenzyl was introduced to the phosphinodiazaphosphole. Both pyrazole phosphines **9** and **10**, also had similar small values $^2J_{PP}$ (7 Hz and 4 Hz, respectively) in accord with this interpretation.

The $^{13}C\{^1H\}$ NMR spectra for the diamino derivatives **3**, **4**, and **5** showed a chemical shift of ~ 155 ppm for the phosphole carbon at the 5-position and also that this phosphorus is coupled to both the σ^2P and the σ^3P centres (**3**: $^2J_{\sigma^2PC}$ 7 Hz, $^2J_{\sigma^3PC}$ 19 Hz; **4**: $^2J_{\sigma^2PC}$ 7 Hz, $^2J_{\sigma^3PC}$ 21 Hz; **5**: $^2J_{\sigma^2PC}$ 7 Hz, $^2J_{\sigma^3PC}$ 21 Hz). A range of 150 ppm to 152 ppm was observed for the ^{13}C chemical shift of the carbon at the 4-position and again this carbon was coupled to both phosphorus atoms (**3**: $^1J_{\sigma^2PC}$ 55 Hz, $^1J_{\sigma^3PC}$ 6 Hz; **4**: $^1J_{\sigma^2PC}$ 55 Hz, $^1J_{\sigma^3PC}$ 9 Hz; **5**: $^1J_{\sigma^2PC}$ 55 Hz, $^1J_{\sigma^3PC}$ 9 Hz for **5**). In all cases the carbon at the 2-position (~ 40.5 ppm) showed a coupling to the σ^2P centre ($^2J_{\sigma^2PC} \sim 17$ Hz). The methyl group at the 5-position (~ 14.3 ppm) was also coupled to the σ^2P centre ($^2J_{\sigma^2PC} \sim 3$ Hz). In the case of compound **3** however, the carbon signal for the dimethyl amino group (40.7 ppm) was a singlet. For **4**, the methylene carbons of the ethylamino group showed a chemical shift of 42.5 ppm and

also coupling to the $\sigma^3\text{P}$ centre ($^2J_{\sigma^3\text{PC}}$ 17 Hz) while the methyl groups were observed to be singlets (14.5 ppm). Similar chemical shifts and coupling constants were observed for **5** (Table 2.3).

The ^1H NMR spectrum also showed significant couplings to the phosphorus centres. The protons for the 2-methyl groups (~3.85 ppm) were coupled to the $\sigma^2\text{P}$ centre (~7 Hz). The protons of the 5-methyl group (~2.20 ppm) appeared as singlets. The dimethylamino group protons (2.55 ppm) of compound **3** were coupled to the $\sigma^3\text{P}$ centre ($^3J_{\sigma^3\text{PH}}$ 9.5 Hz). The splitting pattern for the methylene protons in the diethylamino derivative (**4**), was a doublet of quartets, showing coupling to both the $\sigma^3\text{P}$ and to the methyl protons (3.02 ppm, $^3J_{\sigma^3\text{PH}}$ 9.8 Hz, $^3J_{\text{HH}}$ 7.0 Hz). The methyl protons (1.00 ppm) appeared as triplets, showing coupling only to the methylene protons ($^3J_{\text{HH}}$ 7.0 Hz). The *N*-methylene proton signal for the dipropylamino derivative (**5**) was a doublet of triplets (3.02 ppm, $^3J_{\sigma^3\text{PH}}$ 9.6 Hz, $^3J_{\text{HH}}$ 7.0 Hz) while the signals for the remaining protons for the propyl group (1.10 ppm) appeared as complex multiplets.

As mentioned above, diisopropylamine replaced only one chloride substituent on the *exo*-phosphorus atom, thus making $\sigma^3\text{P}$ unit a stereogenic centre. The bulky diisopropylamino group next to the dimethyldiazaphosphole ring makes the methyl groups in the isopropyl group inequivalent and anisochronous in the NMR spectrum. Several related phosphorus compounds similarly show diastereotopic diisopropylamino groups.²⁰ In this case, only the methine protons showed coupling to the phosphorus centre ($\sigma^3\text{P}$). The broadened $^{13}\text{C}\{^1\text{H}\}$ and ^1H NMR signals for compound **6** indicated that the isopropyl groups were fluxional at room temperature (Figures 2.5 and 2.6).

The $^{13}\text{C}\{^1\text{H}\}$ NMR spectrum for **6** showed sharp signals for the phosphole ring carbons (C-4: 150.3 ppm, $^1J_{\sigma^2\text{PC}}$ 54 Hz, $^1J_{\sigma^3\text{PC}}$ 34 Hz; C-5: 154.2 ppm, $^1J_{\sigma^2\text{PC}}$ 6 Hz, $^1J_{\sigma^3\text{PC}}$ 24 Hz) as well as the 2-methyl group (41.0 ppm, $^2J_{\sigma^2\text{PC}}$ 18 Hz) and the 5-

methyl group (14.7 ppm, $^3J_{\sigma^3PC}$ 5 Hz) at room temperature. The isopropyl groups showed broad pattern of peaks at room temperature and also three ^{13}C NMR peaks were observed indicating that these methyl groups were chemically inequivalent. The broadened peaks for the methylene groups were centred at 49.4 ppm and 46.1 ppm and the methyl group signals were centred at 25.6 ppm, 23.8 ppm, and 21.7 ppm. Cooling the sample to 0°C resulted in a sharpening of the peaks arising from the isopropyl groups and at this temperature two different methylene carbon signals were observed at 49.1 ppm ($^2J_{\sigma^3PC}$ 12 Hz) and 45.4 ppm ($^2J_{\sigma^3PC}$ 26 Hz). The resonances for two methyl carbon atoms for one of the isopropyl groups were similar with only one of the carbon signals coupled to the σ^3P centre (21.4 ppm, $^4J_{\sigma^3PC}$ 3 Hz; 21.1 ppm) while the methyl carbon atoms from the second isopropyl group both showed coupling to the σ^3P centre (27.6 ppm, $^4J_{\sigma^3PC}$ 5 Hz; 24 ppm, $^4J_{\sigma^3PC}$ 24 Hz).

The room temperature 1H NMR spectrum of **6** had also showed fluxional behaviour within the isopropyl group signal set whereas the methyl groups on the phosphole ring gave sharp resonances. The methyl protons at the 2-position gave a signal at 3.91 ppm ($^3J_{\sigma^2PH}$ 7.5 Hz) and the signal for the methyl protons at the 5-position occurred at 2.51 ppm. Coupling to either of the phosphorus centres was not observed for the proton signal at 2.51 ppm. The methylene protons of the isopropyl groups showed signals centred at \sim 3.7 ppm and the signals for methyl groups were centred at \sim 1.3 ppm and \sim 0.9 ppm. At 0°C, the resonances for the methylene protons remained broad but two distinct protons, for which signals were observed (3.79 ppm and 3.44 ppm). The methyl groups of the isopropyl group showed four distinct proton resonances (1.38 ppm, 1.29 ppm, 1.09 ppm, and 0.80 ppm) at this temperature.

At -20°C, the peaks in the isopropyl region of the 1H NMR spectrum had sharpened further. Two distinct methylene proton resonances were now observed centred at 3.76 ppm (doublet of septets, $^3J_{\sigma^3PH}$ 9.9 Hz, $^3J_{HH}$ 6.7 Hz) and at 3.42 ppm

(doublet of septets, $^3J_{\text{C}3\text{P}H}$ 17.7 Hz. doublet $^3J_{\text{HH}}$ 6.7 Hz). Four resonances for the methyl group signals were observed at 1.36 ppm (doublet, $^3J_{\text{HH}}$ 6.7 Hz), 1.28 ppm (doublet, $^3J_{\text{HH}}$ 6.7 Hz), 1.07 ppm (doublet, $^3J_{\text{HH}}$ 6.7 Hz), and 0.78 ppm (doublet, $^3J_{\text{HH}}$ 6.7 Hz). Decoupling experiments showed that the methine protons at 3.76 ppm were coupled to the methyl protons at 1.36 ppm and at 1.26 ppm whereas the methine protons at 3.42 ppm were coupled to the other two methyl protons at 1.07 ppm and at 0.78 ppm, thus a full assignment could be made.

A two-dimensional C,H-correlation (HETCOR) NMR spectrum of compound **6** (Figure 2.7) showed that the two equivalent carbons at 21.2 ppm correlated to the methyl protons at 1.07 ppm and 0.78 ppm. The methyl protons at 1.36 ppm correlated to the carbon at 24.2 ppm while the methyl protons at 1.28 ppm to the carbon at 25.7 ppm. The methine proton at 3.75 ppm correlated to the carbons at 49.2 ppm and the methine proton at 3.41 ppm to the carbon at 45.2 ppm. The protons on the carbons resonating at the higher fields may be influenced by ring currents of the aromatic five-membered ring system which may account for the shift in these signals.

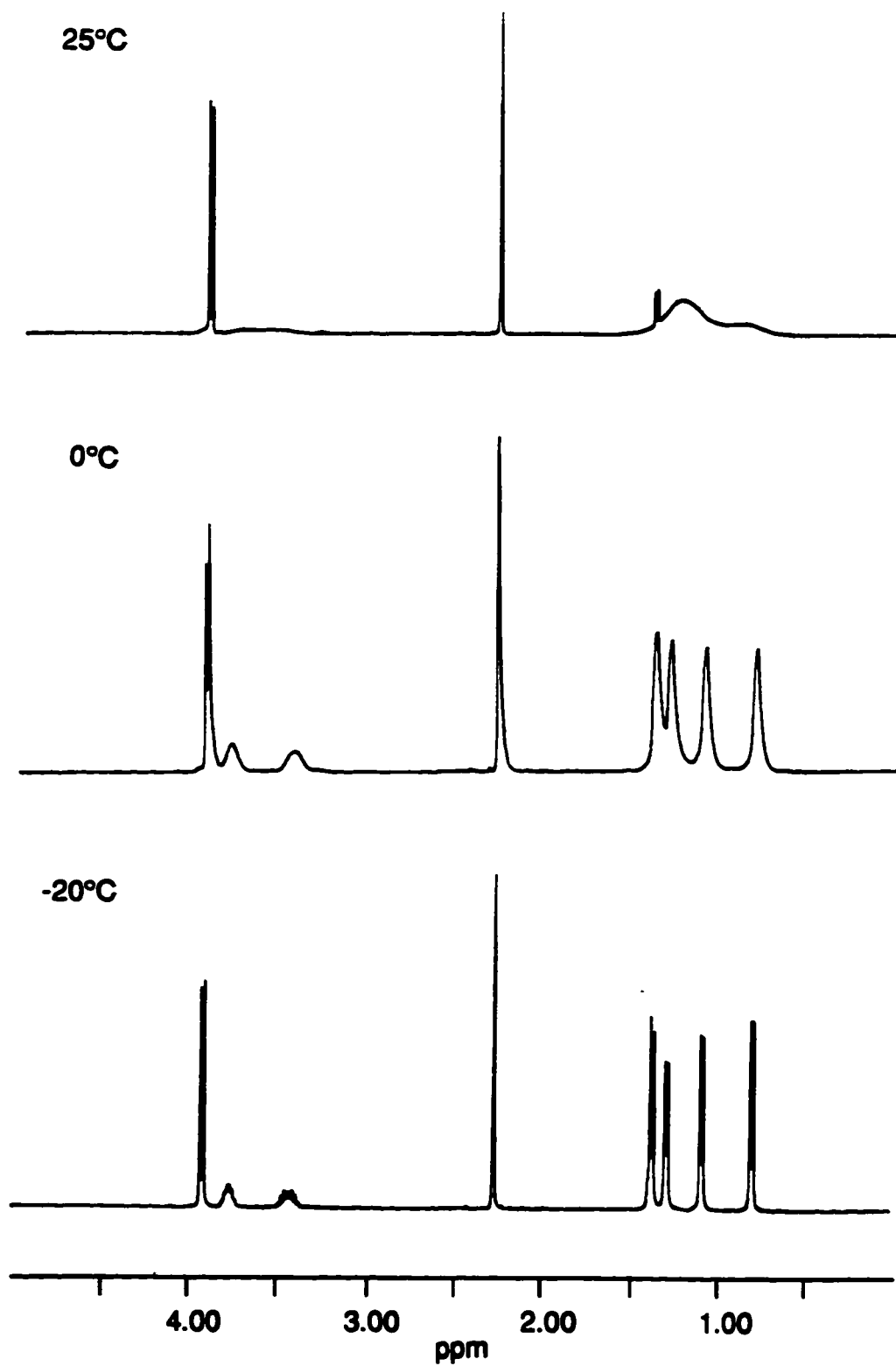


Figure 2.5 ^1H NMR spectra of compound 6 at temperatures between -20°C and 25°C in CDCl_3 .

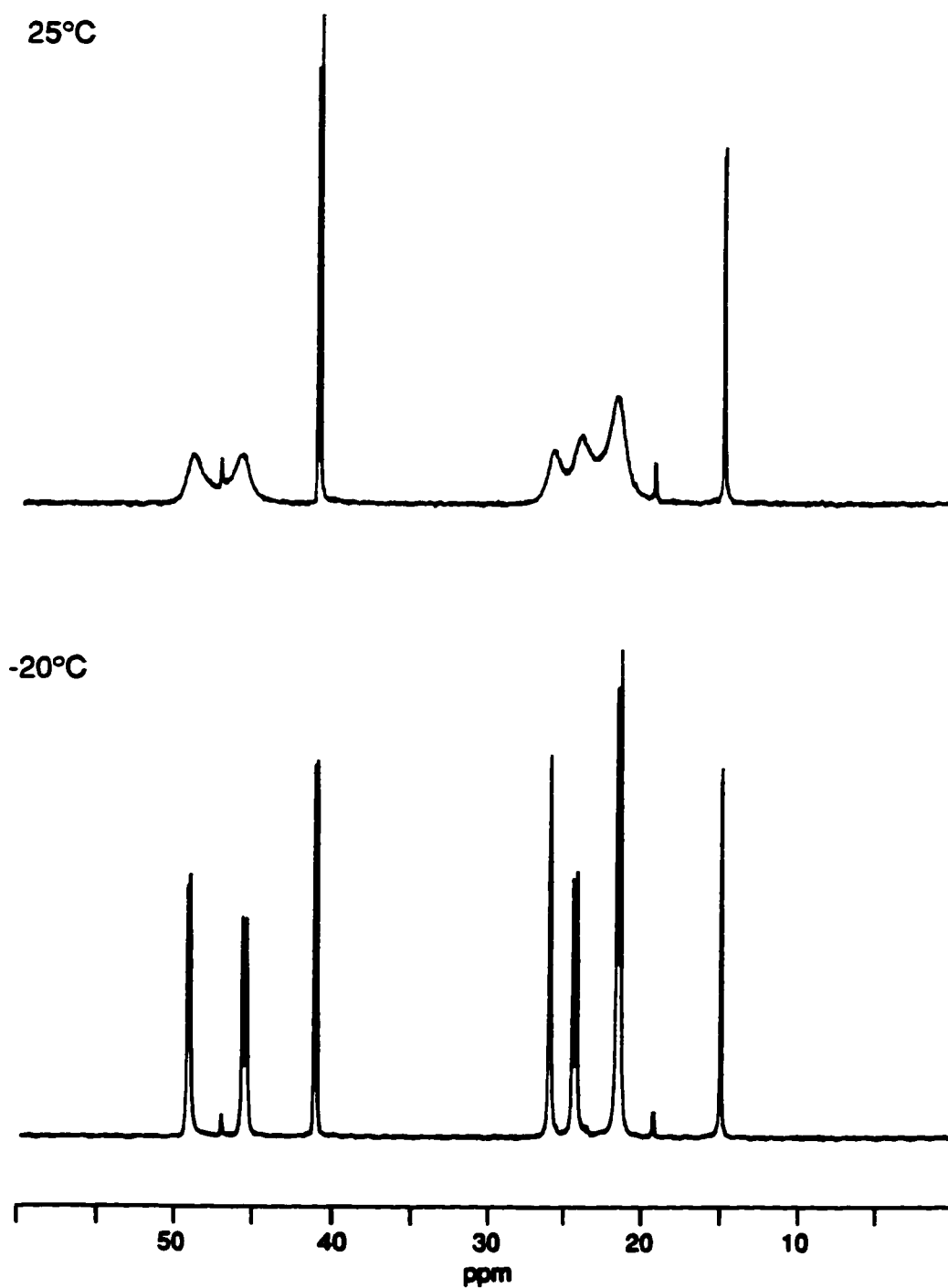


Figure 2.6 Methyl region ^{13}C (^1H) NMR spectra of compound 6 at temperatures between -20°C and 25°C in CDCl_3 .

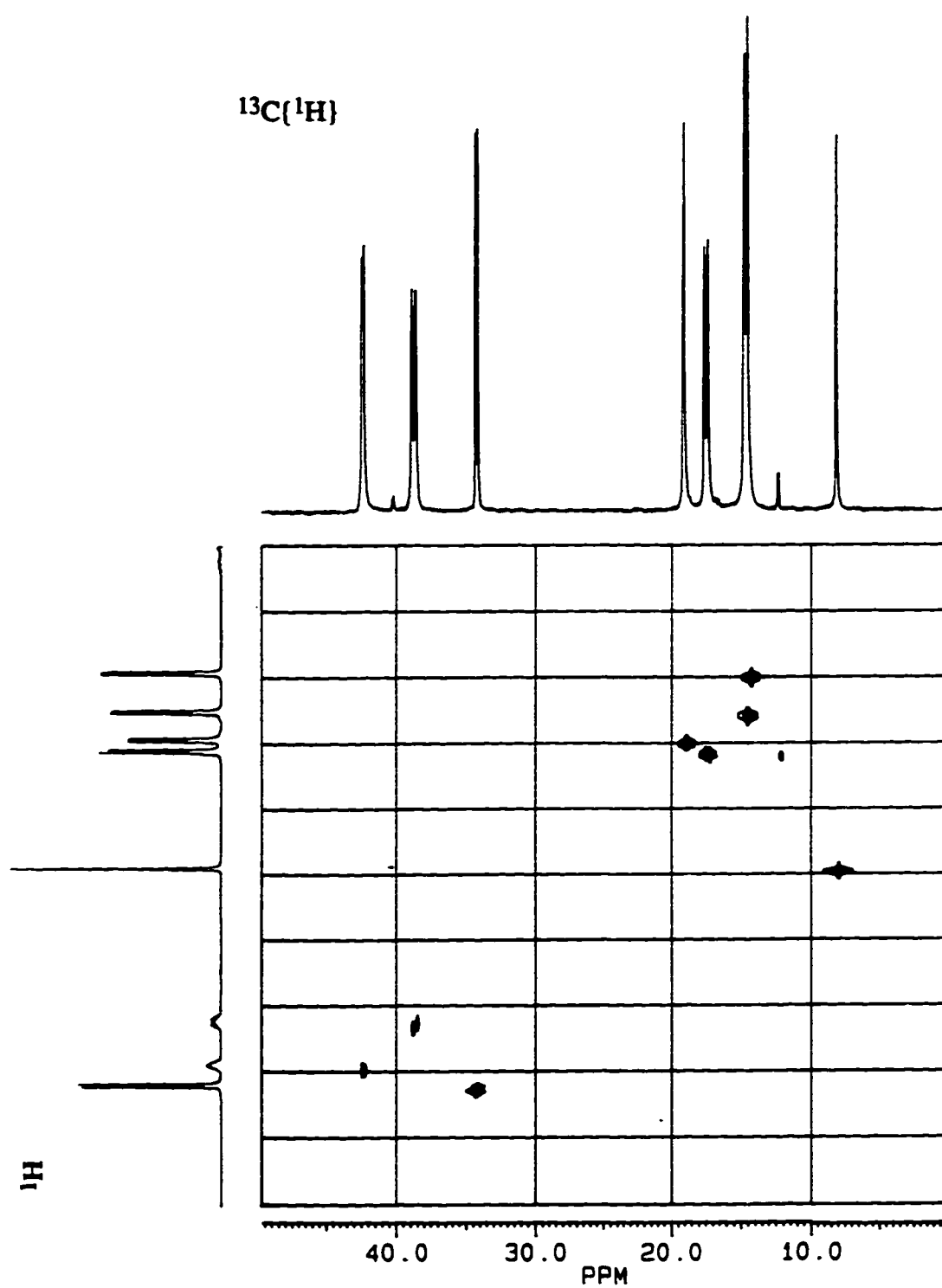


Figure 2.7 Two dimensional C,H-correlation (HETCOR) spectrum for compound **6** at -20°C in CDCl_3 .

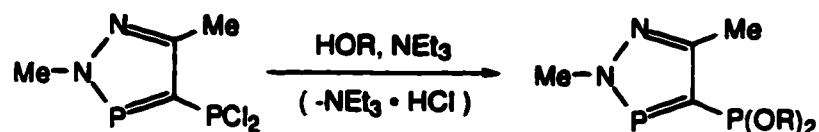
A similar observation was noted in both the $^{13}\text{C}\{^1\text{H}\}$ and ^1H NMR spectra for the chlorodibenzylaminophosphino analogue (7). The methylene carbons of the benzyl groups were diastereotopic as well as fluxional. At room temperature, the $^{13}\text{C}\{^1\text{H}\}$ NMR spectrum showed a broad resonance for the methylene carbons at 51.1 ppm. Upon cooling 7 to 0°C , two broad resonances emerged at 54.5 ppm and at 48.2 ppm. At -30°C , these two peaks had sharpened further and showed a larger $^2\text{J}_{\text{PC}}$ coupling associated with the resonance at 54.5 ppm (39 Hz) and a smaller coupling (14 Hz) associated with the resonance at 48.2 ppm. Unlike the methylene carbons signals, the phosphole carbon signals gave sharp peaks at room temperature (C-4: 150.7 ppm, $^1\text{J}_{\sigma^2\text{PC}}$ 54 Hz, $^1\text{J}_{\sigma^3\text{PC}}$ 36 Hz; C-5: 155.4 ppm, $^1\text{J}_{\sigma^2\text{PC}}$ 5 Hz, $^1\text{J}_{\sigma^3\text{PC}}$ 25 Hz) as were the signals for the 2-methyl group (41.2 ppm, $^2\text{J}_{\sigma^2\text{PC}}$ 18 Hz) and the 5-methyl group (14.9 ppm, $^3\text{J}_{\sigma^3\text{PC}}$ 6 Hz). The signal for the *ipso*-carbon on the phenyl ring (136.4 ppm) also showed coupling to the phosphorus ($^2\text{J}_{\sigma^3\text{PC}}$ 3 Hz).

The ^1H NMR spectrum for compound 7 showed resonances for the methylene protons (4.30 ppm and 4.12 ppm) which were also diastereotopic due to the stereogenic phosphorus centre. Unlike the fluxionality of the signals in the $^{13}\text{C}\{^1\text{H}\}$ NMR spectrum for the carbon at these sites, these protons did not show any fluxional behaviour. The resonance of the methylene group at 4.12 ppm gave the appearance of a triplet because $^3\text{J}_{\sigma^3\text{PH}}$ was similar to the geminal $^2\text{J}_{\text{HH}}$ (15 Hz). The methylene proton signal at 4.30 ppm showed a smaller $^3\text{J}_{\sigma^3\text{PH}}$ (9.5 Hz) where a splitting pattern of a doublet of doublets was observed. The proton resonance for the 2-methyl group (4.03 ppm) showed coupling to the $\sigma^2\text{P}$ centre ($^3\text{J}_{\text{PH}}$ 7.6 Hz). The phosphorus-proton coupling constant for the 4-methyl group (2.44 ppm) was not resolved.

The $^{13}\text{C}\{^1\text{H}\}$ NMR and the ^1H NMR spectra for 8 did not show any evidence of fluxionality.

2.5 Synthesis of 4-(Dialkoxy/aryloxyphosphino)-2,5-dimethyl-2*H*-1,2,3σ²-diazaphospholes

The alkoxy phosphinodiazaphosphole derivatives were synthesized in a similar fashion to the diethylaminophosphinophosphole. In all cases, triethylamine was used as the base (Scheme 2.7).



Scheme 2.7 Preparation of 4-(dialkoxy/aryloxyphosphino)-2,5-dimethyl-2*H*-1,2,3σ²-diazaphospholes.

The alkoxy derivatives prepared were included the 2,2,2-trifluoroethoxy (11), phenoxy (12), pentafluorophenoxy (13), 2,6-difluorophenoxy (14), and pentafluorobenzoyloxy (15) derivatives. These particular alcohol precursors were chosen because they either contain electron-withdrawing fluorine atoms (eg. CF₃ group) or a phenyl ring which inhibits the Arbuzov reaction. The yields of the alkoxy derivatives ranged from 82% for 11 to 74% for 15. All the alkoxyphosphinophospholes were white moisture sensitive solids .

2.5.1 Infrared Data for (Dialkoxy/aryloxyphosphino)-2,5-dimethyl-2*H*-1,2,3σ²-diazaphospholes

The range for the phosphorus-oxygen single bond stretching frequency is 1190-1170 cm⁻¹ when an alkyl group is connected to the oxygen while a range of 1240-1190 cm⁻¹ is observed when aromatic groups are attached to oxygen.¹⁰ For all of the compounds prepared in this series, the ν(P-O) frequencies were observed in the range of 1230 cm⁻¹ to 1184 cm⁻¹. Full infrared data is given in Table 2.4.

2.5.2 Nuclear Magnetic Resonance Properties for the 4-(Dialkoxy/aryloxy-phosphino)-2,5-dimethyl-2*H*-1,2,3σ²-diazaphosphole Series

The phosphorus chemical shifts of the σ³P centre in the dialkoxyphosphino-diazaphospholes differ slightly whereas the σ²P shifts were fairly constant and varied little from the parent diazaphosphole. For the most part, the chemical shifts of the σ³P centres ranged between 170 ppm to 155 ppm (11: 168.1 ppm; 12: 158.1 ppm; 14: 167.5 ppm; 15: 161.0 ppm) all of which are similar to that of the starting phosphinodiazaphosphole **1** (158.1 ppm). The only exception was shown by the pentafluorophenoxy derivative **13** (188.9 ppm), which showed a downfield shift of the resonance towards the difluoro analogue which is due to the electron-withdrawing ability of this highly fluorinated aromatic group.

Even though the ³¹P{¹H} NMR chemical shifts of all the compounds are similar to that of **1**, there is a decrease in the ²J_{PP} values through the series (11: 25 Hz; 12: 36 Hz; 13: 57 Hz; 14: 39 Hz; 15: 23 Hz). The most electron-withdrawing derivative in the series, the pentafluorophenol (**13**), had the largest ²J_{PP} (57 Hz) of all the non-halogen substituted phosphinodiazaphospholes. In all cases the coupling of the fluorine atoms to the σ³P centre was observed. In those compounds which contain fluoroaromatic substituents, the fluorines in the *ortho* position of the aromatic ring were coupled to the σ³P centre (13: ⁴J_{PF} 29 Hz; 14: ⁴J_{PF} 27; 15: ⁵J_{PF} 6 Hz).

The ¹³C{¹H} NMR chemical shift of the carbon signals at the 4-position were fairly consistent throughout the series at 147 ppm and these signals showed coupling to both phosphorus centres (11: 146.44 ppm, ¹J_{σ²PC} 59 Hz, ¹J_{σ³PC} 29 Hz; 12: 147.25 ppm, ¹J_{σ²PC} 57 Hz, ¹J_{σ³PC} 27 Hz; 13: 146.68 ppm, ¹J_{σ²PC} 56 Hz, ¹J_{σ³PC} 27 Hz; 15: 148.02 ppm, ¹J_{σ²PC} 58 Hz, ¹J_{σ³PC} 28 Hz). The chemical shift resonances for the carbon at the 5-position of the ring also showed little variation and again this carbon was coupled to both phosphorus atoms (11: 156.73 ppm, ¹J_{σ²PC} 6 Hz, ¹J_{σ³PC} 23 Hz; 12: 156.56 ppm, ¹J_{σ²PC} 6 Hz, ¹J_{σ³PC} 24 Hz; 13: 157.76 ppm, ¹J_{σ²PC} 4 Hz, ¹J_{σ³PC} 24

Hz; **15**: 156.52 ppm, $^1J_{\sigma^2PC}$ 6 Hz, $^1J_{\sigma^3PC}$ 24 Hz). The chemical shifts for the phenyl carbons were observed between 135 ppm and 145 ppm with the *ipso*-carbon at 129.2 ppm for **13** and 111.3 ppm for **15**. The range for the $^1J_{CF}$ was 210 Hz to 250 Hz. In the case of the perfluoro aromatics, $^2J_{CF}$ was not resolved, however for **11**, the $^1J_{CF}$ was 278 Hz and the $^2J_{CF}$ was 7 Hz.

The ^{19}F NMR spectrum for **11** showed a resonance centred at -75.7 ppm which showed a splitting pattern of a doublet of doublet of triplets being coupled to both phosphorus centres ($^6J_{\sigma^2PF}$ 2.2 Hz and $^4J_{\sigma^3PF}$ 3.5 Hz) and to the two methylene protons (8.4 Hz). For **13**, the chemical shifts for the *ortho*-fluorines were observed at -162.2 ppm, while the *meta*-fluorines were at -154.7 ppm and the *para*-fluorine was observed at -161.2 ppm. Since all the fluorine resonances were second order, it was not possible to obtain the fluorine-fluorine coupling constants. For **15**, the chemical shifts for the *ortho*-fluorines occurred at -162.6 ppm ($^3J_{FF}$ 22 Hz, $^4J_{\sigma^3PF}$ 13 Hz), while the *meta*-fluorines resonated at -143.3 ppm and the *para*-fluorine at -153.5 ppm ($^3J_{FF}$ 21 Hz). The fluorine-fluorine coupling constants were not resolved.

The 1H NMR spectrum for **11** showed the 2-methyl group of the ring at 4.02 ppm and was coupled only to the σ^2P centre (7.9 Hz). The signal for the protons for the 5-methyl group (2.48 ppm) was coupled to both phosphorus centres with the same value for the coupling constant ($^4J_{PH}$ 0.8 Hz). Two signals were observed for the methylene protons (4.21 ppm and 4.06 ppm). In the case of the phenyl derivative (**12**), the 2-methyl group resonance (4.09 ppm) were observably coupled to the σ^2P centre (8.1 Hz) and the 5-methyl group (2.51 ppm) appeared as a singlet. For the compound **13**, coupling of the 2-methyl group was observed to the σ^2P (4.13 ppm, 7.8 Hz) but the 5-methyl group signal (2.65 ppm) which was not coupled appeared as a singlet. The proton resonance for the 2-methyl group in compound **15** showed coupling to the σ^2P centre (4.04 ppm, 7.9 Hz) and the protons for 5-methyl group (2.45 ppm) were again coupled equally to both phosphorus centres ($^4J_{PH}$ 0.8 Hz). As

with **11**, two signals were observed for the methylene group protons (4.93 ppm and 4.83 ppm).

The ^1H NMR spectra of both **11** (Figure 2.8) and **15** revealed that the protons on the methylene group were diastereotopic. The cause for the anisochrony is the unequal magnetic field sensed by the two protons as a result of relative positions of each proton with respect to the ring in the molecule. In the case of **11**, decoupling the phosphorus affected only one proton resonance, that at δ 4.06. The observed coupling to the $\sigma^3\text{P}$ centre was 0.4 Hz. For **15**, the chemical shifts for the methylene protons were broadened due to proton-fluorine coupling and the coupling was not clearly resolved.

2.6 Attempts to Synthesize 4-(Dialkyl/arylphosphino)-2,5-dimethyl-2H-1,2,3 σ^2 -diazaphospholes

The alkylated or arylated 4-(dichlorophosphino)-2,5-dimethyl-2H-1,2,3 σ^2 -diazaphospholes are likely to be useful bisphosphines because of the relatively unreactive phosphorus-carbon bond (i.e. towards the Arbuzov and substitution reactions), the ability to change either the character (i.e. basicity) of the phosphorus centre through the alteration of the electron-donating properties of the alkyl or aryl groups, or the variation of steric bulk around the phosphorus atom. Unfortunately all attempts to synthesize such analogues proved unsuccessful. All alkyl or aryl Grignard reagents explored gave products which according to their $^{31}\text{P}\{^1\text{H}\}$ NMR spectra did not appear to contain the two-coordinate phosphorus centre. In some cases, the removal of the magnesium chloride co-product of the reaction was not possible. When the reaction was done in diethyl ether, the product as well as MgCl_2 would precipitate out of solution. Solvents such as dichloromethane were used in an attempt to extract the phosphinodiazaphosphole from the solid but this resulted in dissolution of all of the material in the flask. Using protic solvents such as water or ethanol in an

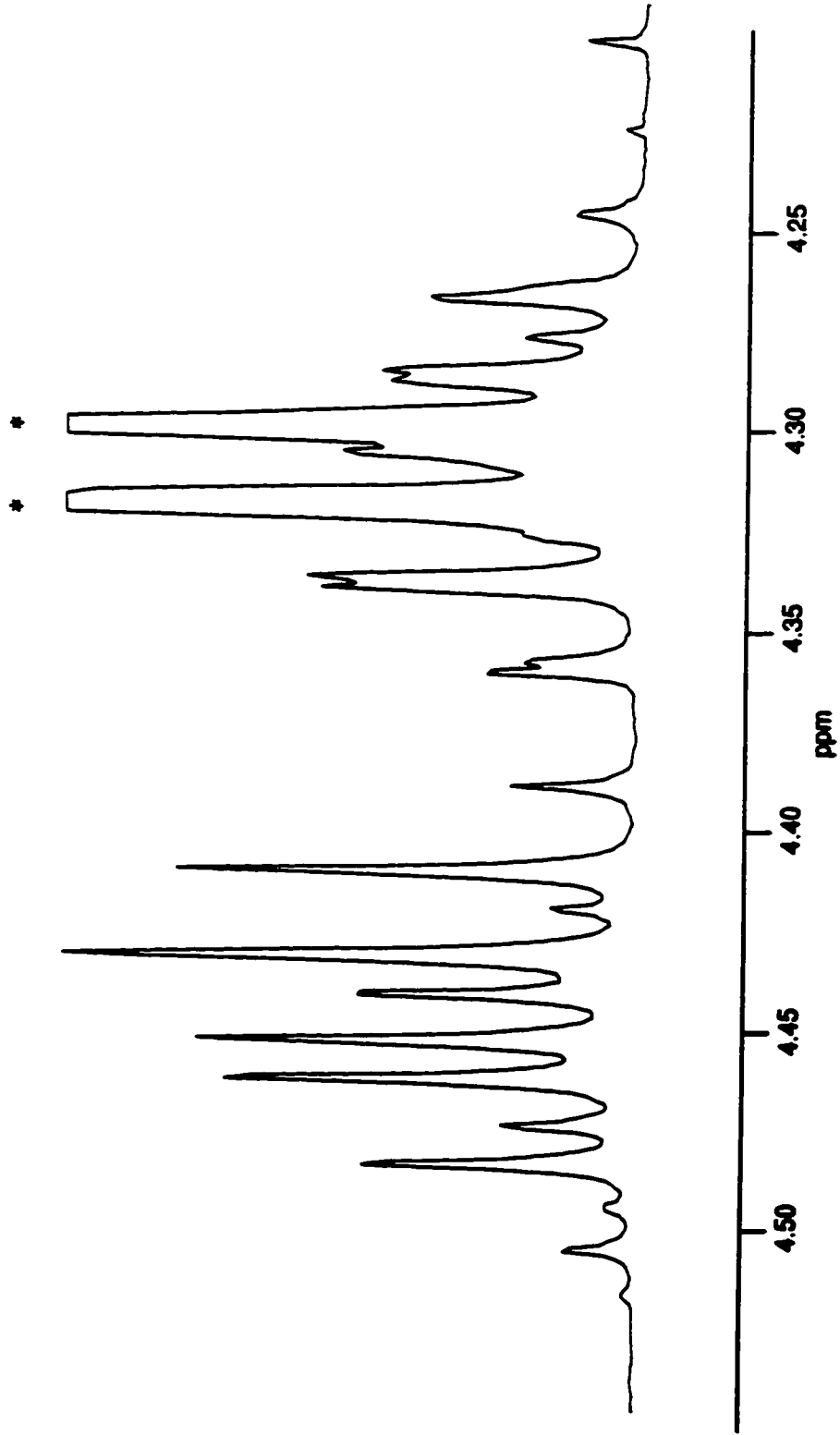


Figure 2.8 ^1H NMR spectrum of the methylene protons of compound **11** in CDCl_3 . Resonance due to the 2-methylamino group of the diazaphosphole ring is indicated with *.

attempt to selectively dissolve the magnesium chloride in the dichloromethane solution by means of a two-phase extraction process resulted in the decomposition of the phosphinodiazaphosphole into acetone methylhydrazone and phosphoric acid. Attempts to preferentially coordinate the magnesium chloride to a hard ligand by adding ligands such as triphenylphosphine oxide or 1,4-dioxane to the reaction mixture resulted in only one equivalent of the $MgCl_2$ adduct precipitating out of solution, thus the separation was incomplete.

The use of tetramethyltin to methylate the phosphinodiazaphosphole was also unsuccessful. Two routes were attempted with tetramethyltin; one trial used the tin reagent in diethyl ether at room temperature while the other reaction was performed without any solvent (neat) at the boiling point of tetramethyltin ($76^\circ C$). Unfortunately neither reaction produced any of the desired methylated product. The use of alkyl lithium reagents, such as methyl lithium, resulted in the nucleophilic attack of the phosphorus-carbon bond (*c.f.* Scheme 1.8 and Scheme 1.9). Zinc alkyls were also ineffective.

2.7 Summary

The dichlorophosphinodiazaphosphole, **1**, was converted to difluoro-, dialkoxy- and diamino phosphinodiazaphospholes. The 2,2,2-trifluoroethoxy member of the alkoxy series gave a compound in which the methylene protons were diastereotopic. The use of bulky diamines such as diisopropylamine, dibenzylamine, and dibenzylamine resulted in limited substitution at the exo-phosphorus to give the asymmetric (chloroaminophosphino)-diazaphosphole. The isopropyl derivative of the aminochlorophosphine (**6**) showed fluxional and diastereotopic diisopropylamino groups in both the 1H and $^{13}C\{^1H\}$ NMR spectra. For the dibenzylamino analogue (**7**), the methylene carbons and protons were also diastereotopic because of the bulky nature of the dibenzyl group and the methylene carbons were also fluxional. The use

of $^{31}\text{P}\{^1\text{H}\}$ NMR spectroscopy was essential in determining the number of chlorines that were displaced from **1**. The two-bond phosphorus-phosphorus coupling increased with the increase in electronegativity of the substituent. These phosphinodiazaphospholes synthesized span a range of basicity and steric bulk at the exo-phosphorus centre.

Table 2.1

³¹P{¹H} NMR Data for 4-(Phosphino)-2,5-dimethyl-2H-1,2,3σ²-diazaphospholes,^{a,b}


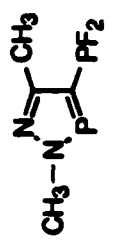
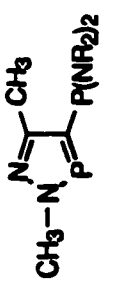
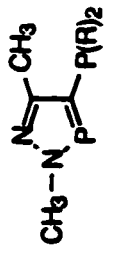
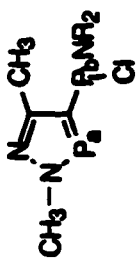

Compound	R	No.	δ σ ² P (ppm)	δ σ ³ P (ppm)	² J _{PP} (Hz)	J _{PF} (Hz)
	-	1	248.51 ^c	158.14 ^c	79	-
	-	2	255.03 ^d	208.84 ^d	107	¹ J _{PF} 1169 ³ J _{PF} 34
	Me Et nPr	3 4 5	243.23 ^c 242.54 ^c 241.53 ^c	86.88 ^c 77.94 ^c 78.99 ^c	33 29 23	- - -
	pyrazole 1,3-dimethyl- pyrazole	9 10	243.84 ^c 242.84 ^c	59.19 ^c 49.28 ^c	7 4	- -

Table 2.1 continued

Compound	R	No.	$\delta \sigma^2P$ (ppm)	$\delta \sigma^3P$ (ppm)	$^2J_{PP}$ (Hz)	J_{PF} (Hz)
	iPr	6	248.53 ^c	120.40 ^c	29	-
	CH ₂ Ph	7	247.43 ^c	127.48 ^c	25	-
	iminodibenzyl	8	246.51 ^c	118.46 ^c	6	-
	CH ₂ CF ₃	11	247.27 ^c	168.09 ^c	25	$^4J_{PF}$ 4
	Ph	12	247.00 ^c	158.13 ^c	36	-
	C ₆ F ₅	13	249.49 ^c	188.89 ^f	57	$^4J_{PF}$ 29
	2,6-F ₂ C ₆ H ₃	14	247.76 ^c	167.54 ^f	39	$^4J_{PF}$ 27
	CH ₂ C ₆ F ₅	15	246.09 ^c	161.04 ^f	23	$^5J_{PF}$ 6

a) Chemical shifts δ in ppm with respect to 85% H₃PO₄.

b) in CDCl₃

c) doublet

d) doublet of triplets

e) doublet of quartets

f) doublet of pentets

Table 2.2

¹H NMR Data for Diazaphosphole Protons in 4-(Phosphino)-2,5-dimethyl-2H-1,2,3σ²-diazaphospholes, a,b

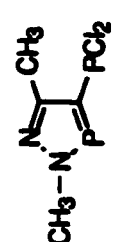
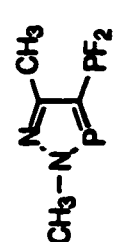
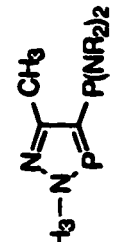
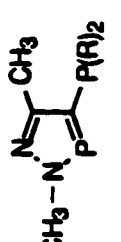
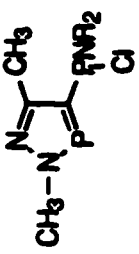
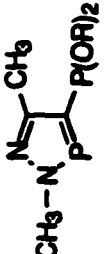
Compound	R	No.	δ CH ₃ -N (ppm)	³ J _{σ²PH} (Hz)	δ C-CH ₃ (ppm)	² J _{PH} (Hz)
	-	1	4.03 ^c	8 ^e	2.51 ^c	2.1
	-	2	4.00 ^d	10.7	2.50	-
	Me Et nPr	3 4 5	3.80 ^c 3.90 ^c 3.93 ^c	7.2 6.8 6.8	2.10 2.27 2.28	- - -
	pyrazole 1,3-dimethyl- pyrazole	9 10	4.04 ^d 4.02 ^d	7.7 7.7	2.38 ^d 2.35 ^d	13.6 13.7

Table 2.2 continued

Compound	R	No.	δ CH ₃ -N (ppm)	$^3J_{\sigma^2PH}$ (Hz)	δ C-CH ₃ (ppm)	$^2J_{PH}$ (Hz)
	iPr	6	3.90 ^c	7.8	2.26	1.6
	CH ₂ Ph	7	4.02 ^c	7.8	2.44 ^d	1.8
	iminodibenzyl	8	3.98 ^c	7.8	2.40 ^d	1.5
	CH ₂ CF ₃	11	4.02	7.9	2.48	n. r.
	Ph	12	4.09 ^c	8.1	2.51	n. r.
	C ₆ F ₅	13	4.13 ^c	7.8	2.65	n. r.
	CH ₂ C ₆ F ₅	15	4.04 ^c	7.9	2.45 ^c	0.8

a) Chemical shifts δ in ppm with respect to SiMe₄.

b) in CDCl₃

c) doublet

d) doublet of doublets

Table 2.3

 $^{13}\text{C}\{^1\text{H}\}$ NMR Data for Diazaphosphole Carbons in 4-(Phosphino)-2,5-dimethyl-2*H*-1,2,3σ²-diazaphospholes, *a,b*

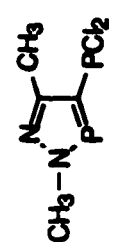
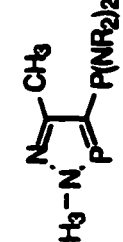
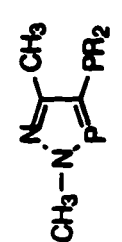


Compound	R	No.	δ N-CH ₃ (ppm)	$^2J_{\sigma^2\text{PC}}$ (Hz)	$\delta_{\text{C-4}}$ (ppm)	$^1J_{\sigma^2\text{PC}}$ (Hz)	$^1J_{\sigma^3\text{PC}}$ (Hz)	$\delta_{\text{C-5}}$ (ppm)	$^2J_{\sigma^2\text{PC}}$ (Hz)	$^2J_{\sigma^3\text{PC}}$ (Hz)	$\delta_{\text{C-CH}_3}$ (ppm)
 <chem>CN(C)C(=N)P(Cl)Cl</chem>	-	1	41.49 ^c	57	150.21 ^d	63	49	156.20 ^d	3	24	14.65 ^c
	-	2	41.51 ^c	19	135.17 ^d	35	6	157.21 ^d	5	19	14.79
		3	40.65 ^c	17	150.95 ^d	54	9	155.68 ^d	7	19	14.24 ^c
 <chem>CN(C)C(=N)P(NR2)2</chem>	Et	4	42.52 ^c	17	153.16 ^d	55	9	155.54 ^d	7	21	14.48 ^c
	Pr	5	42.55 ^c	17	152.69 ^d	55	9	156.05 ^d	7	231	14.39 ^c
 <chem>CN(C)C(=N)P(R)R</chem>	pyrazole	9	41.03 ^c	18	135.77 ^c	18	n.o.	144.63 ^d	n.o.	6	14.95
	3,5-dimethyl- pyrazole	10	41.13 ^c	18	136.27 ^c	18	n.o.	145.53 ^d	n.o.	7	14.95

Table 2.3 continued

Compound	R	No.	δ N-CH ₃ (ppm)	$^2J_{\sigma^2PC}$ (Hz)	δ C-4 (ppm)	$^1J_{\sigma^2PC}$ (Hz)	$^1J_{\sigma^3PC}$ (Hz)	δ C-5 (ppm)	$^2J_{\sigma^2PC}$ (Hz)	$^2J_{\sigma^3PC}$ (Hz)	δ C-CH ₃ (ppm)
 $\text{CH}_3\text{-N}=\text{C}(\text{CH}_3)\text{-P}(\text{OR})_2$	iPr	7	41.26 ^c	18	148.86 ^d	51	32	153.98 ^d	1	28	14.95 ^c
	CH ₂ Ph	8	41.81 ^c	18	150.73 ^d	54	36	155.38 ^d	5	25	15.06 ^c
	imino- dibenzyl	9	41.63 ^c	17	151.07 ^d	53	35	155.52 ^d	6	24	14.99
 $\text{CH}_3\text{-N}=\text{C}(\text{CH}_3)\text{-P}(\text{OR})_2$	CH ₂ CF ₃	11	41.54 ^c	18	146.44 ^d	59	29	156.73 ^d	6	23	14.81
	Ph	12	41.51 ^c	18	147.25 ^d	57	27	156.56 ^d	6	24	14.92
	C ₆ F ₅	13	41.78 ^c	18	146.68 ^d	56	27	157.76 ^d	4	24	15.19
	CH ₂ C ₆ F ₅	15	41.42 ^c	18	148.02 ^d	58	28	156.52 ^d	6	24	14.68

a) Chemical shifts δ in ppm with respect to SiMe₄.b) in CDCl₃

c) doublet

d) doublet of doublets

Table 2.4

Infrared Data for 4-(Phosphino)-2,5-dimethyl-2H-1,2,3σ²-diazaphospholes.

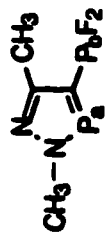

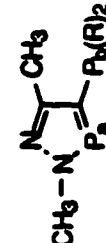
Compound	R	No.	v(P-F) (cm ⁻¹)	v(P-N) (cm ⁻¹)	v(N-C) (cm ⁻¹)	v(P-O) (cm ⁻¹)
	-	2	805, 780	-	-	-
	Me	3	-	713, 656	969, 950	-
	Et	4	-	717, 663	1013, 967	-
	ⁿ Pr	5	-	716, 557	1019, 971	-
	pyrazole	9	-	721	994	-
	1,3-dimethyl- pyrazole	10	-	714	982	-

Table 2.4 continued

Compound	R	No.	v(P-F) (cm ⁻¹)	v(P-N) (cm ⁻¹)	v(N-C) (cm ⁻¹)	v(P-O) (cm ⁻¹)
	iPr	6	-	692	1055	-
	CH ₂ Ph	7	-	680	985	-
	iminodibenzyl	8	-	672	962	-
	CH ₂ CF ₃	11	-	-	-	1175
	Ph	12	-	-	-	1226
	C ₆ F ₅	13	-	-	-	1195
	2,6-F ₂ C ₆ H ₃	14	-	-	-	1187
	CH ₂ C ₆ F ₅	15	-	-	-	1182

2.8 References

- (1) Bhattacharya, A. K.; Thyagarajan, G. *Chem. Rev.* **1981**, *81*, 415.
- (2) Mark, V. *Mech. Mol. Migr.* **1969**, *2*, 319.
- (3) Milobendzki, T. *Chem. Polski* **1917**, *15*, 66.
- (4) Milobendzki, T.; Szulgin, K. *Chem. Abstr.* **1919**, *13*, 2867.
- (5) Luber, J.; Schmidpeter, A. *J. Chem. Soc., Chem. Commun.* **1976**, 887.
- (6) Neda, I.; Fischer, A.; Jones, P. G.; Schmutzler, R. *Phosphorus, Sulfur, and Silicon* **1993**, *78*, 271.
- (7) Cunningham, J., A.F.; Kündig, E. P. *J. Org. Chem.* **1988**, *53*, 1823.
- (8) Weinmaier, J. H.; Brunnhuber, G.; Schmidpeter, A. *Chem. Ber.* **1980**, *113*, 2278.
- (9) Harris, R. K.; Wazeer, M. I. M.; Schlak, O.; Schmutzler, R. *J. Chem. Soc. Dalton Trans.* **1976**, 17.
- (10) Corbridge, D. E. C. In *Topics in Phosphorus Chemistry*; M. Grayson and E. J. Griffith, Ed.; Interscience Publishers: New York, N.Y., 1969; Vol. 6; pp 235.
- (11) Fluck, E.; Heckmann, G. In *Phosphorus-31 NMR Spectroscopy in Stereochemical Analysis*; J. G. Verkade and L. D. Quinn, Ed.; VCH Publishers, Inc.: Deerfield Beach, FL, 1987; Vol. 8; pp 61.
- (12) Verkade, J. G.; Mosbo, J. A. In *Phosphorus-31 NMR Spectroscopy in Stereochemical Analysis*; J. G. Verkade and L. D. Quinn, Ed.; VCH Publishers, Inc.: Deerfield Beach, FL, 1987; Vol. 8; pp 425.
- (13) Tebby, J. C. In *Phosphorus-31 NMR Spectroscopy in Stereochemical Analysis*; J. G. Verkade and L. D. Quinn, Ed.; VCH Publishers, Inc.: Deerfield Beach, FL, 1987; Vol. 8; pp 1.
- (14) Friebolin, H. *Basic One- and Two-Dimensional NMR Spectroscopy*; VCH Publishers: New York, NY, 1991, pp 150.
- (15) Henderson, J., W.A.; Buckler, S. A. *J. Am. Chem. Soc.* **1960**, *82*, 5794.

- (16) Personal communication from Cavell, R. G., University of Alberta, Edmonton, Alberta.
- (17) Grapov, A. F.; Mel'nikov, N. N.; Razvodovskaya, L. V. *Russ. Chem. Rev.* **1979**, *39*, 20.
- (18) Murray, M.; Schmutzler, R. *Z. Chem.* **1968**, *8*, 241.
- (19) Schmutzler, R. *Halogen Chem.* **1967**, *2*, 55.
- (20) Reed, R. W.; Bertrand, G. In *Phosphorus-31 NMR Spectral Properties in Compound Characterization and Structural Analysis.*; L. D. Quinn and J. G. Verkade, Ed.; VCH Publishers, Inc.: New York, NY, 1994; pp 189.

CHAPTER 3

OXIDATION OF 4-(PHOSPHINO)-2,5-DIMETHYL-2H- 1,2,3 σ^2 -DIAZAPHOSPHOLE DERIVATIVES

3.1 Introduction

Altering the chemical nature of one of the phosphorus(III) centres of a bisphosphine modifies its reactivity. A major goal of the synthetic studies described here is to achieve such modifications on only one of the two phosphine centres and to induce differential reactivity. One method of accomplishing such a change is to alter the substituents on one phosphorus centre. Another approach is to oxidize the phosphorus atom from the +3 oxidation state (P(III)) to the +5 oxidation state (P(V)), creating a heterobifunctional phosphine ligand system which presents a phosphine and a different atom (eg. N, O, or S) as binding moieties to metals. In many cases, however, the reagents used to oxidize a bisphosphine results in the oxidation of both phosphorus atoms, and this is especially prevalent when the substituents on both of the phosphorus centres are identical. The syntheses of mono-oxidized bisphosphines are often laborious and yields are frequently low. Creating bisphosphines wherein the phosphorus centres have initially different basicities will favour the oxidation of one of the phosphorus centres over the other. A large enough contrast in basic character ultimately leads to the possibility of exclusively oxidizing only one of the phosphorus centres even under the most rigorous conditions.

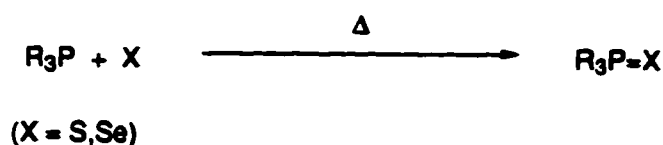
The major question of the electronic orbital structure which best describes the bonding of the phosphorus in the +5 oxidation state has not been fully resolved. The topic has been the subject of recent reviews.¹⁻⁴ Early descriptions of the structure and the bonding in oxidized four coordinate phosphorus(V) compounds invoked d orbital interaction of the phosphorus atom to establish a π overlap with the p orbitals on the

substituent chalcogen or the nitrogen atom of an imine. The use of d orbitals on the phosphorus arose out of the perceived difficulty in the construction of bonding orbitals for hypervalent molecules wherein more bonds to the central atom are needed than can be provided by the octet rule and normal electron pair bonding. A prime example is provided by SF₆, a molecule which does not obey the octet rule. In this case, six sulfur σ bonds must be constructed from six equivalent d²sp³ hybrid components to hold twelve electrons in six pairs. The d orbitals provide the necessary number count of orbitals. Similarly, PF₅ bonding involves dsp² hybrids. The use of d orbitals was also a convenient approach to explain the multiple (apparent π -type, parallel to the C=C bond in ethylene) bonding and the stability of phosphine oxides as well as the shortening of the formally single phosphorus-oxygen bonds in phosphates.

The coordination chemistry of an oxidized phosphorus centre takes on the characteristics of the chemistry of the newly introduced moiety since the oxidized phosphorus centre no longer reacts as a typical Lewis base. This oxidized phosphorus centre becomes part of the molecular backbone. If only one phosphorus atom of a bisphosphine is oxidized, there is still the other phosphorus centre available. Cooperative reactivity with the new donor centre builds a heterobifunctional ligand with one of the functional centres still being a phosphorus moiety. The hardness, or softness, of the remaining phosphine in the bisphosphine ligand can be altered by choosing a variety of chalcogens and/or imino functionalities. The iminophosphine centre also offers the possibility of exploring further variations of the system by changing the substituents on nitrogen (to change the coordination behaviour of the imino group). Finally, systems which offer the possibilities for further reactions at the imino group can be established. A prime example of the latter is illustrated by the trimethylsilyl functionality on the nitrogen. This functionalized imino centre can react with a metal halide to form a sigma bond between the metal centre and the nitrogen *via* the elimination of trimethylsilane chloride (e.g. Scheme 1.5).

3.1.1 Oxidation with Chalcogens

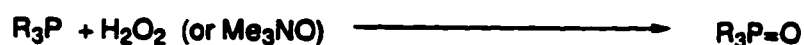
The oxidation of a phosphorus(III) centre is readily achieved by the reaction of the phosphine with chalcogens such as oxygen, elemental sulfur, or elemental selenium. This method allows a certain amount of control over the degree of hardness of the coordinating chalcogen. Phosphine oxides provide a "hard" centre while phosphine selenides create a "soft" coordinating moiety. The oxidative addition of sulfur, selenium, or even tellurium to the phosphorus centre is easily achieved by refluxing a solution of the elemental chalcogen with the phosphine (Scheme 3.1).



Scheme 3.1 Oxidation of a phosphine with an elemental chalcogen.

The tellurophosphoranes are not usually very stable since an equilibrium is established between the phosphorane and the phosphine in solution (i.e. $\text{Te}=\text{P}(\text{V}) \rightleftharpoons \text{Te} + \text{P}(\text{III})$). For the selenium derivatives, there is the added benefit of another NMR active nucleus ^{77}Se ($I = 1/2$, 7.58% natural abundance) for the characterization of the selenophosphoranes, an option which is not available with either oxygen or sulfur.

The synthesis of a phosphine oxide can be achieved through the use of peroxides such as hydrogen peroxide or *tert*-butyl hydroperoxide. Other oxidants include amine oxides such as trimethylamine oxide (Scheme 3.2).



Scheme 3.2 Oxidation of a phosphine with hydrogen peroxide or trimethylamine oxide.

The older models of the bonding between phosphorus and a chalcogen described the bond as a double bond which can be viewed as a type of backbonding wherein the electron density from the lone pair of the oxygen atom is donated into suitable low-lying atomic d orbitals of the phosphorus. As mentioned above, this notion is not now universally accepted. An alternative scheme has been described wherein the $p\pi$ orbital on the oxygen is combined with an antibonding orbital of $e(\pi)$ symmetry on phosphorus to create the necessary acceptor orbital for forming the π bond between phosphorus and oxygen. The interaction is schematically represented in Figure 3.1. The full set of Walsh diagram orbitals for a pyramidal AH_3 system (Figure 3.2) shows the relationship between this $2e$ antibonding orbital and the remaining orbitals in this framework.

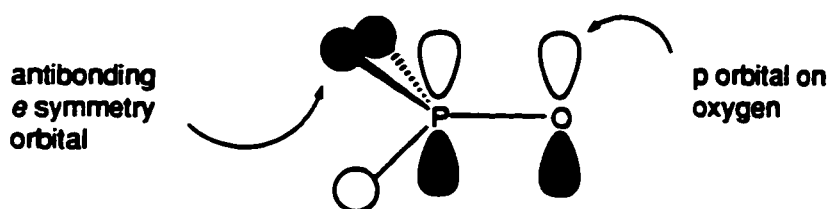


Figure 3.1 Formation of a π bond between phosphorus and oxygen using the oxygen p orbital and an antibonding orbital of e symmetry on phosphorus (the AH_3 moiety). [Reference 4]

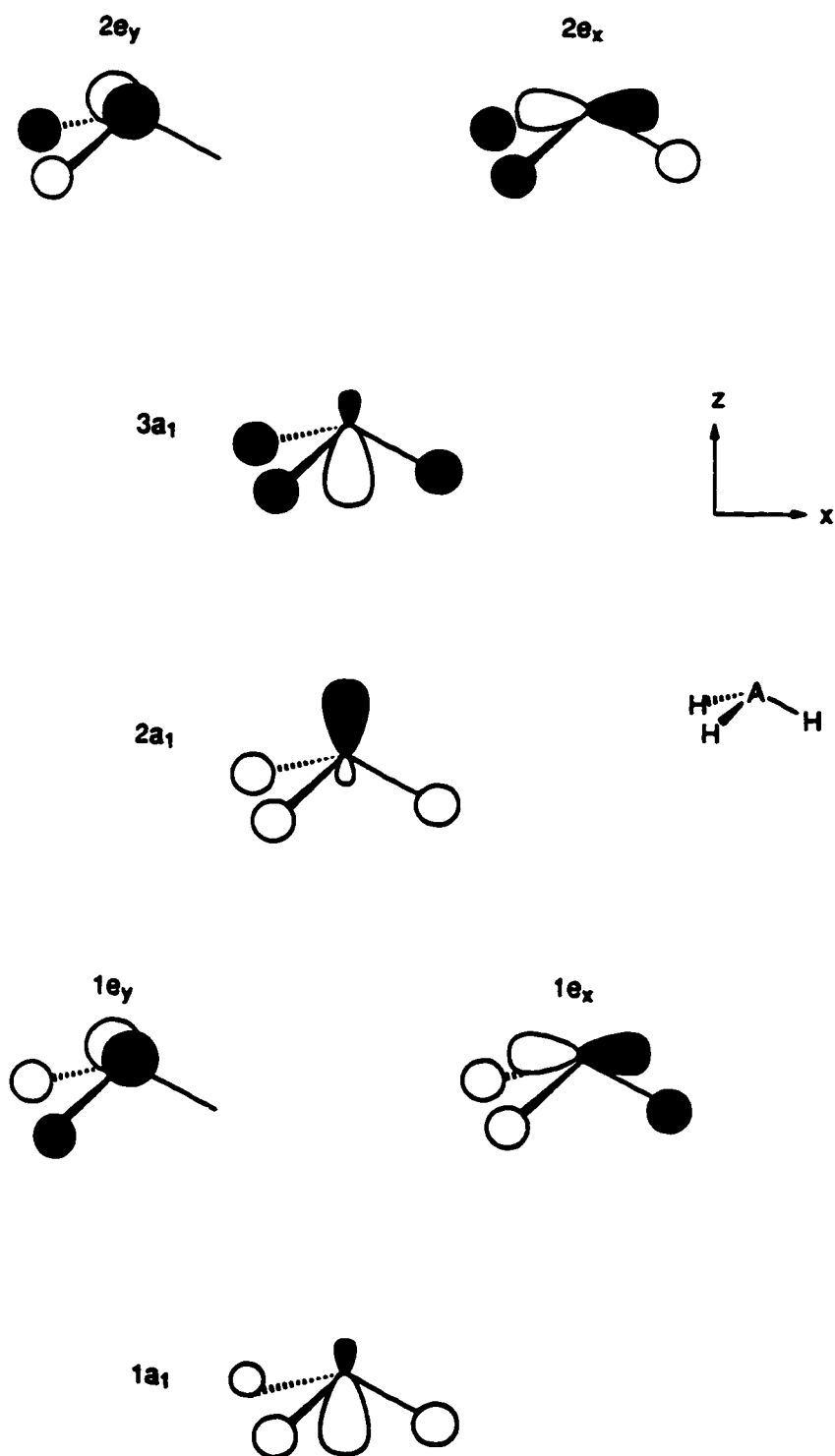


Figure 3.2 Walsh diagram for the pyramidal AH_3 system.

3.1.2 Synthesis of Iminophosphoranes

The addition of an imino moiety to a phosphorus centre can be accomplished by several different reactions:

(a) the Staudinger reaction,⁵ wherein the phosphine reacts with an azide to eliminate N₂ and form the imine,



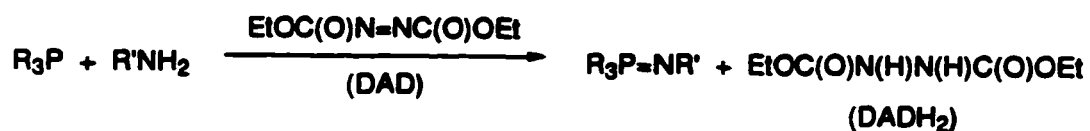
Scheme 3.3 Oxidation of a phosphine *via* the Staudinger reaction.

(b) the Kirsanov reaction,⁶ wherein hydrogen chloride is eliminated from a dichlorophosphorane and a primary amine. In this process, the phosphorus atom is first oxidized by an agent such as elemental chlorine and variants include the removal of the hydrogen chloride as a salt,



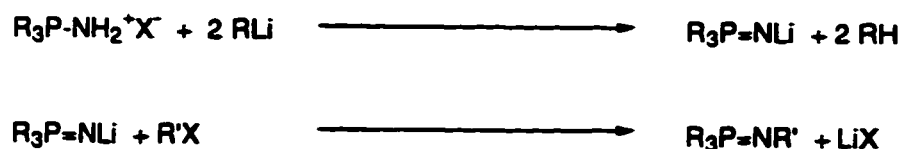
Scheme 3.4 Formation of a phosphinimine *via* the Kirsanov reaction.

(c) the redox-condensation reaction of a phosphine with an amine in the presence of diethyl azodicarboxylate (DEAD or DAD),⁷



Scheme 3.5 Redox-condensation of a phosphine with a primary amine using diethyl azodicarboxylate.

and (d) the deprotonation of an aminophosphinium salt.⁸ This process may be carried out in two steps and the same or a different R group can be placed on the nitrogen.

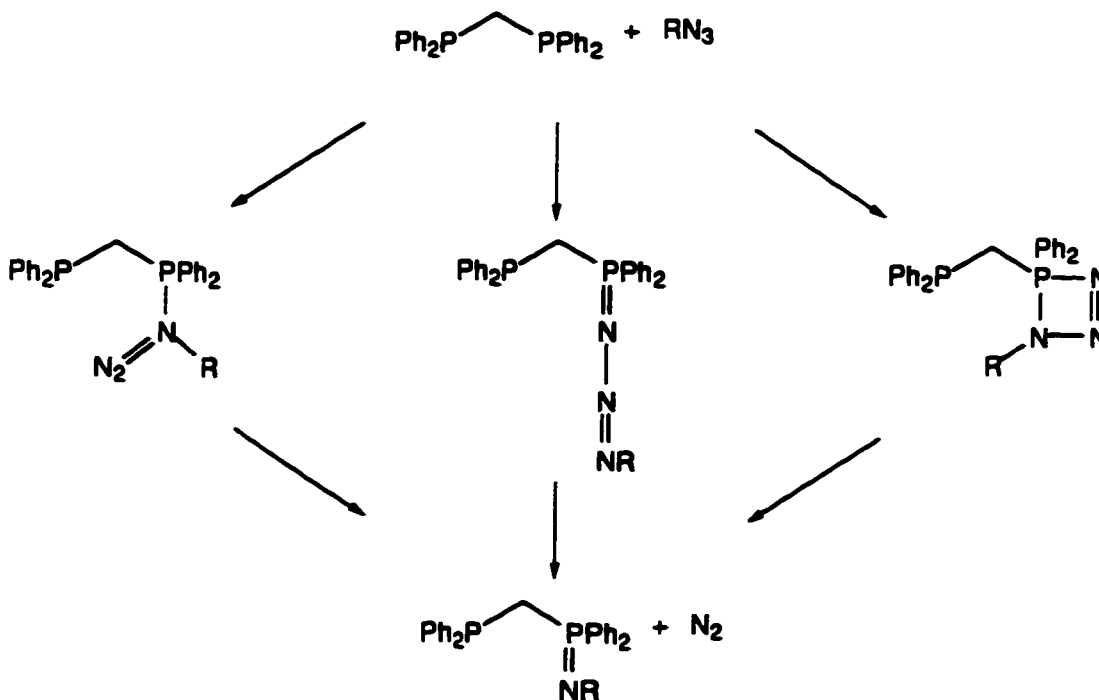


Scheme 3.6 Deprotonation of an aminophosphinium salt and its conversion to an iminophosphorane.

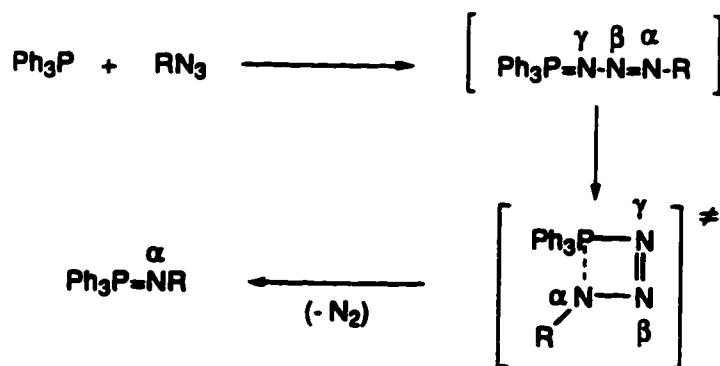
Mechanistic investigations of the Staudinger reaction have shown that the rate of reaction is accelerated by the presence of acceptor groups on the azide⁹ and furthermore it is well established that the α -nitrogen which carries the substituent is retained in the iminophosphorane. To explain these facts, three phosphazide intermediates have been proposed which have either a branched structure,^{10,11} a cyclic structure,¹² or a linear structure¹³ (Scheme 3.7).

The linear form of the primary product has been generally accepted as the most likely because it is consistent with all chemical, spectroscopic, and kinetic data.^{13,14} Mechanistic studies then suggest that the Staudinger reaction proceeds by nucleophilic attack by the phosphorus on the terminal (α) nitrogen of the azide to form the phosphazide and this intermediate, which is most likely the cyclic structure, (which may exist only as a transition state) then dissociates to diatomic nitrogen and to the iminophosphorane (Scheme 3.8).^{15,16}

Further insight into the mechanism of this reaction was provided by the x-ray structure analysis of several relevant metal phosphazides.¹⁷ All of these structures have shown a linear triazide unit in which the terminal nitrogen is bonded to the phosphorus centre. It has also been demonstrated that the phosphorus atom retains its configuration throughout the imine formation,¹⁸⁻²⁰ which further supports the proposed four-centred transition state.



Scheme 3.7 Proposed structures for the phosphazide intermediate.



Scheme 3.8 Mechanism for the Staudinger reaction.

The electronic structures of λ^5 -iminophosphorane systems present problems analogous to those discussed above for phosphine oxides. The structures (Figure 3.3) can be written as either a dipolar resonance form, **a**, or a multiple P-N bonded

resonance form, b, wherein $p\pi-d\pi$ double bonding is involved. An additional form, c, can also be written if the group R' can participate in resonance structures.

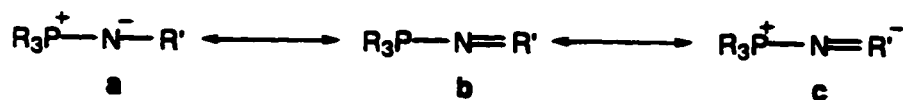


Figure 3.3 Resonance forms of the λ^5 -iminophosphorane system.

The iminophosphoranes are now best described in a fashion similar to the phosphonium ylides with the difference being that the phosphonium ylides are more stable than the imino analogues because of the presence of suitable vacant orbitals on the carbon atom of lower energy than those offered by the nitrogen. One view of the bonding arrangement of the ylides proposes a synergic relationship in which the lone pair of electrons from the phosphorus initially forms a σ bond to the carbon. The extra charge density on the carbon is then delocalized back to the phosphorus by overlapping the p orbital on the ylide with the σ^* LUMO of the phosphine centre (Figure 3.4) in exactly the same manner as was described for the phosphine oxide.

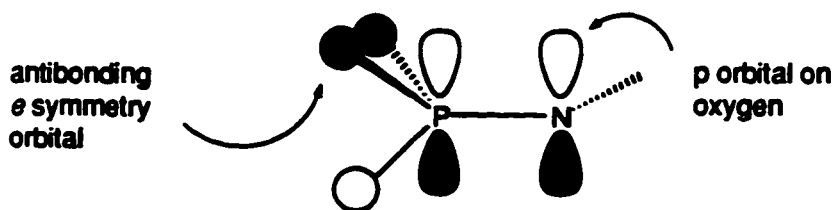


Figure 3.4 Orbitals proposed for the π backbonding between nitrogen and phosphorus. [Reference 4]

Other descriptions of the bonding in phosphonium ylides which are readily extended to imines and chalcogen oxidized phosphines include curved bonds, which have been termed either "bent multiple" bonds or "banana" bonds. More recently, these bonding descriptions have been labelled " τ bonds" or " Ω bonds" (Figure 3.5).³

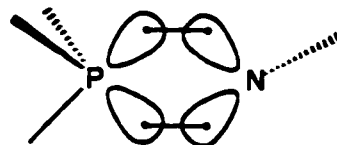


Figure 3.5 Description of the phosphorus-nitrogen double bond as two Ω bonds.

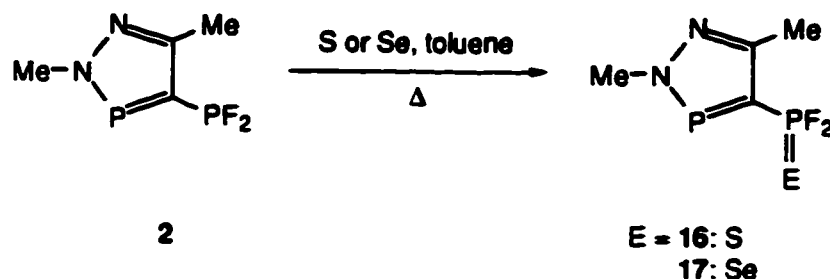
The iminophosphoranes have nominal sp^2 hybridization with one formal electron lone pair on the nitrogen so these molecules are Lewis bases. This electron pair may be protonated or donated to metals. The base strength and donor ability is dependent on the nature of the substituent on the nitrogen and this property motivates the substitution chemistry of the system. When the substituent on the nitrogen is electron-donating, the nitrogen basicity will be enhanced. Electron-withdrawing groups on the nitrogen will reduce its basicity but the ultimate binding of the imine to the metal centre may be additionally dependent on the capability of the metal centre to return electron density *via* backbonding. Our studies focus on the synthesis of a selected series of mixed bisphosphorus molecules to create heterobifunctional ligands which will then be applied to studies of complexation chemistry in Chapter 4.

3.2 Oxidation of 4-(Difluorophosphino)-2,5-dimethyl-2*H*-1,2,3 σ^2 -diazaphosphole.

In all cases, the oxidation of the 4-(difluorophosphino)-2,5-dimethyl-2*H*-1,2,3 σ^2 -diazaphosphole, by either chalcogens or azides, resulted in the exclusive oxidation of the exo-phosphorus centre. This result shows that the lone pair of the two-coordinate phosphorus centre is not in an appropriate orbital to allow reaction with either azides or chalcogens. Steric interactions can be ruled out due to the planar ring system of the diazaphosphole. The compound resulting from the oxidation is a σ^2P - σ^4P phosphine-phosphorane system.

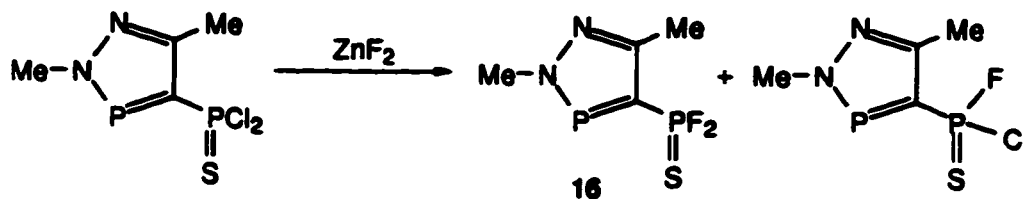
3.2.1 Oxidation with Elemental Chalcogens

The reaction of the 4-(difluorophosphino)phosphole with selenium in refluxing toluene proceeded smoothly over a period of 12 hours. Removal of the excess selenium and toluene gave (difluoroselenophosphorano)diazaphosphole, **17**, in a crystallized yield of 87%. The sulfur analogue, **16**, required a much longer reaction time of 48 hours and was produced in a lower yield (43%). These compounds are extremely sensitive towards moisture.



Scheme 3.9 Oxidation of **2** with elemental sulfur or elemental selenium.

Compound **16** has been previously reported from the reaction of zinc fluoride with 4-(dichlorothiophosphorano)diazaphosphole (**1**) as a mixture of both the chlorofluoro- and difluorophosphorane derivatives (Scheme 3.10). These two compounds were not isolated and were only identified by their $^{31}\text{P}\{^1\text{H}\}$ and the ^1H NMR spectra.²¹



Scheme 3.10 Previously reported synthesis of **16** using zinc fluoride as the fluorinating reagent.

3.2.2 Spectroscopic Characterization of 16 and 17

In both cases the $^{31}\text{P}\{^1\text{H}\}$ NMR spectra showed a large upfield shift for the resonance upon oxidation of the exo-phosphorus centre (16, E = S; 17, E = Se), due to the oxidation of the phosphorus, (E = S: 82.47 ppm; E = Se: 87.50 ppm) and a downfield shift for the signal $\sigma^2\text{P}$ centre (E = S: 264.3 ppm; E = Se: 265.1 ppm). An increase in $^2J_{\text{PP}}$ was also observed (E = S: 112 Hz; E = Se: 119 Hz). The one-bond phosphorus-fluorine coupling constant for the thio derivative, 16, (1132 Hz) was smaller than that for the unoxidized difluorophosphinodiazaphosphole, 2, but the corresponding coupling constants increased slightly in the case of the seleno analogue 17 (1169 Hz).

In most cases where the phosphorus centre carries alkyl or aryl substituents, the phosphorus chemical shift signal in the $^{31}\text{P}\{^1\text{H}\}$ NMR moves downfield upon oxidation. For example, monooxidation of bis(diphenylphosphino)methane (dppm) with trimethylsilyl azide (to give compound VIII) caused a downfield shift of $\Delta\delta$ 21.1 ppm (to -1.1 ppm) for the resonance of the oxidized phosphorus centre while a slight upfield shift of $\Delta\delta$ 5.2 ppm (to -27.4 ppm) was observed for the P(III) centre.²² The downfield shift for the resonance arises from the increased deshielding of the oxidized phosphorus centre caused by the introduction of the new imine moiety. With halogenated phosphines, the opposite trend is observed. The oxidation of the phosphorus centre results in an upfield shift for the phosphorus chemical signal. For example, the chemical shifts of OPF_3 (-36 ppm) and OPCl_3 (2 ppm) both lie upfield from the unoxidized PF_3 (97 ppm) and PCl_3 (219 ppm). Bernard-Moulin and Poulin²³ have calculated the value for the phosphorus chemical shift for OPF_3 which is in good agreement with the experimentally observed values. The authors of this paper were not explicit about how their parameters were optimized, nor did they give their values. They also stressed the importance of the d orbitals and that the shift

values obtained depend critically on the hybridization of the phosphorus. They did not however comment on the role of the d orbitals.

Some of the differences in the shift trends can be traced to the diamagnetic and the paramagnetic terms which compose the shielding contributions in the chemical shift. The diamagnetic term, σ_{dia} , originates in the electronic shielding of the nucleus. The presence of a group in the molecule which donates or withdraws electrons will therefore affect the chemical shift of a nearby nucleus. These diamagnetic effects are major contributors to the proton magnetic resonance spectrum. The paramagnetic term, σ_{para} , can be described as the result of the generation of electronic asymmetry by the electric field of a nearby nucleus. The σ_{para} is inversely proportional to the average electronic excitation energy, so the smaller the difference between the ground and the excited states, the greater is contribution to the shielding. In most cases the diamagnetic term, σ_{dia} , predominates over σ_{para} . For the halophosphines and phosphoranes, however, the contribution of the paramagnetic term is more significant.

The $^{13}\text{C}\{^1\text{H}\}$ NMR spectra for both compounds 16 and 17 showed a two-bond fluorine-carbon coupling ($E = \text{S}$: 24 Hz; $E = \text{Se}$: 24 Hz) which was not observed for the parent compound 2. The reaction with the chalcogens showed a large increase in the $^1J_{\sigma\text{2PC}}$ ($E = \text{S}$: 163 Hz; $E = \text{Se}$: 165 Hz) versus the unoxidized phosphinodiazaphosphole 2 ($^1J_{\sigma\text{2PC}}$ 35 Hz). The one-bond phosphorus-carbon coupling correlates directly with the degree of s character in the P-C bond because the Fermi contact mechanism indicates that coupling will be more effectively transmitted by this mechanism through σ bonds rich in s character. The s character can be distributed differently throughout the bonds to carbon if there is a modification of the bond angles by either ring requirements or unusual steric demands of the substituents and such effects are visible here in the $^{31}\text{P}\{^1\text{H}\}$ NMR spectrum.

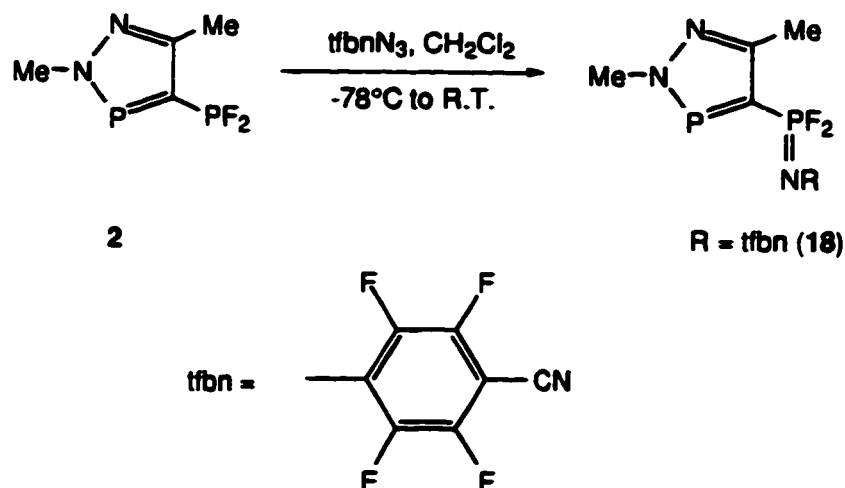
With both compounds, **16** and **17**, the ^{19}F NMR spectrum showed a doublet of doublets for the fluorine resonances. Oxidation of the exo-phosphorus also had a deshielding effect on the fluorine signals (E = S: -41.84 ppm; E = Se: -43.03 ppm). There was a large decrease in the coupling of the fluorine atoms to the $\sigma^2\text{P}$ centre (E = S: 6 Hz; E = Se: 3 Hz) relative to the case of the parent phosphinodiazaphosphole **2** ($^3J_{\sigma^2\text{PF}}$ 34 Hz). The fluorine atom signal of **17** showed further coupling to the selenium (104 Hz) which was also reflected in the ^{77}Se NMR spectrum.

The proton signals in the ^1H NMR spectra of both compounds (**16** and **17**) remained relatively constant upon oxidation of the exo-phosphorus centre. There was a slight downfield shift for the signals for the 2-methyl group protons for **16** (3.94 ppm) and a slight upfield shift in the resonance was observed for **17** (4.02 ppm). Both compounds showed an increase in the phosphorus-proton coupling constant (E = S: $^3J_{\text{PH}}$ 8.6 Hz; E = Se: $^3J_{\text{PH}}$ 8.6 Hz) upon oxidation. The 4-methyl group proton resonances shifted downfield in the case of **16** and coupling was observed to the exo-phosphorus centre (2.39 ppm, $^4J_{\text{PH}}$ 0.9 Hz). The signal for the protons of the same group in the case of **17** remained relatively constant (2.51 ppm) without coupling to either phosphorus centre being observed.

In general, the P-F stretching vibrations in trivalent phosphorus-fluorine compounds absorb at lower frequencies than those of the pentavalent derivatives.^{24,25} Both oxidized difluorophosphino derivatives **16** and **17** showed higher frequencies for the P-F stretching (E = S: $\nu(\text{P-F}) = 853 \text{ cm}^{-1}$, 823 cm^{-1} ; E = Se: $\nu(\text{P-F}) = 869 \text{ cm}^{-1}$, 841 cm^{-1}). For **16** the $\nu(\text{P=S})$ occurred at 726 cm^{-1} while for **17** the $\nu(\text{P=Se})$ was found at 533 cm^{-1} .

3.2.3 Oxidation *via* the Staudinger Reaction; Formation of Iminophosphorane Derivatives

The 4-(difluorophosphino)-2,5-dimethyl-2*H*-1,2,3 σ^2 -phosphole reacted smoothly with *p*-tetrafluorobenzonitrile azide at -78°C in dichloromethane *via* the Staudinger reaction to yield the heterobifunctional phosphine-phosphorane **18** in which the imino moiety is introduced exclusively on the *exo*-phosphorus centre (Scheme 3.11). The compound was recrystallized from dichloromethane at -40°C giving colourless crystals in a yield of 82%.



Scheme 3.11 Reaction of **2** with *p*-tetrafluorobenzonitrile azide.

3.2.4 Spectroscopic Characterization of **18**

With the introduction of this imino functionality into the heterobifunctional bisphosphine, the $^{31}\text{P}\{^1\text{H}\}$ NMR spectrum showed a large upfield shift for the resonance of the *exo*-phosphorus centre of over 200 ppm to 2.66 ppm and a downfield shift for the $\sigma^2\text{P}$ signal to 265.70 ppm and in contrast to the chalcogen derivatives of **2**, $^2\text{J}_{\text{PP}}$ decreased (83 Hz). The $^1\text{J}_{\sigma^4\text{PF}}$ (1145 Hz) had also decreased slightly as did the $^3\text{J}_{\sigma^2\text{PF}}$ (6 Hz) a trend which was similarly observed for both chalcogen derivatives. The most revealing feature of the $^{13}\text{C}\{^1\text{H}\}$ NMR spectrum of **18** is the

signal for the carbon at the 4-position. Upon oxidation, the resonance for this carbon shifted by 10 ppm downfield (125.2 ppm). As in the case of **16** and **17**, there was an increase in the both phosphorus-carbon coupling constants ($^1J_{\sigma^2PC}$ 246 Hz, $^1J_{\sigma^4PC}$ 45 Hz) and a $^4J_{CF}$ was also observed (24 Hz) accompanying oxidation. The large increase in the phosphorus-carbon coupling constant may be explained in terms of resonance structures shown in Figure 3.6.

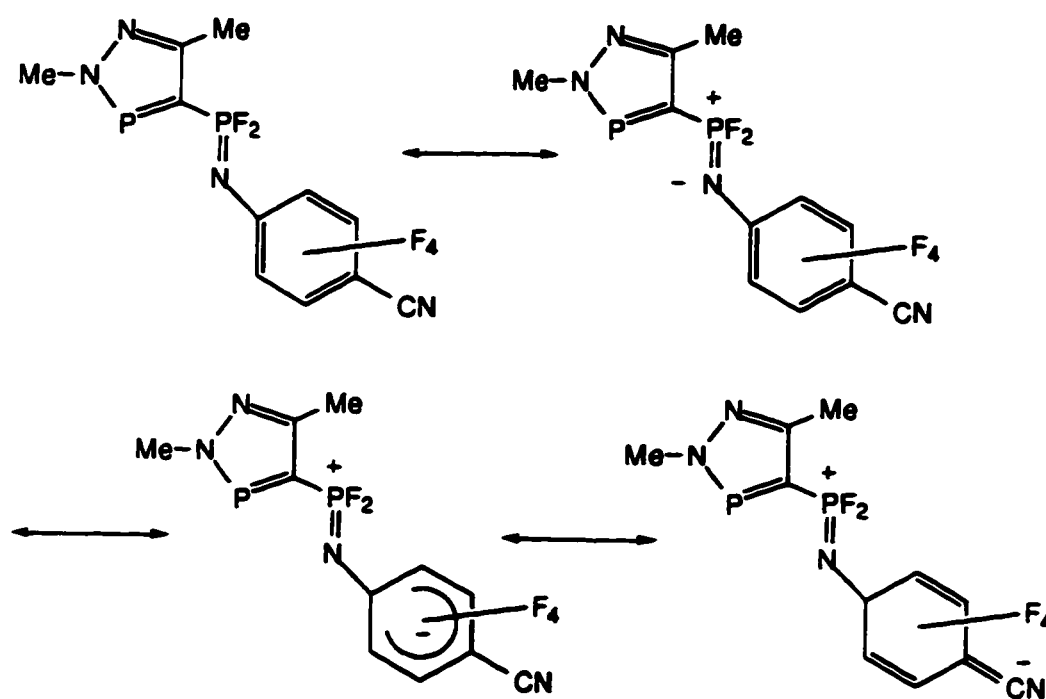


Figure 3.6 Resonance forms for compound **18**.

The resonance forms show that the phosphorus(V) centre would become more positive by means of the dipole changes induced by delocalization into the *p*-cyanotetrafluorophenyl group. This property would then shorten the phosphorus-carbon bond and the resultant increase of the P-C orbital overlap would in turn induce an increase in the $^1J_{PC}$. There was also a marked increase in the $^2J_{\sigma^2PC}$ (45 Hz) for the methyl carbon at the 4-position (125.17 ppm). The carbon at the 5-position was

coupled only to the exo-phosphorus (158.21 ppm, ${}^2J_{\sigma^2PC}$ 13 Hz) while the resonance for the methyl group appeared as a singlet (15.01 ppm).

The ${}^{19}\text{F}$ NMR spectrum demonstrated through the chemical shift of the fluorine atoms on the exo-phosphorus centre that these were not as deshielded as was the case with the chalcogen derivatives (-56.54 ppm). A similar value of ${}^3J_{\sigma^2PF}$ was observed (34 Hz) as that of **16**. The chemical shifts for the *ortho* and the *meta* fluorines on the tfbn ring were -152.81 ppm (${}^4J_{\sigma^4PF}$ 5.7 Hz) and 139.77 ppm, respectively. The ${}^1\text{H}$ NMR spectrum of the proton signals on the ring were relatively constant for both the methyl group at the 2-position (4.14 ppm, ${}^3J_{\sigma^2PC}$ 8.9 Hz) and the methyl group in the 4-position (2.61 ppm).

The solid-state structure of **18** (Figure 3.7) revealed two planar ring systems consisting of the diazaphosphole and the *p*-tetrafluorophenyl with an angle of 26.3° between the rings. The P(41)-N(41)-C(41) bond angle is $141.2(2)^\circ$ and the P(41)-N(41) and N(41)-C(41) bond lengths are 1.514 and 1.363 Å, respectively. The length of this phosphorus-nitrogen double bond is a little shorter than the range of 1.54 to 1.64 Å predicted by the sum of Pauling double bond radii. The angle about the $\sigma^2\text{P}$ centre, N(2)-P(3)-C(4), is $88.20(9)^\circ$. This angle compares with that of the diazaphosphole hydrochloride, XVIII, (88.2°), showing that the diazaphosphole ring system is essentially unaffected by a change in the geometry at the exo-phosphorus and this is supported by the lack of change of the $\sigma^2\text{P}$ signal in the phosphorus NMR. The F(41)-P(41)-F(42) angle is $97.42(7)^\circ$ and the average of the P-F bond distances is 1.537 Å. This phosphorus-fluorine bond length is longer than that observed for a related P(V) compound $\text{Ph}_2\text{FP}=\text{NMe}$ (1.488 Å) which however has a more basic imine centre as a result of the presence of a methyl as opposed to a tfbn substituent on the nitrogen.²⁶ The bond lengths and angles displayed in the phosphole ring system are similar to those of the diazaphosphole and are consistent with an aromatic system.

Table 3.1

Structural Data for Some *N*-Substituted Iminophosphoranes.

Compound	d(P=N)Å	(P=N-R)°	Ref.
18	1.514	141.7	This work
Ph ₂ PCH ₂ PPh ₂ (=NR)			
R = 5-F-2,4-(NO) ₂ C ₆ H ₂	1.589	128.8	27
R = 4-(CN)C ₆ F ₄	1.567	132.9	27
R = SiMe ₃	1.529	150.2	28
Ph ₃ P=NPh	1.602	130.4	29
Ph ₃ P=NCN	1.595	123.0	30
Ph ₃ P=NP(CF ₃) ₂	1.576	131	31
1-(Ph ₂ P)-2-(Ph ₂ P(=NSiMe ₃))C ₆ H ₄	1.529	152.7	32
Me ₃ P=NSiMe ₃	1.542	144.6	33
Ph ₂ FP=NMe	1.469	119.1	26

In Table 3.1, a comparison of the phosphorus-nitrogen double bond of **18** to other iminophosphines is made. It is readily discerned that a short P=N bond length is associated with a large P=N-R angle. In the case of Ph₂FP=NMe, the P=N-C bond angle is 119° therefore the nitrogen can be considered to adopt classical sp² hybridized geometry. In the case of trimethylsilyl iminophosphoranes, the P=N-Si bond angle tends to be very large (*c.f.* Ph₂PCH₂PPh₂(=NSiMe₃), ∠ P=N-Si = 150°; Me₃P=NSiMe₃, ∠ P=N-Si = 145°; 1-(Ph₂P)-2-(Ph₂P(=NSiMe₃))C₆H₄, ∠ P=N-Si = 152°). In the case of **18**, the P=N-C bond angle (142°) is more open than most of the non-silyl iminophosphoranes listed and also has one of the shortest P=N distances (1.514°). It is notable that these parameters indicate a greater P=N bond shortening

and angle widening than was induced by the same imino substituent on the carbon backbone $\text{Ph}_2\text{PCH}_2\text{PPh}_2(=\text{Ntfn})^{27}$ thus it is clear that the interaction also involves the backbone structure. The electron-withdrawing ability of the tfn group in this system suggests that the resonance structure **c** in Figure 3.3 may play a dominant role in the description of the structure of the compound. As mentioned earlier, the P-F bond distance of 1.537\AA is shorter than that usually observed (1.58\AA),³⁴ and this may also be a result of the positive charge induced on the phosphorus(V) atom through the resonance delocalization.

The distance between the $\sigma^2\text{P}$ centre and the imino nitrogen is $3.137(2)\text{\AA}$, which may make it too large to form chelate coordinate complexes but would make it ideal as a bridge between two metal centres. The ability of the ligand to bridge two metals would be aided by its rigid structure and therefore this ligand should be similar in action to the pyridyl phosphines. The *p*-cyanotetrafluorophenylimino moiety (tfn) also stabilizes the bisphosphine but the electron-withdrawing ability of the tfn renders the imino nitrogen much less basic and reduces its coordinating ability thus other imines should be considered as bridging ligands.

The $\nu(\text{CN})$ stretching frequencies for the *p*-cyanotetrafluorophenyl group in the infrared spectrum occurred at 2241 cm^{-1} , shifted to a higher frequency than was observed in the dppm derivatives (2218 cm^{-1} to 2233 cm^{-1}).^{35,36} The P-F stretching frequencies have also shifted to higher frequencies upon oxidation of the exo-phosphorus atom (921 cm^{-1} and 896 cm^{-1}). The $\nu(\text{P}=\text{N})$ vibration was observed at 1498 cm^{-1} .

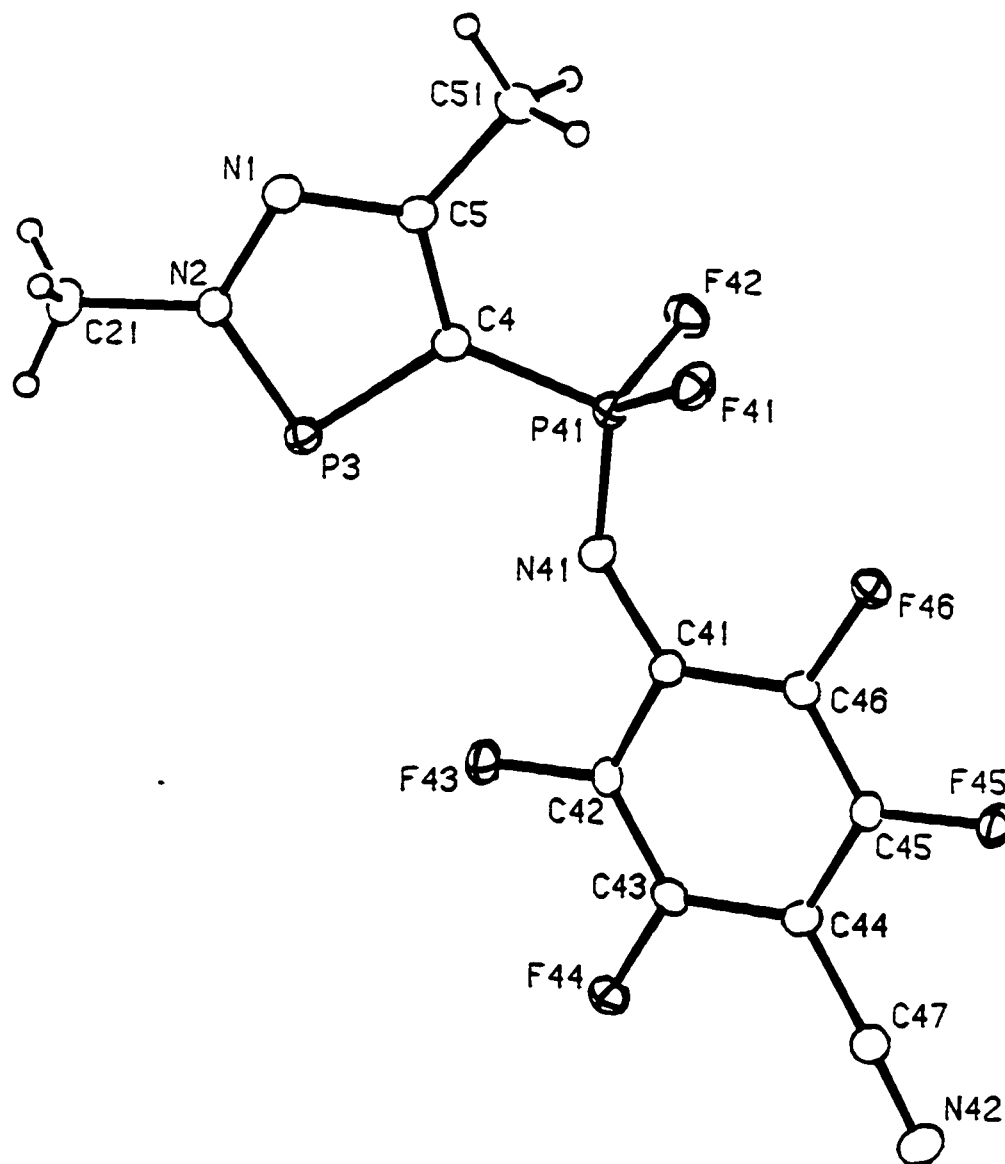


Figure 3.7 Perspective view of 4-(difluoro(*p*-cyanotetrafluorophenyl)imino)phosphorano)-2,5-dimethyl-2*H*-1,2,3 σ^2 -diazaphosphole (18). Non-hydrogen atoms are represented by Gaussian ellipsoids at the 20% probability level. Structure courtesy of Dr. R. McDonald.

Table 3.2

Selected Interatomic Distances (Å) for 4-(Difluoro [*p*-cyanotetrafluorophenyl] imino-phosphorano)-2,5-dimethyl-2*H*-1,2,3σ²-diazaphosphole, (18).

Atom1	Atom2	Distance	Atom1	Atom2	Distance
P3	N2	1.664(2)	N2	C21	1.457(3)
P3	C4	1.720(2)	N41	C41	1.363(3)
P41	F41	1.539(1)	N42	C47	1.136(3)
P41	F42	1.535(1)	C4	C5	1.412(3)
P41	N41	1.514(2)	C5	C51	1.490(3)
P41	C4	1.720(2)	C41	C42	1.404(3)
F43	C42	1.343(2)	C41	C46	1.391(3)
F44	C43	1.340(2)	C42	C43	1.370(3)
F45	C45	1.339(2)	C43	C44	1.381(3)
F46	C46	1.341(2)	C44	C45	1.387(3)
N1	N2	1.358(2)	C44	C47	1.433(3)
N1	C5	1.324(2)	C45	C46	1.374(3)

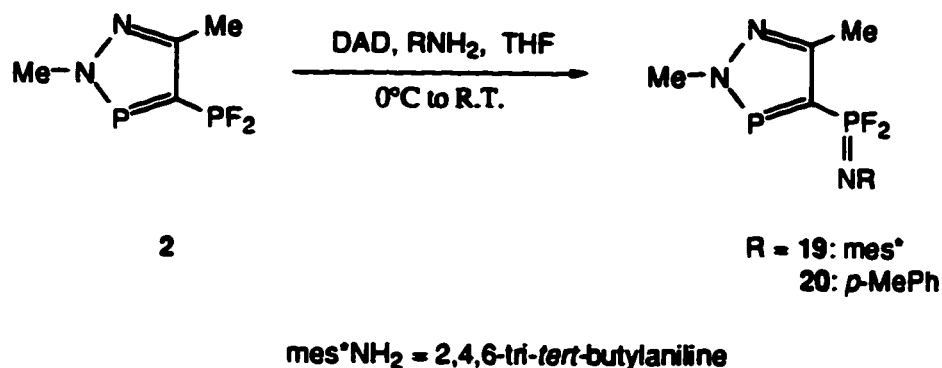
Table 3.3

Selected Interatomic Angles (deg) for 4-(Difluoro(*p*-cyanotetrafluorophenyl)imino-phosphorano)-2,5-dimethyl-2*H*-1,2,3 σ^2 -diazaphosphole, (18).

Atom1	Atom2	Atom3	Angle	Atom1	Atom2	Atom3	Angle
N2	P3	C4	88.20(9)	N41	C41	C46	125.5(2)
F41	P41	F42	97.42(7)	C42	C41	C46	115.8(2)
F41	P41	N41	117.89(9)	F43	C42	C41	119.3(2)
F41	P41	C4	106.57(9)	F43	C42	C43	118.8(2)
F42	P41	N41	114.76(9)	C41	C42	C43	121.9(2)
F42	P41	C4	108.65(8)	F44	C43	C42	119.0(2)
N41	P41	C4	110.5(1)	F44	C43	C44	119.6(2)
N2	N1	C5	109.3(2)	C42	C43	C44	121.4(2)
P3	N2	N1	117.7(1)	C43	C44	C45	117.5(2)
P3	N2	C21	125.7(1)	C43	C44	C47	121.4(2)
N1	N2	C21	116.6(2)	C45	C44	C47	121.1(2)
P41	N41	C41	141.7(2)	F45	C45	C44	119.6(2)
P3	C4	P41	121.0(1)	F45	C45	C46	119.3(2)
P3	C4	C5	110.4(1)	C44	C45	C46	121.2(2)
P41	C4	C5	128.5(2)	C46	C46	C41	118.9(2)
N1	C5	C4	114.4(2)	C46	C46	C45	118.9(2)
N1	C5	C51	118.5(2)	C41	C46	C45	122.2(2)
C4	C5	C51	127.1(2)	N42	C47	C44	179.2(2)
N41	C41	C42	118.6(2)				

3.2.5 Preparation of Iminophosphoranes: Redox-condensation with Diethyl Azodicarboxylate

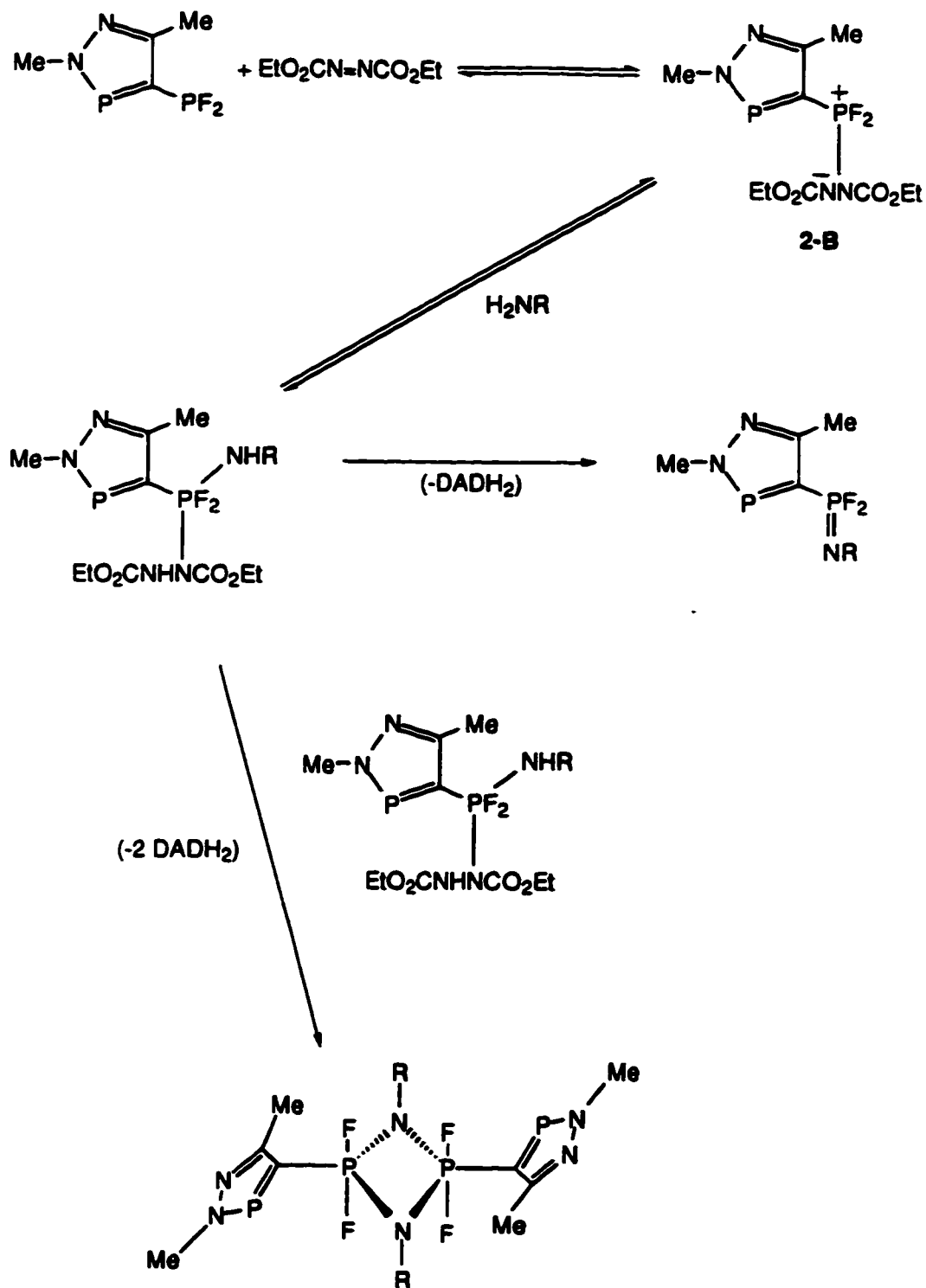
The reaction of the 4-(bis(dimethylamino)phosphino)-2,5-dimethylamino-2H-1,2,3 σ^2 -diazaphosphole with either 2,4,6-tri-*tert*-butylaniline (*mes**NH₂) or *p*-toluidine in the presence of diethyl azodicarboxylate (DAD) gave the σ^2 P- σ^4 P iminophosphorano-diazaphosphole as the major product (Scheme 3.12).



Scheme 3.12 Synthesis of iminophosphoranes *via* redox-condensation.

The oxidation proceeds *via* the betaine intermediate **2-B** (Scheme 3.13) which is stable enough to be observed in the ³¹P{¹H} NMR spectrum, appearing as a peak at 10.34 ppm for the σ^4 P signal and a peak at 266.41 ppm for the σ^2 P resonance. The ²J_{PP} is 96 Hz. In the ¹⁹F NMR spectrum, the chemical shift for the fluorines on the *exo*-phosphorus centre of the betaine intermediate is observed at -27.30 ppm and these fluorine atoms were coupled to both phosphorus centres (¹J _{σ^3 PF} = 971 Hz, ³J _{σ^2 PF} = 51 Hz).

The diethyl hydrazinedicarboxylate (DADH₂) produced during this condensation redox reaction prevented the isolation of these iminophosphoranes because of their similar physical properties. Unlike the iminophosphoranes reported by Bittner,^{7,37} these difluorophosphorano-diazaphospholes were soluble in THF and separation by chromatography was also not possible, thus the methods which were



Scheme 3.13 Formation of the monomeric compounds **19** and **20** and the possible route to the dimeric difluorophosphoranodiazaphospholes (R = *mes**, *p*-MePh).

used by Bittner to purify the compounds could not be applied. The attempted recrystallization of the iminophosphoranodiazaphospholes (**19** and **20**) resulted in the DADH₂ crystallizing out of solution first only when the volume of solvent was reduced to less than 1 mL.

The ³¹P{¹H} NMR spectrum for **19** showed a phosphorus chemical shift for the exo-phosphorus -40.56 ppm with a ²J_{PP} of 88 Hz and the σ²P signal occurred at 266.38 ppm. The ¹⁹F NMR spectrum showed a doublet of doublets for the fluorines on the phosphorus centre (-58.47 ppm, ¹J_{σ³PF} 1079 Hz, ³J_{σ²PF} 10 Hz) which was shifted downfield from the parent compound **2**.

The reaction path depends on the amine used for the redox-condensation. A four-member ring system containing a dimerized aminophosphorane was observed in the reaction of **2** with *p*-toluidine. With the possibility of the dimer being formed, the betaine intermediate must be relatively stable. In the case of the tri-2,4,6-*tert*-butylaniline, the large bulk of the butyl groups should favour the formation of the monomeric iminophosphorane and in agreement, only a small amount of the dimeric species was observed in the ¹⁹F NMR spectrum. With the less bulky *p*-toluidine, there is a greater possibility of the dimeric species being formed.

For the *p*-toluidine derivative, a more complicated ³¹P{¹H} NMR spectrum was observed. The signal for the σ²P centre consisted of one set of doublets (250.14 ppm, ²J_{PP} 110 Hz). Close examination of the region arising from the exo-phosphorus revealed two sets of signals; one set which corresponded to the iminophosphorane **21**, which was sharp, and one other set which was broadened and appeared to be second order. Both sets of resonances had the same chemical shifts and they displayed similar phosphorus-fluorine coupling constants.

The ¹⁹F NMR spectrum of the reaction mixture revealed that three species were present which contained the *p*-toluene functionality on the nitrogen. The resonance for the fluorines of the iminophosphorane species, **20**, was at -58.52 ppm

1077 Hz, $^3J_{\sigma 2PF}$ 10 Hz). One additional aminophosphorane species, showed chemical shifts for inequivalent fluorine signals with one fluorine resonance at -27.27 ppm ($^1J_{\sigma 3PF}$ 756 Hz, $^3J_{\sigma 2PF}$ 10 Hz, $^2J_{FF}$ 90.9 Hz, $^4J_{FF}$ 12.3 Hz) and the other fluorine resonance, at -33.18 ppm, was slightly broadened ($^1J_{\sigma 3PF}$ 734 Hz, $^3J_{\sigma 2PF}$ n.r., $^2J_{FF}$ -80 Hz, $^4J_{FF}$ n.r). A third species showed a broad signal at -49.15 ppm ($^1J_{\sigma 3PF}$ 896 Hz). When the NMR sample was cooled to -10°C, two signals emerged from the broadened resonance which may be attributed to *gauche* and *trans* isomers of the four-membered 1,3,2,4-diazaphosphetidine (Figure 3.8). Similar behaviour has been described for the related diazaphosphetidines $[RF_2PNMe]_2$ (R = Me, Et, OMe).³⁸ For one isomer of 20, the fluorine chemical shift was -51.33 ($^1J_{\sigma 3PF}$ 871 Hz) and the other isomer at -47.38 ($^1J_{\sigma 3PF}$ 910 Hz).

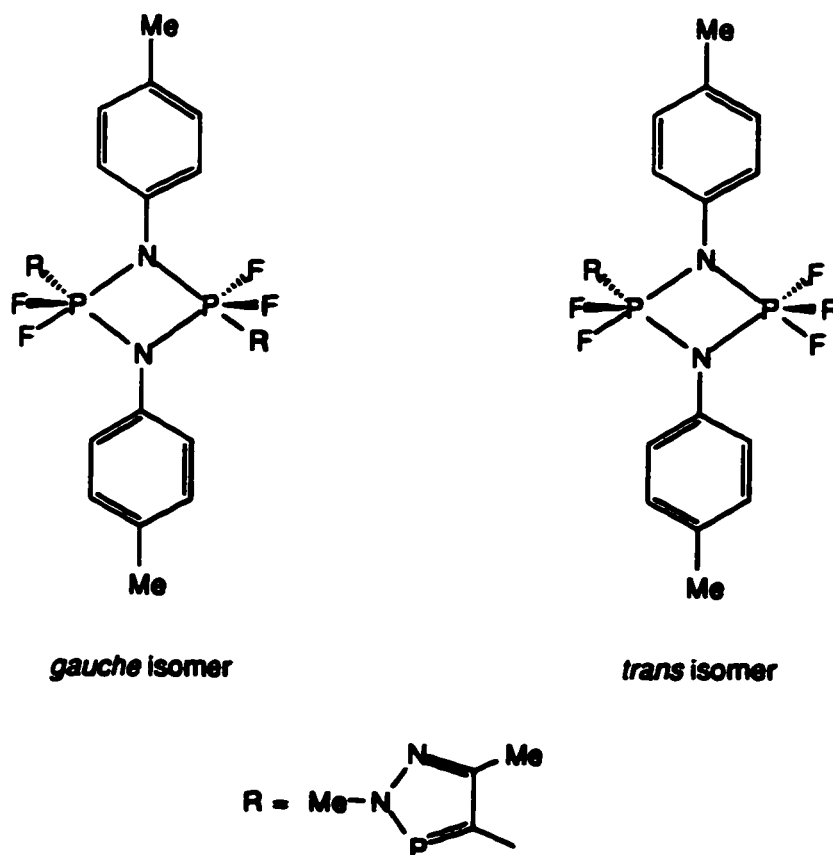
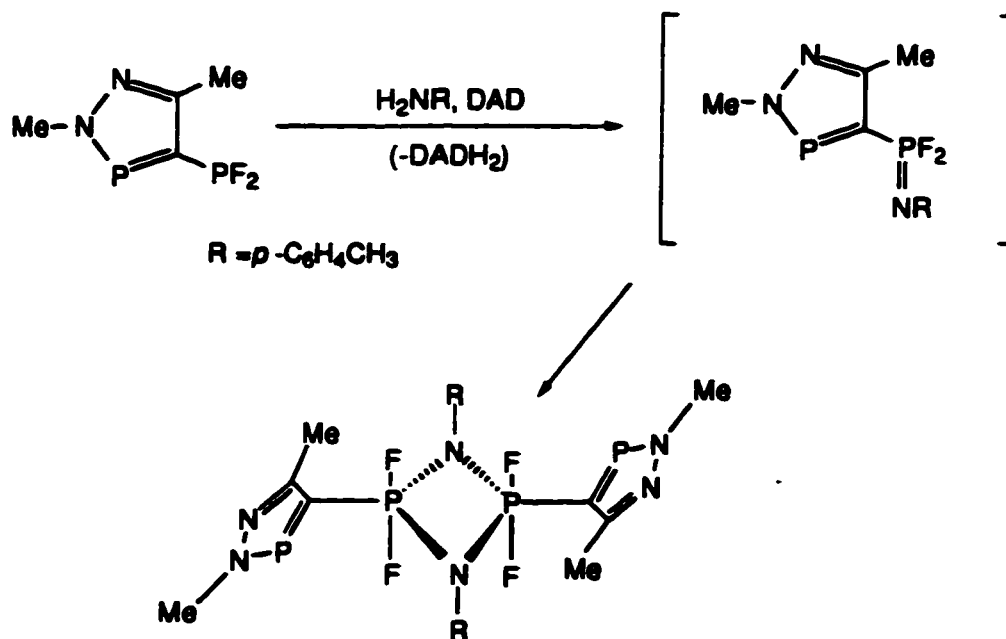


Figure 3.8 *Gauche* and *trans* isomers of compound 20.

Another possible route to the cyclic aminophosphorane is a spontaneous dimerization. It is likely that this dimeric species is more stable than the iminophosphorane (Scheme 3.14).



Scheme 3.14 Dimerization of the iminophosphorane to a phosphetidine.

3.3 Oxidation of 4-(Diaminophosphino)-2,5-dimethyl-2*H*-1,2,3- σ^2 -diazaphospholes

Oxidation of the dimethylamino derivative **3** was explored as a general representative of diaminophosphinodiazaphosphole systems. As in the case of the difluorophosphinodiazaphosphole **2**, oxidation of **3** occurred exclusively at the exo-phosphorus centre to form the $\sigma^2\text{P}-\sigma^4\text{P}$ bisphosphine system. This oxidation of the exo-phosphorus centre was achieved using elemental sulfur, elemental selenium, trimethylsilyl azide, or *p*-tetrafluorobenzonitrile azide. It is interesting to note that the use of electron-withdrawing groups on the azide facilitates the formation of the iminophosphorane since the reaction of *p*-tetrafluorobenzonitrile azide occurs readily at -78°C whereas refluxing conditions are required with the trimethylsilyl azide.

3.3.1 Oxidation with Chalcogens

The oxidation of the dimethylamino derivative **3** with either sulfur or selenium in refluxing toluene resulted in white crystalline products for both chalcogens (**21**, E = S; **22**, E = Se). These compounds are less sensitive towards moisture than their difluoro analogues **16** and **17**.

The $^{31}\text{P}\{^1\text{H}\}$ NMR spectra for both chalcogen derivatives showed a large upfield shift for the exo-phosphorus signal (E = S: 70.83 ppm; E = Se: 66.63 ppm) and a downfield shift for the resonance for the $\sigma^2\text{P}$ centre (E = S: 255.12 ppm; E = Se: 257.19 ppm). An increase in the $^2\text{J}_{\text{PP}}$ was also observed (E = S: 76 Hz; E = Se: 84 Hz). Unlike the difluoro analogues, **17** and **18**, the only coupling observed in the phosphorus spectrum was that between inequivalent phosphorus centres $^2\text{J}_{\text{PP}}$, and this gives the spectrum a typical AX appearance.

The oxidation with the chalcogens yielded a large increase in the phosphorus-carbon coupling constants for the carbon at the 4-position (E = S: 144.68 ppm; E = Se: 145.16 ppm) for $^1\text{J}_{\sigma^2\text{PC}}$ (E = S: 123 Hz; E = Se: 157 Hz) and $^1\text{J}_{\sigma^4\text{PC}}$ (E = S: 47 Hz; E = Se: 43 Hz) relative to the unoxidized phosphinodiazaphosphole **3** ($^1\text{J}_{\sigma^2\text{PC}}$ = 54 Hz; $^1\text{J}_{\sigma^3\text{PC}}$ 9 Hz). There was a decrease in J_{PC} for the carbons at the 5-position (E = S: 155.29 ppm, $^2\text{J}_{\sigma^2\text{PC}}$ 5 Hz, $^2\text{J}_{\sigma^4\text{PC}}$ 5 Hz; E = Se: 154.54 ppm, $^2\text{J}_{\sigma^2\text{PC}}$ n.o., $^2\text{J}_{\sigma^4\text{PC}}$ 5 Hz). There was a slight upfield shift for the 2-methyl carbon signal and $^2\text{J}_{\sigma^2\text{PC}}$ was observed (E = S: 41.18 ppm, $^2\text{J}_{\sigma^2\text{PC}}$ 18 Hz; E = Se: 41.12 ppm, $^2\text{J}_{\sigma^2\text{PC}}$ 18 Hz). Coupling to phosphorus was not observed for the methyl carbons at the 5-position (E = S: 15.60 ppm, E = Se: 15.84 ppm).

In the ^1H NMR spectra, the signals for the 2-methyl protons had shifted downfield slightly (E = S: 3.95 ppm, $^3\text{J}_{\sigma^2\text{PH}}$ 7.9 Hz; E = Se: 3.96 ppm, $^3\text{J}_{\sigma^2\text{PH}}$ 7.9 Hz). The chemical shift for the 4-methyl proton signals were relatively constant throughout the series but a phosphorus-proton coupling was observed to both

phosphorus centres (E = S: 2.50 ppm, $^4J_{\sigma^2\text{P}\text{H}}$ 1.3 Hz, $^4J_{\sigma^4\text{P}\text{H}}$ 1.3 Hz; E = Se: 2.50 ppm, $^4J_{\sigma^2\text{P}\text{H}}$ 1.3 Hz, $^4J_{\sigma^4\text{P}\text{H}}$ 1.0 Hz). The coupling between the protons in the dimethylamino groups to the phosphorus had increased (E = S: 2.63 ppm, $^3J_{\sigma^4\text{P}\text{H}}$ 13.0 Hz; E = Se: 2.64 ppm, $^3J_{\sigma^4\text{P}\text{H}}$ 12.4 Hz).

The infrared spectrum for the thio derivative **22**, showed the stretching frequency $\nu(\text{P}=\text{S})$ at 723 cm^{-1} . For compound **23**, $\nu(\text{P}=\text{Se})$ was observed at 542 cm^{-1} . With both compounds, there was a slight shift to higher frequencies for the P-N stretches (E = S, $\nu(\text{P}-\text{N})$ 735 cm^{-1} and 715 cm^{-1} ; E = Se, $\nu(\text{P}-\text{N})$ 716 cm^{-1} and 692 cm^{-1}).

3.3.2 Iminophosphoranephosphole Derivatives: Oxidation with Azides

The reaction mixture of **3** and two equivalents of trimethylsilyl azide was refluxed in toluene for one day. The toluene and excess azide were removed *in vacuo* to yield **23**, in almost quantitative yield, as an amber viscous oil. Attempts to either crystallize or distill the oil resulted in its decomposition.

To prepare the *p*-cyanotetrafluorophenylimino derivative, **24**, *p*-cyanotetrafluoro-phenyl azide was added to a dichloromethane solution of **3** at -78°C . The solution quickly turned bright yellow, indicating the formation of the phosphazide. The solution was allowed to warm to room temperature and the bright yellow colour slowly faded to light amber. The solvent was removed *in vacuo*, giving an amber oil.

The $^{31}\text{P}\{^1\text{H}\}$ NMR spectra for both imino derivatives **23** and **24** showed a large upfield shift for the signal for the exo-phosphorus centre (E = Ntfn: 44.81 ppm; E = SiMe₃: 8.10 ppm) and a downfield shift for the $\sigma^2\text{P}$ centre resonances (E = Ntfn, 256.09 ppm; E = SiMe₃, 253.50 ppm) with a decrease in the $^2J_{\text{PP}}$ (E = Ntfn: 65 Hz; E = SiMe₃: 68 Hz).

The oxidation with both azides resulted in a large increase in the phosphorus-carbon coupling constants for the carbon at the 4-position of the diazaphosphole ring (E = Ntfbn: 134.03 ppm; E = NSiMe₃: 143.60 ppm) for $^1J_{\sigma 2PC}$ (E = Ntfbn: 147 Hz; E = NSiMe₃: 155 Hz) and $^1J_{\sigma 4PC}$ (E = Ntfbn: 52 Hz; E = NSiMe₃: 49 Hz) as was observed in the case of the chalcogen derivatives. There was a decrease in the J_{PC} value for the carbons at the 5-position of the ring (E = Ntfbn: 155.3 ppm, $^2J_{\sigma 2PC}$ 5 Hz, $^2J_{\sigma 4PC}$ 5 Hz; E = NSiMe₃: 154.5 ppm, $^2J_{\sigma 2PC}$ 7 Hz, $^2J_{\sigma 4PC}$ 5 Hz). There was a slight upfield shift for the 2-methyl carbon resonances and $^2J_{\sigma 2PC}$ was observed (E = Ntfbn: 41.24 ppm, $^2J_{\sigma 2PC}$ 18 Hz; E = NSiMe₃: 40.75 ppm, $^2J_{\sigma 2PC}$ 18 Hz). Coupling to the phosphorus was not observed for the methyl carbons at the 5-position (E = Ntfbn: 15.94 ppm; E = NSiMe₃: 15.05 ppm).

The 1H NMR signals for the 2-methyl group in **23** and **24** shifted downfield slightly upon oxidation (E = Ntfbn: 3.97 ppm, $^3J_{\sigma 2PH}$ 7.9 Hz; E = NSiMe₃: 3.88 ppm, $^3J_{\sigma 2PH}$ 7.4 Hz) relative to the parent diazaphosphole **3**. The chemical shift for the 4-methyl proton signals were relatively unchanged. No phosphorus-proton coupling was observed to either of the phosphorus centres (E = Ntfbn: 2.50 ppm; E = NSiMe₃: 2.50 ppm). The coupling of the protons of the dimethylamino groups to the phosphorus had increased (E = Ntfbn: 2.95 ppm, $^3J_{\sigma 4PH}$ 10.7 Hz; E = NSiMe₃: 2.82 ppm, $^3J_{\sigma 4PH}$ 11.5 Hz).

The $\nu(P=N)$ stretch in the imine appeared at 1377 cm⁻¹ in the infrared spectrum for the trimethylsilyl derivative **23** which is similar to the behaviour of other P=NSiMe₃ compounds.^{22,32} With the tfbn substituent (**24**), $\nu(P=N)$ was observed at 1492 cm⁻¹ along with the characteristic $\nu(CN)$ at 2237 cm⁻¹.

3.4 Oxidation of 4-(Di(2,2,2-trifluoroethoxy)phosphino)-2,5-dimethyl-2H-1,2,3 σ^2 -diazaphosphole

3.4.1 Oxidation using Elemental Selenium and *p*-Cyanotetrafluorophenyl Azide

Compound **6** was oxidized by elemental selenium in refluxing toluene for one day to obtain the $\sigma^2\text{P}$ - $\sigma^4\text{P}$ bisphosphine 4-(di-(2,2,2-trifluoroethoxy)-selenophosphorano-2,5-dimethyl-2H-1,2,3 σ^2 -diazaphosphole, **25**, with a yield of 76% as an off-white moisture-sensitive solid.

Similar conditions used for the reaction of *p*-tetrafluorobenzonitrile azide with **11**, as were for **2** and **3**, at which the addition of the azide took place at -78°C . The solution was stirred overnight and during this time it was allowed to slowly warm up to room temperature. The volatile materials were removed *in vacuo* leaving a white solid. The yield of **26** was 84%.

The $^{31}\text{P}\{^1\text{H}\}$ NMR spectra for both compounds showed two sets of doublets, one corresponding to the $\sigma^2\text{P}$ centre (E = Se: 259.01 ppm; E = Ntfbn: 260.12 ppm) and the other to the $\sigma^3\text{P}$ centre (**25**, E = Se: 87.41 ppm, $^2J_{\text{PP}}$ 108; **26**, E = Ntfbn: 11.95 ppm, $^2J_{\text{PP}}$ 84). Selenium satellites were observed with the selenophosphorane **25** ($^1J_{\text{PSe}}$ 893 Hz), but the value was smaller than that for the difluoro analogue **2** (1022 Hz) and larger than the bisdimethylamine derivative **3** (751 Hz). The ^{77}Se NMR spectrum of **25** revealed a chemical shift for the resonance similar to the other seleno derivative **22** (249.61 ppm) and the signal showed coupling to both phosphorus centres ($^3J_{\sigma^2\text{PSe}}$ 30 Hz; $^1J_{\sigma^4\text{PSe}}$ 893 Hz). Unlike the unoxidized phosphinodiazaphosphole **3**, phosphorus-fluorine coupling was not observed in both compounds.

Upon oxidation by selenium or *p*-cyanotetrafluorophenyl azide the diazaphosphole products resulted in an increase in the phosphorus-carbon coupling constants for the carbon at the 4-position of the diazaphosphole ring but the chemical shift of this carbon signal remained unchanged in both **25** and **26** (E = Se: 144.17

ppm, $^1J_{\sigma 2PC}$ 139 Hz, $^1J_{\sigma 4PC}$ 43 Hz; E = Ntfbn: 128.79 ppm, $^1J_{\sigma 2PC}$ 139 Hz, $^1J_{\sigma 4PC}$ 53 Hz), relative to the parent phosphinodiazaphosphole **11**. A phosphorus-carbon coupling was not observed for the carbon at the 5-position of the diazaphosphole ring for either compound (**25** and **26**) (E = Se: 155.66 ppm; E = Ntfbn: 156.31 ppm). There was a slight upfield shift for the 2-methyl carbon resonances and $^2J_{\sigma 2PC}$ coupling to this carbon was observed (E = Se: 41.38 ppm, $^2J_{\sigma 2PC}$ 18 Hz; E = Ntfbn: 41.45 ppm, $^2J_{\sigma 2PC}$ 18 Hz). Once again coupling to the phosphorus was not observed for either of the methyl carbons at the 5-position of the diazaphosphole ring (E = Se: 14.77 ppm; E = Ntfbn: 14.98 ppm).

The 1H NMR signal for the protons of the 2-methyl group of the ring were shifted downfield slightly (E = Se: 3.96 ppm, $^3J_{\sigma 2PH}$ 8.4 Hz; E = Ntfbn: 4.01 ppm, $^3J_{\sigma 2PH}$ 8.6 Hz). The chemical shifts for the 4-methyl proton signals were relatively unchanged and again, phosphorus-proton coupling was not observed (E = Se: 2.48 ppm; E = Ntfbn: 2.51 ppm). Oxidation of the exo-phosphorus did not alter the values of the chemical shift in the methylene protons of the trifluoroethoxy group (E = Se: 3.89 ppm; E = Ntfbn: 3.94 ppm) relative to the parent compound **11**, though the proton spectrum became a complex second order spectrum as a result of coupling to the fluorine atoms as well as to the exo-phosphorus centre.

The ^{19}F NMR spectra of the oxidized compounds **25** and **26** were greatly simplified, compared to that of the parent phosphine **11**. The splitting pattern for the fluorine signal was a triplet, whereas in **11** this fluorine signal was a doublet of doublet of triplets. The chemical shift values were essentially unchanged after oxidation of the exo-phosphorus centre and the resonances showed coupling to only the methylene protons ($^3J_{FH}$ 8.1 Hz; E = Se: -75.12 ppm, $^3J_{FH}$ 8.0 Hz; E = Ntfbn: -75.35 ppm). The chemical shifts for the *ortho* and the *meta* fluorine resonances on the tfbn ring were observed at -152.95 ppm ($^4J_{\sigma 4PF}$ 5.7 Hz) and 140.95 ppm, respectively.

The $\nu(\text{P}=\text{Se})$ stretching frequency in **25** was assigned to the peak observed at 542 cm^{-1} . In the case of **26**, the $\nu(\text{P}=\text{N})$ stretching frequency was observed at 1489 cm^{-1} and the $\nu(\text{CN})$ frequency at 2235 cm^{-1} .

3.5 The Attempted Oxidation of 4-(Bis(dimethylaminothiophosphorano))-2,5-dimethyl-2*H*-1,2,3 σ^2 -diazaphosphole, **21**.

In an attempt to see whether the vulnerability of the cyclic phosphorus centre to oxidation was affected by the oxidation of the exo-phosphorus centre, 4-(bis(dimethylaminothiophosphorano))-2,5-dimethyl-2*H*-1,2,3 σ^2 -diazaphosphole (**21**) was refluxed in toluene with an excess of trimethylsilyl azide for a period of 24 hours, after which the volatile materials were removed *in vacuo*. The $^{31}\text{P}\{^1\text{H}\}$ NMR spectrum of the remainder showed that there was no change in the chemical shift signal of the cyclic phosphorus centre hence no oxidation had occurred.

3.6 Summary

The oxidation of phosphinodiazaphospholes which contain fluorines, amino groups or alkoxy groups on the exo-phosphorus atom was achieved by either chalcogens or azides to yield products in which there was exclusive oxidation at the exo-phosphorus centre. In addition to the conversion of the trivalent centre to the pentavalent state, a variety of substituents can be introduced to the bisphosphine system to create potential heterobifunctional ligands. The oxidation of the exo-phosphorus centre resulted in a dramatic upfield shift of the phosphorus NMR signals which arise from this phosphorus atom and there was also a substantial increase in the $^1\text{J}_{\text{PC}}$ coupling constants, especially in the system with the *p*-cyanotetrafluorophenyl (tfbn) moiety on the imino group. Oxidation of the difluorophosphinodiazaphosphole with diethyl azodicarboxylate (DAD) gave the iminophosphorane with a 2,4,6-tri-*tert*-butylaniline (mes*) substituent but with

p-toluidine the cyclized diazadiphosphetidine was the major product. Oxidation with trimethylsilyl azide creates the silylimide and there is potential for this compound to undergo further coupling reactions which will be discussed in the next chapter. These alterations of the substituents on the imino nitrogen changes its basicity. Addition of different chalcogens to the exo-phosphorus centre also creates systems with dissimilar basic character at the different donor centres. All of these variations provide many possibilities for "fine-tuning" the reactivity of the bisphosphine which are awaiting to be explored.

Table 3.4

$^3\text{J}[\text{P}\{\text{H}\}]$ NMR Data for Oxidized 4-(Phosphorano)-2,5-dimethyl-2H-1,2,3 σ^2 -diazaphospholes,^{a,b}

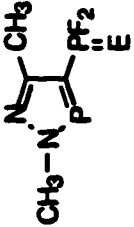
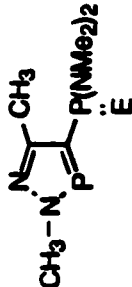
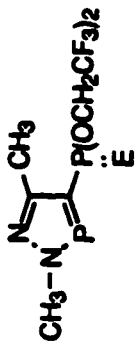
Compound	E	No.	$\delta \sigma^2\text{P}$ (ppm)	$\delta \sigma^4\text{P}$ (ppm)	$^2\text{J}_{\text{PP}}$ (Hz)	$^1\text{J}_{\text{PF}}$ (Hz)	$^1\text{J}_{\text{PSe}}$ (Hz)
	S	16	264.25 ^c	82.47 ^d	112	1133	-
	Se	17	265.10 ^c	87.50 ^d	118	1177	1022
	Nitbn	18	265.70 ^c	2.66 ^d	83	1145	-
	NMes*	19	266.38 ^c	-40.56 ^d	88	962	-
	N(<i>p</i> -MeC ₆ H ₄)	20	266.41 ^c	10.34 ^d	96	971	-
	S	21	255.12 ^c	70.83 ^c	76	-	-
	Se	22	257.19 ^c	66.63 ^c	84	-	751
	Nitbn	23	257.29 ^c	64.81 ^c	65	-	-
	NSiMe ₃	24	253.50 ^c	8.10 ^c	68	-	-

Table 3.4 continued

Compound	E	No.	$\delta \sigma^2\text{P}$ (ppm)	$\delta \sigma^4\text{P}$ (ppm)	$^2J_{\text{PP}}$ (Hz)	$^1J_{\text{PF}}$ (Hz)	$^1J_{\text{PSe}}$ (Hz)
	Se	25	259.01 ^c	87.41 ^c	108	-	893
	Ntfn	26	260.12 ^c	11.95 ^c	84	-	-

a) Chemical shifts δ in ppm with respect to 85% H_3PO_4 .

b) in CDCl_3

c) doublet

d) doublet of triplets

Table 3.5

¹³C (1H) NMR Data for Diazaphosphole Carbons in 4-(Phosphino)-2,5-dimethyl-2H-1,2,3σ²-diazaphospholes.^a

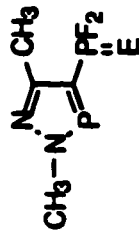
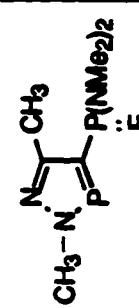
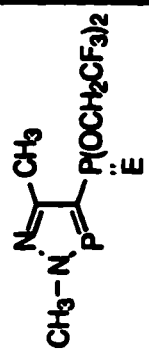
Compound	E	No.	δ N-CH ₃ (ppm)	² J _{σ2PC} (Hz)	δ C-4 (ppm)	¹ J _{σ2PC} (Hz)	¹ J _{σ3PC} (Hz)	δ C-5 (ppm)	² J _{σ2PC} (Hz)	² J _{σ3PC} (Hz)	δ C-CH ₃ (ppm)
 <chem>CN=C(C)P(=O)(F)F</chem> E	S	16	41.49 ^c	17	141.21 ^d	163	59	156.20 ^e	-	1	14.95
	Se	17	41.79 ^c	17	140.39 ^d	160	64	155.46	-	-	15.10
	Nifbn	18	41.92 ^c	18	125.17 ^d	246	45	158.21 ^c	-	13	15.01
	NMes*	19	41.81 ^c	17	140.78 ^d	159	61	155.78	-	-	15.02
	N(p- MeC ₆ H ₄)	20	41.83 ^c	17	141.02 ^d	165	60	156.12	-	-	14.97
 <chem>CN=C(C)P(=O)(N)N</chem> E	S	21	41.18 ^c	18	144.68 ^d	123	47	155.29 ^d	5	5	15.60
	Se	22	41.21 ^c	18	145.16 ^d	157	43	154.54 ^c	-	5	15.84
	Nifbn	23	41.24 ^c	18	134.03 ^d	147	52	156.78 ^d	5	5	15.95
	NSiMe ₃	24	40.75 ^c	18	143.60 ^d	155	49	156.27 ^d	7	7	15.05

Table 3.5 continued

Compound	E	No.	δ N-CH ₃ (ppm)	² J _{σ2PC} (Hz)	δ C-4 (ppm)	¹ J _{σ2PC} (Hz)	¹ J _{σ3PC} (Hz)	δ C-5 (ppm)	² J _{σ2PC} (Hz)	² J _{σ3PC} (Hz)	δ C-CH ₃ (ppm)
	Se	25	41.38 ^c	18	142.17	144	43	155.66	n.r.	n.r.	14.77
	Ntfn	26	41.45 ^c	18	128.79	139	53	156.31 ^d	5	5	14.98

a) Chemical shifts δ in ppm with respect to SiMe₄.

b) in CDCl₃

c) doublet

d) doublet of doublets

Table 3.6

¹H NMR Data for Diazaphosphole Protons in Oxidized 4-(Phosphorano)-2,5-dimethyl-2H-1,2,3σ²-diazaphospholes, a,b

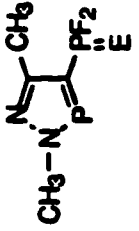
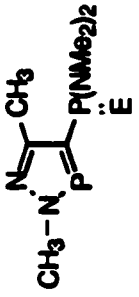
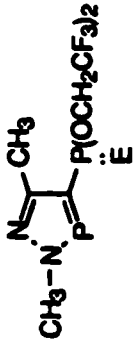
Compound	E	No.	δ CH ₃ -N (ppm)	³ J _{σ²PH} (Hz)	δ C-CH ₃ (ppm)	⁴ J _{σ²PH} (Hz)	⁴ J _{σ³PH} (Hz)
 <chem>CN1C=NC(P1)C(F)(F)E</chem>	S	16	3.94 ^c	8.6	2.39 ^c	-	0.9
	Se	17	4.02 ^c	8.6	2.51	-	-
	Nrfbn	18	4.14 ^c	8.9	2.61	-	n.r.
	NMcs*	19	4.03 ^c	8.4	2.59	-	n.r.
	N(<i>p</i> -MeC ₆ H ₄)	20	4.03 ^c	8.3	2.59	-	-
 <chem>CN1C=NC(P1)C(N)N</chem>	S	21	3.95 ^c	7.7	2.51 ^d	1.5	0.5
	Se	22	3.95 ^c	7.9	2.64 ^d	1.1	1.1
	Nrfbn	23	3.97 ^c	7.9	2.42 ^c	-	-
	SiMe ₃	24	3.88 ^c	7.4	2.41 ^c	n.r	n.r

Table 3.6 continued

Compound	E	No.	δ CH ₃ -N (ppm)	³ J _{σ²PH} (Hz)	δ C-CH ₃ (ppm)	⁴ J _{σ²PH} (Hz)	⁴ J _{σ³PH} (Hz)
	Se	25	3.96 ^c	8.4	2.48	-	-
	Ntfn	26	4.01 ^c	8.6	2.51	-	-

a) Chemical shifts δ in ppm with respect to SiMe₄.


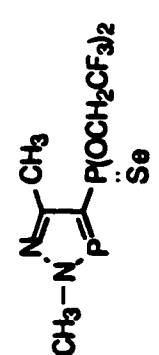
b) in CDCl₃

c) doublet

d) doublet of doublets

Table 3.7

⁷⁷Se NMR Data for 4-(Selenophosphorano)-2,5-dimethyl-2H-1,2,3σ²-diazaphospholes. a,b

Compound	No.	δ Se (ppm)	¹ J _{σ⁴PSe} (Hz)	³ J _{σ²PSe} (Hz)
	2	-245.04 ^c	751	41
	2	-249.61 ^c	893	30

a) Chemical shifts δ in ppm with respect to Me₂Se₂.

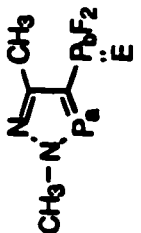
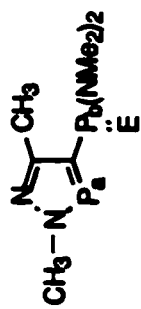
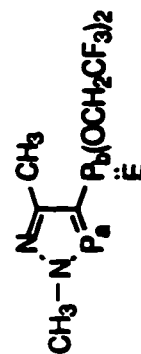
b) in CDCl₃

c) doublet

d) doublet of doublets

Table 3.8

Infrared Data for Oxidized 4-(Phosphorano)-2,5-dimethyl-2H-1,2,3σ²-diazaphospholes.

Compound	E	No.	v(P=E) (cm ⁻¹)	v(P-F) (cm ⁻¹)	v(P-N) (cm ⁻¹)	v(CN) (cm ⁻¹)
	S	16	726	853, 823	-	-
	Se	17	533	869, 841	-	-
	Ntfn	18	1498	921, 896	-	2241
	S	21	723	-	735, 715	-
	Se	22	542	-	716, 692	-
	Ntfn	23	1492	-	851, 816	2237
	NSiMe ₃	24	1377	-	862, 828	-
	Se	25	542	-	-	-
	Ntfn	26	1489	-	-	2235

3.7 References

- (1) Gilheany, D. G. In *The Chemistry of Organophosphorus Compounds*; F. R. Hartley, Ed.; Wiley: New York, 1990; Vol. 1; pp 9.
- (2) Gilheany, D. G. In *The Chemistry of Organophosphorus Compounds*; F. R. Hartley, Ed.; Wiley: New York, 1992; Vol. 2; pp 1.
- (3) Gilheany, D. G. *Chem. Rev.* **1994**, *94*, 1339.
- (4) Gilheany, D. G. In *The Chemistry of Organophosphorus Compounds*; F. R. Hartley, Ed.; Wiley: New York, 1994; Vol. 3; pp 1.
- (5) Staudinger, H.; Meyer, J. *Helv. Chim. Acta.* **1919**, *2*, 635.
- (6) Kirsanov, A. V. *Izv. Akad. Nauk SSSR, Otd. Khim. Nauk* **1950**, 426.
- (7) Bittner, S.; Assaf, Y.; Krief, P.; Pomerantz, M.; Ziemnicka, B. T.; Smith, C. *G. J. Org. Chem.* **1985**, *50*, 1712.
- (8) Appel, R.; Ruppert, I. *Chem. Ber.* **1978**, *111*, 751.
- (9) Leffler, J. E.; Tsuno, T. *J. Org. Chem.* **1963**, *28*, 902.
- (10) Thayer, J. S.; West, R. *Inorg. Chem.* **1964**, *3*, 402.
- (11) Horner, L.; Gross, A. *Liebigs Annal.* **1955**, *591*, 117.
- (12) Goldwhite, H.; Gysegem. St. Schow, P.; Swyke, C. H. *J. Chem. Soc., Dalton Trans.* **1975**, 16.
- (13) Leffler, J. E.; Temple, R. D. *J. Am. Chem. Soc.* **1967**, *89*, 5235.
- (14) Gololobov, Y. G.; Zhmurova, I. N.; Kasukhin, L. F. *Tetrahedron* **1981**, *37*, 437.
- (15) Bock, H.; Schnoller, M. *Angew. Chem. Int. Ed. Eng.* **1968**, *7*, 636.
- (16) Bock, H.; Schnoller, M. *Chem. Ber.* **1969**, *102*, 38.
- (17) Gololobov, Y. G.; Kasukhin, L. F. *Tetrahedron* **1992**, *48*, 1353.
- (18) Heesing, A.; Steinkamp, H. *Chem. Ber.* **1982**, *115*, 2854.
- (19) Baccolini, G.; Todesco, P. E.; Bartoli, G. *Phosphorus Sulfur* **1981**, *10*, 387.

- (20) Wilson, S. R.; Pasternak, A. *Synlett* **1990**, 199.
- (21) Weinmaier, J. H.; Brunnhuber, G.; Schmidpeter, A. *Chem. Ber.* **1980**, *113*, 2278.
- (22) Katti, K. V.; Batchelor, R. J.; Einstein, F. W. B.; Cavell, R. G. *Inorg. Chem.* **1990**, *29*, 808.
- (23) Bernard-Moulin, P.; Pouzard, G. *J. Chim. Phys.* **1979**, *76*, 708.
- (24) Daasch, L. W.; Smith, D. C. *Anal. Chem.* **1951**, *23*, 853.
- (25) Thomas, L. C.; Chittenden, R. A. *Chem. Ind. (London)* **1964**, 1913.
- (26) Adamson, G. W.; Bart, J. C. *J. Chem. Soc. (A)* **1970**, 1452.
- (27) Katti, K. V.; Santarsiero, B. D.; Pinkerton, A. A.; Cavell, R. G. *Inorg. Chem.* **1993**, *32*, 5919.
- (28) Schmidbaur, H.; Bowmaker, G. A.; Kumberger, O.; Müller, G.; Wolfsberger, W. *Z. Naturforsch.* **1990**, *45b*, 476.
- (29) Böhm, E.; Dehnicke, K.; Beck, J.; Hiller, W.; Strähle, J.; Maurer, A.; Fenske, D. *Z. Naturforsch.* **1988**, *43b*, 138.
- (30) Kaiser, J.; Hartung, H.; R., R. *Z. anorg. allg. Chem.* **1980**, *469*, 188.
- (31) Ang, H. G.; Cai, Y. M.; Koh, L. L.; Kwik, W. L. *J. Chem. Soc. Chem. Commun.* **1991**, 850.
- (32) Reed, R. W.; Santarsiero, B.; Cavell, R. G. *Inorg. Chem.* **1996**, *35*, 4292.
- (33) Astrup, E. E.; Bouzga, A. M.; Starzweski, A. O. *J. Mol. Str.* **1987**, *51*, 51.
- (34) Corbridge, D. E. C. *The Structural Chemistry of Phosphorus*; Elsevier Scientific Publishing Co.: New York, 1974, pp 7.
- (35) Imhoff, P.; Van Asselt, R.; Elsevier, C. J.; Vrieze, K.; Goubitz, K.; Van Malssen, K. F.; Stam, C. H. *Phosphorus, Sulphur and Silicon* **1990**, *47*, 401.
- (36) Mozol, V. J. M.Sc. Thesis, University of Alberta, 1993.
- (37) Bittner, S.; Pomerantz, M.; Assaf, Y.; Krief, P.; Xi, S.; Witczak, M. K. *J. Org. Chem.* **1988**, *53*, 1.

- (38) Harris, R. K.; Wazeer, M. I. M.; Schlak, O.; Schmutzler, R. *Phosphorus and Sulfur* **1981**, *11*, 221.

CHAPTER 4

METAL COMPLEXATION OF 4-(PHOSPHINO)-2,5-DIMETHYL-
2*H*-1,2,3σ²-DIAZAPHOSPHOLE DERIVATIVES

4.1 Introduction

The 4-phosphinodiazaphosphole has three possible coordination sites, the two-coordinate nitrogen in the ring, the two-coordinate phosphorus in the ring, and the three-coordinate exo-phosphorus. This phosphinodiazaphosphole is unlikely however to act as a bischelate, such as is observed with bis(diphenylphosphino)methane, because the backbone carbon is sp² hybridized, the P-C-P framework is extremely rigid and the bite angle too large to coordinate to a metal centre to make a four-membered metallacycle. These factors however, along with the presence of two phosphorus centres, suggests that this ligand system could conceivably coordinate to two metal centres in a bridging fashion (Figure 4.1). By exploiting the different basicities of the two phosphorus centres, it may be possible to synthesize heterobimetallic complexes in a stepwise process.



Figure 4.1 Monodentate coordination and bridging action of the phosphino-2,5-dimethyl-2*H*-1,2,3σ²-diazaphospholes with metal centres.

The oxidation of the exo-phosphorus improves the possibility for the phosphoranodiazaphospholes to chelate to form a five-membered metallocycle on one metal (Figure 4.2). Having removed the previous available electron lone pair on the

exo-phosphorus centre by oxidation, coordination of the $\sigma^2\text{P}$ centre may be more favoured. Once again, this ligand system, having two coordinating moieties with different basicities, may possibly form heterobimetallic complexes.



Figure 4.2 Monodentate and chelating coordination of the phosphorano-2,5-dimethyl-2H-1,2,3 σ^2 -diazaphosphole with metal centres.

The characterization of these coordination complexes is aided by $^{31}\text{P}\{^1\text{H}\}$ NMR spectroscopy. The assignment of many of the structures is readily elucidated from the coupling constants between the metal and the phosphorus, $^1J_{\text{PM}}$, and from the coupling constant of the bound phosphorus with the other structural or backbone phosphorus and with other NMR active nuclei such as fluorine present in the molecule.

4.2 Metal Complexes of Phosphines

One characteristic feature of the transition metals is their ability to form complexes with neutral molecules such as carbon monoxide, isocyanides, phosphines, and various molecules with delocalized π orbitals such as olefins. The bonding in transition metal-ligand complexes is usually described in terms of the Dewar-Chat model of a σ -donation accompanied by a synergic π -back-donation.^{1,2} The latter component is essential to stabilization as it reduces the increase in electron density on the metal centre conferred by the σ -donation. For carbon monoxide, it has long been recognized that the acceptance of electron density from the metal centre occurs

through the π^* orbitals of the CO molecule as shown in Figure 4.3. This backbonding also increases the M-CO bond order and concomitantly decreases the C-O bond order.

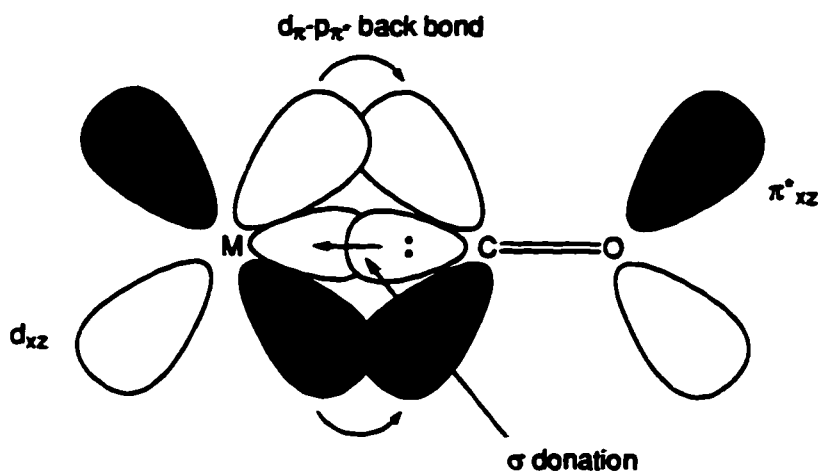


Figure 4.3 Molecular orbital picture of transition metal carbonyls.

For the PR_3 , the parallel classical description of the bonding involves an electron pair donation from the phosphorus and the metal d orbitals back-donate this electron density into empty phosphorus d orbitals in a $d\pi-d\pi$ combination. An alternative view, which has recently gained acceptance, is that the π -back-donation from the metal centre occurs by connecting the metal d orbitals with P-R σ^* antibonding orbitals^{3,4} as shown in Figure 4.4.

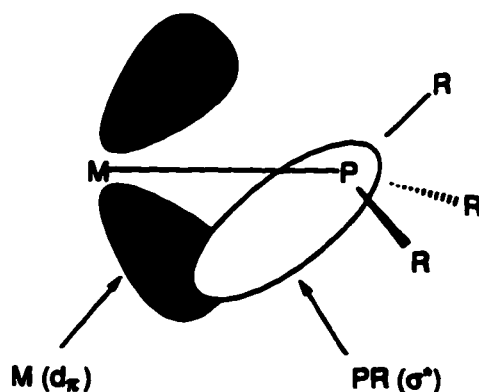


Figure 4.4 Molecular orbital picture of transition metal phosphine complexes showing back donation into the σ^* orbital of the P-R bond.

As the R substituent on the phosphine ligand becomes more electronegative, the orbital used by the R fragment to bond to the phosphorus atom becomes more stable. This then implies that the σ^* orbital of the P-R bond would also become more stable. As the phosphorus contribution to σ^* increases, so does the size of the σ^* lobe that points toward the metal. Both of these factors make the σ^* more accessible for back donation. For phosphines, the resultant order of increasing π -acid character in relation to carbon monoxide is:



The greater π -accepting ability of PF_3 via σ^* orbitals is related to the highly polar phosphorus-fluorine bonds which have characteristically low-lying σ^* orbitals. Since the σ phosphorus-fluorine bond is highly polar towards fluorine, then the σ^* orbital must be highly polar towards the phosphorus, therefore increasing the σ^* -metal d_{π} overlap.^{5,6} The π -acidity of difluorophosphinodiazaphosphole (2), should be greater than that for phosphorus trichloride and similar to that of phosphorus trifluoride.

The increased occupation of the σ^* orbital through back-bonding from the metal would also suggest the the P-R bonds should lengthen slightly upon complexation. This may be masked by the simultaneous shortening of the P-R bond which arises as the result of the donation of the phosphorus electron lone pair to the metal centre, and the consequent decrease in the P(lone pair)-R(bonding pair) repulsions.⁷ The effect on P-R bond lengths may therefore be invisible.

4.3 Complexation Chemistry of 4-(difluorophosphino)-2,5-dimethyl-2H-1,2,3 σ^2 -diazaphosphole (2).

The coordination chemistry of the 4-(difluorophosphino)-2,5-dimethyl-2H-1,2,3 σ^2 -diazaphosphole (2) showed in all cases that the 4-phosphino group, the

exo-phosphorus centre, coordinated to the metal centre, whether the ligand displaced a labile group or was involved in the reduction of the metal centre. The chemistry of the difluorophosphino group was in some ways similar to that observed for phosphites and phosphorus trifluoride. These similarities are attributed to the electron-withdrawing fluorine substituents on the phosphorus atom.

4.3.1 Reactions with Metal Carbonyls.

One equivalent of **2** was reacted with $\text{Cr}(\text{CO})_5(\text{THF})$, generated *in situ* from the photolysis of $\text{Cr}(\text{CO})_6$ in THF. After stirring overnight, the solvent was removed *in vacuo* and the monosubstituted yellow complex $\text{Cr}(\text{CO})_5(\mathbf{2})$ (**27**) was extracted with diethyl ether. The complex was crystallized from diethyl ether at -40°C , yielding bright yellow crystals (72%). Similar to $\text{Cr}(\text{CO})_5(\text{PF}_3)$, complex **27** has a low melting point (64°C).⁸

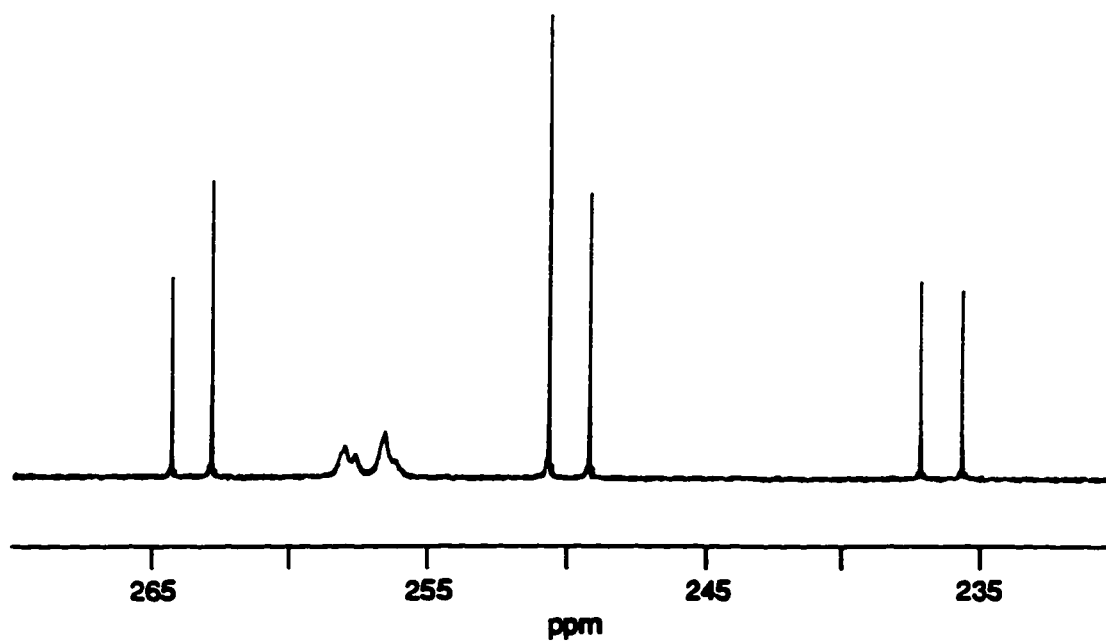
The $^{31}\text{P}\{^1\text{H}\}$ NMR spectra (Figures 4.5, 4.6, and 4.7) were second order. Relative to the free ligand, there was a downfield shift for the resonance of the exo-phosphorus centre of 43 ppm to 249.74 ppm as well as a small downfield shift of 2 ppm for the $\sigma^2\text{P}$ signal (~ 257 ppm). The $^2J_{\text{PP}}$ value increased to ~ 120 Hz while the value $^1J_{\text{PF}}$ was ~ 1106 Hz. The $^{31}\text{P}\{^1\text{H}\}$ NMR spectrum at 81.013 MHz showed the two phosphorus signals to be overlapped and the peak for the $\sigma^2\text{P}$ endo-phosphorus to be skewed and broadened (Figure 4.5a). At a higher field (161.977 MHz), the $^{31}\text{P}\{^1\text{H}\}$ NMR spectrum showed the $\sigma^2\text{P}$ signal merged with one component of the $\sigma^4\text{P}$. The spectrum is still complex (Figure 4.6a) displaying again a second order pattern. At 202.392 MHz, the $(\nu_{\sigma^2\text{P}} - \nu_{\sigma^4\text{P}})$ difference is still not much larger than the value of $^2J_{\text{PP}}$, so the second order $^{31}\text{P}\{^1\text{H}\}$ NMR spectrum was again observed (Figure 4.7a). At all frequencies, the ^{19}F NMR spectra were also second order (Figures 4.5b, 4.6b, and 4.7b). The fluorine chemical shift was centred at -39.45 ppm. Simulation has not been possible.

Table 4.1 **$\nu(\text{CO})$ Assignments in $\text{Cr}(\text{CO})_5\text{L}$ Complexes.**

Complex	$\nu(\text{CO})$ cm^{-1}	Reference
27	2079	This work
$\text{Cr}(\text{CO})_5(\text{PF}_3)$	2083	8
$\text{Cr}(\text{CO})_5(\text{P}(\text{OCH}_2)_3\text{CMe})$	2082	9
$\text{Cr}(\text{CO})_5(\text{P}(\text{OMe})_3)$	2073	10
$\text{Cr}(\text{CO})_5(\text{P}(\text{C}_4\text{H}_9)_3)$	2062	11
$\text{Cr}(\text{CO})_5(\text{P}(\text{NMe}_2)_3)$	2055	12

The IR spectrum showed the two stretching frequencies for the carbonyls at $\nu(\text{CO})$ 2079 cm^{-1} and at $\nu(\text{CO})$ 1938 cm^{-1} . Unfortunately the carbonyl stretching frequencies were not reported for the dichlorophosphinodiazaphosphole or dimethoxyphosphinodiazaphosphole complexes, so a comparison between the two chromium complexes cannot be made. In order to measure the basicity or the π acidity of **2**, the stretching frequency of the A_1 band of other phosphine and phosphites complexes of chromium pentacarbonyl was compared to that of **27**. According to Table 4.1, the basicity of **2** was greater than that of PF_3 (2083 cm^{-1}) and similar to the caged phosphite $\text{P}(\text{OCH}_2)_3\text{CMe}$ (2082 cm^{-1}) but **2** was less basic than $\text{P}(\text{OMe})_3$ (2073 cm^{-1}).

a)



b)

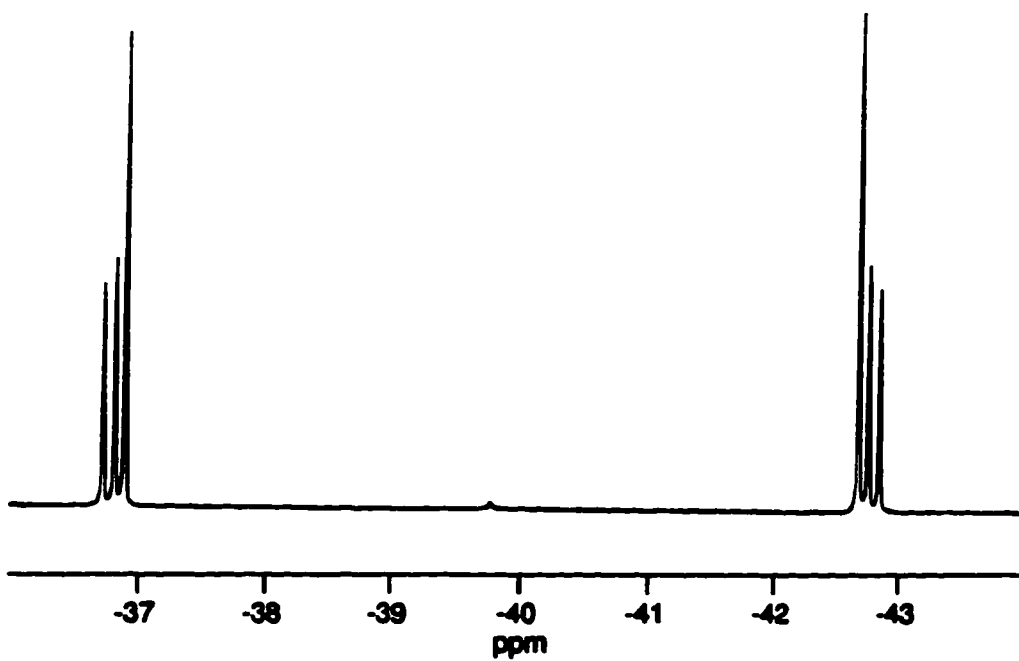


Figure 4.5 (a) $^{31}\text{P}\{^1\text{H}\}$ spectrum at 81.015 MHz and (b) ^{19}F NMR spectrum at 188.313 MHz of **27** in CDCl_3 at room temperature.

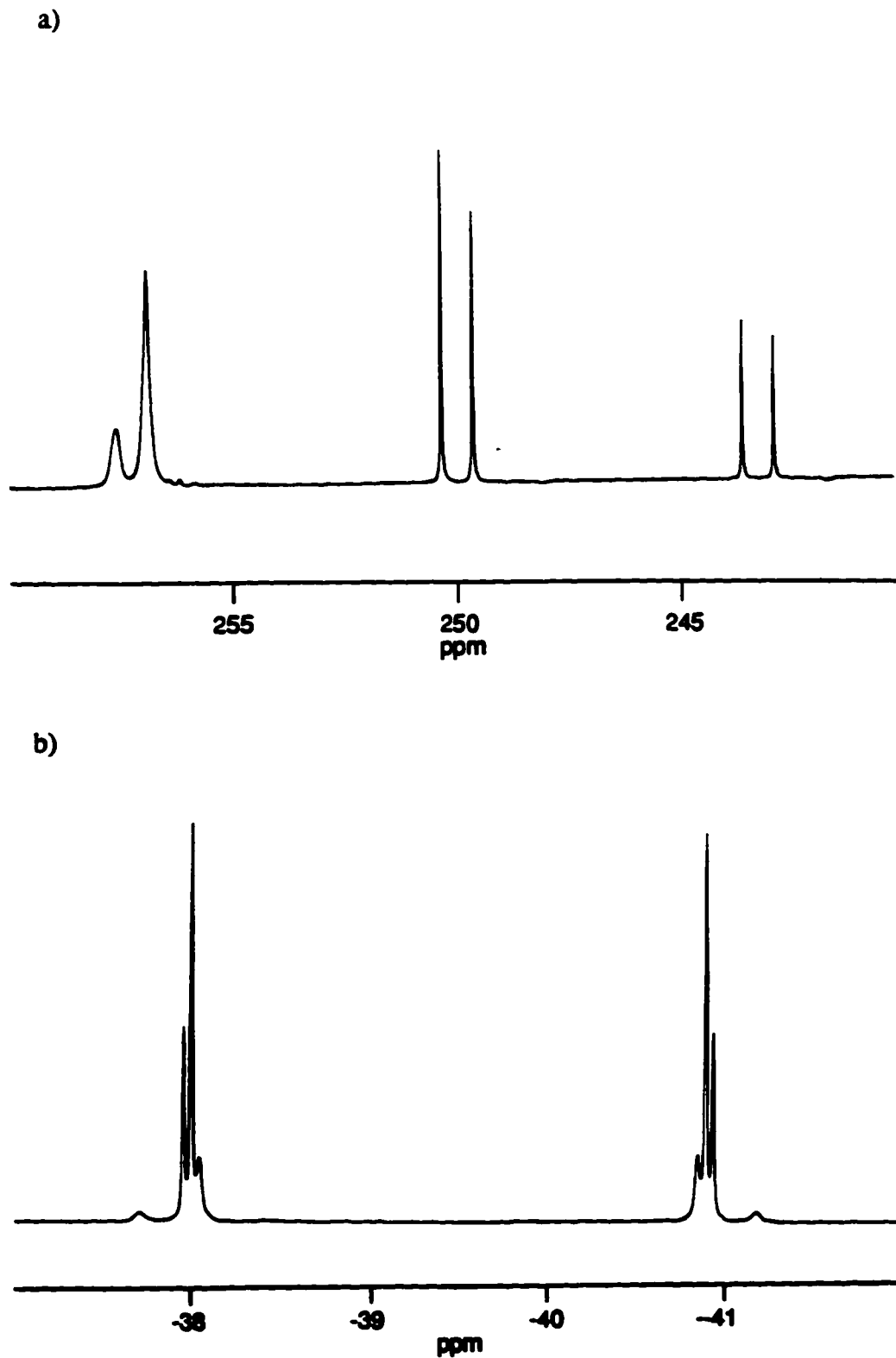


Figure 4.6 (a) $^{31}\text{P}\{^1\text{H}\}$ spectrum at 161.977 MHz and (b) ^{19}F NMR spectrum at 376.503 MHz of **27** in CDCl_3 at room temperature.

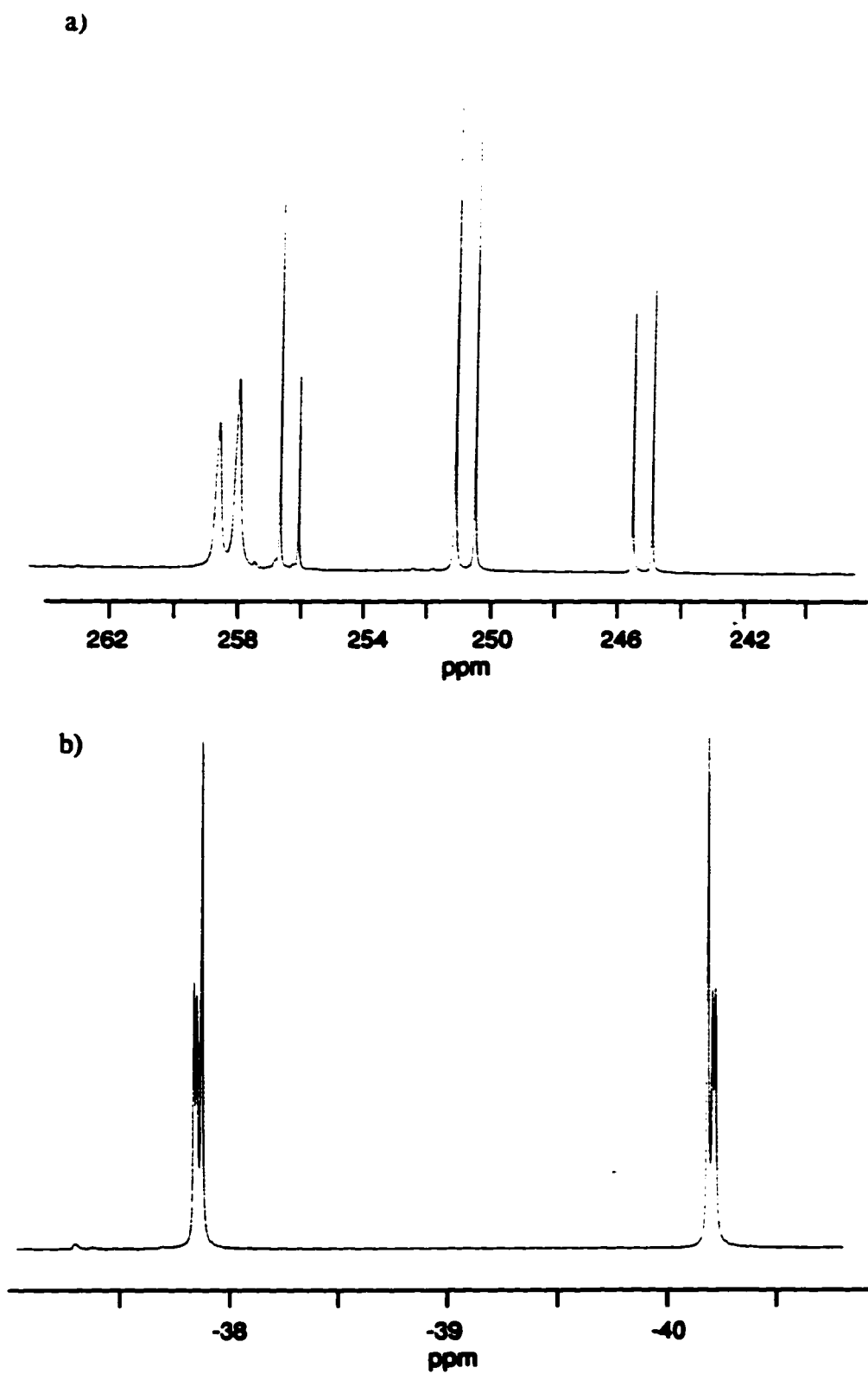


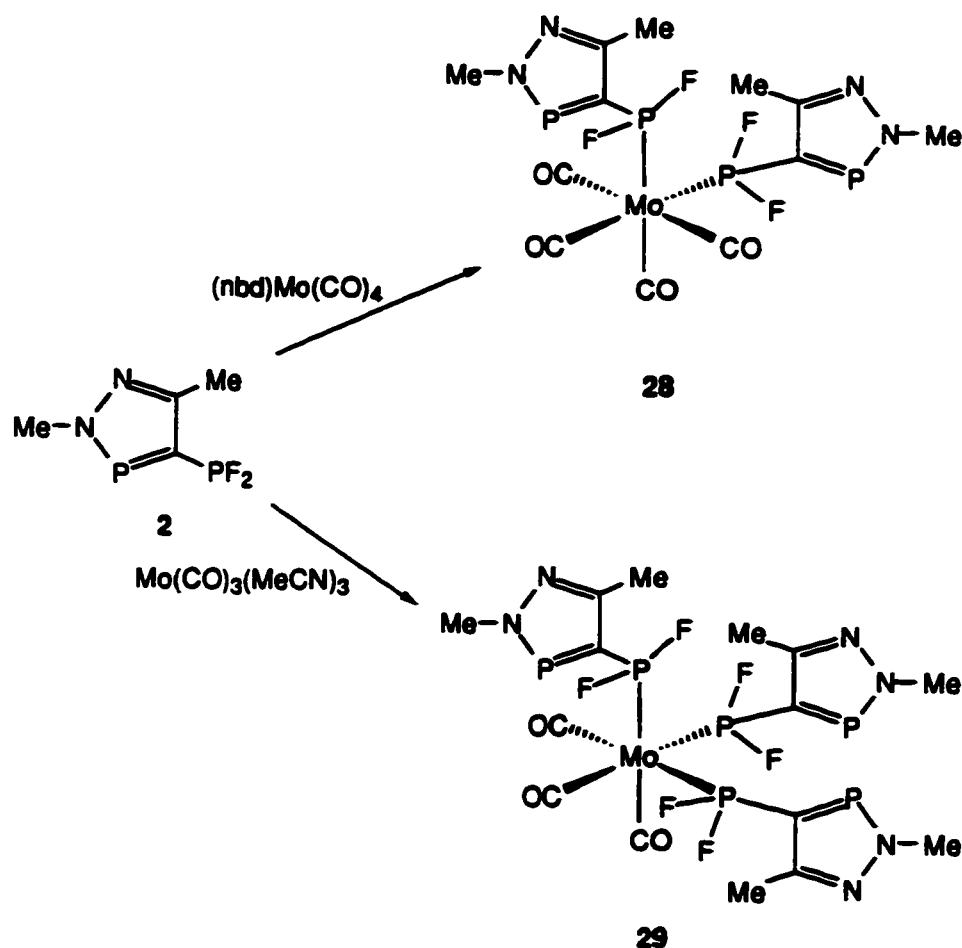
Figure 4.7 (a) $^{31}\text{P}\{^1\text{H}\}$ spectrum at 202.392 MHz and (b) ^{19}F NMR spectrum at 470.304 MHz of **27** in CDCl_3 at room temperature.

A quantitative description of the π acceptor ability of a ligand can be made by comparison of the electronic parameter χ , which was introduced by Tolman.¹³ The electron donor-acceptor properties of phosphines are based on the infrared spectral data for the $\text{LNi}(\text{CO})_3$ complex. The stretching frequencies of the nickel complexes can be estimated from their chromium analogues $\text{Cr}(\text{CO})_5\text{L}$. For **2**, the value of χ is estimated to be 51 cm^{-1} , which is comparable to that for PF_3 ($\chi = 55\text{ cm}^{-1}$).

Addition of **2** to a yellow solution of $\text{Mo}(\text{CO})_5(\text{THF})$ resulted in a slow lightening of the colour. Within a few hours a brown precipitate formed. The removal of THF *in vacuo* resulted in a brown solid. Extraction with diethyl ether and subsequent removal, resulted in a pale yellow oil. The $^{31}\text{P}\{^1\text{H}\}$ NMR spectrum however did not show any identifiable products.

The addition of **2** to an orange solution of $\text{W}(\text{CO})_5(\text{THF})$ caused the solution to quickly darken. A greyish purple solution resulted after stirring overnight. After the removal of the THF *in vacuo*, a greyish purple solid was obtained. The solid liquified to a purple oil after standing for a couple of days. The $^{31}\text{P}\{^1\text{H}\}$ NMR spectrum of the purple oil indicated a mixture of products but isolation of identifiable products could not be accomplished.

In an attempt to place two phosphinodiazaphosphole groups on a molybdenum(0) centre, two equivalents of **2** were reacted with $\text{Mo}(\text{CO})_4(\text{nb})$ (Scheme 4.1). The reaction was stirred overnight in dichloromethane at room temperature. The solvent was removed *in vacuo*, leaving a yellow solid. The compound was recrystallized from dichloromethane/hexane at -40°C to give a 74% yield of *cis*- $\text{Mo}(\text{CO})_4(\text{2})_2$ (**28**).



Scheme 4.1 Formation of the *cis*- $Mo(CO)_4(2)_2$ (**28**) and *fac*- $Mo(CO)_3(2)_3$ (**29**) complexes.

The $^{31}P\{^1H\}$ NMR spectrum of **28** consisted of an $AA'BB'X_2X'_2$ spin system, as is usually observed with disubstituted phosphine metal complexes. The chemical shift for the resonance for the σ^2P atom was centred at 259.74 ppm and the exo-phosphorus signal had shifted downfield, relative to the position of **2**, to 222.99 ppm. From this spectrum, the one-bond phosphorus-fluorine coupling constant was estimated to be 1093 Hz. The ^{19}F NMR spectrum is second order with the chemical shift resonance centred at 42.91 ppm. From the fluorine spectrum, the value for $^2J_{PMP'}$ was calculated to be 33 Hz. The $^1J_{PF}$ and $^3J_{PF}$ values were estimated to be 1091 Hz and 4 Hz, respectively.

Table 4.2 $\nu(\text{CO})$ Assignments in *cis*- $\text{Mo}(\text{CO})_4\text{L}_2$ Complexes.

Complex	$\nu(\text{CO})$ (cm^{-1})	Reference
28	2056, 1974, 1952 a)	This work
$\text{Mo}(\text{CO})_4(\text{PF}_3)_2$	2091, 2022, 2022, 2003	14
$\text{Mo}(\text{CO})_4(\text{P}(\text{OCH}_2)_3\text{CMe})_2$	2045, 1965, 1945 a)	15
$\text{Mo}(\text{CO})_4(\text{P}(\text{OMe})_3)_2$	2037, 1945, 1926, 1921	10
$\text{Mo}(\text{CO})_4(\text{PMe}_3)_2$	2024, 1930, 1901, 1879	16
$\text{Mo}(\text{CO})_4(\text{P}(\text{NMe}_2)_3)_2$	2012, 1908, 1894, 1880	17

a) B_1 and B_2 bands were unresolved.

The carbonyl region of the $^{13}\text{C}\{^1\text{H}\}$ NMR spectrum showed two weak signals for the carbon monoxide. One of the peaks (208.39 ppm) was a doublet that showed coupling to the *trans* phosphorus centre (39 Hz) while the other signal (204.50 ppm) was a singlet. The resonances for the protons in the ^1H NMR spectrum did not change significantly with respect to the uncomplexed ligand.

In order to determine whether the disubstituted complex **28** has a *cis* or *trans* configuration of these ligands, the carbonyl region of the infrared spectrum was examined. The *cis* complexes belong to the C_{2v} point group so 4 peaks are expected, while the *trans* complexes possess D_{4h} symmetry so only one peak should be observed. The IR spectrum showed three peaks at 2056, 1974, and 1952 cm^{-1} so a *cis* structure is assigned with the B_1 and B_2 bands being unresolved. A comparison with other *cis*- $\text{Mo}(\text{CO})_4(\text{PR}_3)_2$ complexes is shown in Table 4.2.

Table 4.3

 $\nu(\text{CO})$ Assignments in *fac*- $\text{Mo}(\text{CO})_3\text{L}_3$ Complexes.^a

Complex	$\nu(\text{CO})$ (cm^{-1})
29	2011, 1945
$\text{Mo}(\text{CO})_3(\text{PF}_3)_3$	2090, 2055
$\text{Mo}(\text{CO})_3(\text{PCl}_3)_3$	2040, 1991
$\text{Mo}(\text{CO})_3(\text{P}(\text{OMe})_3)_3$	1977, 1888
$\text{Mo}(\text{CO})_3(\text{PPh}_3)_3$	1934, 1835
$\text{Mo}(\text{CO})_3(\text{MeCN})_3$	1915, 1783

a) Values taken from Elschenbroich, C.; Salzer, A. *Organometallics - A Concise Introduction*; VCH Publishers: New York, 1989, pp 230.

The complex $\text{Mo}(\text{CO})_3(\text{MeCN})_3$ was reacted with three equivalents of **2** (Scheme 4.1). The resultant product did not show any proton signals in the ^1H NMR spectrum arising from coordinated acetonitrile so the triple substitution appears to have been achieved. Both phosphorus signals were second order in the $^{31}\text{P}\{^1\text{H}\}$ NMR spectrum (Figure 4.8a). The chemical shift for the signal of the two-coordinate phosphorus atom was centred at 255 ppm and was not significantly different from that of the disubstituted molybdenum complex **28**. The signal for the exo-phosphorus centre (224.60 ppm) was more complicated. The fluorine peaks in the ^{19}F NMR were broadened due to unresolved coupling (Figure 4.8b).

The carbonyl region of the infrared spectrum showed only two peaks consistent with a *fac* isomer having C_{3v} symmetry. The infrared pattern was similar to other related molybdenum complexes shown in Table 4.3.

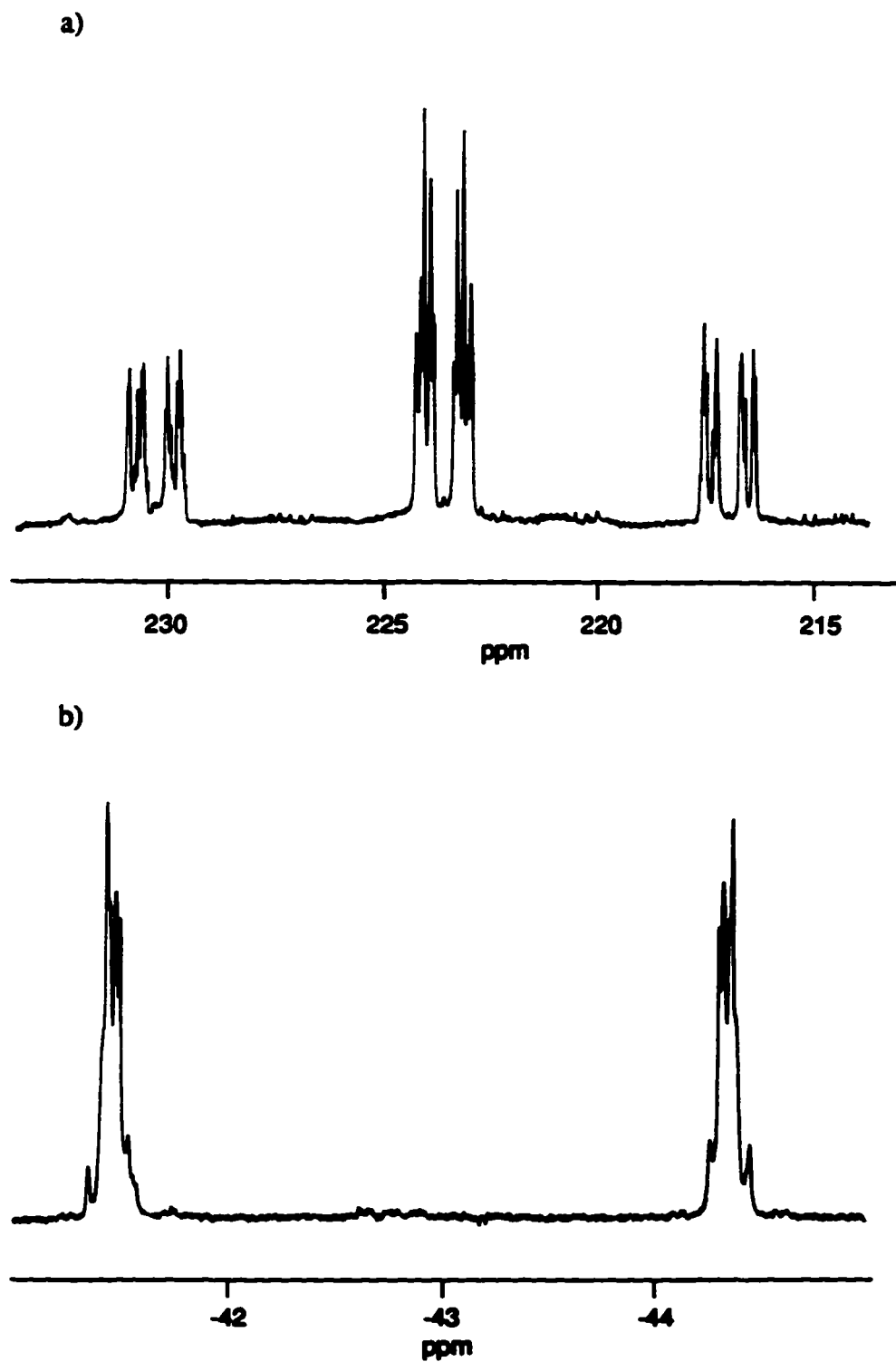


Figure 4.8 (a) ³¹P(¹H) (161.977 MHz) spectrum for the exo-phosphorus region and (b) ¹⁹F NMR (376.503 MHz) spectrum of 29 in CDCl₃.

4.3.2 Reaction with the Prochiral Ruthenium Metal Complex, $\text{CpRu}(\text{PPh}_3)_2\text{Cl}$.

The reaction of **2** with $\text{CpRu}(\text{PPh}_3)_2\text{Cl}$ in refluxing benzene produced the monosubstituted phosphole complex $\text{CpRu}(\text{PPh}_3)(\mathbf{2})\text{Cl}$ (**30**). The $^{31}\text{P}\{^1\text{H}\}$ and the ^{19}F NMR spectra (Figures 4.13a and 4.14a, respectively) indicated that the fluorine atoms on the exo-phosphorus of the phosphinodiazaphosphole were diastereotopic due to the stereogenic ruthenium centre.

The $^{31}\text{P}\{^1\text{H}\}$ NMR spectrum showed a small downfield shift of 4 ppm (259.34 ppm) for the resonance of the $\sigma^2\text{P}$ centre while the signal for the exo-phosphorus centre also experienced a small downfield shift of 8 ppm to 200.04 ppm (Figure 4.10). The signal for the exo-phosphorus showed two different couplings to fluorine atoms as well as coupling to the phosphorus atom in the diazaphosphole ring. Coupling was also observed to the phosphorus of the triphenylphosphine coordinated to the ruthenium. In the ^{19}F NMR spectrum, one of the signals for the fluorines showed a downfield signal of 59 ppm to -27.5 ppm and showed coupling to both phosphorus centres of the diazaphosphole ring ($^1J_{\text{PF}} = 1057$, $^3J_{\text{PF}} = 15$ Hz) and to the other fluorine atom ($^2J_{\text{FF}} = 30$ Hz). The other fluorine resonance was shifted downfield by 47 ppm to -41.0 ppm. The signal for this fluorine was coupled to all three of the phosphorus atoms of the ruthenium complex ($^1J_{\text{PF}} = 1131$ Hz, $^3J_{\text{PF}} = 19$ Hz, and $^3J_{(\text{PPh}_3)\text{F}} = 7$ Hz). Applying the Karplus relationship for vicinal proton-proton coupling leads to the prediction that the fluorine *trans* to the PPh_3 group should show a larger coupling to this phosphorus centre than the fluorine *gauche* to the PPh_3 . This latter coupling should be very small. A Newman projection of the complex is depicted in Figure 4.9. The $^{31}\text{P}\{^1\text{H}\}$ exo-phosphorus spectral region and the ^{19}F NMR spectra were simulated and their comparison is shown in Figure 4.11 and 4.12, respectively. The resultant parameters are given in Table 4.14 .

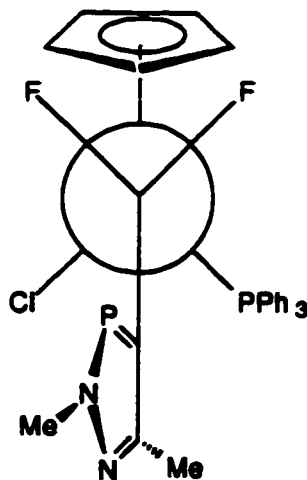


Figure 4.9 Newman projection along the P-Ru bond of compound **30**.

4.3.3 Reactions with Rhodium Complexes.

Wilkinson's discovery that rhodium-phosphine complexes (e.g. $\text{Rh}(\text{PPh}_3)_3\text{Cl}$) provide extremely reactive and selective hydroformylation catalysts¹⁸ opened a large area of application of these rhodium-phosphine complexes for catalytic transformations. Since the initial work, many variations of phosphine-rhodium complex systems have been used in homogeneous catalysis. Detailed studies of the $\text{Rh}(\text{PPh}_3)_3\text{Cl}$ system has led to an understanding of the factors involved in governing the reactivity and the selectivity of the catalytic cycle.¹⁹ Ligands that are strong σ -donors inhibit the reaction, possibly completely, while stronger π -acceptors, such as phosphites, lead to more active and selective hydroformylation catalysts.²⁰⁻²³

The route to the preparation of a wide variety of mononuclear and binuclear $\text{Rh}(\text{I})$ and $\text{Ir}(\text{I})$ complexes begins with the chloro-bridged dimeric complex $[\text{M}(\text{cod})\text{Cl}]_2$ ($\text{M} = \text{Rh}, \text{Ir}$). The addition of two equivalents of a Lewis base to the $[\text{M}(\text{cod})\text{Cl}]_2$ ($\text{M} = \text{Rh}, \text{Ir}$) dimer results in the cleavage of the metal-chlorine bridge to give the monomeric complex containing the Lewis base and a terminal chloride ligand (Scheme 4.2).²⁴⁻²⁷

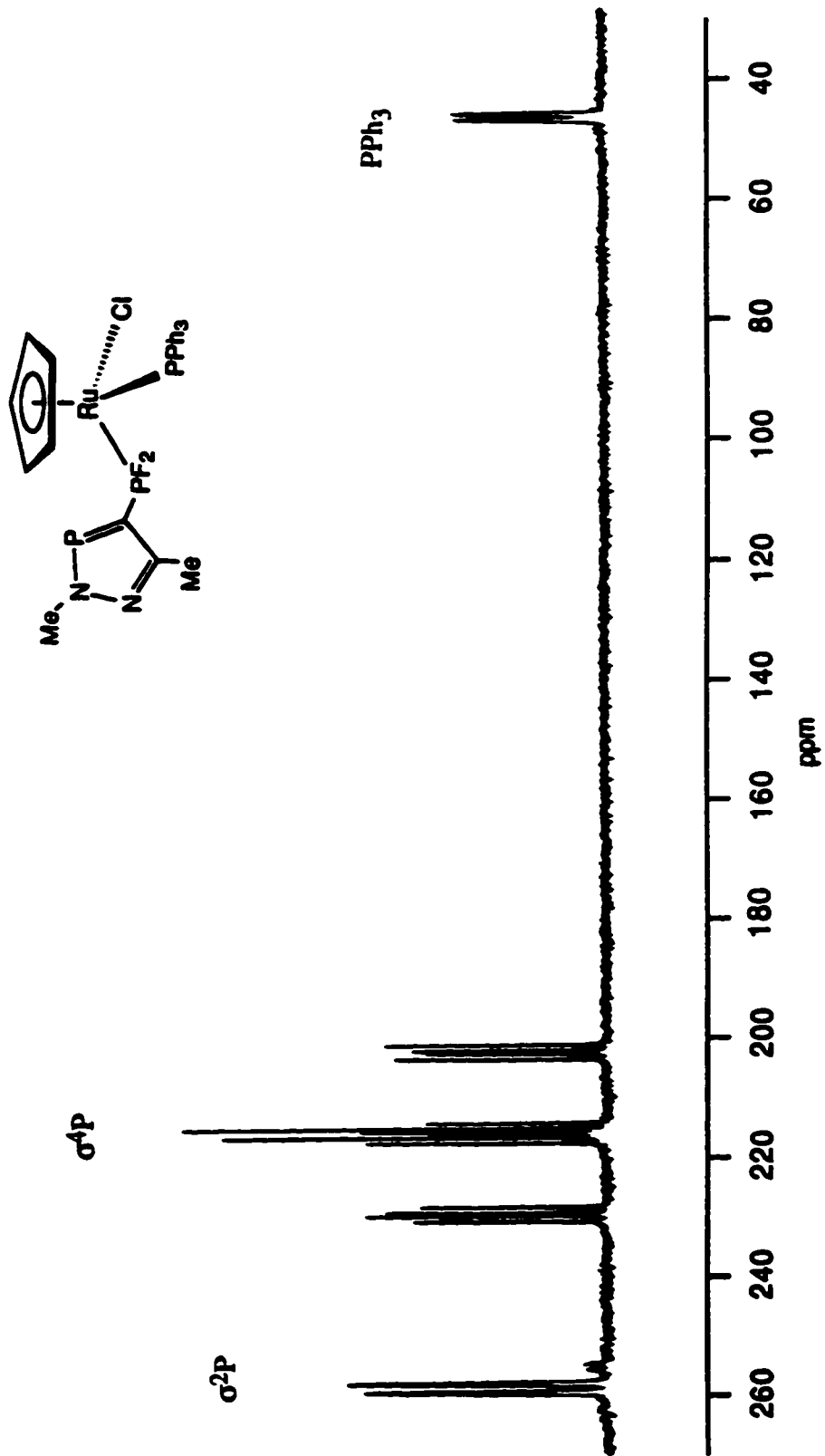
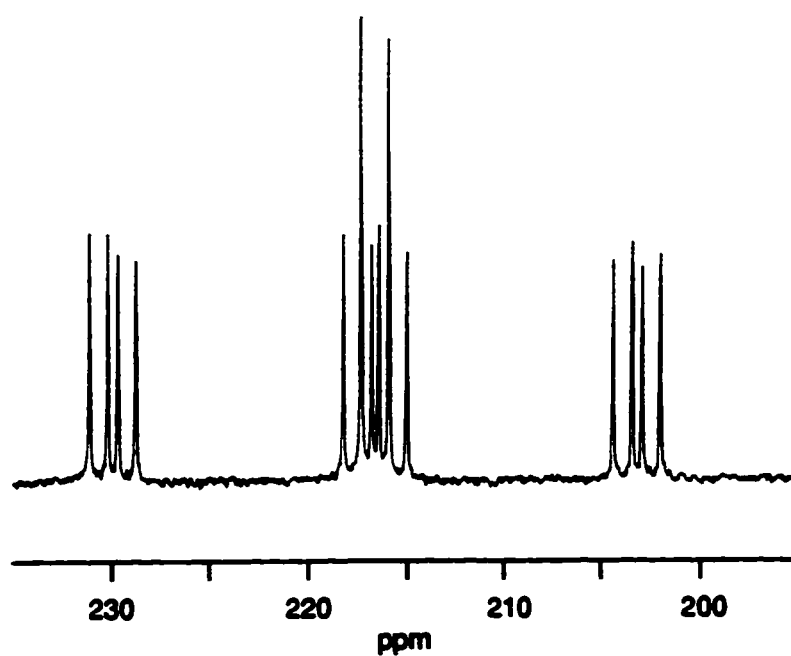


Figure 4.10 The $^{31}\text{P}\{^1\text{H}\}$ NMR (81.015 MHz) of complex 30 in CDCl_3 .

a)



b)

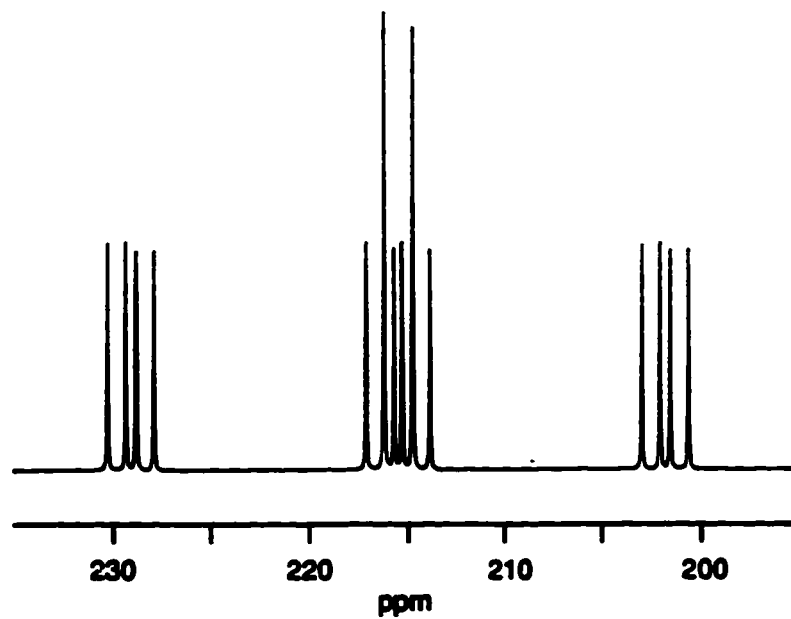


Figure 4.12 (a) $^{31}\text{P}\{^1\text{H}\}$ NMR (81.015 MHz) spectrum in CDCl_3 and (b) simulated spectrum of the exo-phosphorus region for the complex 30.

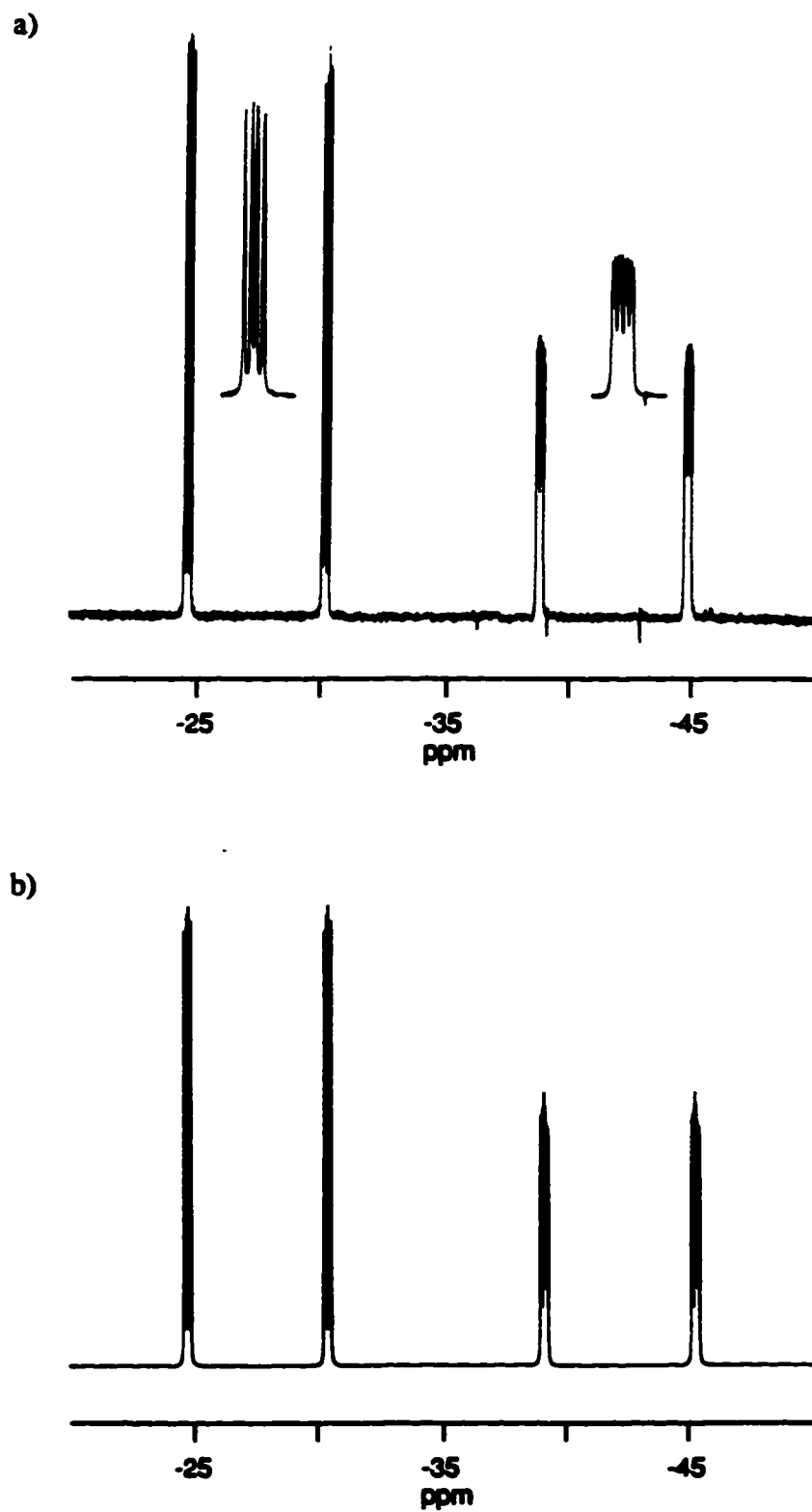


Figure 4.13 (a) ^{19}F NMR (188.313 MHz) spectrum in CDCl_3 and
(b) simulated ^{19}F NMR spectrum for complex 30.



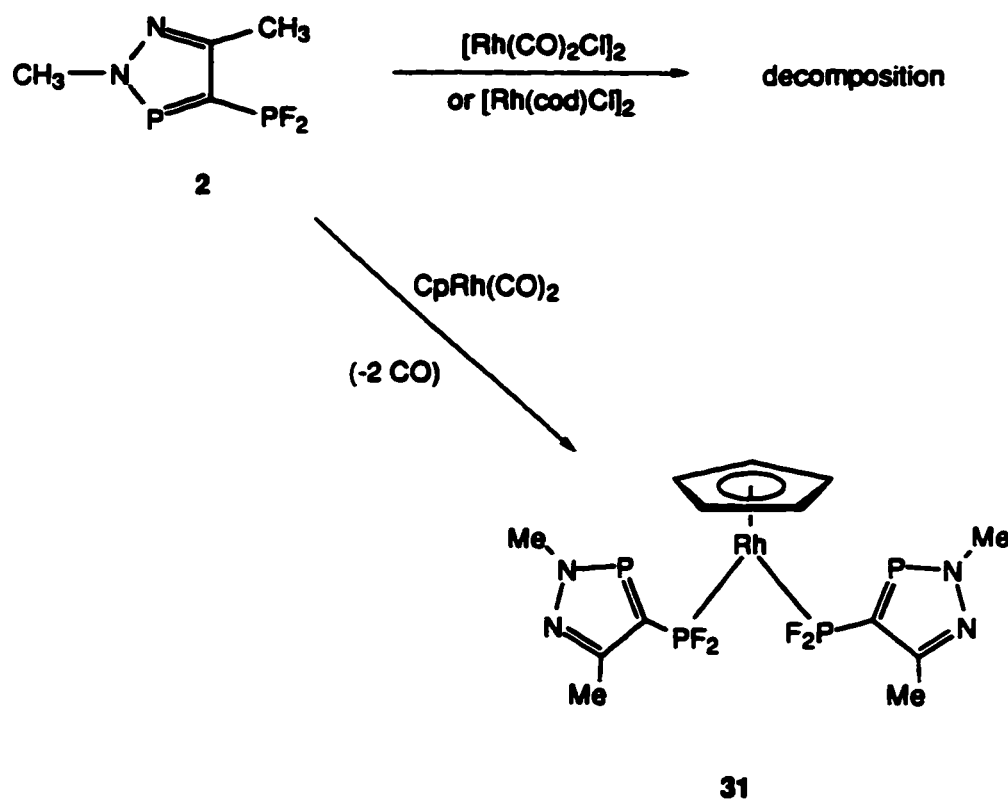
- e.g. L = PPh₃, M = Rh²⁴
 L = THF, M = Rh²⁵
 L = Me₃P(S), M = Rh²⁶
 L = PPh₃, M = Ir²⁷

Scheme 4.2 Reaction of coordinating ligands with [M(cod)Cl]₂ (M = Rh, Ir).

The use of non-coordinating solvents, such as pentane, leads to the displacement of the cyclooctadiene, or related olefin ligands. The rhodium-chlorine bridging bond is then cleaved in the presence of an excess phosphine to give complexes of the type RhCl(phosphine)₃.²⁷ Recent examples include the reaction of trimethylphosphine and [Rh(C₂H₄)₂Cl]₂ where the dimeric rhodium-phosphine complex and, as well, the monomeric rhodium complex Rh(PMe₃)₃Cl were isolated in high yields.²⁸

The incorporation of fluorine into the phosphinodiazaphosphole system would create a ligand with good π acceptor properties for a variety of rhodium(I) precursors. The reaction of **2** with a variety of dimeric rhodium starting complexes such as [Rh(cod)Cl]₂, [Rh(coe)₂Cl]₂, and [Rh(CO)₂Cl]₂ resulted in the decomposition of both the starting phosphine **2** and the rhodium complexes. It is possible that the rhodium-chlorine bridge could not be broken because **2** is a poor σ donor. In comparison, the reaction of phosphorus trifluoride with either of the three rhodium precursors proceeds with the replacement of alkene or carbon monoxide, resulting in the dimeric chloro-bridged complex [RhCl(PF₃)₂]₂, usually in good yield.^{7,29,30} Similar products have resulted from dimethylaminodifluorophosphine and [Rh(C₂H₄)₂Cl]₂.³¹

A move to monomeric rhodium complexes such as $\text{Cp}^*\text{Rh}(\text{cod})$ or $\text{CpRh}(\text{CO})_2$ provided a means of synthesizing phosphine substituted Rh(I) complexes from **2**. It is well known that only one of the carbonyl groups in $\text{CpRh}(\text{CO})_2$ is generally replaced by a phosphine.³² However, here the reaction of **2** with $\text{CpRh}(\text{CO})_2$ resulted in the substitution of both carbonyls to give **31** (Scheme 4.3), a reaction similar to those observed with phosphites.³³



Scheme 4.3 Reactions of **2** with $[\text{Rh}(\text{cod})\text{Cl}]_2$, $[\text{Rh}(\text{CO})_2\text{Cl}]_2$, and $\text{CpRh}(\text{CO})_2$.

The $^{31}\text{P}\{^1\text{H}\}$ and the ^{19}F NMR spectra for the rhodium complex **31**, in Figures 4.13 and 4.14, are both second order. The $^{31}\text{P}\{^1\text{H}\}$ NMR spectrum for the resonance for the $\sigma^4\text{P}$ centre consisted of a 69 line pattern centred at 188.68 ppm while the signal for the $\sigma^2\text{P}$ centre showed a broad doublet (259.81 ppm). The phosphorus spectrum reveals the one-bond phosphorus-rhodium coupling to be extremely large (306 Hz). The $^1\text{J}_{\text{PF}}$ value is approximately 1145 Hz. Due to the

second order nature of the spectrum, no further information could be obtained. In the ^1H NMR spectrum, the cyclopentadienyl protons were not coupled to the exo-phosphorus, as was observed with the related rhodium complex $\text{Cp}^*\text{Rh}(\text{PF}_3)_2$.^{34,35} The fluorine signal was centred at -36.13 ppm. The chemical shift for the ^{103}Rh resonance (-1280 ppm), measured by an inverse detection ^{31}P - ^{103}Rh analysis, lies in a range typical of most CpRhL_2 complexes.³⁶

Decoupling of the fluorine coupling interaction simplified the $^{31}\text{P}\{^1\text{H}\}$ NMR spectra to an 11 line pattern (Figure 4.15). The signal for the $\sigma^2\text{P}$ unit was still second order which implies that both phosphorus centres in the diazaphosphole ring are magnetically inequivalent and this complex could be considered as either an $\text{AA}'\text{DD}'\text{MM}'\text{M}''\text{M}''' \text{X}$ or an $\text{AA}'\text{DD}'\text{M}_2\text{M}'_2\text{X}$ type spin system.

Decoupling of the phosphorus signal at 260 ppm led to the simplification of the fluorine NMR spectrum to a 12 line pattern (Figure 4.16). From this spectrum, the fluorine-rhodium coupling was calculated to be 19 Hz but the $^4\text{J}_{\text{FF}}$ value was not resolved. This spectrum also allows the calculation of the two-bond phosphorus-phosphorus coupling constant of the PF_2 moiety (102 Hz). From this value, the $^1\text{J}_{\text{PF}}$ was then calculated to be 1114 Hz and the $^3\text{J}_{\text{PF}}$ coupling to be 11 Hz. For the related $\text{Cp}^*\text{Rh}(\text{PF}_3)_2$ complex, the analogous coupling constant values obtained were $^2\text{J}_{\text{PP}} = 178$ Hz, $^1\text{J}_{\text{PF}} = 1135$ Hz, $^3\text{J}_{\text{PF}} = 6$ Hz, and $^3\text{J}_{\text{FRh}} = 30$ Hz.³⁴

In the infrared spectrum of **31**, the P-F stretching frequencies had broadened relative to the starting ligand **2**. These peaks were shifted slightly to a higher frequency (835 and 786 cm^{-1}), relative to the starting diazaphosphole **1**. Such a shift is expected since the σ^* orbitals of the P-F is accepting electron density from the metal complex.

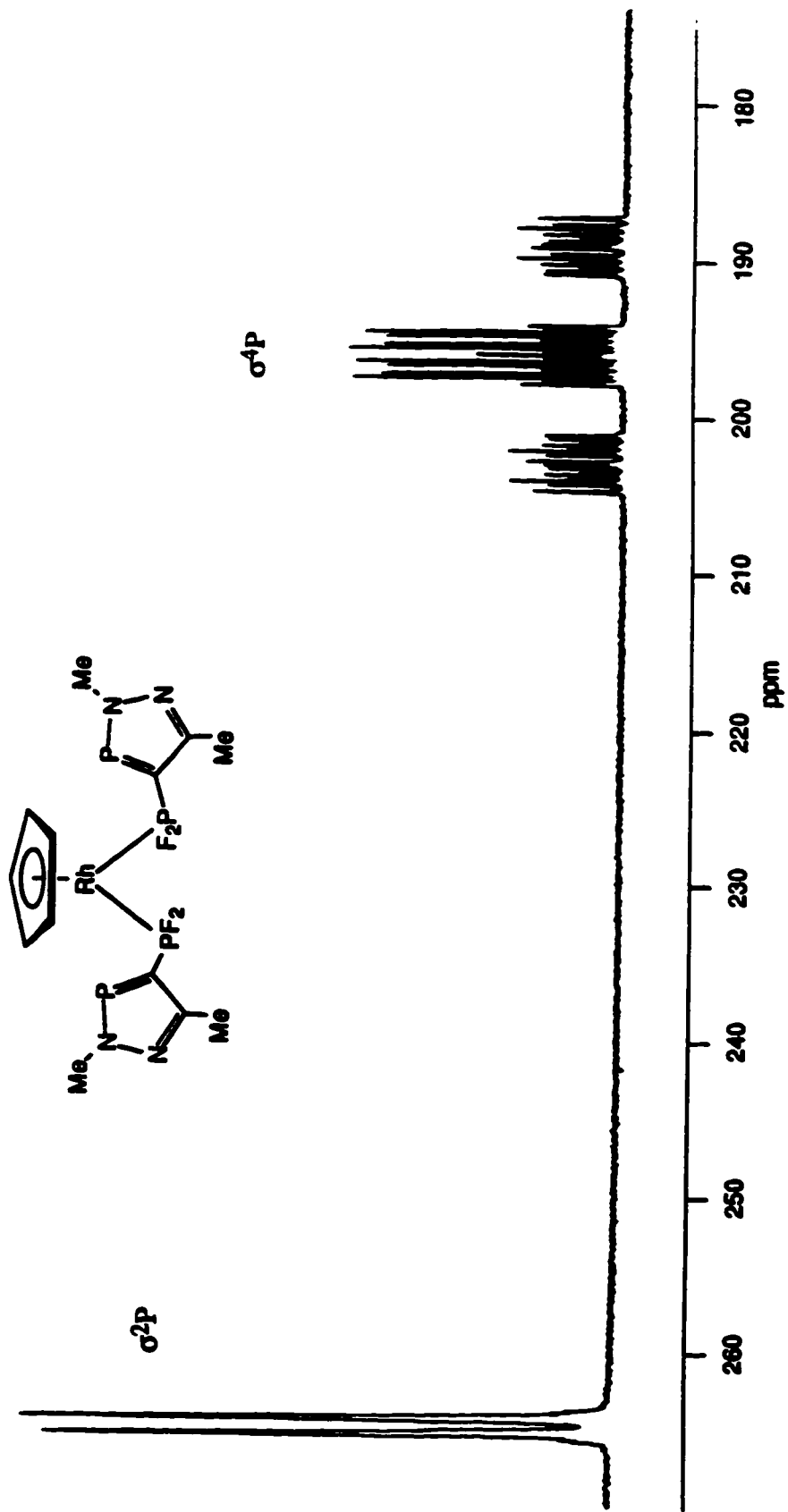


Figure 4.13 The ^{31}P (^1H) NMR (81.015 MHz) spectrum of $\text{CpRh}(\text{2})_2$ in CDCl_3 .

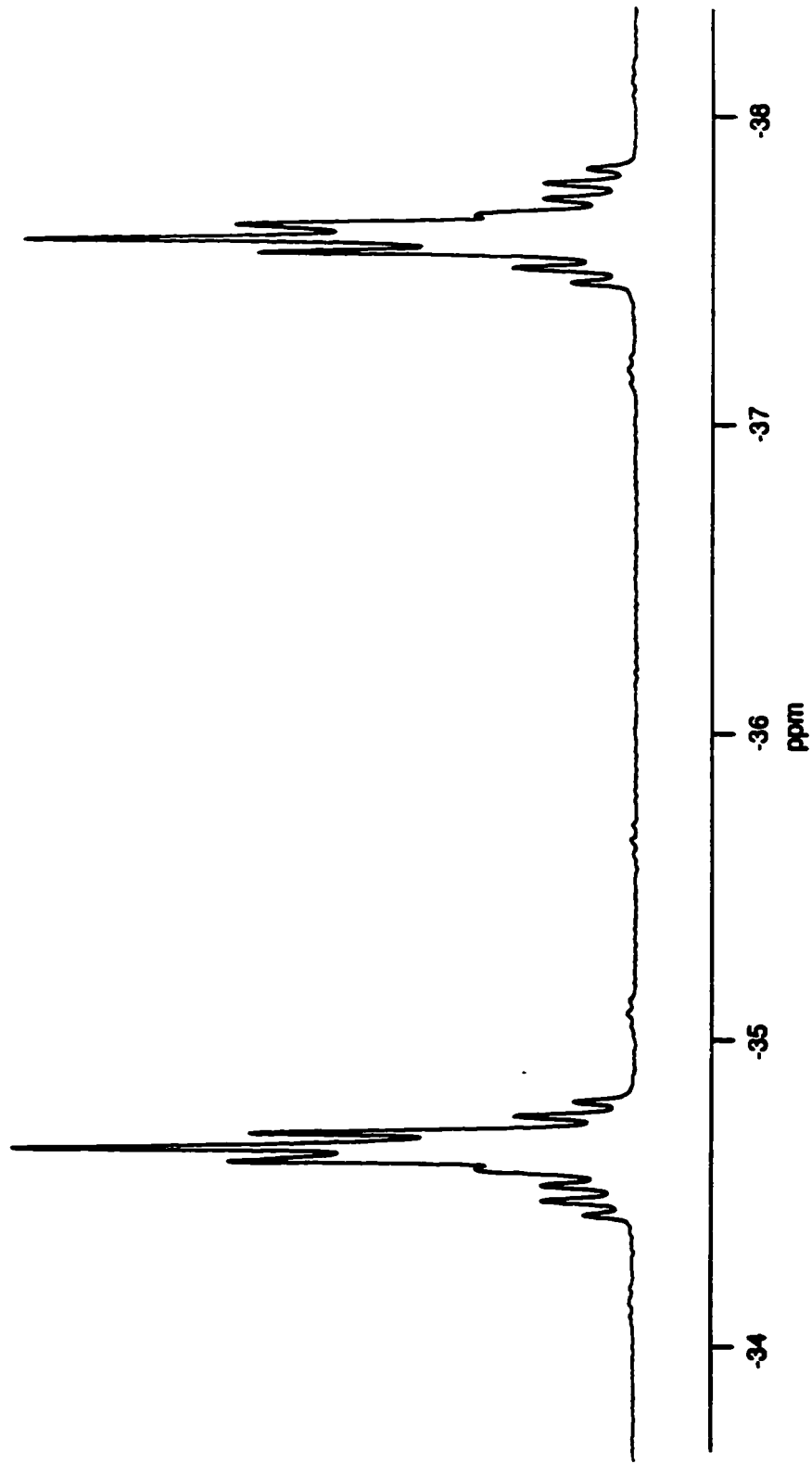


Figure 4.14 The ^{19}F NMR spectrum (188.015 MHz) of $\text{CpRh}(\text{2})_2$ in CDCl_3 .

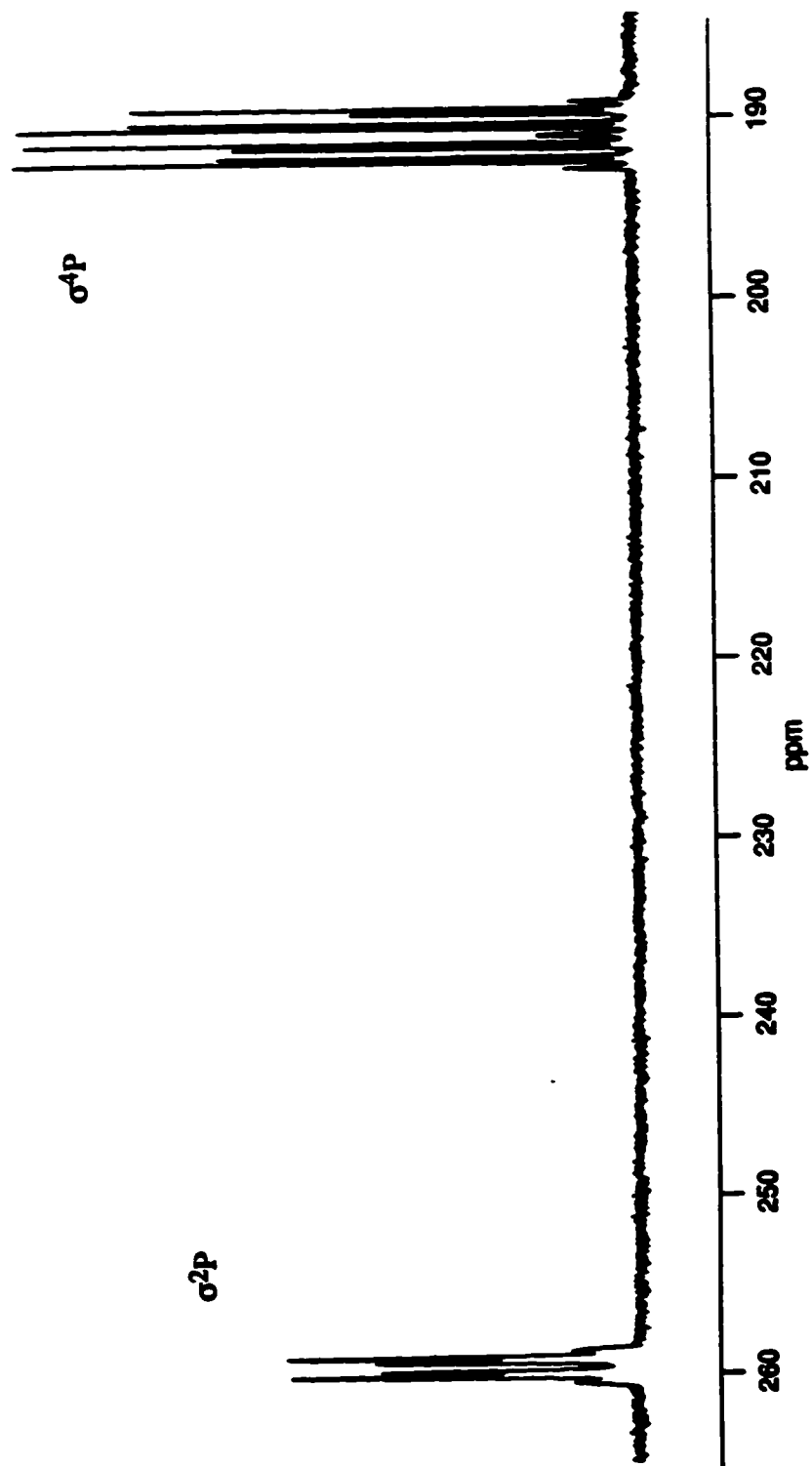


Figure 4.15 The ^{31}P (^{19}F) NMR (81.015 MHz) spectrum of $\text{CpRh}(\text{2})_2$ in CDCl_3 .

$$|{}^2J_{\text{PRh}}| = 19 \text{ Hz}$$

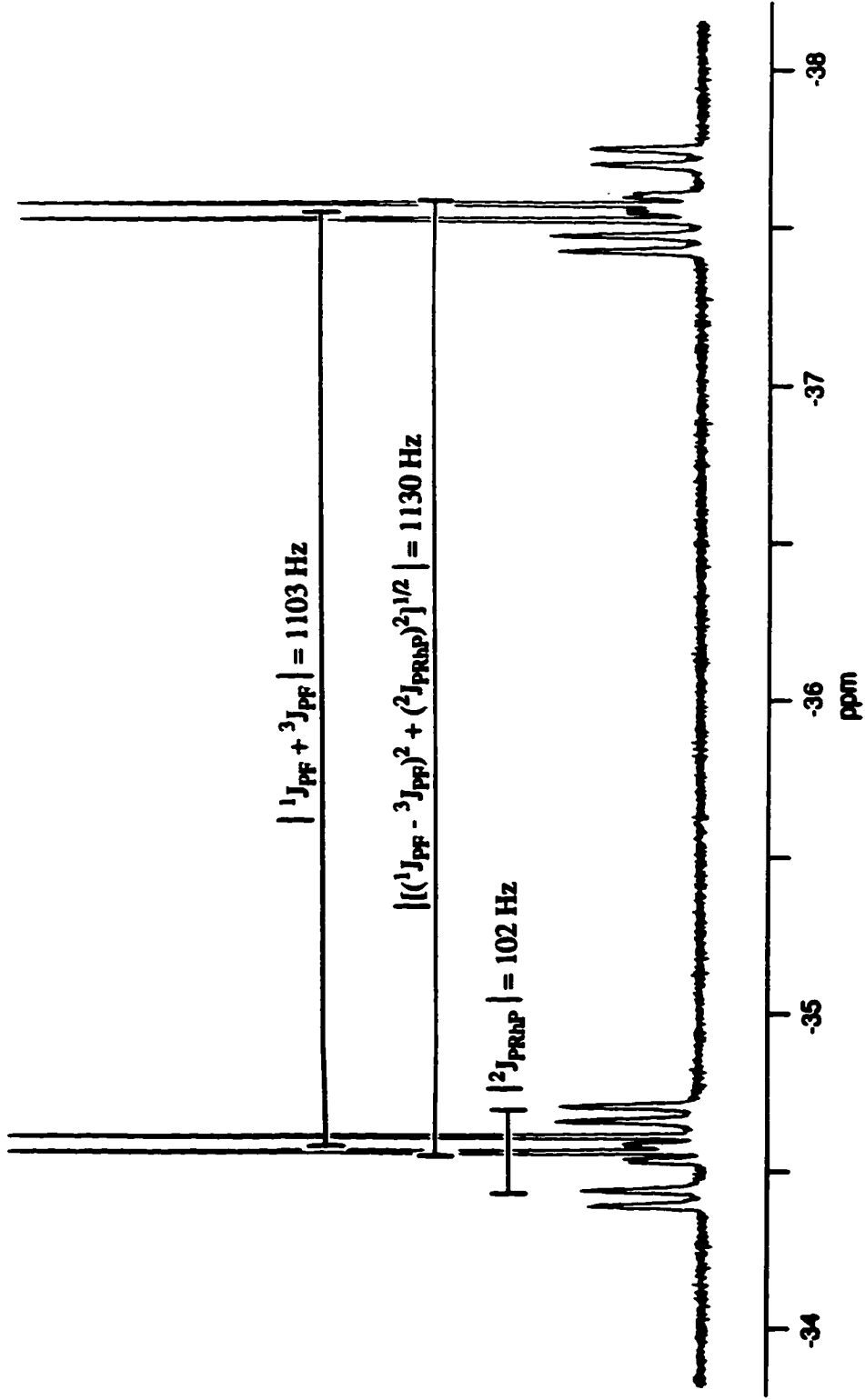


Figure 4.16 The ${}^{19}\text{F}$ (${}^3\text{J}_\text{P}$ at 260 ppm) NMR (188.313 MHz) spectrum of $\text{CpRh}(\text{2})_2$ in CDCl_3 .

A solid-state structure analysis of this complex $\text{CpRh}(\text{CO})_2$ showed a rhodium centre subtended by a cyclopentadienyl ring and two of the fluorophosphinodiazaphole ligands as formulated (Figure 4.17). There is a C_2 axis at the Rh centre (excluding the Cp ring). The angle between rhodium and the two exo-phosphorus centres, $\text{P}(21)\text{-Rh-P}(11)$, is $94.56(5)^\circ$. This angle is smaller than that found for the $(\eta^5\text{-indenyl})\text{Rh}(\text{PMe}_3)_2$ complex (96.69°).³⁷ Here the phosphole rings are planar with the nitrogen at the 2-position also being planar; the sum of the angles about the nitrogen equals 360° . The $\text{P}(22)\text{-N}(23)\text{-N}(24)$ and the $\text{P}(12)\text{-N}(13)\text{-N}(14)$ angles ($117.3^\circ(3)$ and $117.5(3)$, respectively) are wider than those observed for the 2,5-dimethyl-2*H*-1,2,3- σ^2 -diazaphosphole itself (113.8°). The carbon at the 4-position is also planar with the $\text{P}(21)\text{-C}(21)\text{-P}(22)$ angle being 121.6° , showing the sp^2 hybridization of the C(21). The angles about the two $\sigma^2\text{P}$ centres, $\text{N}(23)\text{-P}(22)\text{-C}(21)$ and $\text{N}(13)\text{-P}(12)\text{-C}(11)$ are $88.6(2)^\circ$ and $88.3(2)^\circ$, respectively. These angles are similar to that observed for the phosphole (88.2°).³⁸ Both the $\text{P}(12)\text{-N}(13)$ and the $\text{P}(21)\text{-N}(23)$ bond distance ($1.670(4)\text{\AA}$ and $1.672(3)\text{\AA}$) show some multiple bond character when compared to the normally accepted P-N single bond length (1.77\AA) and typical P-N double bond (1.57\AA) lengths.³⁹ Both two-coordinate phosphorus-carbon bond lengths show multiple bond character ($\text{P}(12)\text{-C}(11)$ and $\text{P}(22)\text{-C}(21) = 1.713\text{\AA}$). A typical value for a P-C single bond is 1.84\AA while that of a P-C double bond is 1.66\AA . The three-coordinate phosphorus-carbon bond lengths are shortened to 1.773\AA . The $\text{F}(11)\text{-P}(11)\text{-F}(12)$ and $\text{F}(21)\text{-P}(21)\text{-F}(22)$ bond angles are $95.3(2)^\circ$ and $96.0(2)^\circ$, respectively, while the average P-F bond distance is 1.569\AA , which is longer than that observed for the oxidized iminophosphinodiazaphosphole, 18 (1.537\AA). The difference in the P-F bond lengths of these two structures shows that that the fluorines play a role in the bonding to the rhodium centre by accepting

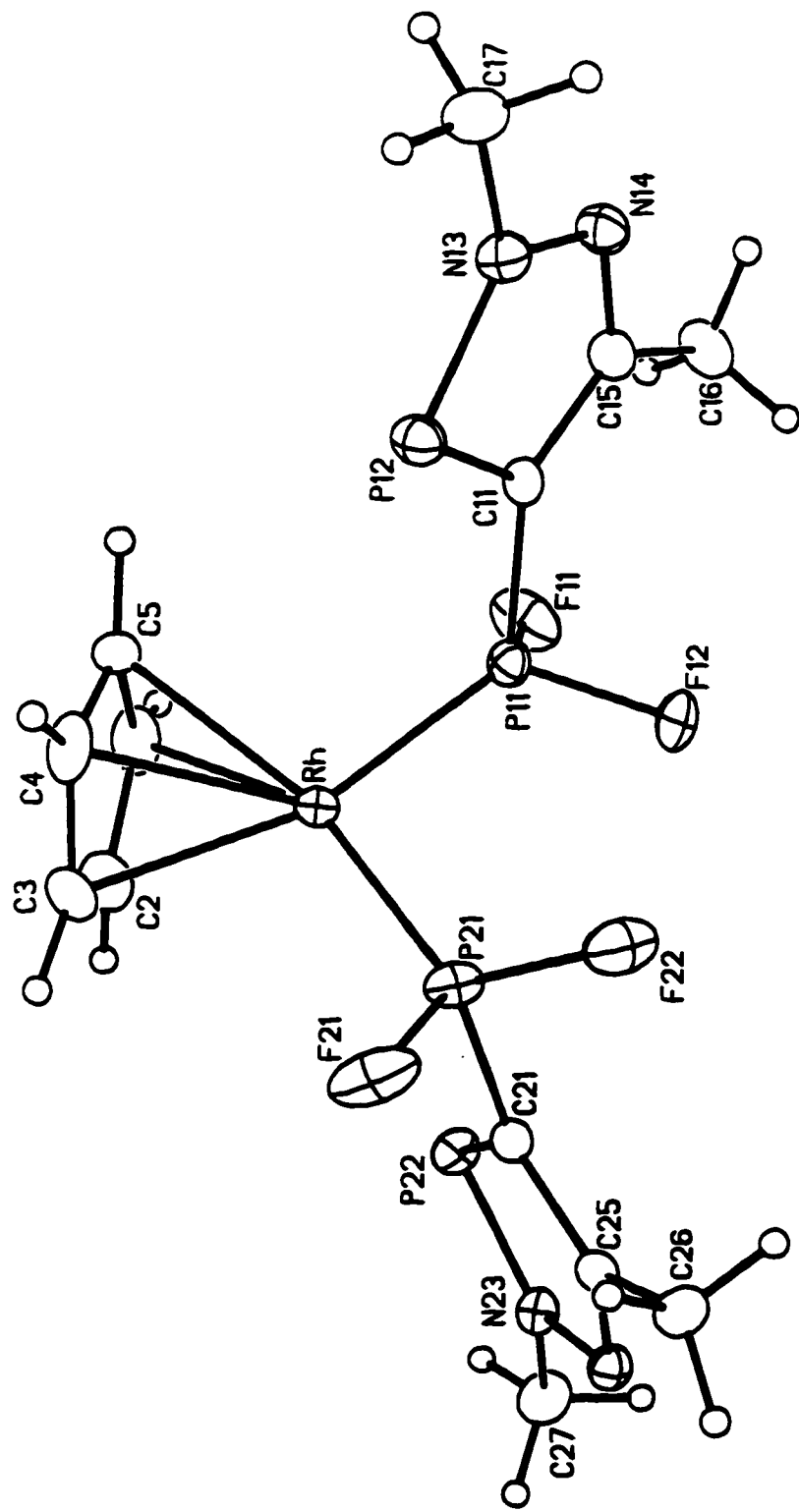


Figure 4.17 The solid-state structure of cyclopentadienylbis(difluoro(2,5-dimethyl-2H-1,2,3-diazaphosphol-4-yl)phosphine)rhodium(I) (31). Non-hydrogen atoms are represented by Gaussian ellipsoids at the 20% probability level. Structure courtesy of Dr. R. McDonald.

Table 4.4

Selected Interatomic Distances (Å) for Cyclopentadienylbis(difluoro(2,5-dimethyl-2*H*-1,2,3σ²-diazaphosphol-4-yl)phosphine)rhodium(I), (31).

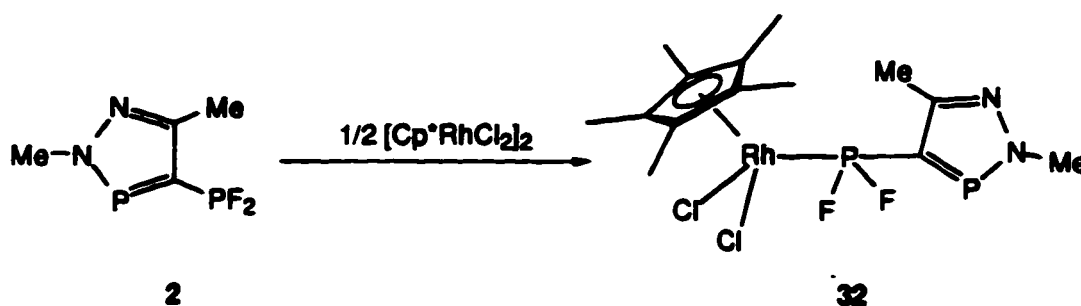
Atom1	Atom2	Distance	Atom1	Atom2	Distance
Rh	P11	2.1334(12)	P22	C21	1.713(4)
Rh	P21	2.1348(12)	N13	C14	1.355(5)
Rh	C1	2.257(5)	N13	C17	1.464(6)
Rh	C2	2.299(5)	N14	C15	1.316(5)
Rh	C3	2.231(5)	N23	C24	1.354(5)
Rh	C4	2.265(4)	N23	C27	1.468(5)
Rh	C5	2.237(4)	N24	C25	1.322(5)
P11	F11	1.574(3)	C1	C2	1.355(7)
P11	F12	1.562(3)	C1	C5	1.392(7)
P11	C11	1.774(4)	C2	C3	1.381(7)
P12	N13	1.671(4)	C3	C4	1.400(7)
P12	C11	1.713(4)	C4	C5	1.399(7)
P21	F21	1.576(3)	C11	C15	1.420(6)
P21	F22	1.563(3)	C15	C16	1.502(7)
P21	C21	1.771(4)	C21	C25	1.408(5)
P22	N23	1.672(4)	C25	C26	1.504(6)

Table 4.5

Selected Interatomic Angles (deg) for Cyclopentadienylbis(difluoro{2,5-dimethyl-2*H*-1,2,3 σ^2 -diazaphosphol-4-yl}phosphine)rhodium(I), (31).

Atom1	Atom2	Atom3	Angle	Atom1	Atom2	Atom3	Angle
P11	Rh	P21	94.56(5)	N13	N14	C15	109.4(4)
Rh	P11	F11	115.95(13)	P22	N23	N24	117.3(3)
Rh	P11	F12	120.59(13)	P22	N23	C27	127.2(3)
Rh	P11	C11	119.02(14)	N24	N23	C27	115.5(3)
F11	P11	F12	95.3(2)	N23	N24	C25	108.8(3)
F11	P11	C11	100.7(2)	P11	C11	P12	119.4(2)
F12	P11	C11	101.0(2)	P11	C11	C15	130.4(3)
N13	P12	C11	88.3(2)	P12	C11	C15	110.2(3)
Rh	P21	F21	114.85(13)	N14	C15	C11	114.6(4)
Rh	P21	F22	119.87(12)	N14	C15	C16	118.4(4)
Rh	P21	C21	122.60(14)	C11	C15	C16	127.0(4)
F21	P21	F22	96.0(2)	P21	C21	P22	121.6(2)
F21	P21	C21	99.0(2)	P21	C21	C25	128.5(3)
F22	P21	C21	99.5(2)	P22	C21	C25	109.8(3)
N23	P22	C21	88.6(2)	N24	C25	C21	115.4(4)
P12	N13	N14	117.5(3)	N24	C25	C26	117.5(4)
P12	N13	C17	126.3(4)	C21	C25	C26	127.0(4)
N14	N13	C17	116.2(4)				

The reaction of the rhodium(III) dimer, $[\text{Cp}^*\text{RhCl}_2]_2$ with **2** was investigated. The reasoning behind this experiment arises from the fact that this rhodium complex does not contain any labile ligands, such as CO or alkenes, so the only reaction possible is the cleavage of the bridging Rh-Cl bond. In this case, the Rh-Cl bond was easily broken by **2** to give the reddish-orange complex $\text{Cp}^*\text{RhCl}_2(\text{2})$ (**32**) in high yield (Scheme 4.4)).



Scheme 4.4 Formation of the rhodium complex **32** with **2**.

The $^{31}\text{P}\{^1\text{H}\}$ NMR spectrum showed an ADMX_2 spin system. There is an upfield shift for the exo-phosphorus centre resonance (188.95 ppm) which is coupled to the rhodium metal centre (216 Hz), the $\sigma^2\text{P}$ centre (102 Hz), and to both fluorine atoms (1170 Hz). The magnitude of the rhodium-phosphorus coupling constant was larger than what is normally observed but smaller than that for the rhodium complex **31** (*c.f.* 305 Hz). The decrease in the $^1\text{J}_{\text{PRh}}$ can be explained in terms of lower π -bonding between the metal centre and the phosphine in the case of Rh(III) complexes compared to the Rh(I) complexes.⁴³ There was a downfield shift of 15 ppm for the signal of the $\sigma^2\text{P}$ centre (269.92 ppm) and a slight decrease in the two-bond phosphorus-phosphorus coupling ($^2\text{J}_{\text{PP}} = 102$ Hz) in the rhodium complex relative to the uncoordinated ligand.

The ^{19}F NMR spectrum of the same sample consisted of a resonance of an apparent doublet of triplets centred at -62.20 ppm with a one-bond phosphorus-

fluorine coupling constant of 1158 Hz. Decoupling the phosphorus signal at 269 ppm collapsed the fluorine signal to a doublet of doublets, giving a value of 11 Hz for both ${}^3J_{\text{O}^2\text{PF}}$ and ${}^2J_{\text{FRh}}$.

Over a period of time (one week), a new species was observed to appear in the ${}^{31}\text{P}\{^1\text{H}\}$ NMR spectrum of the same NMR sample. The chemical shift for the resonance for the two-coordinate phosphorus centre had shifted upfield to 124.54 ppm and now showed coupling to the rhodium metal centre (${}^1J_{\text{O}^2\text{PRh}} = 114$ Hz), which was confirmed by decoupling the fluorine signals. Further coupling was observed to only one fluorine atom (${}^3J_{\text{O}^2\text{PF}} = 12$ Hz), which was also confirmed by selectively decoupling the fluorine signals. The signal for the exo-phosphorus centre was also shifted upfield (93.23 ppm) and showed a similar coupling pattern to that previously observed with ruthenium (complex **30**). In this case, the exo-phosphorus centre signal is coupling to rhodium (${}^1J_{\text{PRh}} = 144$ Hz) as well to two diastereotopic fluorine atoms (${}^1J_{\text{PF}} = 1263$ Hz, ${}^1J_{\text{PF}} = 1319$ Hz), showing a possible stereogenic centre at rhodium.

The ${}^{19}\text{F}$ NMR spectrum of this sample showed two different resonances for the chemical shifts for the fluorine atoms as they are inequivalent. The fluorine signal centre at 14.43 ppm was coupled to rhodium (${}^2J_{\text{FRh}} = 150$ Hz), to the exo-phosphorus centre (${}^2J_{\text{FP}} = 1310$ Hz), and to the two-coordinate phosphorus atom (${}^3J_{\text{O}^2\text{PF}} = 12$ Hz). The other fluorine signal, at -23.07 ppm, was coupled to rhodium (${}^2J_{\text{FRh}} = 116$ Hz) and to the exo-phosphorus centre (${}^2J_{\text{FP}} = 1265$ Hz). These values and assignments were also confirmed by selective phosphorus decoupling.

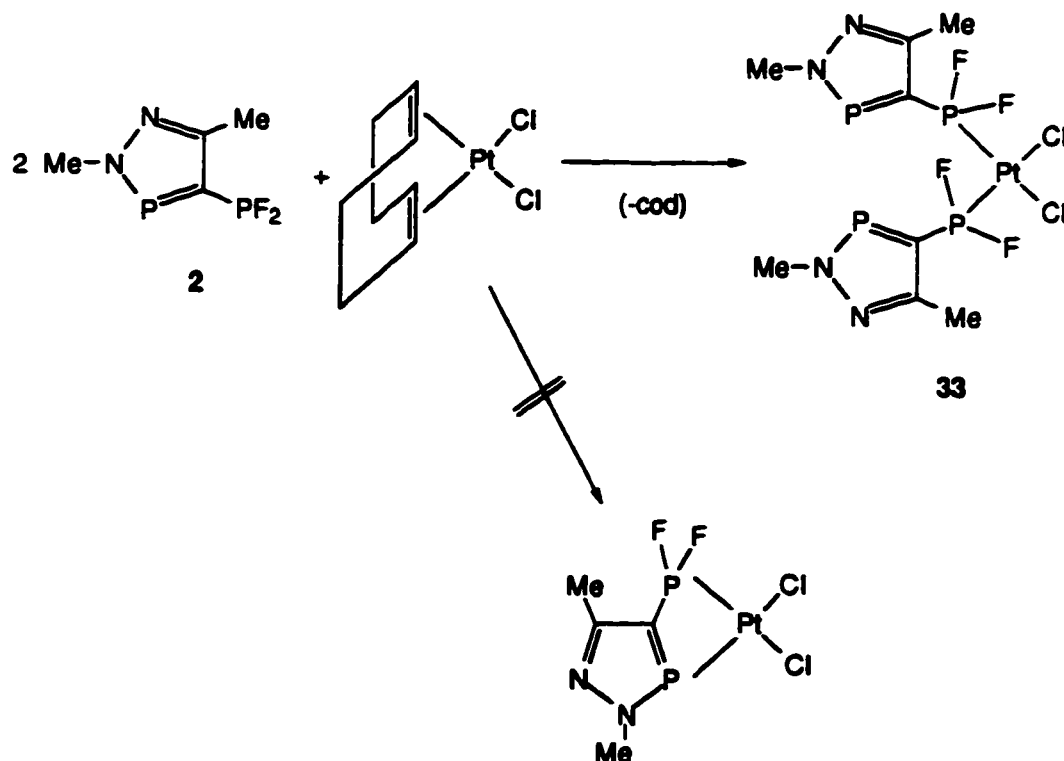
4.3.4 Formation of Complexes with Palladium and Platinum.

A number of platinum(II) complexes have been used for catalytic hydroformylation.⁴⁴ For the most part, these systems are of the type $[\text{PtCl}_2(\text{P-P})]$ where (P-P) is a bisphosphine. The use of Pt(II)-alkyl complexes as precursors with chiral bisphosphines is relatively unknown for asymmetric hydroformylation⁴⁵ even

though carbonylation with Pt(II) complexes containing monodentate phosphine ligands has been extensively investigated.⁴⁶⁻⁴⁹

The reaction of **2** with Pt(cod)Cl₂ resulted in the substitution of the cyclooctadienyl group to yield the *cis*-complex Pt(**2**)₂Cl₂ (**33**). The ³¹P{¹H} NMR spectrum showed no evidence for the formation of a chelated platinum complex, such as platinum satellites associated with the σ²P signal. There was a downfield shift for the resonance for the σ²P centre (271.21 ppm) and an upfield shift for the signal for the *exo*-phosphorus centre (159.29 ppm). The ²J_{PP} had increased to 150 Hz while the ¹J_{PF} had decreased (1125 Hz). A very large phosphorus-platinum one-bond coupling constant (¹J_{PPt} = 5064 Hz) was observed. This value is larger than the typical range of 2300 to 3600 Hz observed for *cis*-PtCl₂(PR₃)₂ complexes.⁵⁰ There have been only a few platinum complexes reported which have ¹J_{PPt} values greater than 5000 Hz.⁵¹⁻⁵³ The one-bond phosphorus-fluorine coupling constant had also increased slightly (1183 Hz). The signal for the chemical shift for the fluorine atoms in the ¹⁹F NMR spectrum was centred at -35.86 ppm and showed coupling to both phosphorus centres (³J_{σ²PF} = 12 Hz, ¹J_{PF} = 1125 Hz).

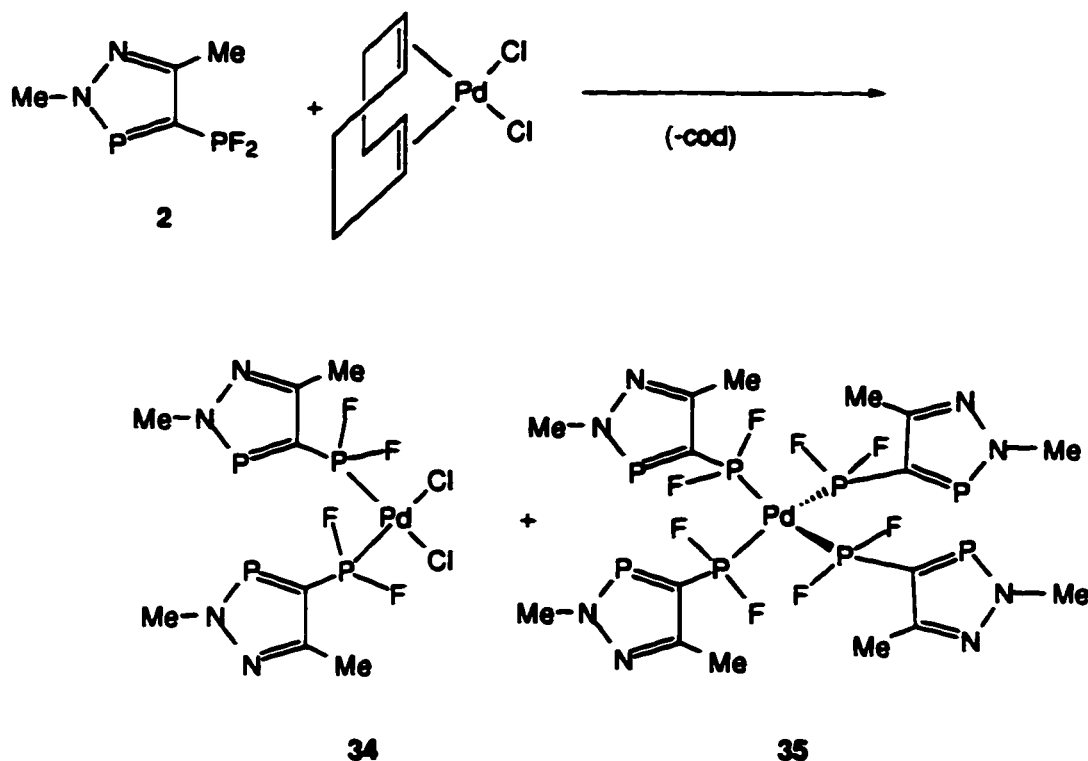
In the case of the reaction of **2** with Pd(cod)Cl₂, the initial yellow solution of the palladium precursor changed first to pale yellow. Over a period of one hour, a deep maroon solution formed. The ³¹P{¹H} NMR spectrum showed a mixture of two products, one being the expected palladium(II) complex, *cis*-Pd(**2**)₂Cl₂ (**34**), and the other one was the reduced palladium(0) complex, Pd(**2**)₄ (**35**) (Scheme 4.6). For both palladium complexes, the resonances for the *exo*-phosphorus centre were broadened. The appearance of the ³¹P{¹H} NMR spectrum of the *cis*-Pd(**2**)₂Cl₂ complex was that of an AMX₂ spin system. An upfield shift was observed for the resonance for the *exo*-phosphorus centre (144.33 ppm) which appeared as a doublet of triplets while the signal, which consisted of a doublet, for the σ²P centre was further shifted downfield at 267.88 ppm. There was an increase in the value for ²J_{PP} (158 Hz) relative to the



Scheme 4.5 Reaction of **2** with $\text{Pt}(\text{cod})\text{Cl}_2$.

starting phosphine **2**. The one-bond phosphorus fluorine coupling constant had also increased slightly (1184 Hz). The chemical shift for the fluorine atoms in the ^{19}F NMR spectrum was centred at -36.42 ppm and showed coupling to both phosphorus centres ($^3J_{\sigma^2\text{PF}} = 15 \text{ Hz}$, $^1J_{\text{PF}} = 1182 \text{ Hz}$)

The phosphorus NMR resonances for both the $\sigma^2\text{P}$ and the exo-phosphorus centres for the $\text{Pd}(0)$ complex appeared much broader than was the case for the $\text{Pd}(\text{II})$ complex **34**. When the NMR sample was cooled to -75°C , the $^{31}\text{P}\{^1\text{H}\}$ NMR spectrum did not show any sharpening of the signals for either $\text{Pd}(0)$ or $\text{Pd}(\text{II})$ complexes. Attempts to crystallize either of these palladium complexes from hexane/dichloromethane resulted only in a maroon oil.



Scheme 4.6 Reaction of **2** with Pd(cod)Cl₂.

Reaction of the Pd(0) complex Pd₂(dba)₃·CHCl₃ with 4 equivalents of **2** gave the complex Pd(**2**)₄ (**35**) as a wine-red powder. As previously observed in the reaction of **2** with Pd(cod)Cl₂, the ³¹P{¹H} NMR showed a broadened signal consisting of a doublet of triplets for the exo-phosphorus centre (202.45 ppm) and a broadened doublet for the σ²P centre (261.17 ppm). Coupling of the fluorines to the exo-phosphorus was smaller (1165 Hz) than with the uncomplexed ligand and there was a large increase in the value of ²J_{PP} (184 Hz). The change in the chemical shift for the resonance for the exo-phosphorus centre in the Pd(0) complex was less than 10 ppm upfield, relative to **2**.

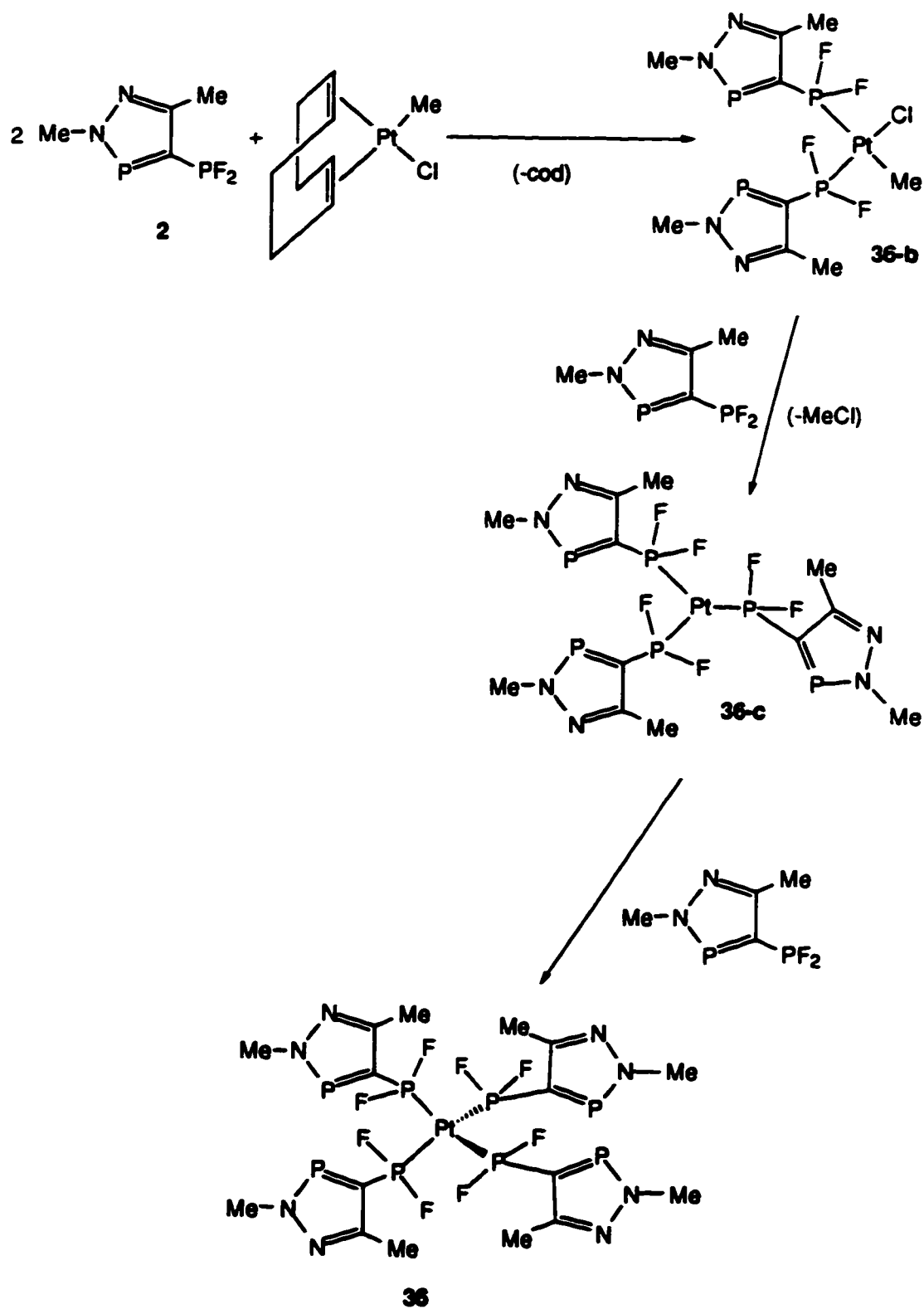
The reaction of [M(PEt₃)Cl₂]₂ (M= Pt or Pd) with **2** gave the metal complexes *trans*-M(PEt₃)(**2**)Cl₂ (**37**, M = Pt; **38**, M= Pd) The ³¹P{¹H} NMR spectrum for the platinum complex **37** showed an upfield shift for the exo-phosphorus centre signal of almost 85 ppm (124.32 ppm) and a 10 ppm (265.81 ppm) shift for the σ² phosphorus

resonance, whereas the signal for the PEt_3 ligand occurred at 18.4 ppm, which has shifted by 10 ppm downfield relative to the starting platinum complex. There was a large increase in the two-bond $\sigma^2\text{P}-\sigma^4\text{P}$ coupling constant (155 Hz) and again, the observed value for $^1J_{\text{PPt}}$ was large (5445 Hz). The $^2J_{\text{P}(\text{PEt}_3)}$ value was 18 Hz. The $^1J_{(\text{PEt}_3)\text{Pt}}$ value decreased substantially from 3845 Hz to 3190 Hz and this was accompanied by a decrease in the $^1J_{\text{PF}}$ to 1112 Hz. These decreases can be attributed to the competition by the phosphine ligands for the available d-electrons on the platinum metal centre. In the square planar *trans* complexes, the two phosphine ligands share the same metal d_π orbitals so that the platinum-phosphorus bonds are weakened. For the *cis* isomer, the two phosphorus ligands do not compete for the same d_π orbital. Since metal-halogen bonds are not considered to have a large π component, more platinum-phosphorus back-bonding can occur, which results in a stronger metal-phosphorus bond. The chemical shift for the fluorine signals in the ^{19}F NMR spectrum was centred at -38.21 ppm and showed coupling to both phosphorus centres ($^3J_{\sigma^2\text{PF}} = 15$ Hz, $^1J_{\text{PF}} = 1115$ Hz).

The signals in the $^{31}\text{P}\{^1\text{H}\}$ NMR spectrum for the palladium complex **38** were broadened, which may be caused by chemical shift anisotropy. An upfield shift for the signal for the exo-phosphorus centre of 49 ppm (160.23 ppm) and a shift of 10 ppm (266.05 ppm) for the $\sigma^2\text{P}$ centre occurred relative to the free phosphine. The chemical shift for the resonance for the PEt_3 group remained relatively unchanged at 42.62 ppm. The $^2J_{\sigma^2\text{PP}}$ value had also increased dramatically (153 Hz), as was observed with the platinum complex. Unlike the $\text{Pt}(\text{PEt}_3)(2)\text{Cl}_2$ complex, $^2J_{\text{PPEt}_3}$ coupling was not observed due to the broadened resonance. There was little change in the $^1J_{\text{PF}}$ value (≈ 1160 Hz) relative to the free phosphine. In the ^{19}F NMR spectrum, the fluorine signal was observed at -35.78 ppm giving a triplet with $^1J_{\text{PF}} = 1165$ Hz.

The reaction of Pt(cod)ClMe and **2** gave the unexpected reductive-elimination reaction product, Pt(0)(**2**)₄ (**36**), which was isolated from the reaction mixture as an orange crystalline solid. A possible mechanism for the formation of this complex is outlined in Scheme 4.7 wherein elimination of chloromethane is proposed. The elimination of chloromethane has been previously observed but as the result of the reduction of platinum from the +4 oxidation state to the +2 oxidation state rather than Pt(II) to Pt(0) as is the case here.⁵⁴ The reaction of phosphorus trifluoride with platinum(II) chloride also resulted in the reduction of platinum to give Pt(PF₃)₄.⁵⁵ Other Pt(0) complexes have been synthesized from fluorinated phosphines by the reductive processes starting from K₂PtCl₄.⁵⁶

When less than two equivalents of **2** were used in the reaction with Pt(cod)ClMe, the complex Pt(**2**)₂ClMe (**36-b**) was observed. The ³¹P{¹H} NMR spectrum (Figure 4.18) showed the signal for one of the σ³ phosphorus centres at 135.6 ppm (¹J_{Pt} 6089 Hz) while the other resonance was observed at 186.61 ppm (¹J_{Pt} 2511 Hz). The difference in the two resonances for the exo-phosphorus centres can be attributed to the greater *trans*-influence of the methyl group relative to the chloride. The *trans* influence is defined as the extent to which a coordinated ligand weakens the bond *trans* to itself in the equilibrium state of that complex. The ligands exhibiting a greater *trans*-influence are strong Lewis bases (σ donors) with minimal π-acceptor properties such as methyl groups, or strong π-acid ligands with synergistically enhanced σ donation. If a ligand is bound to the metal by a strong covalent bond then the bond *trans* must then have a large metal p component and will not be as strong.⁵⁷ The chemical shift for the resonance for the σ²P centre in this complex **36-b** remained the same with only a slight broadening of the peak (265 ppm). The attempted crystallization of Pt(**2**)₂ClMe (**36-b**) resulted only in the platinum(0) complex Pt(**2**)₄, **36**. The complex **36-b** was not structurally



Scheme 4.5 Reductive elimination of Pt(cod)ClMe with 2.

characterized. The only other known structure of a platinum(0) complex containing an organodifluorophosphine ligand is that of $\text{Pt}(\text{CF}_3\text{PF}_2)_4$.⁵⁵

The complex **36** crystallized in the space group, $I\bar{4}2m$. The solid-state structure of this complex revealed a tetrahedral Pt(0) centre, as shown in Figure 4.19. The angles about the platinum for P(1A)-Pt-P(1) and P(1B)-Pt-P(1) are 111.71(8) and 105.1(2), respectively. The phosphole rings are planar with the nitrogen in the 2-position also being planar with the sum of the angles about the nitrogen equalling 360°. The P(2)-N(2)-N(1) angle (115.9°(11)) is slightly wider than that of the phosphole itself (113.8°). The N(2)-P(2)-C(1) angle is 91.7(8)° which is larger than that which was observed for the phosphole (90.4°).⁵⁸ The P(2)-N(2) bond distance of 1.689(15)Å shows some multiple bond character when compared to the normally accepted P-N single bond (1.77Å) while greater than that of a typical P-N double bond (1.64Å). The F-P-F' bond angle is 94.4(5)° while the P-F bond distance is 1.565(6)Å which is longer than that observed for the oxidized iminophosphino-diazaphosphole, **18**, but similar to the $\text{CpRh}(\text{2})_2$ complex **31**.

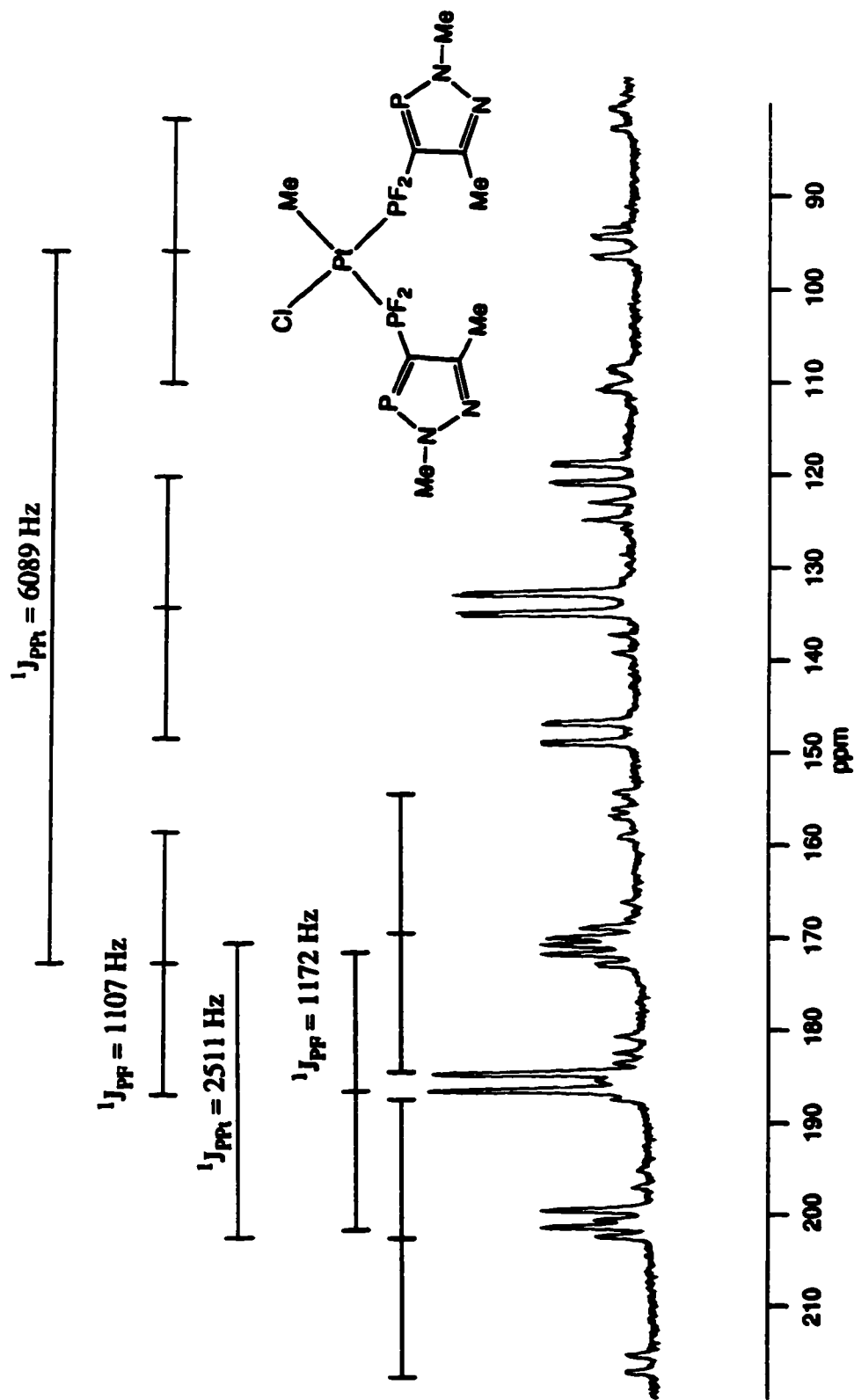


Figure 4.18 The $^{31}\text{P}\{^1\text{H}\}$ NMR (81.015 MHz) spectrum of the exo-phosphorus portion of $\text{Pt}(2)_2\text{ClMe}$ (**38-b**) in CDCl_3 .

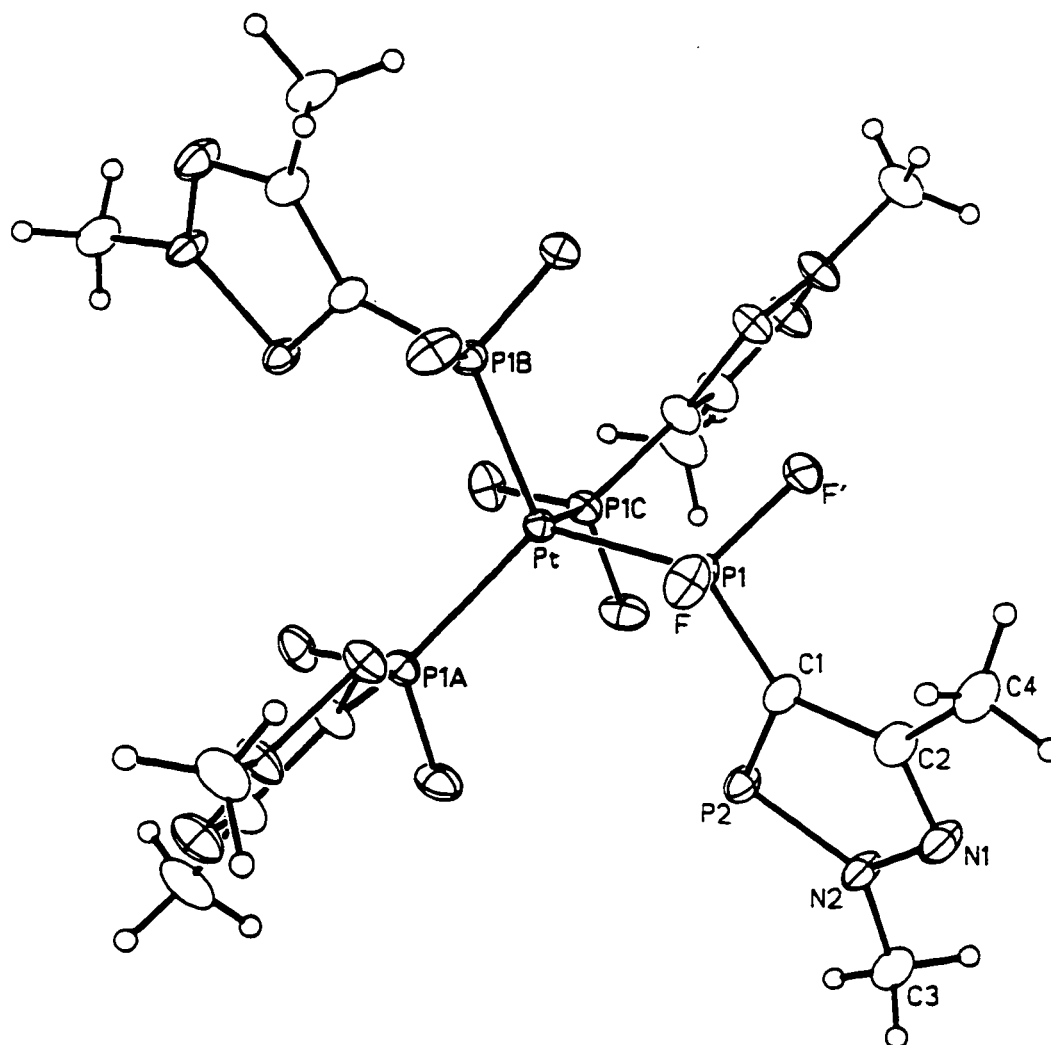


Figure 4.19 The solid-state structure of tetrakis(difluoro(2,5-dimethyl-2*H*-1,2,3 σ^2 -diazaphosphol-4-yl)phosphine)platinum(0) (**36**). Non-hydrogen atoms are represented by Gaussian ellipsoids at the 20% probability level. Hydrogen atoms are shown with arbitrarily small thermal parameters. Structure courtesy of Dr. R. McDonald.

Table 4.6

Selected Interatomic Distances (Å) for Tetrakis(difluoro{2,5-dimethyl-2*H*-1,2,3σ²-diazaphosphol-4-yl}phosphine)platinum(0), (36).

Atom1	Atom2	Distance	Atom1	Atom2	Distance
Pt	P1	2.237(3)	N1	N2	1.380(15)
P1	F	1.565(6)	N1	C2	1.33(2)
P1	C1	1.70(2)	N2	C3	1.42(2)
P2	N2	1.689(15)	C1	C2	1.45(2)
P2	C1	1.72(2)	C2	C4	1.50(2)

Table 4.7

Selected Interatomic Angles (deg) for Tetrakis(difluoro{2,5-dimethyl-2*H*-1,2,3σ²-diazaphosphol-4-yl}phosphine)platinum(0), (36).

Atom1	Atom2	Atom3	Angle	Atom1	Atom2	Atom3	Angle
P1 ^A	Pt	P1	117.1(8)	P2	N2	C3	127.9(12)
P1 ^B	Pt	P1	105.1(2)	N1	N2	C3	116.2(15)
Pt	P1	F	116.8(2)	P1	C1	P2	122.9(10)
Pt	P1	C1	121.2(6)	P1	C1	C2	131.5(14)
F	P1	F	94.4(5)	P2	C1	C2	105.6(13)
F	P1	C1	101.7(4)	N1	C2	C1	119.1(15)
N2	P2	C1	91.7(8)	N1	C2	C4	113.7(14)
N2	N1	C2	107.6(15)	C1	C2	C4	127.1(15)
P2	N2	C2	115.9(11)				

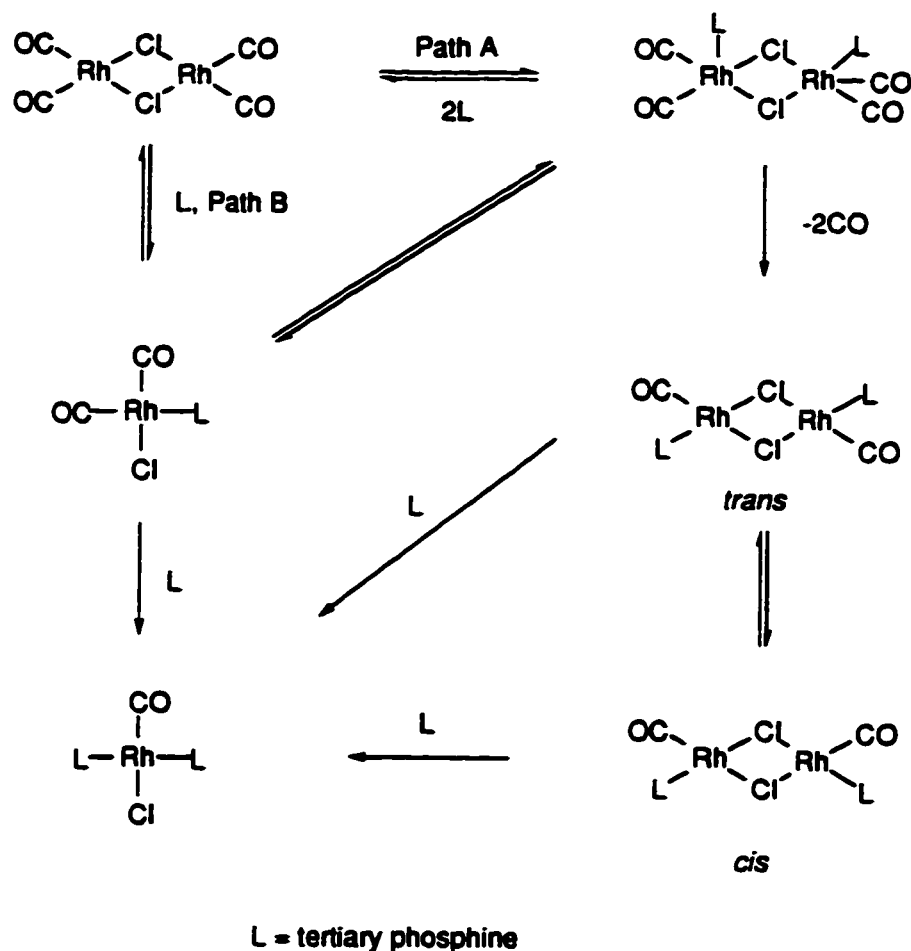
4.4 Metal Complexation of 4-(Bis(dimethylamino)phosphino)-2,5-dimethyl-2H-1,2,3 σ^2 -diazaphosphole (3)

Unlike the difluorophosphinodiazaphosphole **2**, the bis(dimethylamino)-phosphino derivative **3** creates a more basic phosphorus centre due to the presence of the electron-donating methyl groups of the dimethylamino substituents. This diazaphosphole may thus behave more like alkyl and aryl phosphines than **2**. An additional point of difference between **3** and alkyl/aryl phosphines in general is the bulky environment about the coordinating phosphorus centre. With metal complexes, the steric bulk of the dimethylamino groups may congest the metal centre sufficiently to make the complex more stable.

4.4.1 Reactions of 3 with Rhodium Complexes

Unlike the reaction of **2** with the dimeric rhodium complex $[\text{Rh}(\text{CO})_2\text{Cl}]_2$, which gave an identified product, the reaction of **3** resulted in the red complex *trans*- $\text{Rh}(\text{CO})\text{Cl}(\text{3})_2$ (**39**). The complex was recrystallized from diethyl ether/dichloromethane to obtain pale red crystals which were structurally characterized (*vide infra*). A number of *trans*-rhodium complexes have been obtained with other phosphines.⁵⁹ Because of the steric bulk of **3**, the formation of this complex most probably follows Path B in Scheme 4.8, wherein the rhodium dimer is broken first, rather than path A.

The $^{31}\text{P}\{^1\text{H}\}$ NMR spectrum of **39** (Figure 4.20) revealed a second order "triplet" for both phosphorus centres. This "triplet" is the combination of both the two-bond and four-bond $\sigma^2\text{P}-\sigma^4\text{P}$ coupling constant. For this type of spectrum, only the value of $|J_{\text{AX}} + J_{\text{AX}}'|$ can be obtained unless sufficient differences can be extracted from the line patterns inside and outside the major doublet, which in this case is not possible.⁶⁰ The chemical shift of the exo-phosphorus was shifted by 16 ppm downfield to 103.34 ppm while the chemical shift of the $\sigma^2\text{P}$ was relatively



Scheme 4.8 Proposed mechanism for the formation of *trans*-[Rh(CO)Cl(L)₂] from the reaction of [Rh(CO)₂Cl]₂ and a tertiary phosphine.

constant with the value of $|^2J_{\sigma^2P\sigma^4P} + ^4J_{\sigma^2P\sigma^4P}|$ being 51 Hz. The observed one-bond phosphorus-rhodium coupling was 143 Hz, which is within the range frequently observed for $^1J_{PRh}$ in these complexes.⁶⁹ The carbonyl frequency in the infrared spectrum was observed at 1978 cm^{-1} , which is comparable to other rhodium carbonyl chloride alkyl and aryl phosphines listed in Table 4.7.

The solid-state structure of **39** (Figures 4.21 and 4.22) showed a square planar rhodium metal centre wherein both diazaphosphole ligands lie *trans* to each other, as one would anticipate with such bulky phosphines. One interesting feature of the

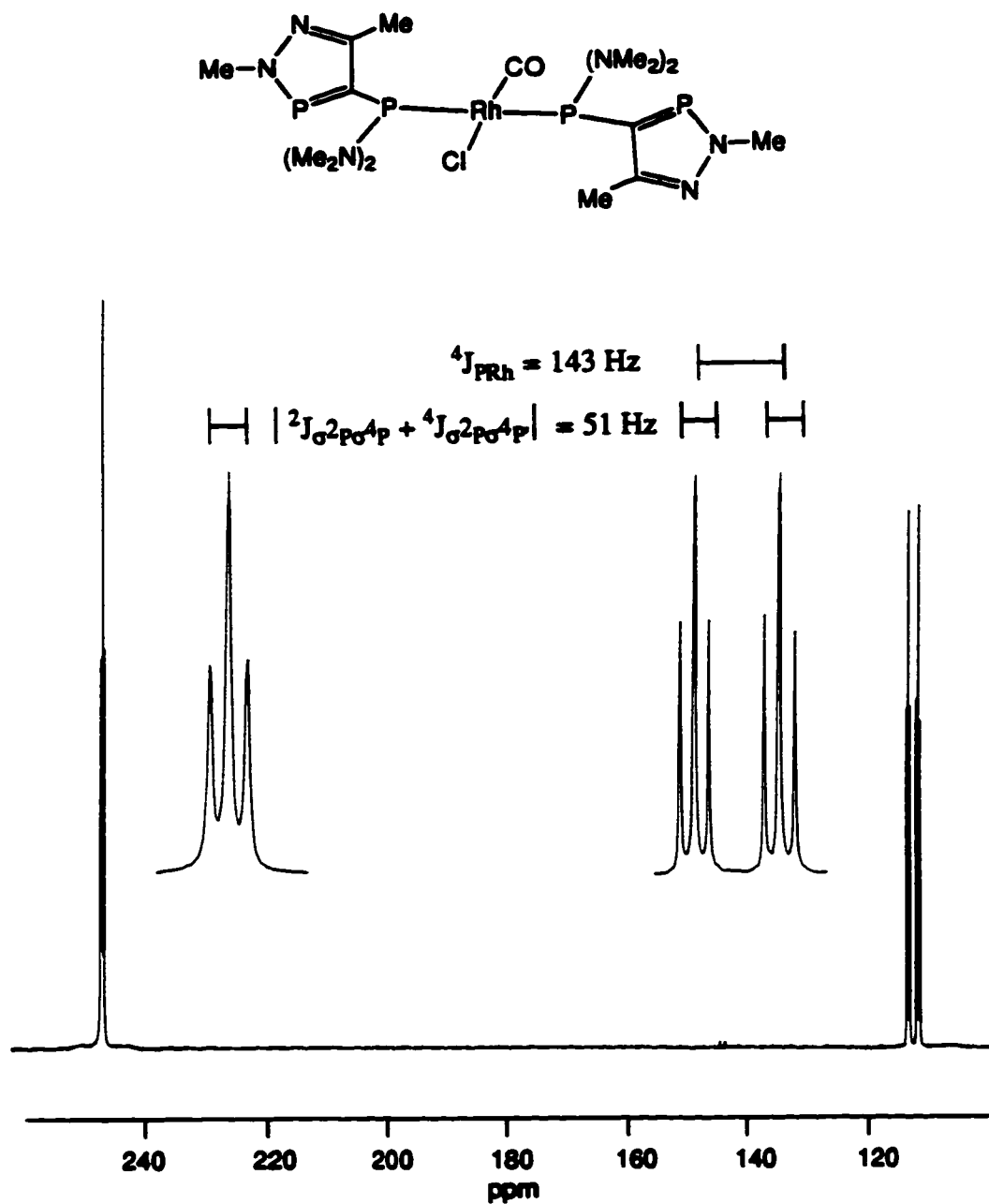


Figure 4.20 The ^{31}P $\{^1\text{H}\}$ NMR (161.977 MHz) spectrum of ((bis(bis-(dimethylamino) [2,5-dimethyl-2H-1,2,3-diazaphosphol-4-yl] phosphine) rhodium(I) complex (39) in CDCl_3 .

Table 4.8Infrared Data (Carbonyl) for *trans*-[RhCl(CO)(L)₂] Complexes.

Compound	$\nu(\text{CO})$ (cm^{-1})	Ref.
39	1978	This work
PPh ₃	1980	61
P(<i>p</i> -MeC ₆ H ₄) ₃	1965	62
PMe ₃	1965	63
P ^t Bu ₃	1923	64
P(2-pyridyl)Ph ₂	1978, 1964	65
P(C ₆ F ₅)Ph ₂	1996	66
P(C ₆ F ₅) ₂ Ph	1982	66
P(C ₆ F ₅) ₃	2004	66
P(OMe) ₃	2014	67
P(OPh) ₃	2018	68

structure is that the diazaphosphole rings are aligned in almost a stacking fashion so that a mirror plane may exist through the Cl-Rh-CO plane. Because of this symmetrical feature, two isomers of the complex were found. These isomers only differ in the exchange of the chlorides and the carbon monoxide ligands. One of the isomers is more predominant than the other (75:25). A similar observation was made with the dimethylphenylphosphine analogue,⁷⁰ where the phenyl rings lay on the same side of the rhodium complex and were orientated towards the carbonyl group. It was rationalized that the orientation of the phenyl rings was due to an electronic interaction between these rings and the carbonyl moiety. A similar effect may be operational here. In the complex **39**, the diazaphosphole rings are oriented

perpendicular to the P(1)-Rh-CO-Cl-P(2) plane of the molecule and parallel to the CO-Rh-Cl axis and so they are parallel to each other. Once again, the phosphole rings are planar, and the angles about the $\sigma^2\text{P}$ centres, C(11)-P(12)-N(13) and C(21)-P(22)-N(23), are $89.1(3)^\circ$ and $88.9(4)^\circ$, respectively. The phosphorus-rhodium distance is 2.33\AA , which is comparable to that of the Rh-P bond length (2.326\AA) in the $\text{Rh}(\text{CO})_2\text{Cl}(\text{PPh}_3)$ complex.⁷¹ The average P-N bond distances of the exophosphorus centre and the dimethylamino groups is 1.683\AA . This distance is shorter than the normally accepted distance of 1.77\AA , which suggests some multiple bonding characteristics in the P-N bond. The dimethylamino nitrogen atoms are planar, with the sum of the angles about the nitrogen centres being 360° . The bond distances and bond angles of the diazaphosphole ring are tantamount to those observed for the rhodium and platinum complexes of the difluoro derivative.

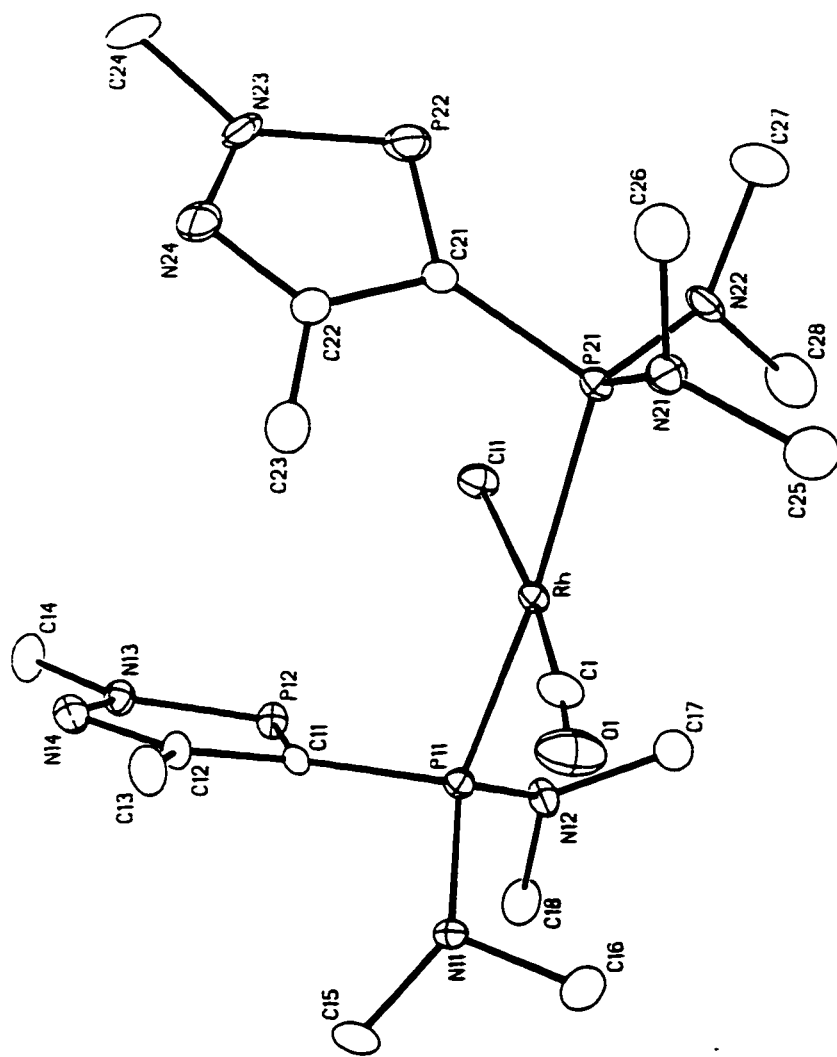


Figure 4.21 Perspective view of the major (75%) isomer of *trans*-chlorocarbonyl-((bis(dimethylamino) [2,5-dimethyl-2H-1,2,3-diazaphosphol-4-yl] phosphine) rhodium(I) (39). Non-hydrogen atoms are represented by Gaussian ellipsoids at 20% probability level. Hydrogen atoms are have been omitted for clarity. Structure courtesy of Dr. R. McDonald.

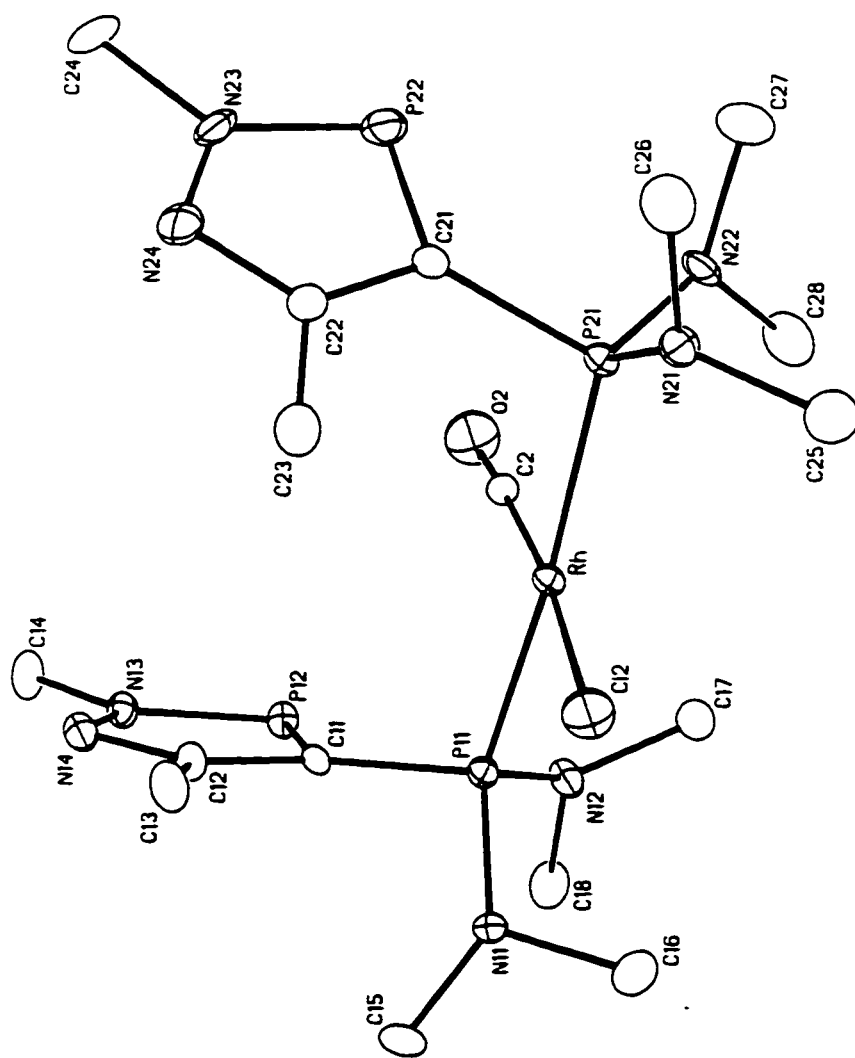


Figure 4.22 View of minor (25%) isomer of **39**. Compared to the major isomer, the positions of the chloro and carbonyl ligands have been exchanged, while the dispositions of the phosphine ligands are unchanged. Structure courtesy of Dr. R. McDonald.

Table 4.9

Selected Interatomic Distances (Å) for *trans*-Chlorocarbonyl(bis(bis-(dimethylamino) {2,5-dimethyl-2*H*-1,2,3σ²-diazaphosphol-4-yl} phosphine))-rhodium(I), (39).

Atom1	Atom2	Distance	Atom1	Atom2	Distance
Rh	C11	2.395(4) ^a	N11	C15	1.455(8)
Rh	C12	2.46(2) ^b	N11	C16	1.455(8)
Rh	P11	2.333(2)	N12	C17	1.462(8)
Rh	P21	2.326(2)	N12	C18	1.455(8)
Rh	C1	1.777(13) ^a	N13	N14	1.350(7)
Rh	C2	1.77(1) ^b	N13	C14	1.434(8)
P11	N11	1.695(5)	N14	C12	1.344(8)
P11	N12	1.683(6)	N21	C25	1.455(8)
P11	C11	1.784(7)	N21	C26	1.480(8)
P12	N13	1.678(6)	N22	C27	1.457(8)
P12	C11	1.704(7)	N22	C28	1.468(9)
P21	N21	1.686(6)	N23	N24	1.356(9)
P21	N22	1.668(6)	N23	C24	1.473(8)
P21	C21	1.795(7)	N24	C22	1.325(9)
P22	N23	1.679(7)	C11	C12	1.409(9)
P22	C21	1.712(7)	C12	C13	1.495(9)
O1	C1	1.13(2) ^a	C21	C22	1.413(10)
O2	C2	1.12(1) ^b	C22	C23	1.499(9)

a) Major (75%) isomer.

b) Minor (25%) isomer.

Table 4.10

Selected Interatomic Angles (deg) for *trans*-Chlorocarbonyl(bis(bis(dimethylamino)-(2,5-dimethyl-2*H*-1,2,3σ²-diazaphosphol-4-yl)phosphine))rhodium(I), (39).

Atom1	Atom2	Atom3	Angle	Atom1	Atom2	Atom3	Angle
C11	Rh	P11	86.71(10) ^a	N21	P21	N22	108.9(3)
C11	Rh	P21	87.18(10) ^a	N21	P21	C21	101.5(3)
C11	Rh	C1	173.6(4) ^a	N22	P21	C21	106.2(3)
C12	Rh	P11	92.9(7) ^b	N23	P22	C21	88.9(4)
C12	Rh	P21	92.7(7) ^b	P11	N11	C15	124.4(5)
C12	Rh	C1	172.4(41) ^b	P11	N11	C16	115.5(5)
P11	Rh	P21	173.33(8)	C15	N11	C16	112.6(6)
P11	Rh	C1	93.6(4) ^a	P11	N12	C17	120.0(5)
P11	Rh	C2	88.14) ^b	P11	N12	C18	120.1(5)
P21	Rh	C1	92.1(4) ^a	C17	N12	C18	112.5(6)
P21	Rh	C2	85.9(12) ^b	P21	N21	C25	114.8(5)
Rh	P11	N11	117.4(2)	P21	N21	C26	123.0(5)
Rh	P11	N12	111.7(2)	C25	N21	C26	111.5(6)
Rh	P11	C11	110.7(2)	P21	N22	C27	123.2(6)
N11	P11	N12	109.4(3)	P21	N22	C28	120.6(5)
N11	P11	C11	103.8(3)	C27	N22	C28	112.4(6)
N12	P11	C11	102.5(3)	Rh	C1	O1	175.9(13) ^a
N13	P12	C11	89.1(3)	Rh	C2	O2	177.9(44) ^b
Rh	P21	N21	117.5(2)	P11	C11	P12	122.9(4)
Rh	P21	N22	112.0(2)	P21	C21	P22	126.0(4)
Rh	P21	C21	109.7(2)				

a) Major (75%) isomer.

b) Minor (25%) isomer.

4.4.2 Reactions of 3 with Palladium and Platinum Precursors

The reaction of 3 with $M(\text{cod})\text{Cl}_2$ ($M = \text{Pd}, \text{Pt}$) resulted in the simple displacement of the cyclooctadienyl group to give $M(\mathbf{3})_2\text{Cl}_2$ ($M = \text{Pd}$ (40), Pt (41)). In both cases, the $^{31}\text{P}\{^1\text{H}\}$ NMR spectrum showed the same pattern of the deceptively simple second order "triplet" that was observed with the rhodium complex 39. For the palladium complex 40, the chemical shift for the exo-phosphorus occurred at 86.94 ppm with the $\sigma^2\text{P}$ resonance at 249.63 ppm. The major splitting, $|2J_{\sigma^2\text{P}\sigma^4\text{P}} + 4J_{\sigma^2\text{P}\sigma^4\text{P}}|$, was 51 Hz. For the platinum complex 41, the signals were observed at 248.88 ppm and 80.59 ppm for the $\sigma^2\text{P}$ and the exo-phosphorus, respectively. The value of $|2J_{\sigma^2\text{P}\sigma^4\text{P}} + 4J_{\sigma^2\text{P}\sigma^4\text{P}}|$ was 57 Hz. The one-bond phosphorus-platinum coupling constant in these cases was much smaller than observed in the platinum complexes with 2 ($^1J_{\text{PPt}} = 2918$ Hz). The ^{195}Pt NMR spectrum gave a chemical shift of 179.04 ppm.

The reaction of 3 with $\text{Pt}(\text{cod})\text{ClMe}$ produced the *cis*- $\text{Pt}(\mathbf{3})_2\text{ClMe}$ complex (42) unlike that obtained for the reaction with 2. The $^{31}\text{P}\{^1\text{H}\}$ NMR spectrum showed only one signal for the exo-phosphorus centre (75.21 ppm, $|2J_{\sigma^2\text{P}\sigma^4\text{P}} + 4J_{\sigma^2\text{P}\sigma^4\text{P}}| = 53$ Hz). Both exo-phosphorus centres are equivalent so the complex formed must be the *trans* isomer. Had the *cis* isomer been formed as was observed with 2, the two $^1J_{\text{PP}}$ values would be different due to the *trans*-influence, and a similar pattern to that observed in the complex 38-b would result. The ^{195}Pt spectrum showed an $\text{A}_2\text{D}_2\text{MX}_3$ spin system. The platinum is coupled to both phosphorus atoms ($^1J_{\text{PPt}} = 3554$ Hz, $^3J_{\text{PPt}} = 50$ Hz) as well as to the protons of the methyl group ($^2J_{\text{HPt}} = 83$ Hz), which gives rise to a splitting pattern of a triplet of triplets of quartets (Figure 4.23).

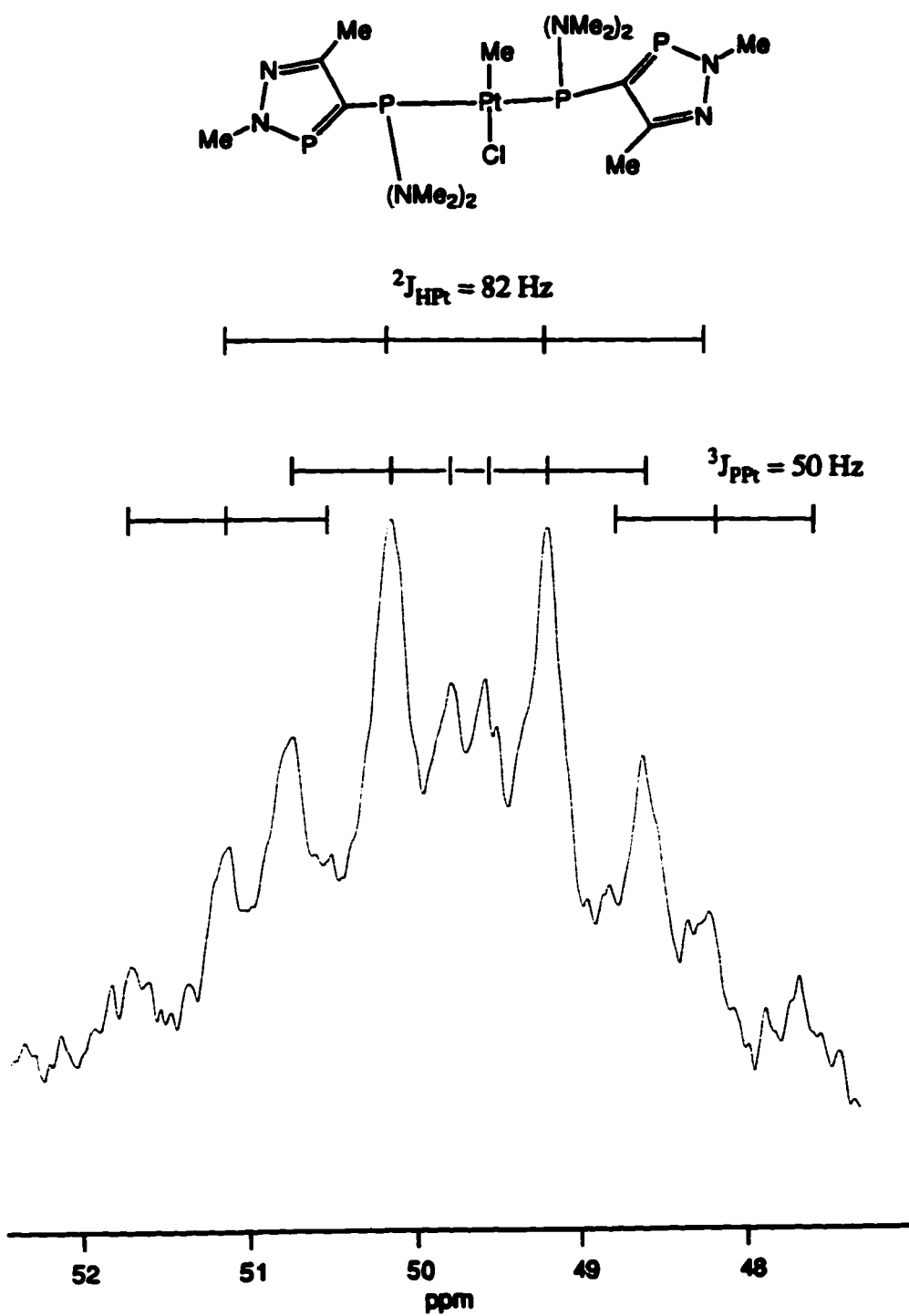


Figure 4.23 The ^{195}Pt NMR (21.40 MHz) spectrum of $\text{Pt}(\text{3})_2\text{MeCl}$ (42) in CDCl_3 .

4.5 Metal Complexation of 4-((2,2,2-Trifluoroethoxy)phosphino)-2,5-dimethyl-2H-1,2,3 σ^2 -diazaphosphole (11)

Placing alkoxy groups on the exo-phosphorus centre creates a phosphorus atom which is more basic than it is in **2**. It is also less basic than the amino derivatives such as **3** though the centre is not as bulky. The nucleophilic character of alkyl phosphites has been used to reduce metal centres.⁷² The electron-withdrawing 2,2,2-trifluoroethoxy group on the exo-phosphorus atom also inhibits the Arbuzov reaction by providing a phosphorus centre which is not as nucleophilic as an alkyl phosphite.

As was observed in the case of **3**, the reaction of **11** with $[\text{Rh}(\text{CO})_2\text{Cl}]_2$ resulted in the formation of the *trans*- $[\text{Rh}(\text{CO})\text{Cl}(\mathbf{11})_2]$ complex (**43**). The $^{31}\text{P}\{^1\text{H}\}$ NMR spectrum of this compound was second order, showing a spectrum consisting of two deceptively similar simple "triplets", as was observed with complexes derived from **3**. Surprisingly, chemical shift of the exo-phosphorus signal was only reduced by 8 ppm (159.78 ppm) upon complexation whereas the signal for the $\sigma^2\text{P}$ centre experienced a greater shift downfield of 14.5 ppm (251.88 ppm). The major spacing for $|2J_{\sigma^2\text{P}\sigma^4\text{P}} + 4J_{\sigma^2\text{P}\sigma^4\text{P}}|$ was 52 Hz. The $^1J_{\text{PRh}}$ coupling constant was 187 Hz.

The fluorine NMR spectrum of **43** showed a single resonance at -74.50 ppm for the fluorines of the trifluoroethoxy group, which was unchanged from that of the uncomplexed phosphinodiazaphosphole **11**. Unlike the parent diazaphosphole **11**, however, coupling to either the $\sigma^2\text{P}$ centre or the protons was not resolved. This observation was consistent with the proton spectrum where only two broadened resonances were seen for the diastereotopic protons (4.353 ppm and 4.585 ppm). Even at higher magnetic fields, the coupling to other nuclei remained unresolved.

The $^{13}\text{C}\{^1\text{H}\}$ NMR spectrum of **43** showed an upfield shift for the resonance for the carbon at the 4-position of the ring which was coupled to both phosphorus centres (135.26 ppm, $^1J_{\sigma^2\text{PC}} = 84$ Hz, $^1J_{\sigma^3\text{PC}} = 42$ Hz). The carbon at the 5-position

of the ring showed only coupling to the exo-phosphorus centre (155.57 ppm, ${}^2J_{\sigma^4PC}$ 10 Hz). The resonance for the trifluoromethyl carbon showed coupling to the exo-phosphorus (122.19 ppm, ${}^3J_{\sigma^4PC} = 9$ Hz, ${}^1J_{CF} = 277$ Hz). Coupling to only the fluorines was observed in the methylene carbon signals (64.83 ppm, ${}^2J_{CF} = 39$ Hz) but the coupling to the phosphorus was unresolved.

The infrared spectrum of **43** showed the carbon monoxide stretching frequency at 2010 cm^{-1} . Comparing the $\nu(\text{CO})$ stretching frequency of the rhodium carbonyl complex **43** with similar *trans*-rhodium carbonyl chlorine complexes listed in Table 4.7 suggests that the π -bonding characteristics are similar to this of the phosphites $\text{P}(\text{OMe})_3$ (2014 cm^{-1}) and $\text{P}(\text{OPh})_3$ (2018 cm^{-1}). There was a slight shift in the P-O stretching frequency (1165 cm^{-1}) on coordination.

The palladium and platinum complexes $[\text{M}(\mathbf{11})_2\text{Cl}_2]$ (**44**: M = Pd; **45**: M = Pt) were synthesized from the their respective $\text{M}(\text{cod})\text{Cl}_2$ precursors. The palladium complex **44** showed an AA'XX' spin system in the ${}^{31}\text{P}\{^1\text{H}\}$ NMR spectrum. The signal for the two-coordinate phosphorus centre was found at 256.43 ppm, further deshielded than it was in the rhodium complex **43**. As for the exo-phosphorus centre, it was shifted upfield by 37 ppm to 131.16 ppm. The value for the $|{}^2J_{\sigma^2P\sigma^4P} + {}^4J_{\sigma^2P\sigma^4P}'|$ was 51 Hz for **44**.

The platinum analogue **45** did not show any second order behaviour in the phosphorus NMR spectrum. Similar to the palladium complex **44**, a downfield shift for the resonance of the $\sigma^2\text{P}$ unit (256.78 ppm) was observed while the signal for the exo-phosphorus was even further shifted upfield (104.37 ppm). Relative to the parent diazaphosphole **11**, there was an increase in the two-bond phosphorus-phosphorus coupling from 25 Hz to 58 Hz. The electron-withdrawing ability of the trifluoroethoxy parallels that of the difluoro analogue **2** in that the value of the ${}^1J_{\sigma^4PPt}$ coupling was also large (4811 Hz).

4.6 Metal Complexation of Oxidized 4-(Phosphorano)-2,5-dimethyl-2*H*-1,2,3σ²diazaphospholes

The unoxidized phosphinodiazaphospholes have a large bite angle induced by the rigid structure of the P-C-P backbone and as such are reluctant to form chelates. The larger bite angle of the chalcogen derivatives of the phosphoranodiazaphospholes offers the opportunity to form a chelate complex with a single metal. The imino group afforded by azide oxidation of the exo-phosphorus offers a more versatile functionality on the exo-phosphorus atom because it is possible to change the substituent carried on the nitrogen of this imine centre. This alteration allows for the "fine-tuning" of the Lewis basicity of the nitrogen, and as a consequence affects its coordination capacity towards transition metals.



Figure 4.25 Possible metallacycles formed using the phosphino- and phosphoranodiazaphospholes.

4.6.1 Metal Complexation of 4-(bis(dimethylamino)phosphorano)-2,5-dimethyl-2*H*-1,2,3σ²diazaphospholes

The oxidized species, 4-(bis(dimethylamino)thiophosphorano)-2,5-dimethyl-2*H*-1,2,3σ²-diazaphosphole, **21**, and (bis(dimethylamino)selenophosphorano)-2,5-dimethyl-2*H*-1,2,3σ²-diazaphosphole, **22**, were reacted with a number of metal complexes such as Cr(CO)₅(THF). Unfortunately there was no clear evidence in the ³¹P{¹H} NMR of the formation of a monodentate complex, coordinating either through the two-coordinate phosphorus atom or the nitrogen of the imino group.

The reaction of $\text{Mo}(\text{cht})(\text{CO})_3$ with **21** did show the formation of a complex in the $^{31}\text{P}\{^1\text{H}\}$ NMR spectrum. The spectrum showed an upfield shift for the signal for the $\sigma^2\text{P}$ (224.67 ppm) as well as a dowfield shift for the $\sigma^4\text{P}$ resonance (113.21 ppm) with a decrease in the two-bond phosphorus-phosphorus coupling constant (82 Hz). These observations imply the formation of a tripodal chelate using the endocyclic phosphorus atom and the nitrogens of the amino groups. The phosphoranodiazaphosphole would then occupy one face of the octahedral molybdenum metal centre in a *fac* orientation as shown in Figure 4.25. The definitive structure of this complex could not be established and proper formulation awaits further work.

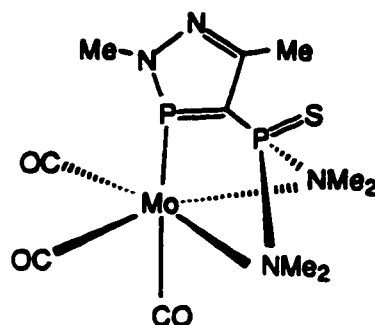


Figure 4.25 Possible structure for the reaction of **21** with $\text{Mo}(\text{cht})(\text{CO})_3$.

4.6.2 Iminophosphorano Metal Complexes

Isoelectronic with R_3PO , the iminophosphorano compounds form stable complexes with Lewis acid metal halides. While phosphine oxides form donor-acceptor complexes (C), the anionic iminophosphoranes form complexes wherein any short distance between the metal and nitrogen is interpreted as a double bond (D).



Though the metal-nitrogen-phosphorus linkage is generally linear, a number of complexes with smaller bond angles are known.⁷³ The bending of the M-N-P moiety is described by the contribution of the resonance structures shown in Figure 4.26.

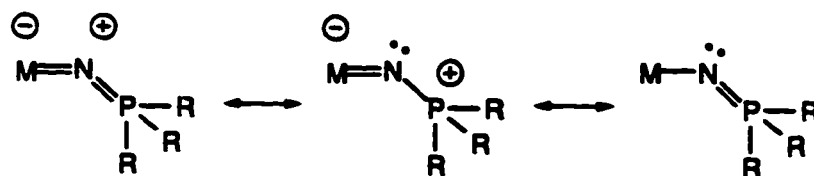
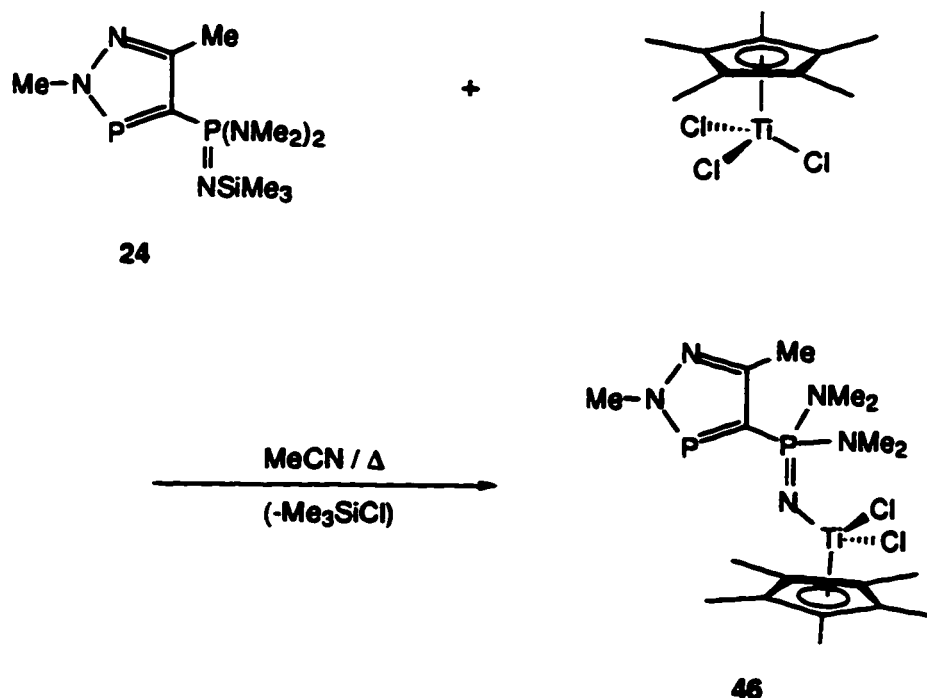


Figure 4.26 Resonance structures of the iminophosphorano metal complexes with a non-linear M-N-P moiety.

The infrared spectra of the iminophosphorane metal complexes have a characteristic absorption $\sim 1100\text{ cm}^{-1}$, which is assigned as the antisymmetric stretching vibration of the M-N-P group. The corresponding symmetrical stretch generally lies below 600 cm^{-1} , but this has only been reliably assigned for a few examples. The linear linkages tend to have the largest difference between the two stretching frequencies. For example, the complex $[\text{MoCl}_4(\text{NPPH}_3)(\text{pyridine})]\cdot\text{CH}_2\text{Cl}_2$,⁷⁴ shows two stretching frequencies at 1130 cm^{-1} and 560 cm^{-1} , which corresponds to a difference of 570 cm^{-1} and in this case the Mo-N-P bond angle is 177° . In the case of $[\text{Re}(\text{NO})(\text{NPPH}_3)\text{Cl}_3(\text{OPPh}_3)]$,⁷⁵ the difference of the two stretching frequencies is 390 cm^{-1} and the Re-N-P bond angle is 139° .

The employment of the trimethylsilyliminophosphorano derivative of **3** with metal chlorides provides a means for the formation of a metal-nitrogen sigma bond. The reaction of **23** with Cp*TiCl₃ at elevated temperatures in acetonitrile resulted in formation of the iminophosphorano titanium complex **46** (Scheme 4.9).



Scheme 4.9 Synthesis of the titanium complex **46**.

The ³¹P{¹H} NMR spectrum shows a shift to a lower field for the resonance for the two-coordinate phosphorus centre (260.87 ppm) and a shift of 34 ppm to 40.87 ppm downfield for the iminophosphorane centre signal. The ¹J_{PP} had increased to 84 Hz. The carbon signal for the methyl groups of the trimethylsilyl moiety (3.56 ppm for **21**) disappears from the ¹³C{¹H} NMR, as the result of the loss of trimethylsilyl chloride and provides evidence for the formation of the titanium-nitrogen sigma bond.

The infrared spectrum shows a strong absorption at 1091 cm⁻¹ due to the antisymmetric stretch of the P-N-Ti group. For a comparison, other Ti-N-P linkages

show asymmetric stretching frequencies ranging from 986 cm^{-1} for $\text{CpTiCl}_2(\text{NPMe}_3)^{76}$ to 1110 cm^{-1} for $[\text{Ph}_2\text{P}(\text{NSiMe}_3)_2]\text{Ti}(\text{NPNSiMe}_3)^{77}$

The crystallization of the complex **46** from acetonitrile provided x-ray quality crystals. From the solid-state structure shown in Figure 4.28, the N2-P1-C5 angle of the diazaphosphole ring is 89.3° , which is similar to those shown in other structures reported in this thesis. One important feature of the structure is the angle of 161.5° for the Ti-N-P linkage. This angle is comparable to others listed in Table 4.11. The bonding description of phosphinimate complexes with an end-on arrangement is shown in Figure 4.27. An angle of 180° for M-N-P is expected in this case. One reason for the deviation from 180° may be the steric effects about the titanium metal centre which arise from the pentamethylcyclopentadienyl ring and the two dimethylamino groups on the exo-phosphorus centre. The Ti-N distance is shorter than the sum of the single-bond covalent radii, hence the phosphinimate is probably a three-electron donor. The P=N distance is slightly shorter than the other titanium complexes in Table 4.11. The shortening of this bond length may be a consequence of continued conjugation through to the diazaphosphole ring, hence an increase in the $^2J_{\text{PP}}$ value. The P-N distance of the exo-phosphorus atom and the dimethylamino groups is also shortened considerably (1.649 \AA), also showing multiple bonding character.

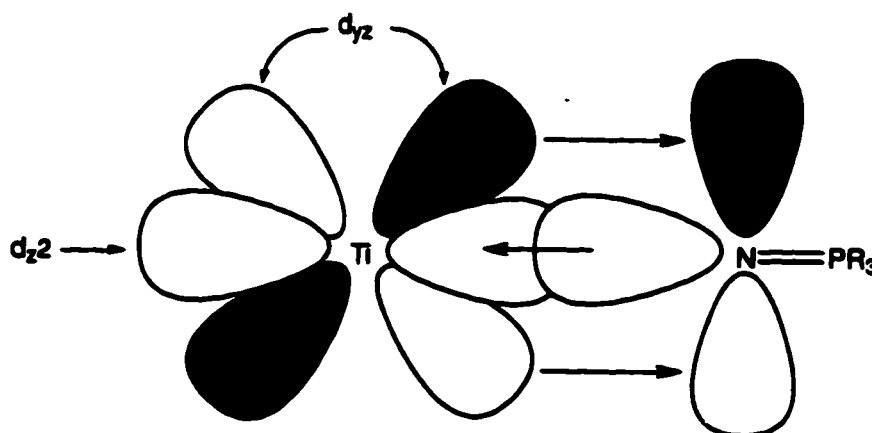


Figure 4.27 End-on titanium-nitrogen multiple bonding in a phosphinimate.

Table 4.11**Structural Data for Iminophosphorano Complexes of Titanium.**

Complex	\angle Ti-N=P	Ti-N (Å)	N=P (Å)	Reference
46	161.3(5) $^\circ$	1.781(6)	1.669(6)	This work
CpTiCl ₂ (NPPPh ₃)	174.7(9) $^\circ$	1.78(1)	1.56(1)	78
CpTiCl ₂ (NPPPh ₂ NS(O)Me ₂)	158.7(1) $^\circ$	1.764(2)	1.595(2)	79
[Ph ₂ P(NSiMe ₃) ₂]Ti(NPNSiMe ₃)	170.3(7) $^\circ$	1.792(9)	1.561(9)	77
Cp*TiF ₂ (NPPPh ₃)	152.7(4) $^\circ$	1.809(6)	1.567(6)	80
1,2-C ₂ H ₂ (Ph ₂ PNTiF ₂ Cp*) ₂	150.4(3) $^\circ$	1.806(5)	1.562(5)	80
TiCl ₃ [NPPPh ₂ NPPPh ₂ N(SiMe ₃) ₂]	177.5(2) $^\circ$	1.721(3)	1.62.3(3)	81
Cp*TiCl ₂ (NPPPh ₂ NHSiMe ₃)	164.9(9) $^\circ$	1.781(3)	1.581(3)	81
CpTiCl ₂ (NPM ₃)	170.7(2) $^\circ$	1.746(3)	1.586(3)	76
TiCl ₂ (NPPPh ₃) ₂	166.6(2) $^\circ$	1.790(3)	1.568(3)	82

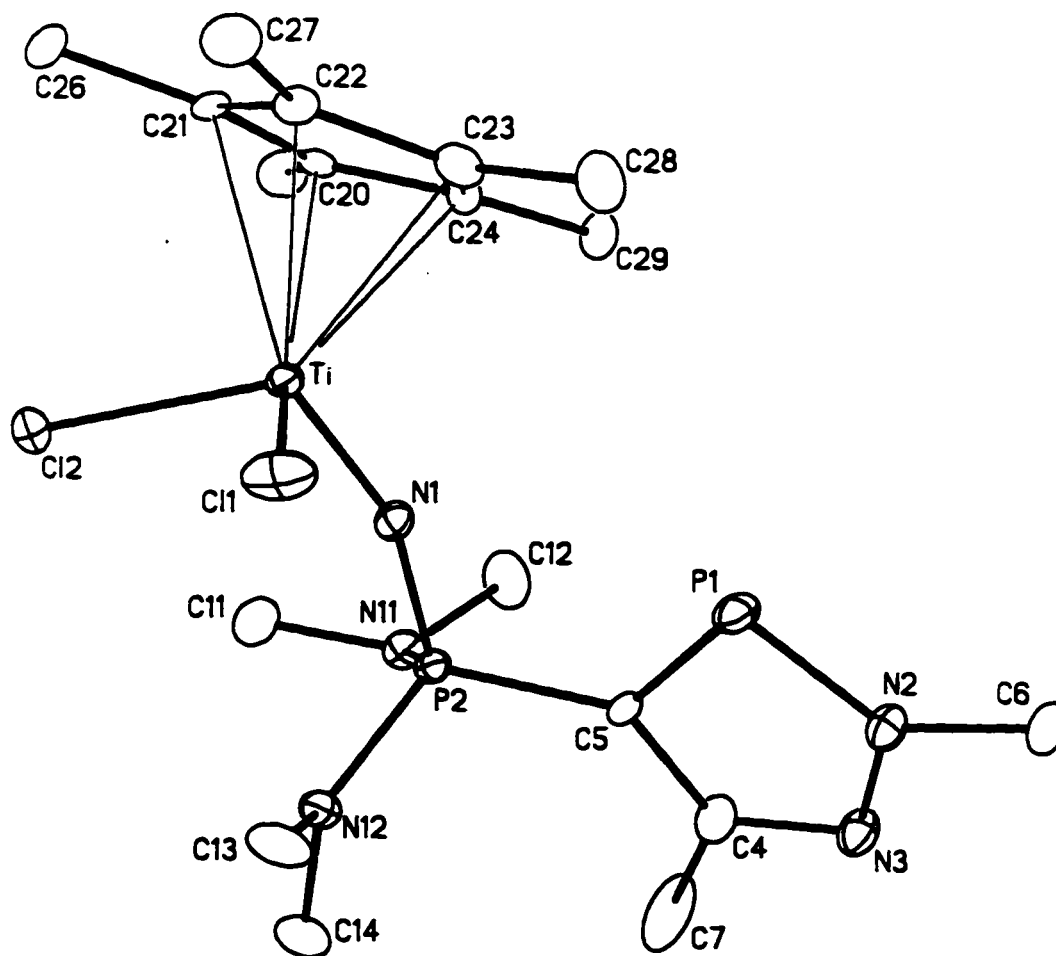


Figure 4.28 Perspective view of the $[(\eta^5\text{-C}_5\text{Me}_5)\text{TiCl}_2(\text{N}=\text{P}(\text{NMe}_2)_2)\text{-}(2,5\text{-dimethyl-}2H\text{-}1,2,3\sigma^2\text{-diazaphosphol-4-yl})]$ (**46**) showing the atom labelling scheme. Non-hydrogen atoms are represented by Gaussian ellipsoids at the 20% probability level. Hydrogen atoms have been omitted. Structure courtesy of Dr. R. McDonald.

Table 4.12

Selected Interatomic Distances (Å) for $[(\eta^5\text{-C}_5\text{Me}_5)\text{TiCl}_2(\text{N}=\text{P}(\text{NMe}_2)_2)\text{-}(2,5\text{-dimethyl-}2H\text{-}1,2,3\sigma^2\text{-diazaphosphol-}4\text{-yl})]$, (46).

Atom1	Atom2	Distance	Atom1	Atom2	Distance
Ti	C11	2.306(3)	N11	C11	1.472(11)
Ti	C12	2.314(3)	N11	C12	1.457(13)
Ti	N1	1.781(6)	N12	C13	1.473(12)
Ti	C20	2.368(8)	N12	C14	1.450(11)
Ti	C21	2.436(7)	C4	C5	1.411(10)
Ti	C22	2.448(8)	C4	C7	1.507(12)
Ti	C23	2.382(9)	C20	C21	1.446(11)
Ti	C24	2.347(9)	C20	C24	1.432(11)
P1	N2	1.669(6)	C20	C25	1.488(12)
P1	C5	1.721(7)	C21	C22	1.400(11)
P2	N1	1.592(6)	C21	C26	1.487(11)
P2	N11	1.651(7)	C22	C23	1.428(12)
P2	N12	1.645(7)	C22	C27	1.479(12)
P2	C5	1.778(7)	C23	C24	1.387(12)
N2	N3	1.363(9)	C23	C28	1.498(13)
N3	C4	1.330(10)	C24	C29	1.506(12)
N2	C6	1.464(9)			

Table 4.13

Selected Interatomic Angles (deg) for $[(\eta^5\text{-C}_5\text{Me}_5)\text{TiCl}_2(\text{N}=\text{P}(\text{NMe}_2)_2)\text{-}(2,5\text{-dimethyl-}2H\text{-}1,2,3\sigma^2\text{-diazaphosphol-4-yl})]$ (46).

Atom1	Atom2	Atom3	Angle	Atom1	Atom2	Atom	Angle
C11	Ti	C12	102.71(12)	N2	N3	C4	108.5(6)
C11	Ti	N1	103.7(3)	P2	N11	C11	116.5(6)
C12	Ti	N1	101.7(2)	P2	N11	C12	119.4(7)
N2	P1	C5	89.3(3)	C11	N11	C12	112.9(8)
N1	P2	C5	107.1(3)	P2	N12	C13	118.1(6)
N1	P2	N11	116.6(4)	P2	N12	C14	124.5(7)
N1	P2	N12	110.6(4)	C13	N12	C14	112.7(8)
C5	P2	N11	108.4(4)	N3	C4	C5	116.1(7)
C5	P2	N12	112.2(4)	N3	C4	C7	117.4(7)
N11	P2	N12	102.0(4)	C5	C4	C7	126.4(7)
Ti	N1	P2	161.3(5)	P1	C5	P2	118.4(4)
P1	N2	N3	117.1(5)	P1	C5	C4	108.9(5)
P1	N2	C6	127.2(6)	P2	C5	C4	132.1(6)
N3	N2	C6	115.7(6)				

4.6 Summary

The 4-phosphinodiazaphosphole systems showed quite a varied coordination chemistry related to the effects of the different substituents on the exo-phosphorus centre. The chromium pentacarbonyl complexes of the phosphinodiazaphosphole **2** showed that this ligand has similar π acceptor abilities to that of the phosphorus trihalides, PF_3 and PCl_3 . The replacement of either two or three CO ligands gave the *cis*- $\text{Mo}(\text{CO})_4(\mathbf{2})_2$ and the *fac*- $\text{Mo}(\text{CO})_3(\mathbf{2})_3$, respectively. The replacement of one of the PPh_3 groups in the complex $\text{CpRu}(\text{PPh}_3)_2\text{Cl}$ gave the asymmetric ruthenium complex $\text{CpRu}(\text{PPh}_3)(\mathbf{2})\text{Cl}$ where the fluorine atoms were diastereotopic. Unlike the reactions involving PF_3 , the carbon monoxide ligands of $[\text{Rh}(\text{CO})_2\text{Cl}]_2$ could not be replaced nor could the Rh-Cl bridge be cleaved by ligand **2**. The compound **2**, however, readily substituted the CO ligands in the monomeric rhodium complex $\text{CpRh}(\text{CO})_2$. The $^{31}\text{P}\{^1\text{H}\}$ NMR spectrum of this complex gave a complex second order splitting pattern for the exo-phosphorus centre. A very large one-bond phosphorus-rhodium coupling constant value of 305 Hz was observed. The initial reaction of **2** with the dimeric complex $[\text{Cp}^*\text{RhCl}_2]_2$ resulted in the complex $\text{Cp}^*\text{Rh}(\mathbf{2})\text{Cl}_2$. Over a period of time, another complex was formed where the cyclic-phosphorus centre was coordinated to the rhodium centre. In the case of either $\text{Pd}(\text{cod})\text{Cl}_2$ or $\text{Pt}(\text{cod})\text{ClMe}$, the reduced metal complexes $\text{M}(\mathbf{2})_4$ ($\text{M} = \text{Pd}, \text{Pt}$) were isolated. The initial product of the reaction of **2** with $\text{Pt}(\text{cod})\text{ClMe}$ gave the disubstituted complex $\text{Pt}(\mathbf{2})_2\text{ClMe}$. The $^{31}\text{P}\{^1\text{H}\}$ NMR spectrum for $\text{Pt}(\mathbf{2})_2\text{ClMe}$ showed a resonance for each of the exo-phosphorus centres with different values for the one-bond phosphorus-platinum coupling constant. This observation is attributed to the *trans*-influence of the methyl and the chloride substituents in the square-planar platinum metal centre.

The bis(dimethylamino)phosphino derivative **3** formed the *trans*-complex $\text{Rh}(\mathbf{3})_2(\text{CO})\text{Cl}$ upon reaction with $[\text{Rh}(\text{CO})_2\text{Cl}]_2$. The steric bulk about the

exo-phosphorus centre with **3** resulted in the formation of the *trans*-Pt(**3**)₂ClMe complex even though *cis* complexes tend to be the preferred isomeric structure for monodentate phosphines, which may be due to steric factors. The metal complexation chemistry of the trifluoroethoxy derivative **11** gave complexes of rhodium, palladium and platinum which were generally similar to those of typical monodentate phosphines.

The metal complexation reactions of the phosphoranodiazaphospholes were not as successful as the reactions of their unoxidized counterparts. The reason for this difficulty is the inability of the $\sigma^2\text{P}$ centre to chelate to metal centres to form five-membered metallacycles. The trimethylsilyliminophosphorano derivative reacted to give the iminatophosphorano titanium complex **47**. This reaction demonstrates the potential of using the elimination of trimethylsilyl chloride to form metal-nitrogen sigma bonds.

Table 4.14

$^{31}\text{P}\{^1\text{H}\}$ and ^{19}F NMR Data for Metal Complexes with 4-(Difluorophosphino)-2,5-dimethyl-2H-1,2,3 σ^2 -diazaphospholes. a,b

Complex	No.	$\delta \sigma^2\text{P}$ (ppm)	$\delta \sigma^4\text{P}$ (ppm)	$^2J_{\text{PP}}$ (Hz)	δF (ppm)	$^1J_{\sigma^2\text{PF}}$ (Hz)	$^3J_{\sigma^4\text{PF}}$ (Hz)
$\text{Cr}(\text{CO})_5(2)$	27	257.18 ^c	249.76 ^d	120	-39.78 ^e	1137	17
$\text{Mo}(\text{CO})_4(2)_2$	28	259.74 ^c	208.8 ^d	81	-41.52 ^d	1091	4
$\text{Mo}(\text{CO})_3(2)_3$	29	255.10 ^e	224.60 ^e		-42.92 ^e		
$\text{CpRu}(\text{PPh}_3)(2)\text{Cl}$	30	258.90 ^f	216.59 ^f	116	-27.55 ^f	1057	19
					-42.92 ^h	1131	15
$\text{CpRh}(2)_2$	31	259.90 ^d	188.52 ^d		-36.13 ^d		

Table 4.14 continued

Complex	No.	$\delta \sigma^2\text{P}$ (ppm)	$\delta \sigma^4\text{P}$ (ppm)	$^2J_{\text{PP}}$ (Hz)	δF (ppm)	$^1J_{\sigma^2\text{PF}}$ (Hz)	$^3J_{\sigma^4\text{PF}}$ (Hz)
$\text{Cp}^*\text{Rh}(\text{2})\text{Cl}_2$	32	269.50 ^c	188.23 ^d	103	-62.32 ^b	1158	13
<i>cis</i> - $\text{Pt}(\text{2})_2\text{Cl}_2$	33	271.21 ^c	159.29 ^d	150	-36.13 ^c	1130	
<i>cis</i> - $\text{Pd}(\text{2})_2\text{Cl}_2$	34	268.88 ^c	144.33 ^d	158	-39.42 ^c	1184	n.r.
$\text{Pd}(\text{2})_4$	35	258.90 ^c	188.90 ^d	116	-43.24 ^c	1131	n.r.
$\text{Pt}(\text{2})_4$	36	267.88 ^c	164.90 ^d	190	-43.02 ^c	1130	n.r.

Table 4.14 continued

Complex	No.	$\delta \sigma^2\text{P}$ (ppm)	$\delta \sigma^4\text{P}$ (ppm)	$^2J_{\text{PP}}$ (Hz)	δF (ppm)	$^1J_{\sigma^2\text{PF}}$ (Hz)	$^3J_{\sigma^4\text{PF}}$ (Hz)
<i>trans</i> -Pt(2)(PEt ₃)Cl ₂	37	265.81 ^c	124.32 ^d	155	-43.02 ⁱ	1115	15
<i>trans</i> -Pd(2)(PEt ₃)Cl ₂	38	266.05 ^c	160.23 ^d	150	-38.31 ⁱ	1125	13

a) Chemical shifts δ in ppm in CDCl₃ with respect to 85% H₃PO₄.

b) in CDCl₃

c) doublet

d) doublet of triplets

e) second order

f) doublet of doublet of doublets

g) doublet of doublet of triplets

h) doublet of doublet of doublet of doublets

i) doublet of doublets

Table 4.15

³¹P{¹H} NMR Data for Metal Complexes of 4-(Bis(dimethylamino)phosphino)-2,5-dimethyl-2H-1,2,3σ²-diazaphospholes, a,b

Complex	No.	δ σ ² P (ppm)	δ σ ⁴ P (ppm)	² J _{PP} ^d (Hz)
<i>trans</i> -Rh(CO)(3) ₂ Cl	39	246.92 ^c	103.34 ^c	51
<i>trans</i> -Pd(3) ₂ Cl ₂	40	249.72 ^c	86.94 ^c	51
<i>trans</i> -Pt(3) ₂ Cl ₂	41	249.69 ^c	80.63 ^c	57
<i>trans</i> -Pt(3) ₂ ClMe	42	267.88 ^c	75.21 ^c	53

a) Chemical shifts δ in ppm in CDCl₃ with respect to 85% H₃PO₄.

b) in CDCl₃

c) second order

d) |²J_{σ²Pσ⁴P} + 4J_{σ²Pσ⁴P}|

e) doublet

Table 4.16

^{31}P (^1H) NMR Data for Metal Complexes of 4-(Bis(2,2,2-trifluoroethoxy)phosphino)-2,5-dimethyl-2H-1,2,3- σ^2 -diazaphospholes, a,b

Complex	No.	$\delta \sigma^2\text{P}$ (ppm)	$\delta \sigma^4\text{P}$ (ppm)	$^2J_{\text{PP}}$ (Hz)
<i>trans</i> -Rh(CO)(11) $_2$ Cl	43	251.88 ^c	159.78 ^c	52 ^d
<i>trans</i> -Pd(11) $_2$ Cl $_2$	44	256.43 ^c	131.22 ^c	-
<i>cis</i> -Pt(11) $_2$ Cl $_2$	45	249.69 ^c	80.63 ^c	58

a) Chemical shifts δ in ppm in CDCl_3 with respect to 85% H_3PO_4 .

b) in CDCl_3

c) second order

d) $|2J_{\sigma^2\text{P}\sigma^4\text{P}} + 4J_{\sigma^2\text{P}\sigma^4\text{P}}|$

e) doublet

Table 4.17

³¹P{¹H} NMR Data for Metal Complexes of 4-(Bis(dimethylamino)iminophosphorano)-2,5-dimethyl-2H-1,2,3σ²-diazaphospholes.^{a,b}

Complex	No.	δ σ ² P (ppm)	δ σ ⁴ P (ppm)	2J _{PP} (Hz)
Cp*TiCl ₂ (23)	47	260.87 ^c	40.87 ^c	84

a) Chemical shifts δ in ppm in CDCl₃ with respect to 85% H₃PO₄.

b) in CDCl₃

c) doublet

4.7 References

- (1) Dewar, M. J. S. *Bull. Soc. Chem. Fr.* **1951**, *18*, C71.
- (2) Chatt, J.; Duncanson, L. A. *J. Chem. Soc.* **1953**, 2939.
- (3) Orpen, A. G.; Connelly, N. G. *J. Chem. Soc., Chem. Commun.* **1985**, 1310.
- (4) Pacchioni, G.; Bagus, P. S. *Inorg. Chem.* **1992**, *31*, 4391.
- (5) Marynick, D. S. *J. Am. Chem. Soc.* **1984**, *106*, 4064.
- (6) Nixon, J. F. In *Advances in Inorganic Chemistry and Radiochemistry*; H. J. Emeléus and A. G. Sharpe, Ed.; Academic Press, Inc.: Orlando, 1985; Vol. 29; pp 41.
- (7) Crabtree, R. H. *The Organometallic Chemistry of the Transition Metals*; 2nd ed.; John Wiley & Sons, Inc.: New York, 1994, pp 83.
- (8) Strohmeier, W.; Müller, F.-J. *Chem. Ber.* **1967**, *100*, 2812.
- (9) Verkade, J. G.; McCarley, R. E.; Hendricker, D. G.; King, R. W. *Inorg. Chem.* **1965**, *4*, 228.
- (10) Mathieu, R.; Lenzi, M.; Poilblanc, R. *Inorg. Chem.* **1970**, *9*, 2030.
- (11) Magee, T. A.; Matthews, C. N.; Wang, T. S.; Woliz, J. H. *J. Am. Chem. Soc.* **1961**, *83*, 3200.
- (12) Faber, G. C.; Dobson, G. R. *Inorg. Chem.* **1968**, *7*, 584.
- (13) Tolman, C. A. *J. Am. Chem. Soc.* **1970**, *92*, 2953.
- (14) Stelzer, O.; Unger, E. *Chem. Ber.* **1975**, *108*, 1246.
- (15) Vanderbroucke, J., A.C.; Hendricker, D. G.; McCarley, R. E.; Verkade, J. G. *Inorg. Chem.* **1968**, *7*, 1825.
- (16) Jenkins, J. M.; Verkade, J. G. *Inorg. Chem.* **1967**, *6*, 2250.
- (17) Poilblanc, R.; Bigorgne, M. **1962**, 1301.
- (18) Evans, D.; Osborn, J. A.; Wilkinson, G. *J. Chem. Soc. (A)* **1968**, 3133.

- (19) Moulijn, J. A.; van Leeuwen, P. W. N. M.; van Santen, R. A. *Catalysis-An Intergrated Approach to Homogeneous, Heterogeneous and Industrial Catalysis.*; Elsevier: Amsterdam, 1995, pp 199.
- (20) RajanBabu, T. V.; T.A., A. *Tetrahedron Lett.* **1994**, *25*, 4295.
- (21) Chan, A. S. C.; Pai, C.-C.; Yang, T. K.; Chen, S.-M. *J. Chem. Soc. Chem. Commun.* **1995**, 2031.
- (22) Leeuwen, P. W. N. M.; Roobeek, C. F. *J. Organomet. Chem.* **1983**, *258*, 343.
- (23) Unruh, J. D.; Christenson, J. R. *J. Mol. Catal.* **1982**, *14*, 19.
- (24) Ainscough, E. W.; Brodie, A. M.; Mentzer, E. *J. Chem. Soc. Dalton Trans.* **1973**, 2167.
- (25) Chatt, J.; Venanzi, L. M. *J. Chem. Soc.* **1957**, 4735.
- (26) Li, M. P.; Drago, R. S. *J. Am. Chem. Soc.* **1976**, *98*, 5129.
- (27) Denise, B.; Pannetier, G. *J. Organomet. Chem.* **1978**, *148*, 155.
- (28) Binger, P.; Haas, J.; Glaser, G.; Goddard, R.; Krüger, C. *Chem. Ber.* **1994**, *127*, 1927.
- (29) Clement, D. A.; Nixon, J. F. *J. Chem. Soc. Dalton Trans.* **1972**, 2553.
- (30) Bennett, M. A.; Patmore, D. J. *Inorg. Chem.* **1971**, *10*, 2387.
- (31) Clement, D. A.; Nixon, J. F. *J. Chem. Soc. Dalton Trans.* **1973**, 195.
- (32) Oliver, A. J.; Graham, W. A. G. *Inorg. Chem.* **1970**, *9*, 243.
- (33) Schuster-Woldan, H. G.; Basolo, F. *J. Am. Chem. Soc.* **1966**, *88*, 1657.
- (34) King, R. B.; Efraty, A. *J. Am. Chem. Soc.* **1972**, *94*, 3768.
- (35) King, R. B.; Efraty, A. *J. Am. Chem. Soc.* **1971**, *93*, 5260.
- (36) Goodfellow, R. J. In *Multinuclear NMR*; J. Mason, Ed.; Plenum Press: Ney York, 1987; pp 521.
- (37) Marder, T. B.; Calabrese, J. C.; Roe, D. C.; Tulip, T. H. *Organometallics* **1987**, *6*, 2012.

- (38) Friedrich, P.; Huttner, G.; Luber, J.; Schmidpeter, A. *Chem. Ber.* **1978**, *111*, 1558.
- (39) Corbridge, D. E. C. *The Structural Chemistry of Phosphorus*; Elsevier Scientific Publishing Co.: New York, 1974, pp 7.
- (40) Collman, J. P.; Hegedus, L. S.; Norton, J. R.; Finke, R. G. *Principles and Applications of Organotransition Metal Chemistry*; University Science Books: Mill Valley, Ca., 1987, pp 306.
- (41) Hart-Davies, J.; Graham, W. A. G. *Inorg. Chem.* **1971**, 1653.
- (42) Werner, H. *Angew. Chem. Int. Ed. Engl.* **1983**, *22*, 927.
- (43) Appleton, T. G.; Clark, H. C.; Manzer, L. E. *Coord. Chem. Rev.* **1973**, *10*, 335.
- (44) Agbossou, F.; Carpentier, J.-F.; Montreux, A. *Chem. Rev.* **1995**, *95*, 2485.
- (45) Scrivanti, A.; Beghetto, V.; Bastianini, A.; Menchi, G. *Organometallics* **1996**, *15*, 4687.
- (46) Adamson, G. W.; Bart, J. C. J. *J. Chem. Soc. (A)* **1970**, 1452.
- (47) Anderson, G. K.; Cross, R. J. *J. Chem. Soc. Dalton Trans.* **1980**, 1434.
- (48) Anderson, G. K.; Clark, H. C.; Davies, J. A. *Organometallics* **1982**, *1*, 64.
- (49) Anderson, G. K.; Cross, R. *Acc. Chem. Res.* **1984**, *17*, 67.
- (50) Verkade, J. G.; Mosbo, J. A. In *Phosphorus-31 NMR Spectroscopy in Stereochemical Analysis*; J. G. Verkade and L. D. Quinn, Ed.; VCH Publishers, Inc.: Deerfield Beach, FL, 1987; Vol. 8; pp 425.
- (51) Heaton, B. Ph.D. Thesis Thesis, University of Sussex, Brighton,
- (52) Chatt, J.; Mason, R.; Meek, D. W. *J. Am. Chem. Soc.* **1975**, *97*, 3826.
- (53) Anderson, G. K.; Cross, R. J.; Manojlovic-Muir, L.; Muir, K. W.; Solomon, T. *J. Organomet. Chem.* **1979**, *170*, 385.
- (54) van der Boom, M. E.; Kraatz, H.-B.; Ben-David, Y.; Milstein, D. *J. Chem. Soc. Chem. Commun.* **1996**, 2167.

- (55) Nixon, J. F.; Sexton, M. D. *J. Chem. Soc. (A)* **1970**, 321.
- (56) Heuer, L.; Jones, P. G.; Schmutzler, R.; Schomburg, D. *New J. Chem.* **1990**, *14*, 891.
- (57) Nixon, J. F.; Pidcock, A. In *Ann. Rev. NMR Spec.*; E. F. Mooney, Ed.; Academic Press: New York, 1969; Vol. 2; pp 345.
- (58) Luber, J.; Schmidpeter, A. *Angew. Chem. Int. Ed. Eng.* **1976**, *15*, 111.
- (59) Hughes, R. P. In *Comp. Organomet. Chem.*; G. Wilkinson, F. G. A. Stone and E. W. Abel, Ed.; Pergamon Press: New York, N.Y., 1982; Vol. 5; pp 296.
- (60) Harris, R. K. *Can. J. Chem.* **1964**, *42*, 2275.
- (61) Vaska, L.; Peone, J., *J. J. Chem. Soc. Chem Commun.* **1971**, 418.
- (62) Evans, D.; Osborn, J. A.; Wilkikson, G. *Inorg. Synth.* **1967**, *11*, 99.
- (63) Browning, J.; Goggin, P. L.; Goodfellow, R. J.; Norton, M. G.; Rattray, A. J. M.; Taylor, B. F.; Mink, J. *J. Chem. Soc. Dalton Trans.* **1977**, 2061.
- (64) Schumann, H.; Heisler, M.; Pickardt, J. *Chem. Ber.* **1977**, *110*, 1020.
- (65) Wajda, K.; Pruchnik, F.; Lis, T. *Inorg. Chim. Acta* **1980**, *40*, 207.
- (66) Kermitt, R. D. W.; Nichols, D. I.; Peacock, R. D. *J. Chem. Soc. (A)* **1968**, 1898.
- (67) Wu, M. L.; Desmond, M. J.; Drago, R. S. *Inorg. Chem.* **1979**, *18*, 679.
- (68) Dutta, D. K.; Singh, M. M. *Transition Met. Chem.* **1980**, *4*, 244.
- (69) Pregosin In *Phosphorus-31 NMR Spectroscopy in Stereochemical Analysis*; J. G. Verkade and L. D. Quinn, Ed.; VCH Publishers, Inc.: Deerfield Beach, FL, 1987; Vol. 8; pp 465.
- (70) Schumann, H.; Jurgis, S.; Eisen, M.; Blim, J. *Inorg. Chim. Acta* **1990**, *172*, 191.
- (71) Chen, Y.-J.; Wang, J.-C.; Wang, Y. *Acta Crys.* **1991**, *C47*, 2441.
- (72) Cook, B. W.; Miller, R. G. J.; Todd, P. F. *J. Organomet. Chem.* **1969**, *19*, 421.
- (73) Dehnicke, K.; Strähle, J. *Polyhedron* **1989**, *8*, 707.

- (74) Völp, K.; Willing, W.; Müller, U.; Denicke, K. *Z. Naturforsch.* **1986**, *41b*, 1196.
- (75) Mronga, N.; Weller, F.; Denicke, K. *Z. Anorg. Allg. Chem.* **1983**, *502*, 35.
- (76) Rübenstahl, T.; Weller, F.; Harms, K.; Denicke, K.; D., F.; Baum, G. *Z. anorg. allg. Chem.* **1994**, *620*, 1741.
- (77) Witt, M.; Roesky, H. W.; Stalke, D.; Pauer, F.; Henkel, T.; G.M., S. *J. Chem. Soc. Dalton Trans.* **1989**, 2173.
- (78) Latham, I. A.; Leugh, G. J.; Huttner, G.; I., J. *J. Chem. Soc. Dalton Trans.* **1986**, 377.
- (79) Roesky, H. W.; Schrumpf, F.; Noltemeyer, M. *Z. Naturforsch.* **1989**, *44b*, 35.
- (80) Sotoodeh, M.; Leichtweis, I.; Roesky, H. W.; Noltemeyer, M.; Schmidt, H.-G. *Chem. Ber.* **1993**, *126*, 913.
- (81) Hasselbring, R.; Leichtweis, I.; Noltemeyer, M.; Roesky, H. W.; Schmodt, H.-G.; Herzog, A. *Z. anorg. allg. Chem.* **1993**, *619*, 1543.
- (82) Rübenstahl, T.; Weller, F.; Wocadlo, S.; Massa, W.; Denicke, K. *Z. anorg. allg. Chem.* **1995**, *621*, 953.

CHAPTER 5

EXPERIMENTAL

All experimental manipulations were performed under an atmosphere of dry argon using standard Schlenk techniques. The deuterated solvents, CDCl_3 and CD_2Cl_2 , were distilled over P_2O_5 and stored over molecular sieves under argon before use. All other solvents were dried according to Appendix A.3.

Nuclear magnetic resonance spectra were recorded on Bruker WH-200, WH-300, WH-400, and Varian Unity 500 spectrometers using as the reference the deuterium signal of the solvent employed (respective operating frequencies: $^1\text{H} = 200.133$ and 400.135 MHz, $^{13}\text{C} = 50.323$, 75.469 , and 100.614 MHz, $^{31}\text{P} = 81.015$, 161.977 , and 202.392 MHz, $^{19}\text{F} = 188.313$, 376.503 , and 470.304 MHz, $^{77}\text{Se} = 76.312$ MHz, $^{195}\text{Pt} = 85.629$ MHz. External standards used were SiMe_4 (C and H), 85% H_3PO_4 , CECl_3 , Me_2Se . The ^{103}Rh and ^{195}Pt chemical shifts are reported as absolute frequencies (Ξ) at 3.16 MHz¹ and 21.40 MHz,² respectively. CDCl_3 and CD_2Cl_2 were used as both solvent and the internal lock. Positive shifts lie downfield in all cases. NMR spectra were simulated using the Bruker software Parameter Adjustment in NMR by Iteration Calculation (PANIC). Chemical ionization (CI) spectra were recorded using ammonia at 16 eV on an AEI MS50 spectrometer. Low-resolution mass spectra (electron impact, EI) were recorded at 16 or 70 eV on an AEI MS50 spectrometer. Positive ion fast atom bombardment mass spectra (FAB-MS) were obtained by using Xe fast atoms on a customized AEI MS9 spectrometer.

Infrared spectra were recorded as CH_2Cl_2 casts on KBr cells using a Nicolet 7199 Infrared Spectrometer or obtained as solution samples held between KBr (0.05 mm) on a Nicolet MX-1 FT IR Spectrometer. Elemental analyses were performed by

the Microanalytical Services Laboratory at the University of Alberta. Melting points were determined on samples in sealed melting point capillaries and are uncorrected. Crystal structure determinations were carried out by Dr. R. McDonald at the Structure Determination Lab, Department of Chemistry, University of Alberta.

The following materials were obtained commercially and used as received unless otherwise indicated: *tert*-butylamine (Mallinckrodt, distilled over KOH), chloroplatinic acid hexahydrate (Strem), chromium hexacarbonyl (Aldrich), 15-crown-5 (Aldrich), dicyclopentadiene (Terochem), *N,N*-dimethylaminotrimethylsilane (Petrarch), diethylamine (Aldrich, distilled over KOH), 2,5-dimethylpyrazole (Aldrich), dipropylamine (T.J. Baker, distilled over KOH), diisopropylamine (Aldrich, distilled over KOH), *p*-fluorophenol (Aldrich), methyl hydrazine (Aldrich), molybdenum hexacarbonyl (Strem), palladium chloride (Strem), phenol (Aldrich), pentafluorophenol (Aldrich), pentafluorobenzyl alcohol (Aldrich), phosphorus trichloride (Aldrich), platinum chloride (Strem), potassium tetrachloroplatinate (Strem), pyrazole (Aldrich), sodium fluoride (Fisher), sodium azide (Fisher), pentafluorobenzonitrile (Aldrich), pentamethylcyclopentadienyl-titanium trichloride (Strem), rhodium(III) chloride (Aldrich), ruthenium(III) chloride hydrate (BDH), selenium (Aldrich), sulfur (Aldrich), *p*-toluidine (T.J. Baker, sublimed), 2,4,6-tri-*tert*-butylaniline (Aldrich), trimethylsilyl azide (Lancaster), 2,2,2-trifluoroethanol (Alpha, distilled over 4Å molecular sieves), triphenylphosphine (Aldrich), tungsten hexacarbonyl (Aldrich). The ligands and metal complexes that were used as starting materials are listed in Table 5.1 along with the reference for their preparation.

Table 5.1**Starting Materials Prepared**

Compound	Reference
Mo(nbd)(CO) ₄	3
Pentamethylcyclopentadiene	4
Pd(PhCN) ₂ Cl ₂	5
Pd(cod)Cl ₂	6
Pd ₂ (dba) ₃ ·CHCl ₃	7
[Pd(PEt ₃)Cl ₂] ₂	8
Pt(PhCN) ₂ Cl ₂	5
Pt(cod)Cl ₂	6
Pt(cod)ClMe	9
[Pt(PEt ₃)Cl ₂] ₂	10,11
[Rh(coe)Cl] ₂	12
[Cp* ₂ RhCl] ₂	13
[Rh(cod)Cl] ₂	14
[Rh(CO) ₂ Cl] ₂	15
CpRu(PPh ₃) ₂ Cl	16
TiCp	17

5.1 Ligand Synthesis

Synthesis of 4-(Dichlorophosphino)-2,5-dimethyl-2*H*-1,2,3σ²-diazaphosphole, (1).

Acetone methylhydrazone (50 mL) was added over a period of 45 minutes to a 500 mL round bottom flask containing a large excess of phosphorus trichloride (250 mL) at -60°C under argon. After the addition, the solution was allowed to warm slowly to room temperature (22°C) and then the mixture was refluxed for a period of two days. The reaction mixture was then stored at -40°C for a period of two days. The solution was filtered under argon and excess phosphorus trichloride removed *in vacuo*. The chlorinated phosphole was obtained by distillation under argon as a colourless to pale yellow liquid. Compound 1 was again filtered under argon to remove any of the hydrogen chloride adduct which had crystallized. The yield of 4-(dichlorophosphino)-2,5-dimethyl-2*H*-1,2,3σ²-diazaphosphole (1) ranged from 66.4 g to 83.6 g (50% to 63%). **B.P.** = 90-95°C @ 2 torr. **NMR Data** (CDCl₃) ³¹P{¹H}: P(σ²): δ 248.51 (d, ²J_{PP} 79 Hz), P(σ³): δ 158.14 (d, ²J_{PP} 79 Hz).

Synthesis of 4-(Difluorophosphino)-2,5-dimethyl-2*H*-1,2,3σ²-diazaphosphole, (2).

To a suspension of NaF (11.80 g, 0.281 mol), with 5 drops of 15-crown-5, in 50 mL of acetonitrile, 4-(dichlorophosphino)-2,5-dimethyl-2*H*-1,2,3σ²-diazaphosphole, 1, (10.0 mL, 70.5 mmol) was added *via* syringe at room temperature (22°C). The suspension was refluxed for 24 hours. The solution was filtered through Celite and the Celite was washed with (2 x 5 mL) of acetonitrile. The fluorinated phosphole was obtained by distillation under argon as a colourless liquid. The yield of 4-(difluorophosphino)-2,5-dimethyl-2*H*-2*H*-1,2,3σ²-diazaphosphole (2) was 9.84 g (76.7%). The compound was stored at -40°C. **B.P.** = 172°C @ 720 torr. **Formula**

Weight: 182.05 g/mol. **Anal.** for $C_4H_6F_2N_2P_2$: C, 26.39; H, 3.32; N, 15.39 %.
Found: C, 26.09; H, 3.30; N, 15.46%. **MS (CL. m/z):** 183 (M+1, 100%). **IR Data** (neat, cm^{-1}): $\nu(P-F)$ 805 (s), 780 (s). **NMR Data** ($CDCl_3$): $^{31}P\{^1H\}$: $P(\sigma^2)$: δ 255.03 (dt, $^2J_{PP}$ 81 Hz, $^3J_{PF} \approx 30$ Hz), $P(\sigma^3)$: δ 208.84 (dt, $^2J_{PP}$ 81 Hz, $^1J_{PF}$ 1169 Hz). 1H : C- $\underline{C}H_3$ δ 2.50 (s), N- $\underline{C}H_3$ δ 4.00 (d, $^3J_{\sigma^2PH}$ 8.2 Hz). $^{13}C\{^1H\}$: C- $\underline{C}H_3$ δ 14.79 (d, $^3J_{PC}$ 17 Hz), N- $\underline{C}H_3$ δ 41.51 (d, $^2J_{\sigma^2PC}$ 19 Hz), P- \underline{C} -P δ 135.17 (d, $^1J_{PC}$ 35 Hz), N- \underline{C} - $\underline{C}H_3$ δ 157.21 (dd, $^2J_{\sigma^2PC}$ 5 Hz, $^2J_{\sigma^3PC}$ 18 Hz). ^{19}F : δ -89.33 (dd, $^1J_{\sigma^3PF}$ 1169 Hz, $^3J_{\sigma^2PF}$ 34 Hz).

Synthesis of 4-(Bis(dimethylamino)phosphino)-2,5-dimethyl-2H-1,2,3 σ^2 -diazaphosphole, (3).

A solution of *N,N*-dimethylaminotrimethylsilane (23.0 mL, 0.144 mol) in 25 mL of dichloromethane was added dropwise to a solution of 1 (10.0 mL, 70.5 mmol) in 75 mL of dichloromethane at 0°C. After the addition, the solution was allowed to warm up to room temperature (22°C) and stirred for 24 hours during this time the solution became light yellow. The solvent and excess *N,N*-dimethylaminotrimethylsilane were removed *in vacuo*, leaving a light yellow liquid. The phosphole was distilled at 93-96°C @ 0.6 torr and remained light yellow. The yield of 3 was 13.88 g (84.8%). **Formula Weight:** 232.20 g/mol. **Anal.** for $C_8H_{18}N_4P_2$: C, 41.38; H, 7.81; N, 24.13%. **Found:** C, 41.25; H, 7.36; N, 24.21%. **MS (CL. m/z):** 233 (M+1, 100%). **IR Data** (neat, cm^{-1}): $\nu(P-N)$ 713 (s), 656 (s), $\nu(N-C)$ 969 (s), 950 (s). **NMR Data** ($CDCl_3$): $^{31}P\{^1H\}$: $P(\sigma^2)$: δ 243.23 (d, $^2J_{PP}$ 33 Hz), $P(\sigma^3)$: δ 86.88 (d, $^2J_{PP}$ 33 Hz). 1H : C- $\underline{C}H_3$ δ 2.10 (s), $P(\sigma^2)$ -N- $\underline{C}H_3$ δ 3.80 (d, $^3J_{\sigma^2PH}$ 7.2 Hz), $P(\sigma^3)$ -N- $\underline{C}H_3$ δ 2.55 (d, $^3J_{\sigma^3PH}$ 9.8 Hz). $^{13}C\{^1H\}$: C- $\underline{C}H_3$ δ 14.24 (d, $^3J_{PC}$ 4 Hz), $P(\sigma^2)$ -N- $\underline{C}H_3$ δ 40.54 (s), P- \underline{C} -P δ 150.95 (dd, $^1J_{\sigma^2PC}$ 54 Hz, $^1J_{\sigma^3PC}$ 9 Hz), N- \underline{C} - $\underline{C}H_3$ δ 155.68 (dd, $^2J_{\sigma^2PC}$ 7 Hz, $^2J_{\sigma^3PC}$ 19 Hz), $P(\sigma^3)$ -N- $\underline{C}H_3$ δ 40.65 (d, $^2J_{\sigma^3PC}$ 17 Hz).

Synthesis of 4-(Bis(diethylamino)phosphino)-2,5-dimethyl-2*H*-1,2,3σ²-diazaphosphole, (4).

A solution of **1** (10.0 mL, 70.5 mmol) in 100 mL of ether was added dropwise to a solution of diethylamine (32.0 mL, 309.3 mmol) in 250 mL of ether at 0°C, during this time the precipitate of Et₂NH·HCl was immediately observed. The solution was stirred for one day after slowly be allowed to warm up to room temperature (22°C). The solvent and excess diethylamine were removed *in vacuo*, leaving a yellow liquid. The phosphole was distilled at 125-128°C @ 0.06 torr and and remained yellow. The yield of **4** was 15.53 g (76.4%). Formula Weight: 288.31 g/mol. Anal. for C₁₂H₂₆N₄P₂: C, 49.99; H, 9.09; N, 19.43%. Found: C, 49.82; H, 9.03; N, 19.60%. MS (CI, m/z): 289 (M+1, 100%). IR Data (neat, cm⁻¹): ν(P-N) 717 (s), 663 (s), ν(N-C) 1013 (s), 967 (s). NMR Data (CDCl₃): ³¹P{¹H}: P(σ²): δ 242.54 (d, ²J_{PP} 29 Hz), P(σ³): δ 77.94 (d, ²J_{PP} 29 Hz). ¹H: C-CH₃ δ 2.27 (s), P(σ²)-N-CH₃ δ 3.90 (d, ³J_{σ²PH} 6.9 Hz), N-CH₂-CH₃ δ 3.02 (dt, ³J_{σ³PH} 6.9 Hz, ³J_{HH} 6.9 Hz), N-CH₂-CH₃ δ 0.97 (t, ³J_{HH} 6.9 Hz). ¹³C{¹H}: C-CH₃ δ 14.68 (d, ³J_{PC} 5 Hz), P(σ²)-N-CH₃ δ 40.64 (d, ²J_{σ²PC} 18 Hz), P-C-P δ 153.09 (dd, ¹J_{σ²PC} 54 Hz, ¹J_{σ³PC} 12 Hz), N-C-CH₃ δ 156.05 (dd, ²J_{σ²PC} 9 Hz, ²J_{σ³PC} 24 Hz), P(σ³)-N-CH₂-CH₃ δ 42.45 (d, ²J_{σ³PC} 23 Hz), P(σ³)-N-CH₂-CH₃ δ 14.39 (s).

Synthesis of 4-(Bis(dipropylamino)phosphino)-2,5-dimethyl-2*H*-1,2,3σ²-diazaphosphole, (5).

A solution of **1** (10.0 mL, 70.5 mmol) in 100 mL of ether was added dropwise to a solution of diethylamine (20.0 mL, 146 mmol) and triethylamine (10.7 mL, 148 mmol) in 250 mL of ether at 0°C. During the addition, a precipitate of Et₃N·HCl was immediately observed. After the addition, the solution was allowed to warm up to room temperature (22°C) and stirred for 1 day. The solvent and excess dipropylamine

were removed *in vacuo*, leaving an orange liquid. The phosphole was distilled at 149-155°C @ 0.06 torr and remained orange in colour. The yield of **5** was 17.60 g (72.5 %). **Formula Weight**: 344.42 g/mol. **Anal.** for C₁₆H₃₄N₄P₂: C, 55.80; H, 9.95; N, 16.27%. Found: C, 55.76; H, 9.96; N, 16.38%. **MS (CL. m/z)**: 345 (M+1, 100%). **IR Data** (neat, cm⁻¹): ν(P-N) 716 (s), 557 (s), ν(N-C) 1019 (s), 971 (s). **NMR Data** (CDCl₃) ³¹P{¹H}: P(σ²): δ 241.53 (d, ²J_{PP} 23 Hz), P(σ³): δ 78.99 (d, ²J_{PP} 23 Hz). ¹H: C-CH₃ δ 2.28 (s), P(σ²)-N-CH₃ δ 3.93 (d, ³J_{σ²PH} 6.8 Hz), N-CH₂-CH₃ δ 3.02 (dd, ³J_{σ³PH} 9.6 Hz, ³J_{HH} 7.0 Hz), N-CH₂-CH₂-CH₃ δ 1.17 (dt, ³J_{HH} 6.9 Hz, ³J_{HH} 6.8 Hz), N-CH₂-CH₂-CH₃ δ 0.97 (t, ³J_{HH} 6.8 Hz). ¹³C{¹H}: C-CH₃ δ 14.39 (s), P(σ²)-N-CH₃ δ 40.55 (d, ²J_{σ²PC} 17 Hz), P-CH₂-P δ 152.69 (dd, ¹J_{σ²PC} 55 Hz, ¹J_{σ³PC} 9 Hz), N-CH₂-CH₃ δ 156.05 (dd, ²J_{σ²PC} 9 Hz, ²J_{σ³PC} 24 Hz), P(σ³)-N-CH₂-CH₃ δ 42.45 (d, ²J_{σ³PC} 22 Hz), P(σ³)-N-CH₂-CH₃ δ 14.39 (s).

Synthesis of 4-(Chloro(diisopropylamino)phosphino)-2,5-dimethyl-2H-1,2,3σ²-diazaphosphole, (**6**).

A solution of **1** (10.0 mL, 70.5 mmol) in 100 mL of ether was added dropwise to a solution of diisopropylamine (32.0 mL, 309 mmol) in 250 mL of ether at 0°C. During the addition, a precipitate of ⁱPr₂NH·HCl was immediately observed. After the addition, the solution was allowed to warm up to room temperature (22°C) and stirred for 1 day. The solvent and excess diisopropylamine were removed *in vacuo*, leaving a light yellow solid. The phosphole was recrystallized from hexane and stored at -25°C for 1 day to produce a colourless crystalline material. The phosphole was also sublimed at 80-85°C @ 1.0 torr. The yield of **6** was 15.06 g (76.4 %). **Formula Weight**: 279.69 g/mol. **Anal.** for C₁₀H₂₀ClN₃P₂: C, 42.94; H, 7.21; Cl, 12.68; N, 15.02%. Found: C, 42.87; H, 7.29; Cl, 12.87; N, 14.77%. **MS (CL. m/z)**: 280 (M+1, 100%). **IR Data** (CH₂Cl₂ cast, cm⁻¹): ν(P-N) 692 (s), ν(N-C) 1055 (s). **NMR Data** (CDCl₃) ³¹P{¹H}: P(σ²): δ 248.53 (d, ²J_{PP} 30 Hz), P(σ³): δ 120.40 (d, ²J_{PP} 30 Hz).

^1H : C-CH₃ δ 2.31 (dd, $^4J_{\sigma^2\text{PH}}$ 1.4 Hz, $^4J_{\sigma^3\text{PH}}$ 1.4 Hz), P(σ^2)-N-CH₃ δ 3.97 (dd, $^3J_{\sigma^2\text{PH}}$ 7.6 Hz, $^5J_{\sigma^3\text{PH}}$ 0.9 Hz), N-CH-(CH₃)₂ δ 3.35 (sept., $^3J_{\text{HH}}$ 6.4 Hz), N-CH-CH₃ δ 1.45 (d, $^3J_{\text{HH}}$ 6.4 Hz). $^{13}\text{C}\{^1\text{H}\}$: C-CH₃ δ 14.44 (d, $^3J_{\text{PC}}$ 6 Hz), P(σ^2)-N-CH₃ δ 41.24 (d, $^2J_{\sigma^2\text{PC}}$ 18 Hz), P-C-P δ 153.09 (dd, $^1J_{\sigma^2\text{PC}}$ 54 Hz, $^1J_{\sigma^3\text{PC}}$ 12 Hz), N-C-CH₃ δ 156.05 (dd, $^2J_{\sigma^2\text{PC}}$ 9.4 Hz, $^2J_{\sigma^3\text{PC}}$ 24 Hz), P(σ^3)-N-CH₂-CH₃ δ 42.45 (d, $^2J_{\sigma^3\text{PC}}$ 23 Hz), P(σ^3)-N-CH₂-CH₃ δ 14.39 (s).

Synthesis of 4-(Chloro(dibenzylamino)phosphino)-2,5-dimethyl-2H-1,2,3 σ^2 -diazaphosphole, (7).

A solution of 1 (1.0 mL, 7.05 mmol) in 30 mL of ether was added dropwise to a solution of dibenzylamine (2.8 mL, 14.6 mmol) and triethylamine (2.1 mL, 15 mmol) in 25 mL of ether at 0°C, during this time the precipitate of Et₂NH·HCl was immediately observed. The solution was stirred for one day after slowly be allowed to warm up to room temperature (22°C). The solvent and triethylamine were removed *in vacuo*, leaving an off-white solid. The phosphole was recrystallized from hexane to produce a light brown solid. The yield of 7 was 1.91 g (72.1%). **Formula Weight:** 375.78 g/mol. **Anal.** for C₁₈H₂₀ClN₃P₂: C, 57.53; H, 5.36; Cl, 9.43; N, 11.18%. Found: C, 57.42; H, 5.29; Cl, 9.72; N, 11.00%. **MS (Cl, m/z):** 376 (M+1, 100%). **IR Data** (CH₂Cl₂ cast, cm⁻¹): $\nu(\text{P-N})$ 680 (s), $\nu(\text{N-C})$ 985 (s). **NMR Data** (CDCl₃) $^{31}\text{P}\{^1\text{H}\}$: P(σ^2): δ 247.43 (d, $^2J_{\text{PP}}$ 25 Hz), P(σ^3): δ 127.48 (d, $^2J_{\text{PP}}$ 25 Hz). ^1H : C-CH₃ δ 2.44 (d, $^4J_{\sigma^2\text{PH}}$ 1.8 Hz, $^4J_{\sigma^3\text{PH}}$ 1.8 Hz), P(σ^2)-N-CH₃ δ 4.02 (dd, $^3J_{\sigma^2\text{PH}}$ 7.6 Hz, $^5J_{\sigma^3\text{PH}}$ 0.9 Hz), N-CH₂-C₆H₅ δ 5.35 (m), N-CH₂-C₆H₅ δ 7.2-8.4 (m). $^{13}\text{C}\{^1\text{H}\}$: C-CH₃ δ 14.44 (d, $^3J_{\text{PC}}$ 5.5 Hz), P(σ^2)-N-CH₃ δ 41.81 (d, $^2J_{\sigma^2\text{PC}}$ 18 Hz), P-C-P δ 150.73 (dd, $^1J_{\sigma^2\text{PC}}$ 54 Hz, $^1J_{\sigma^3\text{PC}}$ 36 Hz), N-C-CH₃ δ 155.38 (dd, $^2J_{\sigma^2\text{PC}}$ 5 Hz, $^2J_{\sigma^3\text{PC}}$ 25 Hz), P(σ^3)-N-CH₂-C₆H₅ δ 40.32 (d, $^2J_{\sigma^3\text{PC}}$ 23 Hz).

Synthesis of 4-(Chloro(iminodibenzyl)phosphino)-2,5-dimethyl-2H-1,2,3 σ^2 -diazaphosphole, (8).

A solution of **1** (1.0 mL, 7.05 mmol) in 30 mL of ether was added dropwise to a solution of DBU (2.2 mL, 14.6 mmol) and triethylamine (2.1 mL, 15 mmol) in 25 mL of ether at 0°C. During the addition, a precipitate of Et₃N·HCl was immediately observed. After the addition, the solution was allowed to warm up to room temperature (22°C) and stirred for 1 day. The solvent was removed *in vacuo*, leaving a light brown solid. The phosphole was precipitated from hexane from a dichloromethane solution as beige powder. The yield of **8** was 0.87 g (33.2%). Formula Weight: 373.76 g/mol. Anal. for C₁₈H₁₈ClN₃P₂: C, 57.84; H, 4.85; Cl, 9.40; N, 11.24%. Found: C, 57.93; H, 4.72; Cl, 9.21; N, 11.09%. MS (CL m/z): 374 (M+1, 62%). IR Data (CH₂Cl₂ cast, cm⁻¹): ν (P-N) 672 (s), ν (N-C) 962 (s). NMR Data (CDCl₃) ³¹P{¹H}: P(σ^2): δ 246.51 (d, ²J_{PP} 6 Hz), P(σ^3): δ 118.46 (d, ²J_{PP} 6 Hz). ¹H: C-CH₃ δ 2.40 (dd, ⁴J_{PH} 1.5 Hz, ⁴J_{PH} 1.4 Hz), P(σ^2)-N-CH₃ δ 3.98 (dd, ³J_{PH} 7.8 Hz, ⁵J_{PH} 0.9 Hz), iminodibenzyl alkyl H δ 5.26 (m), iminodibenzyl phenyl H δ 7.2-8.4 (m). ¹³C{¹H}: C-CH₃ δ 14.94 (s), P(σ^2)-N-CH₃ δ 41.63 (d, ²J_{PC} 17 Hz), P-C-P δ 151.07 (dd, ¹J _{σ^2 PC} 53 Hz, ¹J _{σ^3 PC} 35 Hz), N-C-CH₃ δ 155.52 (dd, ²J _{σ^2 PC} 9 Hz, ²J _{σ^3 PC} 24 Hz), iminodibenzyl alkyl C δ 34.85 (s), iminodibenzyl phenyl C: δ 131 - 1178 (s), P(σ^3)-N-C δ 143.11 (d, ²J _{σ^3 PC} 5 Hz).

Synthesis of 4-(Dipyrazolephosphino)-2,5-dimethyl-2H-1,2,3 σ^2 -diazaphosphole, (9).

A solution of **1** (1.0 mL, 7.05 mmol) in 30 mL of ether was added dropwise to a solution of pyrazole (0.9940 g, 14.6 mmol) and triethylamine (2.1 mL, 15 mmol) in 25 mL of ether at 0°C, during this time the precipitate of Et₂NH·HCl was immediately observed. The solution was stirred for one day after slowly be allowed to warm up to room temperature (22°C). The solvent and excess triethylamine were removed *in*

vacuo, leaving a white solid. The yield of **9** was 1.55 g (78.9 %). **Formula Weight**: 278.19 g/mol. **Anal.** for C₁₀H₁₂N₆P₂: C, 43.18; H, 4.35; N, 30.21%. Found: C, 42.62; H, 4.12; N, 27.31%. **MS (CL, m/z)**: 279 (M+1, 100%). **IR Data** (CH₂Cl₂ cast, cm⁻¹): ν(P-N) 721 (s), 665 (s). **NMR Data** (CDCl₃) ³¹P{¹H}: P(σ²): δ 243.84 (d, ²J_{PP} 7 Hz), P(σ³): δ 59.18 (d, ²J_{PP} 7 Hz). ¹H: C-CH₃ δ 2.38 (dd, ⁴J_{σ²PH} 1.6 Hz, ⁴J_{σ³PH} 1.6 Hz), P(σ²)-N-CH₃ δ 4.04 (d, ³J_{σ²PH} 7.7 Hz), pyrazole: P(σ³)-N-CH δ 7.95 (dd, ³J_{σ³PH} 2.4 Hz, ³J_{HH} 2.4 Hz), P(σ³)-N-N-C-H δ 7.78 (d, ³J_{HH} 1.3 Hz), N-CH-CH δ 6.35 (dd, ³J_{HH} 2.4 Hz, ³J_{HH} 1.3 Hz). ¹³C{¹H}: C-CH₃ δ 14.95 (d, ³J_{PC} 10.4 Hz), P(σ²)-N-CH₃ δ 41.03 (d, ²J_{σ²PC} 18 Hz), P-C-P δ 153.09 (dd, ¹J_{Pσ²C} 54 Hz, ¹J_{Pσ³C} 12 Hz), N-C-CH₃ δ 156.05 (dd, ²J_{Pσ²C} 9 Hz, ²J_{Pσ³C} 24 Hz), pyrazole: P(σ³)-N-CH-CH δ 142.45 (d, ²J_{σ³PC} 31 Hz), P(σ³)-N-N-CH- δ 135.51 (s), P(σ³)-N-CH-CH δ 104.39 (s).

Synthesis of 4-(Bis(3,5-dimethylpyrazole)phosphino)-2,5-dimethyl-2H-1,2,3σ²-diazaphosphole, (10).

A solution of **1** (1.0 mL, 7.05 mmol) in 30 mL of ether was added dropwise to a solution of 3,5-dimethylpyrazole (1.403 g, 14.6 mmol) and triethylamine (2.1 mL, 15 mmol) in 25 mL of ether at 0°C. During the addition, a precipitate of Et₃N·HCl was immediately observed. After the addition, the solution was allowed to warm up to room temperature (22°C) and stirred for 1 day. The solvent and excess triethylamine were removed *in vacuo*, leaving a white solid. The yield of **10** was 1.94 g (82.4 %). **Formula Weight**: 334.30 g/mol. **Anal.** for C₁₄H₂₀N₆P₂: C, 50.30; H, 6.03; N, 25.14%. Found: C, 50.54; H, 6.30; N, 25.04%. **MS (CL, m/z)**: 335 (M+1, 100%). **NMR Data** (CDCl₃) ³¹P{¹H}: P(σ²): δ 242.83 (d, ²J_{PP} 4 Hz), P(σ³): δ 49.28 (d, ²J_{PP} 4 Hz). ¹H: C-CH₃ δ 2.26 (dd, ⁴J_{σ²PH} 1.7 Hz, ⁴J_{σ³PH} 1.7 Hz), P(σ²)-N-CH₃ δ 4.02 (d, ³J_{σ²PH} 7.5 Hz), pyrazole: P(σ³)-N-C-CH₃ δ 2.41 (s), P(σ³)-N-N-C-CH₃ δ 2.23 (s), N-C-CH δ 5.85 (s). ¹³C{¹H}: C-CH₃ δ 14.68 (d, ³J_{PC} 5 Hz), P(σ²)-N-CH₃ δ

40.64 (d, $^2J_{\sigma^2PC}$ 18 Hz), P-C-P δ 153.09 (dd, $^1J_{P\sigma^2C}$ 54 Hz, $^1J_{P\sigma^3C}$ 12 Hz), N-C-CH₃ δ 156.05 (dd, $^2J_{\sigma^2PC}$ 9 Hz, $^2J_{\sigma^3PC}$ 24 Hz), pyrazole: P(σ^3)-N-C-CH₃ δ 145.63 (d, $^2J_{\sigma^3PC}$ 33 Hz), P(σ^3)-N-N-C-CH₃ δ 130.51 (s), P(σ^3)-N-CH-CH δ 104.98 (s).

Synthesis of 4-(Bis(2,2,2-trifluoroethoxy)phosphino)-2,5-dimethyl-2H-1,2,3 σ^2 -diazaphosphole, (11)

A solution of 1 (2.5 mL, 18 mmol) in 25 mL of ether was added dropwise to a solution of 2,2,2-trifluoroethanol (2.6 mL, 36 mmol) and triethylamine (5.0 mL, 38 mmol) in 125 mL of ether at 0°C, during this time the precipitate of Et₃NH·HCl was immediately observed. The solution was stirred for one day after slowly be allowed to warm up to room temperature (22°C). The solvent, excess trifluoroethanol, and triethylamine were removed *in vacuo*, leaving a white solid. The phosphole was recrystallized from hexane and stored at -10°C for 1 day. The phosphole was also sublimed at 65-70°C @ 0.1 torr. The yield of 11 was 5.52 g (89.6 %). **Formula Weight:** 342.12 g/mol. **Anal.** for C₈H₁₀F₆N₂O₂P₂: C, 28.09; H, 2.95; N, 8.19%. Found: C, 27.40; H, 2.92; N, 8.06%. **MS (EI, m/z):** 342 (M, 100%), 259 (M-CH₂CF₃, 45%). **IR Data** (CH₂Cl₂ cast, cm⁻¹): ν (P-O) 1175 (s). **NMR Data** (CDCl₃) $^{31}P\{^1H\}$: P(σ^2): δ 247.27 (d(broad), $^2J_{PP}$ 25 Hz), P(σ^3): δ 168.09 (ds, $^2J_{PP}$ 25 Hz, $^4J_{PF}$ 4 Hz). 1H : C-CH₃ δ 2.48 (dd, $^4J_{\sigma^2PH}$ 2 Hz, $^4J_{\sigma^3PH}$ 2 Hz), P(σ^2)-N-CH₃ δ 4.02 (d, $^3J_{\sigma^2PH}$ 7.9 Hz), P(σ^3)-N-O-CH₂CF₃ δ 2.41 (m), δ 2.09 (m). $^{13}C\{^1H\}$: C-CH₃ δ 14.81 (d, $^3J_{\sigma^3PC}$ 6 Hz), P(σ^2)-N-CH₃ δ 41.54 (d, $^2J_{\sigma^2PC}$ 18 Hz), P-C-P δ 146.44 (dd, $^1J_{\sigma^2PC}$ 59 Hz, $^1J_{\sigma^3PC}$ 29 Hz), N-C-CH₃ δ 156.73 (dd, $^2J_{\sigma^2PC}$ 5 Hz, $^2J_{\sigma^3PC}$ 23 Hz), P(σ^3)-O-CH₂-CF₃ δ 63.30 (dq, $^2J_{\sigma^3PC}$ 8 Hz, $^2J_{FC}$ 36 Hz), P(σ^3)-O-CH₂-CF₃ δ 123.49 (dq, $^3J_{\sigma^3PC}$ 6 Hz, $^1J_{FC}$ 278 Hz). ^{19}F : δ -75.70 (ddq, $^4J_{\sigma^3PF}$ 4 Hz, $^6J_{\sigma^2PF}$ 2 Hz, $^3J_{FH}$ 8 Hz).

Synthesis of 4-(Bis(phenoxy)phosphino)-2,5-dimethyl-2H-1,2,3 σ^2 -diazaphosphole, (12).

A solution of **1** (1.0 mL, 7.05 mmol) in 20 mL of ether was added dropwise to a solution of phenol (0.339 g, 14.4 mmol) and triethylamine (2.1 mL, 15 mmol) in 30 mL of ether at 0°C. During the addition, a precipitate of Et₃N·HCl was immediately observed. After the addition, the solution was allowed to warm up to room temperature (22°C) and stirred for 1 day. The solvent and excess triethylamine were removed *in vacuo*, leaving a white solid. The yield of **12** was 2.05 g (88.2%). Formula Weight: 330.26 g/mol. Anal. for C₁₆H₁₆N₂O₂P₂: C, 58.19; H, 4.88; N, 8.48%. Found: C, 58.14; H, 4.92; N, 8.56%. MS (CI, m/z): 331 (M+1, 100%). IR Data (CH₂Cl₂ cast, cm⁻¹): ν (P-O) 1226 (s). NMR Data (CDCl₃) ³¹P{¹H}: P(σ^2): δ 247.00 (d(broad), ²J_{PP} 36 Hz), P(σ^3): δ 158.13 (d, ²J_{PP} 36 Hz). ¹H: C-CH₃ δ 2.51 (s (broad)), P(σ^2)-N-CH₃ δ 4.09 (d, ³J _{σ^2 PH} 8.1 Hz). ¹³C{¹H}: C-CH₃ δ 14.92 (s), P(σ^2)-N-CH₃ δ 41.51 (d, ²J _{σ^2 PC} 18 Hz), P-C-P δ 146.68 (dd, ¹J _{σ^2 PC} 57 Hz, ¹J _{σ^3 PC} 27 Hz), phenyl C: δ 139 - 127 (s).

Synthesis of 4-(Bis(pentafluorophenoxy)phosphino)-2,5-dimethyl-2H-1,2,3 σ^2 -diazaphosphole, (13).

A solution of **1** (1.0 mL, 7.05 mmol) in 20 mL of ether was added dropwise to a solution of pentafluorophenol (2.65 g, 14.4 mmol) and triethylamine (2.1 mL, 15 mmol) in 30 mL of ether at 0°C. During the addition, a precipitate of Et₃N·HCl was immediately observed. After the addition, the solution was allowed to warm up to room temperature (22°C) and stirred for 1 day. The solvent and excess triethylamine were removed *in vacuo*, leaving a white solid. The phosphole was recrystallized from hexane and stored at -10°C for 1 day. The yield of **13** was 1.79 g (49.8%). Formula Weight: 510.17 g/mol. Anal. for C₁₆H₆F₁₀N₂O₂P₂: C, 37.67; H, 1.19; N, 5.49%. Found: C, 37.24; H, 1.12; N, 5.59%. MS (CI, m/z): 511 (M+1, 100%). IR Data

(CH₂Cl₂ cast, cm⁻¹): ν (P-O) 1195 (s). NMR Data (CDCl₃) ³¹P{¹H}: P(σ^2): δ 248.49 (d(broad), ²J_{PP} 57 Hz), P(σ^3): δ 188.89 (dp, ²J_{PP} 25 Hz, ⁴J_{PP} 29 Hz). ¹H: C-CH₃ δ 2.65 (s (broad)), P(σ^2)-N-CH₃ δ 4.13 (d, ³J _{σ^2 PH} 7.8 Hz). ¹³C{¹H}: C-CH₃ δ 15.19 (s), P(σ^2)-N-CH₃ δ 41.78 (d, ²J _{σ^2 PC} 18 Hz), P-C-P δ 146.68 (dd, ¹J _{σ^2 PC} 56 Hz, ¹J _{σ^3 PC} 27 Hz), N-C-CH₃ δ 157.76 (dd, ²J _{σ^2 PC} 4 Hz, ²J _{σ^3 PC} 24 Hz), phenyl C: δ 149 - 122. ¹⁹F (second order): δ -75.70 (m).

Synthesis of 4-(Bis(2,6-difluorophenoxy)phosphino)-2,5-dimethyl-2H-1,2,3 σ^2 -diazaphosphole, (14).

A solution of **1** (1.0 mL, 7.05 mmol) in 20 mL of ether was added dropwise to a solution of 2,6-difluorophenol (1.87 g, 14.4 mmol) and triethylamine (2.1 mL, 15 mmol) in 30 mL of ether at 0°C, during this time the precipitate of Et₂NH·HCl was immediately observed. The solution was stirred for one day after slowly be allowed to warm up to room temperature (22°C). The solvent and excess triethylamine were removed *in vacuo*, leaving a white solid. NMR Data (CDCl₃) ³¹P{¹H}: P(σ^2): δ 247.76 (d, ²J_{PP} 34 Hz), P(σ^3): δ 167.54 (dp, ²J_{PP} 25 Hz, ⁴J_{PF} 27 Hz). IR Data (CH₂Cl₂ cast, cm⁻¹): ν (P-O) 1187 (s).

Synthesis of 4-(Bis(2-(2,3,4,5-pentafluorophenyl)ethoxy)phosphino)-2,5-dimethyl-2H-1,2,3 σ^2 -diazaphosphole, (15).

A solution of **1** (1.0 mL, 7.05 mmol) in 25 mL of ether was added dropwise to a solution of 2,3,4,5,6-pentafluorobenzyl alcohol (2.85 g, 14.4 mmol) and triethylamine (2.1 mL, 15 mmol) in 125 mL of ether at 0°C. During the addition, a precipitate of Et₃N·HCl was immediately observed. After the addition, the solution was allowed to warm up to room temperature (22°C) and stirred for 1 day. The solvent and excess triethylamine were removed *in vacuo*, leaving a white solid. The phosphole was recrystallized from hexane and stored at -10°C for 1 day. The yield of **15** was

2.90 g (76.4 %). **Formula Weight:** 538.22 g/mol. **Anal.** for $C_{18}H_{10}F_{10}N_2O_2P_2$: C, 40.17; H, 2.87; N, 5.20%. Found: C, 39.78; H, 2.82; N, 5.32 %. **MS (CI, m/z):** 539 (M+1, 100%). **IR Data** (CH_2Cl_2 cast, cm^{-1}): $\nu(P-O)$ 1182 (s). **NMR Data** ($CDCl_3$) $^{31}P\{^1H\}$: $P(\sigma^2)$: δ 246.09 (d(broad), $^2J_{PP}$ 23 Hz), $P(\sigma^3)$: δ 161.04 (dp, $^2J_{PP}$ 23 Hz, $^5J_{PF}$ 6 Hz). 1H : C- $\underline{C}H_3$ δ 2.45 (d, $^4J_{PH}$ 0.8 Hz), $P(\sigma^2)$ -N- $\underline{C}H_3$ δ 4.04 (dd, $^3J_{\sigma^2PH}$ 7.8 Hz, $^5J_{\sigma^3PH}$ 0.5 Hz). $^{13}C\{^1H\}$: C- $\underline{C}H_3$ δ 14.68 (s), $P(\sigma^2)$ -N- $\underline{C}H_3$ δ 41.42 (d, $^2J_{\sigma^2PC}$ 18 Hz), P- \underline{C} -P δ 148.02 (dd, $^1J_{\sigma^2PC}$ 58 Hz, $^1J_{\sigma^3PC}$ 28 Hz), N- \underline{C} - $\underline{C}H_3$ δ 156.52 (dd, $^2J_{\sigma^2PC}$ 6 Hz, $^2J_{\sigma^3PC}$ 24 Hz), phenyl C: δ 149 - 122. ^{19}F (second order): δ -75.70 (m).

5.2 Oxidation of the 4-Phosphinodiazaphosphole.

Synthesis of 4-(Difluorothiophosphorano)-2,5-dimethyl-2*H*-1,2,3 σ^2 -diazaphosphole, (16).

Sulfur (0.116 g, 3.6 mmol) was added to a solution of **2** (0.5 mL, 3.6 mmol) in 10 mL of toluene and heated to reflux for 48 hours. The solvent was removed *in vacuo*, leaving a yellow liquid which contained some sulfur. Diethyl ether was added (5 mL) and the solution was filtered through Celite. The ether and excess **2** were then removed *in vacuo*, leaving a light yellow oil. The yield of **16** was 0.403 g (52.3%). **Formula Weight:** 214.11 g/mol. **Anal.** for C₄H₆F₂N₂P₂S: C, 22.44; H, 2.82; N, 13.08; S, 14.97%. Found: C, 22.42; H, 2.95; N, 13.09; S 14.79%. **MS (EI, m/z):** 214 (M, 29%), 182 (M-S, 100%). **IR Data** (CH₂Cl₂ cast, cm⁻¹): ν (P=S) 726 (w), ν (P-F) 853 (s), 823 (s). **NMR Data** (CDCl₃) ³¹P{¹H}: P(σ^2): δ 264.25 (d, ²J_{PP} 112 Hz), P(σ^3): δ 82.47 (²J_{PP} 112 Hz, ¹J_{PF} 1133 Hz). ¹H: C-CH₃ δ 2.39 (d, ⁴J_{PH} 01 Hz), P(σ^2)-N-CH₃ δ 3.94 (d, ³J _{σ^2 PH} 9 Hz). ¹³C{¹H}: C-CH₃ δ 14.79 (s), P(σ^2)-N-CH₃ δ 41.62 (d, ²J _{σ^2 PC} 18 Hz), P-C-P δ 137.15 (ddt, ¹J _{σ^2 PC} 163 Hz, ¹J _{σ^3 PC} 43 Hz, ²J_{CF} 24.1 Hz), N-C-CH₃ δ 155.84 (d, ²J _{σ^2 PC} 6 Hz). ¹⁹F: δ -41.84 (dd, ¹J _{σ^3 PF} 1132 Hz, ³J _{σ^2 PF} 6 Hz).

Synthesis of 4-(Difluoroselenophosphorano)-2,5-dimethyl-2*H*-1,2,3 σ^2 -diazaphosphole, (17).

Selenium (0.592 g, 7.5 mmol) was added to a solution of **2** (1.00 mL, 7.2 mmol) in 15 mL of toluene and heated to reflux for 12 hours. The solution was cooled then filtered through Celite and washed with (2 x 5 mL) toluene. The solvent was removed *in vacuo*, leaving a colourless moisture-sensitive crystalline material. The yield of **17** was 1.80 g (95.6%). **Formula Weight:** 261.01 g/mol. **Anal.** for C₄H₆F₂N₂P₂Se: C, 18.41; H, 2.32; N, 10.73%. Found: C, 18.02; H, 2.16; N,

10.58%. MS (EI, m/z): 262 (M, 26%), 182 (M-Se, 100%). IR Data (CH₂Cl₂ cast, cm⁻¹): ν(P=Se) 533 (m) ν(P-F) 869 (s), 841 (s). NMR Data (CDCl₃) ³¹P{¹H}: P(σ²): δ 265.25 (d, ²J_{PP} 118 Hz), P(σ³): δ 87.65 (dt Se sat. 8%, ²J_{PP} 118 Hz, ¹J_{PF} 1177 Hz, ¹J_{PSe} 1021 Hz). ¹H: C-CH₃ δ 2.43 (dd, ⁴J_{σ²PH} 0.9 Hz, ⁴J_{σ³PH} 0.9 Hz), P(σ²)-N-CH₃ δ 4.03 (d, ³J_{σ²PH} 12 Hz). ¹³C{¹H}: C-CH₃ δ 15.10 (s), P(σ²)-N-CH₃ δ 41.79 (d, ²J_{σ²PC} 17 Hz), P-C-P δ 140.39 (dd, ¹J_{σ²PC} 160 Hz, ¹J_{σ³PC} 64 Hz), N-C-CH₃ δ 155.46 (s). ¹⁹F: δ -43.03 (dd, ¹J_{σ³PF} 1169 Hz, ³J_{σ²PF} 34 Hz).

Synthesis of 4-(difluoro(*p*-cyanotetrafluorophenyl)iminophosphorano)-2,5-dimethyl-2*H*-1,2,3σ²-diazaphosphole, (18).

The *p*-cyanotetrafluorophenyl azide (1.0 mL, 7.2 mmol) was added dropwise with a syringe into a stirred solution containing **2** (1.0 mL, 7.2 mmol), dissolved in 15 mL of dichloromethane at -78°C (acetone/Dry Ice). The solution became yellow coloured a few minutes after the addition. It was left to warm to room temperature (22°C) and stirred overnight, by this time the solution was colourless. The volume was reduced to ~5 mL and stored at -40°C overnight to produce colourless crystals. The yield of **18** was 2.39 g (89.7%). M.P. = 123°C. Formula Weight: 370.13 g/mol. Anal. for C₁₁H₆F₆N₄P₂: C, 35.70; H, 1.63; N, 15.14%. Found: C, 35.12; H, 1.68; N, 15.28%. MS (EI, m/z): 370 (M, 100%). IR Data (CH₂Cl₂ cast, cm⁻¹): ν(P=N) 1498 (s), ν(P-F) 921 (s), 896 (s), ν(CN) 2241 (s). NMR Data (CDCl₃) ³¹P{¹H}: P(σ²): δ 265.25 (d, ²J_{PP} 83 Hz), P(σ³): δ 2.66 (dt, ²J_{PP} 83 Hz, ¹J_{PF} 1145 Hz). ¹H: C-CH₃ δ 2.61 (s (broad)), P(σ²)-N-CH₃ δ 4.14 (d, ³J_{σ²PH} 9 Hz). ¹³C{¹H}: C-CH₃ δ 15.01 (s), P(σ²)-N-CH₃ δ 41.92 (d, ²J_{σ²PC} 18 Hz), P-C-P δ 125.17 (dd, ¹J_{σ²PC} 246 Hz, ¹J_{σ³PC} 45 Hz), N-C-CH₃ δ 158.21 (d, ²J_{σ³PC} 13 Hz). ¹⁹F: δ -56.54 (dd, ¹J_{PF} 1169 Hz, ³J_{PF} 34 Hz), *m*-F tbn δ 139.77 (m), *o*-F tbn δ -152.81 (m).

Synthesis of 4-(difluoro{2,4,6-tri-*tert*-butylphenylimino}phosphorano)-2,5-dimethyl-2*H*-1,2,3σ²-diazaphosphole, (19).

A solution of diethyl azodicarboxylate (0.6 mL, 3.8 mmol) in 5 ml of THF was added dropwise into a stirred solution containing **2** (0.5 mL, 3.6 mmol) and 2,4,6-tri-*tert*-butylaniline (0.941 g, 3.6 mmol) dissolved in 10 mL of THF and maintained at 0°C. The addition took for 30 minutes. The solution was then stirred for 12 hours at room temperature (22°C). The initial red solution formed on mixing slowly disappeared a few hours after the addition. **Formula Weight:** 441.48 g/mol. **MS (EI, m/z):** 441 (M, 15%). **NMR Data** (CDCl₃) ³¹P{¹H}: P(σ²): δ 266.38 (d, ²J_{PP} 96 Hz), P(σ³): δ -40.56 (dt, ²J_{PP} 88 Hz, ¹J_{σ³PF} 1062 Hz). ¹H: N-C-CH₃ δ 2.59 (s), P(σ²)-N-CH₃ δ 4.03 (d, ³J_{σ²PH} 8.4 Hz), ^tBu CH₃ δ 1.39 (s). ¹³C{¹H}: C-CH₃ δ 15.02 (s), P(σ²)-N-CH₃ δ 41.81 (d, ¹J_{σ²PC} 17 Hz), P-C-P δ 140.78 (dd, ²J_{σ²PC} 159 Hz, ²J_{σ³PC} 61 Hz), N-C-CH₃ δ 155.78 (s). ¹⁹F: δ -58.41 (dd, ¹J_{σ²PF} 1079 Hz, ³J_{σ³PF} 10 Hz).

Synthesis of 4-(difluoro{*p*-methylphenylimino}phosphorano)-2,5-dimethyl-2*H*-1,2,3σ²-diazaphosphole, (20).

A solution of diethyl azodicarboxylate (0.6 mL, 3.9 mmol) in 5 ml of THF was slowly added dropwise (over 30 minutes) to a stirred solution containing **2** (0.5 mL, 3.6 mmol) and *p*-toluidine (0.386 g, 3.6 mmol) dissolved in 10 mL of THF at 0°C. The solution was then stirred at room temperature (22°C) for 12 hours. The initial red colour of the solution slowly lightened over a period of a few hours following the completion of the addition. **Formula Weight:** 287.19 g/mol. **MS (EI, m/z):** 287 (M, 100%). **NMR Data** (CDCl₃) ³¹P{¹H}: P(σ²): δ 266.41 (d, ²J_{PP} 96 Hz), P(σ³): δ 10.34 (dt, ²J_{PP} 96 Hz, ¹J_{σ³PF} 971 Hz). ¹H: C-CH₃ δ 2.59 (s), P(σ²)-N-CH₃ δ 4.03 (d, ³J_{PH} 8.3 Hz). ¹³C{¹H}: C-CH₃ δ 14.97 (s), P(σ²)-N-CH₃ δ 41.83 (d, ²J_{σ²PC} 17

Hz), P-C-P δ 141.02 (dd, $^2J_{\sigma^2PC}$ 165 Hz, $^2J_{\sigma^3PC}$ 60 Hz), N-C-CH₃ δ 156.12 (s). ^{19}F : δ -58.41 (d (broad), $^1J_{PF}$ 971 Hz).

Synthesis of 4-(Bis(Dimethylamino)thiophosphorano)-2,5-dimethyl-2H-1,2,3 σ^2 -diazaphosphole, (21).

Sulfur (0.154 g, 4.8 mmol) was added to a solution of 3 (1.0 mL, 4.8 mmol) in 10 mL of toluene and heated to reflux for 48 hours. The solvent was removed *in vacuo*, leaving a yellow liquid which contained some sulfur. Diethyl ether was added (5 mL) and the solution was filtered through Celite. The ether was then removed *in vacuo*. The yield of 22 was 1.14 g (89.5%). M.P. = 135-138°C. Formula Weight: 264.26 g/mol. Anal. for C₈H₁₈N₄P₂S: C, 36.36; H, 6.87; N, 21.20; S, 12.13%. Found: C, 36.42; H, 6.95; N, 21.09; S 11.79%. MS (EI, m/z): 264 (M, 80%). IR Data (CH₂Cl₂ cast, cm⁻¹): ν (P=S) 723 (w), ν (P-N) 735 (s), 715 (s). NMR Data (CDCl₃) ^{31}P { 1H }: P(σ^2): δ 255.12 (d, $^2J_{PP}$ 76 Hz), P(σ^3): δ 70.83 ($^2J_{PP}$ 76 Hz). 1H : C-CH₃ δ 2.51 (dd, $^4J_{PH}$ 1.5 Hz, $^4J_{\sigma^2PH}$ 0.5 Hz), P(σ^2)-N-CH₃ δ 3.95 (d, $^3J_{\sigma^2PH}$ 7.7 Hz). ^{13}C { 1H }: C-C-CH₃ δ 14.95 (s), P(σ^2)-N-C-CH₃ δ 41.49 (d, $^2J_{\sigma^2PC}$ 17 Hz), P-C-P δ 141.21 (dd, $^2J_{\sigma^2PC}$ 123 Hz, $^2J_{\sigma^3PC}$ 47 Hz), P(σ^3)-N-C-CH₃ δ 40.29 (d, $^2J_{\sigma^3PC}$ 5 Hz).

Synthesis of 4-(Bis(Dimethylamino)selenophosphorano)-2,5-dimethyl-2H-1,2,3 σ^2 -diazaphosphole, (22).

Selenium (0.381 g, 4.8 mmol) was added to a solution of 2 (1.0 mL, 4.8 mmol) in 10 mL of toluene and heated to reflux for 12 hours. The solution was cooled then filtered through Celite and washed with (2 x 5 mL) toluene. The solvent was removed *in vacuo*, to leave an off-white, moisture sensitive crystalline material. The phosphole was recrystallized from toluene. The yield of 23 was 1.47 g (96.7%). Formula Weight: 311.16 g/mol. Anal. for C₈H₁₈N₄P₂Se: C, 30.88; H, 5.83; N,

18.01%. Found: C, 31.02; H, 5.90; N, 17.78%. M.P. = 148-150°C. IR Data (CH₂Cl₂ cast, cm⁻¹): ν (P=Se) 542 (m), ν (P-N) 716 (s), 692 (s). MS (EI, m/z): 313 (M+1, 100%). NMR Data (CDCl₃) ³¹P{¹H}: P(σ^2): δ 257.19 (d, ²J_{PP} 84 Hz), P(σ^3): δ 66.63 (dt Se sat. 8%, ²J_{PP} 84 Hz, ¹J_{PSe} 751 Hz). ¹H: C-CH₃ δ 2.64 (dd, ⁴J_{PH} 1.1 Hz, ⁴J_{PH} 1.1 Hz), P(σ^2)-N-CH₃ δ 3.95 (d, ³J _{σ^2 PH} 7.9 Hz). ¹³C{¹H}: C-CH₃ δ 15.60 (s), P(σ^2)-N-CH₃ δ 41.21 (d, ²J _{σ^2 PC} 18 Hz), P-C-P δ 147.16 (dd, ²J _{σ^2 PC} 157 Hz, ²J _{σ^3 PC} 43 Hz), P(σ^3)-N-CH₃ δ 40.54 (d, ²J _{σ^3 PC} 5 Hz). ⁷⁷Se: δ -245.04 (dd, ³J _{σ^2 PF} 41 Hz, ¹J _{σ^3 PF} 751 Hz).

Synthesis of 4-(Bis(Dimethylamino)(trimethylsilylimino)phosphorano)-2,5-dimethyl-2H-1,2,3 σ^2 -diazaphosphole, (23).

Trimethylsilyl azide (1.3 mL, 10 mmol) was added to a solution of 2 (0.5 mL, 4.8 mmol) in 10 mL of acetonitrile and heated to reflux for 24 hours. The solution was cooled and the volatiles were removed *in vacuo*, to leave an light amber oil. Formula Weight: 319.40 g/mol. MS (EI, m/z): 319 (M, 37%). IR Data (CH₂Cl₂ cast, cm⁻¹): ν (P=N) 1492 (s), ν (P-N) 851 (s), 816 (s). NMR Data (CDCl₃) ³¹P{¹H}: P(σ^2): δ 253.50 (d, ²J_{PP} 68 Hz), P(σ^3): δ 8.10 (d, ²J_{PP} 68 Hz). ¹H: C-CH₃ δ 2.41 (s), P(σ^2)-N-CH₃ δ 3.88 (d, ³J_{PH} 7.4 Hz), Si-CH₃ δ 0.12 (s). ¹³C{¹H}: C-CH₃ δ 15.05 (s), P(σ^2)-N-CH₃ δ 40.75 (d, ²J _{σ^2 PC} 18 Hz), P-C-P δ 143.60 (dd, ²J _{σ^2 PC} 155 Hz, ²J _{σ^3 PC} 49 Hz), P(σ^3)-N-CH₃ δ 40.27 (d, ²J _{σ^3 PC} 7 Hz).

Synthesis of 4-(Bis(Dimethylamino)(*p*-cyanotetrafluorophenylimino)-phosphorano)-2,5-dimethyl-2H-1,2,3 σ^2 -diazaphosphole, (24).

The *p*-cyanotetrafluorophenyl azide (0.7 mL, 4.8 mmol) was added dropwise with a syringe into a stirred solution containing 3 (0.5 mL, 4.8 mmol), dissolved in 15 mL of dichloromethane at -78°C (acetone/Dry Ice). The solution became yellow in colour a few minutes after the addition. It was left to warm to room temperature (22°C)

and stirred overnight; by this time the solution was colourless. The solvent was removed *in vacuo*, to leave an off-white, moisture sensitive crystalline material. The yield of **24** was 1.51 g (75.3%). **Formula Weight:** 420.29 g/mol. **Anal.** for $C_{15}H_{18}F_4N_6P_2$: C, 42.87; H, 4.32; N, 20.00%. Found: C, 42.67; H, 4.25; N, 20.09%. **M.P.** = 152°C (dec.). **MS (EI, m/z):** 420 (M, 100%). **IR Data** (CH_2Cl_2 cast, cm^{-1}): $\nu(P=N)$ 1377 (s), $\nu(P-N)$ 862 (s), 828 (s), $\nu(CN)$ 2237 (s). **NMR Data** ($CDCl_3$) $^{31}P\{^1H\}$: $P(\sigma^2)$: δ 257.29 (d, $^2J_{PP}$ 65 Hz), $P(\sigma^3)$: δ 64.81 (d, $^2J_{PP}$ 65 Hz). 1H : C- $\underline{C}H_3$ δ 2.42 (s), $P(\sigma^2)$ -N- $\underline{C}H_3$ δ 3.97 (d, $^3J_{\sigma^2PH}$ 7.9 Hz). $^{13}C\{^1H\}$: C- $\underline{C}H_3$ δ 15.95 (s), $P(\sigma^2)$ -N- $\underline{C}H_3$ δ 41.24 (d, $^2J_{\sigma^2PC}$ 18 Hz), P- \underline{C} -P δ 134.03 (dd, $^2J_{\sigma^2PC}$ 147 Hz, $^2J_{\sigma^3PC}$ 52 Hz), $P(\sigma^3)$ -N- $\underline{C}H_3$ δ 40.78 (d, $^2J_{\sigma^3PC}$ 5 Hz). ^{19}F (second order): *m*-F tbn δ 139.77, *o*-F tbn δ -152.81.

Synthesis of 4-(Bis(2,2,2-trifluoroethoxy)selenophosphorano)-2,5-dimethyl-2*H*-1,2,3 σ^2 -diazaphosphole, (**25**).

Selenium (0.205 g, 2.6 mmol) was added to a solution of **11** (0.135 g, 2.5 mmol) in 10 mL of toluene which was then heated to reflux for 12 hours. The solution was cooled then filtered through Celite and washed with (2 x 5 mL) toluene. The solvent was removed *in vacuo*, leaving an off-white, moisture sensitive crystalline material. The product was recrystallized from toluene. The yield of **25** was 1.03 g (98.2%). **Formula Weight:** 421.08 g/mol. **Anal.** for $C_8H_{10}F_6N_2O_2P_2Se$: C, 22.82; H, 2.39; N, 6.65%. Found: C, 22.51; H, 2.45; N, 6.62%. **M.P.** = 132-134°C. **MS (EI, m/z):** 422 (M, 100%). **IR Data** (CH_2Cl_2 cast, cm^{-1}): $\nu(P=Se)$ 542 (m). **NMR Data** ($CDCl_3$) $^{31}P\{^1H\}$: $P(\sigma^2)$: δ 259.01 (d, $^2J_{PP}$ 108 Hz), $P(\sigma^3)$: δ 87.81 (d Se sat. 8%, $^2J_{PP}$ 108 Hz, $^1J_{PSe}$ 893 Hz). 1H : C- $\underline{C}H_3$ δ 2.48 (s), $P(\sigma^2)$ -N- $\underline{C}H_3$ δ 3.96 (d, $^3J_{PH}$ 8.4 Hz), $P(\sigma^3)$ -N-O- $\underline{C}H_2CF_3$ δ 2.39 (m). $^{13}C\{^1H\}$: C- $\underline{C}H_3$ δ 14.77 (s), $P(\sigma^2)$ -N- $\underline{C}H_3$ δ 41.38 (d, $^2J_{PC}$ 18 Hz), P- \underline{C} -P δ 142.17 (dd, $^2J_{\sigma^2PC}$ 144 Hz, $^2J_{\sigma^3PC}$ 43 Hz), $P(\sigma^3)$ -O- $\underline{C}H_2$ - $\underline{C}F_3$ δ 65.68 (dq, $^2J_{\sigma^3PC}$ 6 Hz, $^2J_{FC}$ 36 Hz), $P(\sigma^3)$ -O- $\underline{C}H_2$ - $\underline{C}F_3$ δ

123.89 (dq, $^3J_{\sigma^3PC}$ 6 Hz, $^1J_{FC}$ 278 Hz). ^{19}F : δ -75.20 (t, $^3J_{FH}$ 8 Hz). ^{77}Se : δ -249.61 (dd, $^3J_{\sigma^2PF}$ 30 Hz, $^1J_{\sigma^3PF}$ 893 Hz).

Synthesis of 4-(Bis(2,2,2-trifluoroethoxy)(*p*-cyanotetrafluorophenylimino)phosphorano)-2,5-dimethyl-2*H*-1,2,3 σ^2 -diazaphosphole, (26).

The *p*-cyanotetrafluorophenyl azide (0.4 mL, 2.5 mmol) was added dropwise with a syringe into a stirred solution containing **11** (0.141 mL, 2.5 mmol), dissolved in 15 mL of dichloromethane. The solution was maintained at $-78^\circ C$ (acetone/Dry Ice). The solution became yellow a few minutes after the addition. It was left to warm to room temperature ($22^\circ C$) and stirred overnight, by this time the solution was colourless. The solvent was removed in vacuo, leaving an off-white crystalline material. The phosphole was recrystallized from toluene. The yield of **26** was 1.09 g (82.3%). **Formula Weight**: 530.20 g/mol. **Anal.** for $C_{15}H_{10}F_{10}N_4O_2P_2$: C, 33.98; H, 1.90; N, 10.57%. Found: C, 33.62; H, 1.79; N, 10.55%. **M.P.** = $122^\circ C$. **MS (EL *m/z*)**: 530 (M, 31%). **IR Data** (CH_2Cl_2 cast, cm^{-1}): $\nu(P=N)$ 1489 (s), $\nu(CN)$ 2235 (m). **NMR Data** ($CDCl_3$) $^{31}P\{^1H\}$: $P(\sigma^2)$: δ 260.12 (d, $^2J_{PP}$ 84 Hz), $P(\sigma^3)$: δ 11.95 (d, $^2J_{PP}$ 84 Hz). 1H : C- CH_3 δ 2.48 (s), $P(\sigma^2)$ -N- CH_3 δ 4.01 (d, $^3J_{\sigma^2PH}$ 8.6 Hz). $^{13}C\{^1H\}$: C- CH_3 δ 14.98 (s), $P(\sigma^2)$ -N- CH_3 δ 41.45 (d, $^2J_{\sigma^2PC}$ 18 Hz), P-C-P δ 128.79 (dd, $^2J_{\sigma^2PC}$ 139 Hz, $^2J_{\sigma^3PC}$ 53 Hz), $P(\sigma^3)$ -O- CH_2 - CF_3 δ 66.08 (dq, $^2J_{\sigma^3PC}$ 5 Hz, $^2J_{FC}$ 36 Hz), $P(\sigma^3)$ -O- CH_2 - CF_3 δ 124.21 (q, $^1J_{FC}$ 278 Hz). ^{19}F : δ -75.43 (t, $^3J_{FH}$ 8 Hz), *m*-F tbn δ 139.77, *o*-F tbn δ -152.81.

5.3 Metal Complexation

Synthesis of Cr(CO)₅(2), (27).

A Schlenk flask containing a solution of Cr(CO)₆ (0.475 g, 2.2 mmol) in 100 mL of THF in an ice bath was photolyzed (450-Watt mercury lamp) for 1.5 hours (monitored by IR). The phosphole (2) (0.30 mL, 2.2 mmol) was then added by syringe and the solution was stirred overnight at room temperature (22°C). The solution gradually changed colour from orange to greenish-yellow. The solvent was removed *in vacuo*, to leave a greenish-yellow solid. The solid was dissolved in 10 mL of diethyl ether and filtered through Celite. The resultant bright yellow solution was concentrated to ~1 mL and stored at -40°C for 24 hours, to give yellow crystals. The yield of 25 was 0.58 g (70 %). M.P. = 52-55°C. Formula Weight: 374.10 g/mol. Anal. for C₉H₆CrF₂N₂O₂P₂: C, 28.90; H, 1.62; N, 7.49%. Found: C, 28.99; H, 1.87; N, 7.75%. IR Data: (CH₂Cl₂ cast, cm⁻¹): ν(CO): 2079 (m), 1938 (vs). MS (FAB, m/z): 374 (M, 100%). NMR Data (CDCl₃) ³¹P{¹H}: P(σ²): δ 257.18 (dt (broad), ²J_{PP} 120 Hz, ³J_{PF} 1122 Hz), P(σ³): δ 249.76 (dt, ²J_{PP} 120 Hz, ¹J_{PF} 1122 Hz). ¹H: C-CH₃ δ 2.57 (s), P(σ²)-N-CH₃ δ 4.05 (d, ³J_{σ²PH} 8.3 Hz). ¹³C{¹H}: C-CH₃ δ 15.48 (s), P(σ²)-N-CH₃ δ 41.76 (d, ²J_{σ²PC} 18.6 Hz), P-C-P δ 150.56 (dd, ¹J_{σ²PC} 12 Hz, ¹J_{σ³PC} 6 Hz), N-C-CH₃ δ 155.29 (s), CO δ 204.50 (s), CO δ 208.41 (d, ²J_{PC} 40 Hz). ¹⁹F: δ -39.78 (dd, ¹J_{PF} 1137 Hz, ³J_{PF} 17 Hz).

Attempted Synthesis of Mo(CO)₅(2).

A Schlenk flask containing a solution of Mo(CO)₆ (0.190 g, 0.72 mmol) in 100 mL of THF in an ice bath was photolyzed (450-Watt mercury lamp) for 2 hours (monitored by IR). The phosphole (2) (0.10 mL, 0.72 mmol) was added by syringe and the solution was stirred overnight at room temperature (22°C). The solution gradually changed colour from yellow to pale brown. The solvent was removed *in*

vacuo, to leave a light brown solid. The $^{31}\text{P}\{^1\text{H}\}$ NMR spectrum did not show the formation of the desired complex.

Synthesis of *cis*- $\text{Mo}(\text{CO})_4(\mathbf{2})_2$, (**28**).

A solution of the phosphole, (**2**) (0.50 mL, 3.60 mmol) in 10 mL of dichloromethane was added dropwise at room temperature to a solution of $\text{Mo}(\text{nbd})(\text{CO})_4$ (0.540 g, 1.80 mmol) in 15 mL of dichloromethane and stirred for 12 hours at room temperature (22°C). The solution was concentrated to ~5 mL and hexane was added until the solution became slightly turbid. The solution was stored at -40°C overnight to give an off-white powder. The yield of **28** was 0.686 g (66.7%). M.P. = 78-80°C (dec.). Formula Weight: 572.08 g/mol. Anal. for $\text{C}_{12}\text{H}_{12}\text{F}_4\text{MoN}_4\text{O}_4\text{P}_4$: C, 25.19; H, 2.11; N, 9.79 %. Found: C, 25.00; H, 1.97; N, 9.72%. MS (FAB, m/z): 572 (M, 25%). IR Data (CH_2Cl_2 solution, cm^{-1}): $\nu(\text{CO})$: 2056 (m), 1974 (m), 1952 (vs). NMR Data (CDCl_3) $^{31}\text{P}\{^1\text{H}\}$: $\text{P}(\sigma^2)$: δ 259.74 (second order), $\text{P}(\sigma^3)$: δ 216.59 ((second order), $^1J_{\text{PF}}$ 1091 Hz). ^1H : C- $\underline{\text{C}}\text{H}_3$ δ 2.57 (s), $\text{P}(\sigma^2)\text{-N-}\underline{\text{C}}\text{H}_3$ δ 4.05 (d, $^3J_{\sigma^2\text{PH}}$ 8.3 Hz). $^{13}\text{C}\{^1\text{H}\}$: C- $\underline{\text{C}}\text{H}_3$ δ 15.51 (s), $\text{P}(\sigma^2)\text{-N-}\underline{\text{C}}\text{H}_3$ δ 41.75 (d, $^2J_{\sigma^2\text{PC}}$ 17 Hz), $\text{P-}\underline{\text{C}}\text{-P}$ δ 151.34 (dd, $^1J_{\sigma^2\text{PC}}$ 12 Hz, $^1J_{\sigma^3\text{PC}}$ 6 Hz), $\text{N-}\underline{\text{C}}\text{-CH}_3$ δ 154.32 (s), CO δ 208.32 (s), CO δ 212.35 (d, $^2J_{\text{PC}}$ 35 Hz). ^{19}F : δ -41.52 (dd, $^1J_{\text{PF}}$ 1091 Hz, $^3J_{\text{PF}}$ 4 Hz).

Synthesis of *fac*- $\text{Mo}(\text{CO})_3(\mathbf{2})_3$, (**29**).

A solution of $\text{Mo}(\text{CO})_6$ (0.50 mL, 3.60 mmol) in 25 mL of acetonitrile was refluxed for a period of 24 hours, during this time the solution turned yellow. A solution of the phosphole, (**2**), (1.7 mL, 12.2 mmol) in 5 mL of acetonitrile was added dropwise at room temperature (22°C) to the $\text{Mo}(\text{MeCN})_3(\text{CO})_3$ solution which was then stirred for 12 hours at room temperature. The solution was concentrated to ~2 mL and the solution was stored at -25°C for two days to give pale yellow needles. The

yield of **29** was 1.11 g (45.2%). **M.P.** = 123°C (dec.). **Formula Weight:** 726.12 g/mol. **Anal.** for $C_{15}H_{18}F_6MoN_6O_3P_6$: C, 24.81; H, 2.50; N, 11.57%. Found: C, 24.75; H, 2.55; N, 11.62%. **MS (FAB, m/z):** 726 (M, 15%). **IR Data:** (CH_2Cl_2 solution, cm^{-1}): $\nu(CO)$: 2011 (s), 1945 (s). **NMR Data** ($CDCl_3$) $^{31}P\{^1H\}$: $P(\sigma^2)$: δ 255.10 (second order), $P(\sigma^3)$: δ 224.60 (second order). 1H : C- CH_3 δ 2.57 (s), $P(\sigma^2)$ -N- CH_3 δ 4.05 (d, $^3J_{\sigma^2PH}$ 8.3 Hz). $^{13}C\{^1H\}$: C- CH_3 δ 15.48 (s), $P(\sigma^2)$ -N- CH_3 δ 41.67 (d, $^2J_{\sigma^2PC}$ 19 Hz), P- C -P δ 150.92 (dd, $^1J_{\sigma^2PC}$ 11 Hz, $^1J_{\sigma^3PC}$ 6 Hz), N- C - CH_3 δ 153.68 (s), CO δ 201.36 (s), CO δ 209.65 (d, $^2J_{P\sigma^3C}$ 37 Hz). ^{19}F (second order): δ -42.92 .

Attempted Synthesis of $W(CO)_5(2)$.

A Schlenk flask containing a solution of $W(CO)_6$ (0.190 g, 0.72 mmol) in 100 mL of THF in an ice bath was photolyzed (450-Watt Hg mercury lamp) for 2 hours (monitored by IR). The phosphole (**2**) (0.10 mL, 0.72 mmol) was added by syringe and the solution was stirred overnight at room temperature (22°C). The solution gradually changed colour from yellow to pale brown. The solvent was removed *in vacuo*, to leave a light brown solid. The solid was dissolved in 10 mL of diethyl ether and filtered through Celite and washed with an additional 10 mL of ether. The solution was concentrated to ~1 mL and stored at -40°C for 24 hours to give bright yellow crystals.

Synthesis of $CpRu(PPh_3)_2Cl$, (**30**).

To a solution of $CpRu(PPh_3)_2Cl$ (0.523 g, 0.72 mmol) in 25 mL of benzene, the phosphole, **2** (0.1 mL, 0.72 mmol) was added *via* syringe. The solution was heated to reflux for 24 hours. The solution was cooled and the solvent was removed *in vacuo* to leave an orange oily material. The oil was washed with hot hexanes. Recrystallization from diethyl ether/dichloromethane yielded orange crystals. The yield

of **30** was 0.357 g (76.7%). M.P. = 112°C. Formula Weight: 645.96 g/mol. Anal. for $C_{27}H_{26}ClF_2N_2P_3Ru$: C, 50.20; H, 4.06; Cl 5.46; N, 4.34%. Found: C, 50.15; H, 4.02; Cl 5.60; N, 4.37%. MS (FAB, m/z): 646 (M, 17.8%), 611 (M-Cl, 31.5%), 429 (M-Cl-2, 100%). IR Data: (CH_2Cl_2 cast, cm^{-1}): $\nu(P-F)$: 843 (s), 792 (s). NMR Data ($CDCl_3$) $^31P\{^1H\}$: $P(\sigma^2)$: δ 258.90 (ddd, $^2J_{PP}$ 116 Hz, $^3J_{PF}$ 19 Hz, $^3J_{PF}$ 15 Hz), $P(\sigma^3)$: δ 216.59 (dddd, $^2J_{PP}$ 116 Hz, $^1J_{PF}$ 1131 Hz, $^1J_{PF}$ 1057 Hz, $^2J_{PPh_3}$ 74 Hz), PPh_3 : δ 48.16 (dd, $^2J_{PPh_3}$ 74 Hz, $^3J_{PF}$ 7 Hz). 1H : C- CH_3 δ 2.52 (s), $P(\sigma^2)$ -N- CH_3 δ 3.97 (d, $^3J_{\sigma^2PH}$ 8.0 Hz), Cp δ 4.70 (s), phenyl H δ 7.3-7.6 (m). $^{13}C\{^1H\}$: C- CH_3 δ 15.49 (s), $P(\sigma^2)$ -N- CH_3 δ 44.88 (d, $^2J_{\sigma^2PC}$ 17 Hz), P- C -P δ 138.32 (d, $^1J_{\sigma^2PC}$ 345 Hz), N- C - CH_3 δ 154.36 (s). ^{19}F : F_1 : δ -27.55 (ddd, $^2J_{FF}$ 30 Hz, $^1J_{\sigma^3PF}$ 1057 Hz, $^3J_{\sigma^2PF}$ 19 Hz), F_2 : δ -42.92 (dddd, $^2J_{FF}$ 30 Hz, $^1J_{\sigma^3PF}$ 1131 Hz, $^3J_{\sigma^2PF}$ 15 Hz, $^3J_{FPPh_3}$ 7 Hz).

Synthesis of $CpRh(2)_2$, (**31**).

To a solution of $[Rh(CO)_2Cl]_2$ (0.11g, 0.29 mmol) in 10 mL of hexanes, $TlCp$ (0.19 g, 0.73 mmol) was added. The solution was heated to reflux overnight then filtered through Celite. The Celite was washed with 2.5 mL of hexanes and the phosphole, (**2**), (0.1 mL, 0.72 mmol) was added by syringe to the solution of $CpRh(CO)_2$ and the mixture was stirred at room temperature (22°C) for 4 hours. The solution was then reduced to half its volume and stored at -40°C for 24 hours, giving orange crystals which were suitable for x-ray diffraction. A second crop was obtained by reducing the volume of hexanes and storing the concentrated solution at -40°C. The yield of **31** was 0.262 g (68.3%). M.P. = 93-94°C. Formula Weight: 532.10 g/mol. Anal. for $C_{13}H_{17}F_4N_4P_4Rh$: C, 29.34; H, 3.22; N, 10.53 %. Found: C, 29.36; H, 2.86; N, 10.13 %. MS (FAB, m/z): 532 (M, 100%), 350 (M-2, 85%), 168 (CpRh, 66%). IR Data: (CH_2Cl_2 cast, cm^{-1}): $\nu(P-F)$: 835 (s), 786 (s). NMR Data ($CDCl_3$) $^31P\{^1H\}$ (second order): $P(\sigma^2)$: δ 259.9 (d(broad), $^2J_{PP}$ -116 Hz), $P(\sigma^3)$: δ 188.5

(second order, $^2J_{PP} \sim 116$ Hz, $^1J_{PF}$ 1114 Hz, $^1J_{PRh}$ 356 Hz). 1H : C-CH₃ δ 2.48 (s), P(σ^2)-N-CH₃ δ 3.97 (d, $^3J_{\sigma^2PH}$ 8 Hz), Cp δ 5.32 (s). $^{13}C\{^1H\}$: C-CH₃ δ 15.49 (s), P(σ^2)-N-CH₃ δ 44.88 (d, $^2J_{\sigma^2PC}$ 17 Hz), P-C-P δ 138.35 (d, $^1J_{\sigma^2PC}$ 35 Hz), N-C-CH₃ δ 154.48 (s). ^{19}F (second order): δ -36.13 ($^2J_{FRh}$ 19 Hz, $^1J_{PF}$ 1114 Hz). ^{103}Rh : δ -1278 ppm.

Attempted synthesis of [Rh(2)₂Cl]₂.

A solution of the phosphole, (2), (0.1 mL, 0.72 mmol) in 10 mL of dichloromethane was added dropwise at room temperature (22°C) to a solution of [Rh(CO)₂Cl]₂ (0.140 g, 0.36 mmol) in 15 mL of dichloromethane and stirred for 4 hours during which a red precipitate formed. The $^{31}P\{^1H\}$ NMR spectrum did not indicate that the desired product had formed.

Synthesis of Cp*RhCl₂(2), (32).

A solution of the phosphole, (2), (0.1 mL, 0.72 mmol) in 10 mL of dichloromethane was added dropwise at room temperature to a solution of [Cp*RhCl₂]₂ (0.167 g, 0.36 mmol) in 15 mL of dichloromethane and stirred for 4 hours. The solution was reduced to ~3 mL and 10 mL of hexanes was added. The solution was stored overnight at room temperature (22°C). During this time reddish-orange crystals formed. The yield of 32 was 0.277 g (78.3%). M.P. = 135-140°C (dec.). Formula Weight: 491.09 g/mol. Anal. for C₁₄H₂₁Cl₂F₂N₂P₂Rh: C, 34.24; H, 4.31; Cl, 14.44, N, 5.70%. Found: C, 33.99; H, 4.20; Cl, 15.20, N, 5.82%. MS (EAB, m/z): 491 (M+1, 5%). IR Data: (CH₂Cl₂ cast, cm⁻¹): ν (P-F): 756 (s), 786 (s). NMR Data (CDCl₃) $^{31}P\{^1H\}$: P(σ^2): δ 259.9 (d, $^2J_{PP}$ 102 Hz), P(σ^3): δ 188.5 (ddt, $^2J_{PP}$ 102 Hz, $^1J_{\sigma^3PF}$ 1170 Hz, $^1J_{\sigma^3PRh}$ 216 Hz). 1H : C-CH₃ δ 2.48 (s), P(σ^2)-N-CH₃ δ 3.97 (d, $^3J_{\sigma^2PH}$ 8 Hz), C₅-(CH₃)₅ δ 1.95 (s). $^{13}C\{^1H\}$: C-CH₃ δ 15.49 (s), P(σ^2)-N-CH₃ δ 44.88 (d, $^2J_{\sigma^2PC}$ 17 Hz), P-C-P δ 148.35 (d, $^1J_{\sigma^2PC}$ 35 Hz), N-C-

CH₃ δ 156.70 (s), C₅-(CH₃)₅ δ 102.42 (d, ¹J_{CRh} 4 Hz) C₅-(CH₃)₅ δ 9.72 (s). ¹⁹F: δ -36.13 (²J_{FRh} 19 Hz, ¹J_{σ³PF} 1173 Hz)

Synthesis of *trans*-Pt(2)₂Cl₂, (33).

A solution of the phosphole, (2), (0.10 mL, 0.72 mmol) in 10 mL of dichloromethane was added dropwise at room temperature (22°C) to a solution of Pt(cod)Cl₂ (1.35 g, 0.36 mmol) in 15 mL of dichloromethane and stirred for 4 hours. The solution was concentrated to ~5 mL and hexane was added until the solution became slightly turbid. The solution was stored at -40°C overnight to give an off-white powder. The yield of 33 was 0.196 g (86.3%). M.P. = 129°C (dec.). Formula Weight: 630.09 g/mol. Anal. for C₈H₁₂Cl₂F₄N₄P₄Pt: C, 15.25; H, 1.92; Cl 11.25; N, 8.89%. Found: C, 15.11; H, 1.96; Cl 11.50; N, 8.81%. MS (FAB, m/z): 630 (M, 7%). IR Data: (CH₂Cl₂ cast, cm⁻¹): ν(P-F): 852 (s), 793 (s). NMR Data (CDCl₃) ³¹P{¹H}: P(σ²): δ 271.21 (d, ²J_{PP} 150 Hz), P(σ³): δ 159.29 (dt, Pt sat., ²J_{PP} 150 Hz, ¹J_{σ³PF} 1125 Hz, ¹J_{PPt} 5064 Hz). ¹H: C-CH₃ δ 2.48 (s), P(σ²)-N-CH₃ δ 3.96 (d, ³J_{σ²PH} 8 Hz). ¹³C{¹H}: C-CH₃ δ 15.49 (s), P(σ²)-N-CH₃ δ 44.92 (d, ²J_{σ²PC} 17 Hz), P-C-P δ 148.63 (d, ¹J_{σ²PC} 34.7 Hz), N-C-CH₃ δ 155.01 (s). ¹⁹F: δ -36.13 (²J_{FPt} 190 Hz, ¹J_{σ³PF} 1130 Hz).

Synthesis of *cis*-Pd(2)₂Cl₂, (34) and Pd(2)₄, (35).

A solution of the phosphole, (2), (0.25 mL, 1.8 mmol) in 10 mL of dichloromethane was added dropwise at room temperature (22°C) to a solution of Pd(cod)Cl₂ (0.257 g, 0.90 mmol) in 15 mL of dichloromethane and stirred for 4 hours. NMR Data (CDCl₃) ³¹P{¹H}: Pd(0): P(σ²): δ 258.90 (d, ²J_{PP} 116 Hz), P(σ³): δ 144.33 (dt (broad), ²J_{PP} 116 Hz, ¹J_{σ³PF} 1131 Hz); Pd(II): P(σ²): δ 267.88 (d, ²J_{PP} 158 Hz), P(σ³): δ 144.33 (dt (broad), ²J_{PP} 158 Hz, ¹J_{σ³PF} 1184 Hz).

Synthesis of Pd(2)₄, (35).

To a solution of Pd₂(dba)₃ (0.137 g, 0.15 mmol) in 15 mL of dichloromethane, a solution of the phosphole, (2), (0.1 mL, 0.72 mmol) in 10 mL of dichloromethane was added dropwise at room temperature (22°C) and stirred for 4 hours. The solution was concentrated to ~5 mL and hexane was added until the solution became slightly turbid. The solution was stored at -40°C overnight to give a maroon powder. The yield of 36 was 0.116 g (92.7%). M.P. = 115°C (dec.). Formula Weight: 834.60 g/mol. Anal. for C₁₆H₂₄F₈N₈P₈Pd: C, 23.03; H, 2.90; N, 13.43%. Found: C, 23.23; H, 2.95; N, 13.42%. MS (FAB, m/z): 838 (M, 4%). IR Data: (CH₂Cl₂ cast, cm⁻¹): ν(P-F): 833 (s), 778 (s). NMR Data (CDCl₃) ³¹P{¹H}: P(σ²): δ 257.88 (d, ²J_{PP} 118 Hz), P(σ³): δ 144.33 (dt (broad), ²J_{PP} 116 Hz, ¹J_{σ³PF} 1129 Hz). ¹H: C-CH₃ δ 2.48 (s), P(σ²)-N-CH₃ δ 3.97 (d, ³J_{σ²PH} 8.0 Hz). ¹³C{¹H}: C-CH₃ δ 15.46 (s), P(σ²)-N-CH₃ δ 44.88 (d, ²J_{σ²PC} 18.6 Hz), P-C-P δ 146.96 (d, ¹J_{σ²PC} 37 Hz), N-C-CH₃ δ 155.84 (s). ¹⁹F: δ -36.42 (²J_{σ²PF} 15 Hz, ¹J_{σ³PF} 1130 Hz).

Synthesis of Pt(2)₄, (36).

To a solution of Pt(cod)ClMe (0.127 g, 0.36 mmol) in 15 mL of dichloromethane, a solution of the phosphole, (2), (0.1 mL, 0.72 mmol) in 10 mL of dichloromethane was added dropwise at room temperature (22°C) and stirred for 4 hours. The solution was concentrated to ~5 mL and hexane was added until the solution became slightly turbid. The solution was stored at -40°C overnight to yield orange crystals. The yield of 36 was 0.208 g (62.7%). M.P. = 136°C. Formula Weight: 923.29 g/mol. Anal. for C₁₆H₂₄F₈N₈P₈Pt: C, 20.81; H, 2.62; N, 12.14%. Found: C, 20.65; H, 2.68; N, 12.26%. MS (FAB, m/z): 924 (M+1, 25%). IR Data: (CH₂Cl₂ cast, cm⁻¹): ν(P-F): 832 (s), 771 (s). NMR Data (CDCl₃) ³¹P{¹H}: P(σ²): δ 267.88 (d, ²J_{PP} 158 Hz), P(σ³): δ 144.33 (dt (broad), ²J_{PP} 158 Hz, ¹J_{PF} 1184 Hz). ¹H: C-CH₃ δ 2.47 (s), P(σ²)-N-CH₃ δ 3.99 (d, ³J_{σ²PH} 8.0 Hz). ¹³C{¹H}: C-CH₃ δ

15.49 (s), P(σ^2)-N- $\underline{\text{C}}\text{H}_3$ δ 44.88 (d, $^2J_{\sigma^2\text{PC}}$ 16 Hz), P- $\underline{\text{C}}\text{-P}$ δ 148.35 (d, $^1J_{\sigma^2\text{PC}}$ 30 Hz), N- $\underline{\text{C}}\text{-CH}_3$ δ 154.23 (s). ^{19}F : δ -36.13 (d, Pt sat., $^2J_{\text{FPt}}$ 190 Hz, $^1J_{\text{PF}}$ 1156 Hz).

Synthesis of *trans*-Pt(PEt₃)Cl(2)₄, (37)

A solution of the phosphole, (2), (0.05 mL, 0.72 mmol) in 10 mL of dichloromethane was added dropwise at room temperature (22°C) to a solution of [Pt(PEt₃)Cl₂]₂ (0.138 g, 0.18 mmol) in 15 mL of dichloromethane and stirred for 4 hours. The solution was concentrated to ~5 mL and hexane was added until the solution became slightly turbid. The solution was stored at -40°C overnight to give an off-white powder. The yield of 37 was 0.089 g (86.3%). M.P. = 122°C (dec.). Formula Weight: 566.20 g/mol. Anal. for C₁₀H₂₁Cl₂F₂N₂P₃Pt: C, 21.21; H, 3.74; Cl 12.52; N, 4.95%. Found: C, 21.35; H, 3.72; Cl 12.62; N, 4.91%. MS (FAB, m/z): 566 (M, 7%). IR Data: (CH₂Cl₂ cast, cm⁻¹): $\nu(\text{P-F})$: 842 (s), 790 (s). NMR Data (CDCl₃) $^{31}\text{P}\{^1\text{H}\}$: P(σ^2): δ 265.81 (d, $^2J_{\text{PP}}$ 155 Hz), P(σ^3): δ 124.32 (ddt, Pt sat., $^2J_{\text{PP}}$ 155 Hz, $^1J_{\sigma^3\text{PF}}$ 1112 Hz, $^2J_{\sigma^3\text{PPEt}_3}$ 18 Hz, $^1J_{\sigma^3\text{PPt}}$ 5445 Hz), PEt₃: δ 18.40 (d, Pt sat., $^2J_{\text{PP}}$ 18 Hz, $^1J_{\text{PPt}}$ 3190 Hz). ^1H : C- $\underline{\text{C}}\text{H}_3$ δ 2.48 (s), P(σ^2)-N- $\underline{\text{C}}\text{H}_3$ δ 3.97 (d, $^3J_{\text{PH}}$ 8.0 Hz). $^{13}\text{C}\{^1\text{H}\}$: C- $\underline{\text{C}}\text{H}_3$ δ 15.49 (s), P(σ^2)-N- $\underline{\text{C}}\text{H}_3$ δ 44.88 (d, $^2J_{\sigma^2\text{PC}}$ 15 Hz), P- $\underline{\text{C}}\text{-P}$ δ 148.35 (d, $^1J_{\sigma^2\text{PC}}$ 31 Hz), N- $\underline{\text{C}}\text{-CH}_3$ δ 154.48 (d, $^2J_{\sigma^2\text{PC}}$ 3 Hz, $^2J_{\sigma^3\text{PC}}$ 18 Hz). ^{19}F : δ -38.21 (dd, $^3J_{\sigma^2\text{PF}}$ 15 Hz, $^1J_{\sigma^3\text{PF}}$ 1115 Hz).

Synthesis of *trans*-Pd(PEt₃)Cl(2)₄, (38)

A solution of the phosphole, (2), (0.05 mL, 0.36 mmol) in 10 mL of dichloromethane was added dropwise at room temperature (22°C) to a solution of [Pd(PEt₃)Cl₂]₂ (0.216 g, 0.36 mmol) in 15 mL of dichloromethane and stirred for 4 hours. The solution was concentrated to ~5 mL and hexane was added until the solution became slightly turbid. The solution was stored at -40°C overnight to give a yellowish powder. The yield of 38 was 0.269 g (78.3%). M.P. = 111°C (dec.).

Formula Weight: 477.51 g/mol. **Anal.** for $C_{10}H_{21}Cl_2F_2N_2P_3Pd$: C, 25.15; H, 4.43; Cl 14.85; N, 5.87%. **Found:** C, 25.11; H, 4.56; Cl 14.99; N, 5.78 %. **MS (FAB, m/z):** 479 (M,+1 9%). **IR Data:** (CH_2Cl_2 cast, cm^{-1}): $\nu(P-F)$: 849 (s), 788 (s). **NMR Data** ($CDCl_3$) $^{31}P\{^1H\}$: $P(\sigma^2)$: δ 266.05 (d, $^2J_{PP}$ 150 Hz), $P(\sigma^3)$: δ 160.23 (dt, $^2J_{PP}$ 150 Hz, $^1J_{PF}$ 1125 Hz), PEt_3 : δ 18.40 (s). 1H : C- CH_3 δ 2.48 (s), $P(\sigma^2)$ -N- CH_3 δ 3.97 (d, $^3J_{PH}$ 8.0 Hz). $^{13}C\{^1H\}$: C- CH_3 δ 15.61 (s), $P(\sigma^2)$ -N- CH_3 δ 44.88 (d, $^2J_{\sigma^2PC}$ 18 Hz), P- C -P δ 148.35 (d, $^1J_{\sigma^2PC}$ 30 Hz), N- C - CH_3 δ 152.53 (d, $^2J_{\sigma^2PC}$ 4 Hz, $^2J_{\sigma^3PC}$ 12 Hz). ^{19}F : δ -38.21 (dd, $^3J_{\sigma^2PF}$ 15 Hz, $^1J_{\sigma^3PF}$ 1115 Hz).

Synthesis of *trans*-RhCl(CO)(3)₂, (39).

A solution of the phosphole 3 (0.25 mL, 1.2 mmol) in 10 mL of dichloromethane was added dropwise at room temperature (22°C) to a solution of $[Rh(CO)_2Cl]_2$ (0.117 g, 0.30 mmol) in 15 mL of dichloromethane and stirred for 4 hours. The solution was concentrated to ~5 mL and hexane was added until the solution became slightly turbid. The solution was stored at -40°C overnight to yield pale red crystals. The yield of 39 was 0.149 g (78.7%). **M.P.** = 178°C (dec.). **Formula Weight:** 630.78 g/mol. **Anal.** for $C_{17}H_{36}ClN_8OP_4Rh$: C, 29.95; H, 5.65; Cl 11.05; N, 17.46%. **Found:** C, 30.40; H, 5.89; Cl 11.35; N, 17.72%. **MS (FAB, m/z):** 631 (M+1, 5%), 602 (M-CO, 22%). **IR Data:** (CH_2Cl_2 solution, cm^{-1}): $\nu(CO)$: 1978 (s). **NMR Data** ($CDCl_3$) $^{31}P\{^1H\}$: $P(\sigma^2)$: δ 246.92(t, $|^2J_{\sigma^2P\sigma^4P} + ^4J_{\sigma^2P\sigma^4P}|$ 51 Hz), $P(\sigma^3)$: δ 103.34 (t, $|^2J_{\sigma^2P\sigma^4P} + ^4J_{\sigma^2P\sigma^4P}|$ 51 Hz). 1H : C- CH_3 δ 2.43 (dd, $^4J_{PH}$ 0.9 Hz), $P(\sigma^2)$ -N- CH_3 δ 4.03 (d, $^3J_{\sigma^2PH}$ 12.2 Hz), $P(\sigma^3)$ -N- CH_3 δ 2.72 (d, $^3J_{\sigma^3PH}$ 7.6 Hz). $^{13}C\{^1H\}$: C- CH_3 δ 14.37 (s), $P(\sigma^2)$ -N- CH_3 δ 41.88 (d, $^2J_{\sigma^2PC}$ 18 Hz), P- C -P δ 143.45 (dd, $^2J_{\sigma^2PC}$ 145 Hz, $^2J_{\sigma^3PC}$ 45 Hz), N- C - CH_3 δ 156.72 (dd, $^2J_{\sigma^2PC}$ 5 Hz, $^2J_{\sigma^3PC}$ 18 Hz).

Synthesis of *trans*-Pd(3)₂Cl₂, (40).

A solution of the phosphole 3 (0.25 mL, 1.2 mmol) in 10 mL of dichloromethane was added dropwise at room temperature (22°C) to a solution of Pt(cod)Cl₂ (0.171 g, 0.60 mmol) in 15 mL of dichloromethane and stirred for 4 hours. The solution was concentrated to ~5 mL and hexane was added until the solution became slightly turbid. The solution was stored at -40°C overnight to give a light yellow crystals. The yield of 40 was 0.130 g (67.6%). M.P. = 186°C (dec.). Formula Weight: 641.72 g/mol. Anal. for C₁₆H₃₆Cl₂N₈P₄Pd: C, 29.95; H, 5.65; Cl 11.05; N, 17.46%. Found: C, 29.92; H, 5.72; Cl 11.35; N, 17.49%. MS (FAB, m/z): 641 (M+1, 5%). NMR Data (CDCl₃) ³¹P{¹H}: P(σ²): δ 249.72 (t, |²J_{σ²Pσ⁴P} + ⁴J_{σ²Pσ⁴P}| 51 Hz), P(σ³): δ 86.94 (t, |²J_{σ²Pσ⁴P} + ⁴J_{σ²Pσ⁴P}| 51 Hz). ¹H: C-CH₃ δ 2.43 (dd, ⁴J_{P_H} 0.9 Hz), P(σ²)-N-CH₃ δ 4.03 (d, ³J_{σ²P_H} 12.2 Hz), P(σ³)-N-CH₃ δ 2.68 (d, ³J_{σ³P_H} 7.8 Hz). ¹³C{¹H}: C-CH₃ δ 14.37 (s), P(σ²)-N-CH₃ δ 41.88 (d, ²J_{σ²PC} 18 Hz), P-C-P δ 143.45 (dd, ²J_{σ²PC} 143 Hz, ²J_{σ³PC} 45 Hz), N-C-CH₃ δ 156.72 (s).

Synthesis of *trans*-Pt(3)₂Cl₂, (41).

A solution of the phosphole 3 (0.25 mL, 1.2 mmol) in 10 mL of dichloromethane was added dropwise at room temperature (22°C) to a solution of Pt(cod)Cl₂ (0.117 g, 0.60 mmol) in 15 mL of dichloromethane and stirred for 4 hours. The solution was concentrated to ~5 mL and hexane was added until the solution became slightly turbid. The solution was stored at -40°C overnight to give an off-white powder. The yield of 41 was 0.172 g (78.6%). M.P. = 191-193°C (dec.). Formula Weight: 730.41 g/mol. Anal. for C₁₆H₃₆Cl₂N₈P₄Pt: C, 26.31; H, 4.97; Cl 9.71; N, 15.34%. Found: C, 26.51; H, 5.09; Cl 9.75; N, 15.37%. MS (FAB, m/z): 730 (M+1, 11%). NMR Data (CDCl₃) ³¹P{¹H}: P(σ²): δ 249.69 (t, |²J_{σ²Pσ⁴P} + ⁴J_{σ²Pσ⁴P}| 57 Hz), P(σ³): δ 80.63 (dt, Pt sat. |²J_{σ²Pσ⁴P} + ⁴J_{σ²Pσ⁴P}| 57 Hz, ¹J_{σ³P_{Pt}} 2918 Hz). ¹H:

C-CH₃ δ 2.43 (dd, ⁴J_{PH} 0.9 Hz), P(σ²)-N-CH₃ δ 4.02 (d, ³J_{PH} 12.2 Hz), P(σ³)-N-CH₃ δ 2.76 (d, ³J_{σ³PH} 7.2 Hz). ¹³C{¹H}: C-CH₃ δ 14.73 (s), P(σ²)-N-CH₃ δ 41.92 (d, ²J_{PC} 18 Hz), P-C-P δ 148.45 (dd, ²J_{σ²PC} 138 Hz, ²J_{σ³PC} 32 Hz), N-C-CH₃ δ 156.27 (s). ¹⁹⁵Pt: δ 179.04 (t, ¹J_{σ³Pt} 2918 Hz).

Synthesis of *trans*-PtMeCl(3)₂, (42).

A solution of the phosphole 3 (0.25 mL, 1.2 mmol) in 10 mL of dichloromethane was added dropwise at room temperature (22°C) to a solution of Pt(cod)ClMe (0.117 g, 0.30 mmol) in 15 mL of dichloromethane and stirred for 4 hours. The solution was concentrated to ~5 mL and hexane was added until the solution became slightly turbid. The solution was stored at -40°C overnight to give a light yellow powder. The yield of 42 was 0.194 g (77.6%). M.P. = 156°C (dec.). Formula Weight: 709.99 g/mol. Anal. for C₁₇H₃₉ClN₈P₄Pt: C, 28.76; H, 5.54; Cl 4.99; N, 15.78%. Found: C, 28.60; H, 5.59; Cl 4.35; N, 15.86%. MS (FAB. m/z): 711 (M+1, 5%). NMR Data (CDCl₃) ³¹P{¹H}: P(σ²): δ 248.29 (t, |²J_{σ²Pσ⁴P} + ⁴J_{σ²Pσ⁴P}| 53 Hz), P(σ³): δ 75.21 (t Pt sat., |²J_{σ²Pσ⁴P} + ⁴J_{σ²Pσ⁴P}| 53 Hz, ¹J_{σ³Pt} 3351 Hz). ¹H: C-CH₃ δ 2.34 (dd, ⁴J_{PH} 0.9 Hz), P(σ²)-N-CH₃ δ 4.03 (d, ³J_{σ²PH} 12.2 Hz), P(σ³)-N-CH₃ δ 2.74 (d, ³J_{σ³PH} 7.6 Hz). ¹³C{¹H}: C-CH₃ δ 14.37 (s), P(σ²)-N-CH₃ δ 41.78 (d, ²J_{σ²PC} 18 Hz), P-C-P δ 144.53 (dd, ²J_{σ²PC} 154 Hz, ²J_{σ³PC} 54 Hz), N-C-CH₃ δ 156.72 (s). ¹⁹⁵Pt: δ 354.40 (ttq, ¹J_{σ³Pt} 3351 Hz, ³J_{σ²Pt} 50 Hz, ²J_{PtH} 82 Hz).

Synthesis of *trans*-Rh(CO)Cl(11)₂, (43).

A solution of the phosphole 11 (0.146 g, 0.42 mmol) in 10 mL of dichloromethane was added dropwise at room temperature (22°C) to a solution of [Rh(CO)₂Cl]₂ (0.021 g, 0.053 mmol) in 15 mL of dichloromethane and stirred for 4 hours. The solution was reduced to ~3 mL and 10 mL of hexanes was added. The

solution was stored overnight at room temperature during which time a light orange powder formed. The yield of **43** was 0.068 g (75.3%). M.P. = 189°C (dec.). Formula Weight: 850.60 g/mol. Anal. for $C_{17}H_{20}ClF_{12}N_4O_5P_4Rh$: C, 24.00; H, 2.37; Cl, 4.17, N, 6.59%. Found: C, 24.06; H, 2.30; Cl, 4.28, N, 6.55%. MS (FAB, m/z): 850 (M, 20%). NMR Data ($CDCl_3$) $^{31}P\{^1H\}$: $P(\sigma^2)$: δ 251.88 ("t", $|2J_{\sigma^2P\sigma^4P} + 4J_{\sigma^2P\sigma^4P}|$ 52 Hz), $P(\sigma^3)$: δ 159.78 (d"t", $|2J_{\sigma^2P\sigma^4P} + 4J_{\sigma^2P\sigma^4P}|$ 52 Hz, $^1J_{PRh}$ 187 Hz). 1H : C- CH_3 δ 2.48 (s), $P(\sigma^2)$ -N- CH_3 δ 3.97 (d, $^3J_{\sigma^2PH}$ 8.0 Hz), $P(\sigma^3)$ -N-O- CH_2 δ 4.4-4.2 (m (broad)). $^{13}C\{^1H\}$: C- CH_3 δ 15.49 (s), $P(\sigma^2)$ -N- CH_3 δ 44.93 (d, $^2J_{\sigma^2PC}$ 19 Hz), P- C -P δ 149.36 (d, $^1J_{\sigma^2PC}$ 30 Hz), N- C - CH_3 δ 155.03 (s). ^{19}F : δ -74.57 (s).

Synthesis of *trans*-PdCl₂(**11**)₂, (**44**).

A solution of the phosphole **11** (0.193 g, 0.57 mmol) in 10 mL of dichloromethane was added dropwise at room temperature (22°C) to a solution of Pd(cod)Cl₂ (0.081 g, 0.28 mmol) in 15 mL of dichloromethane and stirred for 4 hours. The solution was reduced to ~3 mL and 10 mL of hexanes was added. The solution was stored overnight at room temperature during which time a yellow powder formed. The yield of **44** was 1.889 g (78.3%). M.P. = 168°C (dec.). Formula Weight: 861.54 g/mol. Anal. for $C_{16}H_{20}Cl_2F_{12}N_4O_4P_4Pd$: C, 22.31; H, 2.34; Cl, 8.23, N, 6.50%. Found: C, 22.12; H, 2.30; Cl, 8.42, N, 6.62%. MS (FAB, m/z): 861 (M, 5%). NMR Data ($CDCl_3$) $^{31}P\{^1H\}$: $P(\sigma^2)$: δ 256.43 ("t", $|2J_{\sigma^2P\sigma^4P} + 4J_{\sigma^2P\sigma^4P}|$ 51 Hz), $P(\sigma^3)$: δ 131.22 ("t", $|2J_{\sigma^2P\sigma^4P} + 4J_{\sigma^2P\sigma^4P}|$ 51 Hz). 1H : C- CH_3 δ 2.33 (s), $P(\sigma^2)$ -N- CH_3 δ 4.05 (d, $^3J_{\sigma^2PH}$ 8.0 Hz) $P(\sigma^3)$ -N-O- CH_2 δ 4.6-4.3 (m (broad)). $^{13}C\{^1H\}$: C- CH_3 δ 15.49 (s), $P(\sigma^2)$ -N- CH_3 δ 44.36 (d, $^2J_{\sigma^2PC}$ 18 Hz), P- C -P δ 148.62 (d, $^1J_{\sigma^2PC}$ 35 Hz), N- C - CH_3 δ 154.48 (s). ^{19}F : δ -74.57 (s).

Synthesis of *cis*-PtCl₂(11)₂, (45).

A solution of the phosphole **3** (0.151 g, 0.44 mmol) in 10 mL of dichloromethane was added dropwise at room temperature (22°C) to a solution of Pt(cod)Cl₂ (0.083 g, 0.22 mmol) in 15 mL of dichloromethane and stirred for 4 hours. The solution was concentrated to ~5 mL and hexane was added until the solution became slightly turbid. The solution was stored at -40°C overnight to give an off-white powder. The yield of **45** was 0.162 g (77.6%). M.P. = 172°C (dec.). Formula Weight: 950.23 g/mol. Anal. for C₁₆H₂₀Cl₂F₁₂N₄O₄P₄Pt: C, 20.22; H, 2.12; Cl 7.46, N, 5.90%. Found: C, 20.35; H, 2.25; Cl 7.35; N, 6.01%. MS (FAB, m/z): 951 (M+1, 13%). NMR Data (CDCl₃) ³¹P{¹H}: P(σ²): δ 256.78(d, ²J_{PP} 58 Hz.), P(σ³): δ 104.35 (d Pt sat., ²J_{PP} 58 Hz, ¹J_{PPt} 4811). ¹H: C-CH₃ δ 2.35 (dd, ⁴J_{PH} 0.9 Hz), P(σ²)-N-CH₃ δ 4.09 (d, ³J_{σ²PH} 12.2 Hz), P(σ³)-N-O-CH₂ δ 4.6-4.4 (m (broad)). ¹³C{¹H}: C-CH₃ δ 14.53 (s), P(σ²)-N-CH₃ δ 41.36 (d, ²J_{σ²PC} 18 Hz), P-C-P δ 144.65 (dd, ²J_{σ²PC} 145 Hz, ²J_{σ³PC} 45 Hz), N-C-CH₃ δ 156.72 (dd, ²J_{σ²PC} 5 Hz, ²J_{σ³PC} 18 Hz). ¹⁹F: δ -74.57 (s).

Reaction of **21** with Mo(CO)₃(cht).

A solution of Mo(CO)₆ (0.50 g, 3.60 mmol) in 25 mL of acetonitrile was heated to reflux for a period of 24 hours, during this time the solution turned yellow. A solution of the phosphole, (**21**), (1.7 mL, 12.2 mmol) in 5 mL of acetonitrile was dropwise at room temperature (22°C) to the Mo(MeCN)₃(CO)₃ solution and stirred for 12 hours at room temperature. The solvent was removed *in vacuo*, to leave a light brown solid. The ³¹P{¹H} NMR spectrum did not shown the formation of the desired complex.

Synthesis of Cp*TiCl₂(N=(23))₂, (46).

Trimethylsilyl azide (0.65 mL, 5 mmol) was added to a solution of **2** (0.25 mL, 2.4 mmol) in 10 mL of acetonitrile and heated to reflux for 24 hours. The solution was cooled and the volatiles were removed *in vacuo*. Fresh acetonitrile (15 mL) was then added to this flask along with Cp*TiCl₃ (0.695 g, 4.8 mmol). The solution was refluxed for a period of 24 hours. As the solution cooled to room temperature, orange crystals appeared. The yield of **46** was 9.84 g (62.8%). M.P. = 145°C (dec.). Formula Weight: 500.25 g/mol. Anal. for C₁₈H₃₃Cl₂N₅P₂Ti: C, 43.22; H, 6.65; Cl 14.12; N, 14.00 %. Found: C, 43.32; H, 6.72; Cl 14.26; N, 14.08 %. MS (FAB, m/z): 500 (M+1, 5%). IR Data: (CH₂Cl₂ cast, cm⁻¹): ν(P-N-Ti): 1091 (s). NMR Data (CDCl₃) ³¹P{¹H}: P(σ²): δ 260.87 (d, ²J_{PP} 84 Hz), P(σ³): δ 40.87 (d, ²J_{PP} 84 Hz). ¹H: C-CH₃ δ 2.43 (dd, ⁴J_{PH} 0.9 Hz), P(σ²)-N-CH₃ δ 4.03 (d, ³J_{PH} 12.2 Hz), P(σ³)-N-CH₃ δ 3.76 (d, ³J_{PH} 8.2 Hz), C₅-(CH₃)₅ δ 1.98 (s).. ¹³C{¹H}: C-CH₃ δ 14.37 (s), P(σ²)-N-CH₃ δ 41.88 (d, ²J_{PC} 18 Hz), P(σ³)-N-CH₃ δ 40.03 (d, ²J_{PC} 3 Hz), P-C-P δ 143.25 (dd, ²J_{σ2PC} 45 Hz, ²J_{σ3PC} 23 Hz), N-C-CH₃ δ 156.72 (dd, ²J_{σ2PC} 5 Hz, ²J_{σ3PC} 18 Hz), C₅-(CH₃)₅ δ 97.78 (s) C₅-(CH₃)₅ δ 9.93 (s).

5.4 References

- (1) Mann, B. E. In *NMR of Newly Accessible Nuclei*; P. Laszlo, Ed.; Academic Press: London, 1983; Vol. 2; pp 301.
- (2) Kidd, R. G.; Goodfellow, R. J. In *NMR and the Periodic Table*; R. K. Harris and B. E. Mann, Ed.; Academic Press: London, 1978; pp 249.
- (3) King, R. B. *Organomet. Syn.* **1965**, *1*, 124.
- (4) Threlkel, R. S.; Bercaw, J. E.; Seidler, P. F.; Stryker, J. M.; Bergman, J. D. *Org. Syn.* **1987**, *65*, 42.
- (5) Anderson, G. K.; Lin, M. *Inorg. Synth.* **1990**, *28*, 61.
- (6) Drew, D.; Doyle, J. R. *Inorg. Synth.* **1990**, *28*, 348.
- (7) Ukai, T.; Kawazura, H.; Ishii, Y.; Bonnet, J. J.; Ibers, J. A. *J. Organomet. Chem.* **1974**, *65*, 253.
- (8) Chatt, J.; Venanzi, L. M. *J. Chem. Soc.* **1957**, 2351.
- (9) Clark, H. C.; Manzer, L. E. *J. Organomet. Chem.* **1973**, *59*, 411.
- (10) Baratta, W.; Pregosin, P. S. *Inorg. Chim. Acta* **1993**, *209*, 85.
- (11) Chatt, J.; Venanzi, L. M. *J. Chem. Soc.* **1955**, 2787.
- (12) van der Ent, A.; Onderdelinden *Inorg. Synth.* **1990**, *28*, 90.
- (13) Amouri, H. E.; Gruselle, M.; Jaouén, G. *Syn. React. Inorg. Met.-Org. Chem.* **1994**, *24*, 395.
- (14) Giordano, G.; Crabtree, R. H. *Inorg. Synth.* **1990**, *28*, 88.
- (15) McCleverty, J. A.; Wilkinson, G. *Inorg. Synth.* **1990**, *28*, 84.
- (16) Bruce, M. I.; Hameister, C.; Swincer, A. G.; Wallis, R. C. *Inorg. Synth.* **1990**, *28*, 270.
- (17) Nielson, A. J.; Rickard, C. E. F.; Smith, J. M. *Inorg. Synth.* **1990**, *28*, 315.

CHAPTER 6

CONCLUSION AND FUTURE PROSPECTS

6.1 Conclusion

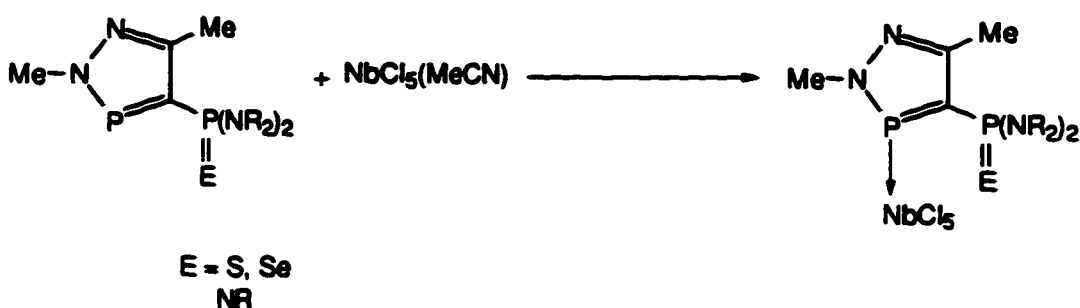
In a series of reactions it was demonstrated that the chlorine substituents on the exo-phosphorus centre of the bisphosphine 4-(dichlorophosphino)-2,5-dimethyl-2*H*-1,2,3 σ^2 -diazaphosphole (1) could be replaced with a variety of groups and so the chemical nature of this phosphorus atom was altered. Complexation studies, assessed in more detail below, showed that these ligands with their rigid structure and large bite angle seemed to preclude chelation of these compounds as bidentate ligands. Instead they served as monodentate ligands wherein only the exo-phosphorus centre coordinated to the metal centre.

The ability to develop oxidized derivatives of this bisphosphine by reactions with chalcogens and azides created a series of heterobifunctional bisphosphines. The iminophosphorano compounds in the series can also employ different substituents on the imine nitrogen in order to control the basicity of that nitrogen centre. In the case of the trimethylsilyl functionality on the iminophosphorane, it was possible to react this moiety with a metal halide to give the class of complexes known as phosphorane iminato metal complexes by means of trimethylsilyl chloride elimination.

6.2 Coordination of the σ^2 P Centre

The availability of the iminophosphorano metal complexes would provide a means of synthesizing heterobimetallic complexes if the σ^2 phosphorus centre could be coordinated to a metal centre. Though the lack of reactivity of the σ^2 P centre encountered in this work did not permit chemistry involving the two-coordinate phosphorus centre to be extensively explored, there are a few known complexes

wherein coordination of this centre has been achieved (usually involving the late transition metals^{1,2}) thus reactions at this centre seem to be feasible. Reactions with palladium tend to favour to coordination of the nitrogen of the diazaphosphole ring, while the use of platinum encourages the coordination of the $\sigma^2\text{P}$ centre. The reaction of high oxidation state third-row transition metal, such as $\text{NbCl}_5(\text{MeCN})$, may be able to involve the two-coordinate phosphorus centre as illustrated in Scheme 6.1.

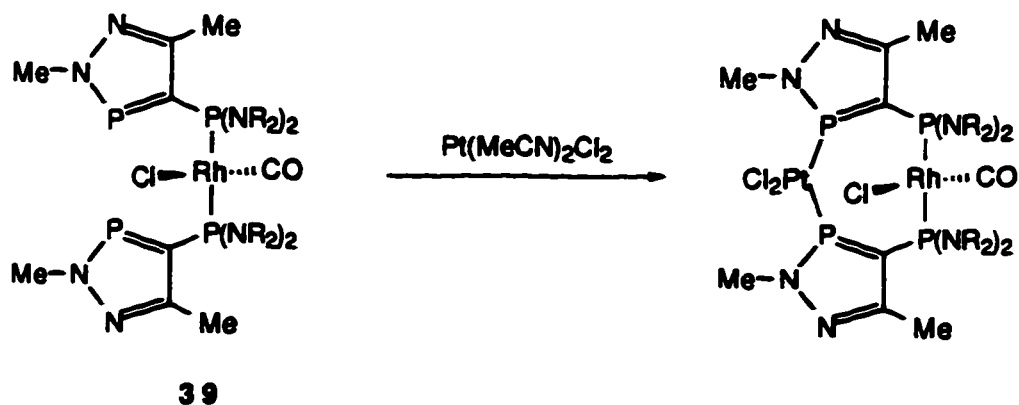


Scheme 6.1 Possible coordination of the $\sigma^2\text{P}$ centre with niobium.

Once again, competition with the nitrogen in the 2-position of the diazaphosphole ring may complicate the reactions by being the preferred site of coordination.

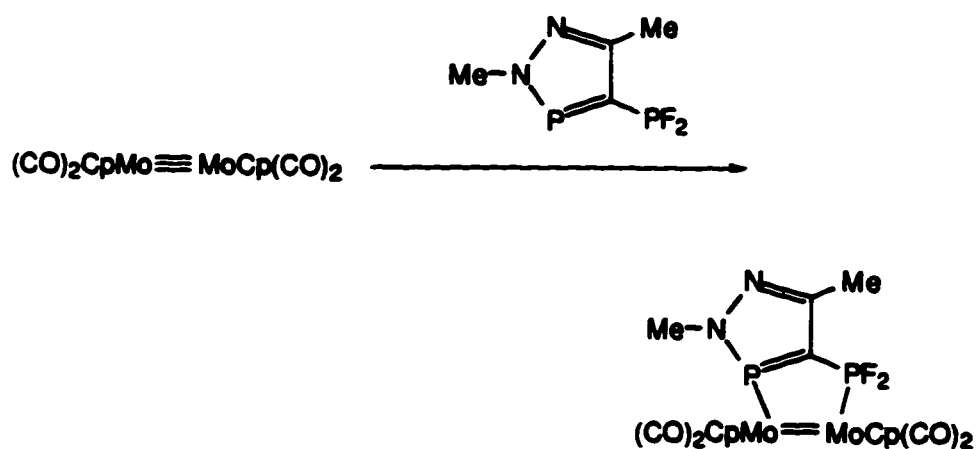
6.3 Bimetallic Complexes

As mentioned in chapter 4, the orientation of the diazaphosphole ring systems in the rhodium carbonyl chloride complex **39** containing the dimethylaminophosphino ligand **3** shows a potentiality for this ligand system to bridge between two metal centres, creating A-frame type complexes (Scheme 6.2) similar to those observed with the *dppm* and pyridyl phosphine ligands. Once again the use of the late transition metal may encourage the formation of such heterobimetallic complexes. The most probable candidates for successful synthesis of a heterobimetallic would be the $\text{Pt}(\text{MeCN})_2\text{Cl}_2$ or the $\text{Pt}(\text{benzonitrile})_2\text{Cl}_2$ starting materials since these complexes contain labile ligands *trans* to each other.



Scheme 6.2 Synthesis of an A-frame bimetallic from the rhodium complex **39**.

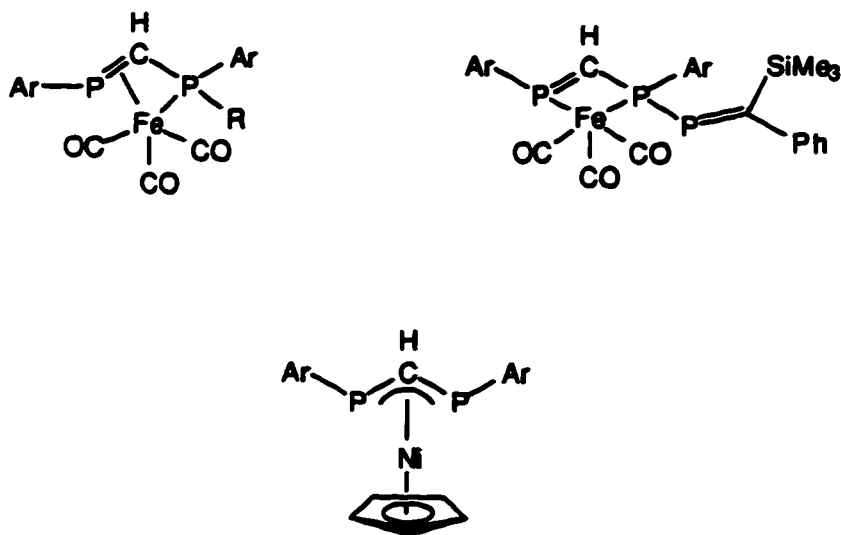
Other materials that may provide optional access to bimetallics systems are the coordinatively unsaturated $[\text{CpM}(\text{CO})_2]_2$ ($\text{M} = \text{Cr}, \text{Mo}, \text{W}$) (Scheme 6.3). These complexes are known to form bridging bimetallic complexes with *dppm*.³ The flexibility of *dppm* yields a number of *anti-syn* isomers in the reaction mixture. Our rigid phosphinodiazaphospholes, especially the bulky diamino derivatives, may simplify the reaction and preferentially yield products with only one conformation.



Scheme 6.3 Formation of molybdenum bimetallics from the phosphinodiazaphosphole **2**.

6.4 Allyl-Type Metal Complexes

Bulky amines amines such diisopropylamine provided a means of synthesizing the asymmetric 4-(chlorodiisopropylphosphino)diazaphosphole in high yield. With one chlorine substituent still available, there is potential for transforming this compound with metal anions to yield allyl-like complexes; a process which is similar to that observed with chlorodiphosphapropene.^{4,5}



6.5 Coordination of the Imino-Nitrogen

Another possible way in which the phosphinophosphole could coordinate to a metal centre would use the ring as a π -bonded ligand. In order to achieve η^5 coordination of the phosphole ring, the lone pair of the exo-phosphorus must be prevented from complexation, since the $\sigma^3\text{P}$ has a greater tendency to coordinate. Our oxidized phosphoranophospholes wherein the exocyclic phosphorus has been transformed to a P(V) could favour the formation of phosphole ring complexes (Figure 6.1).

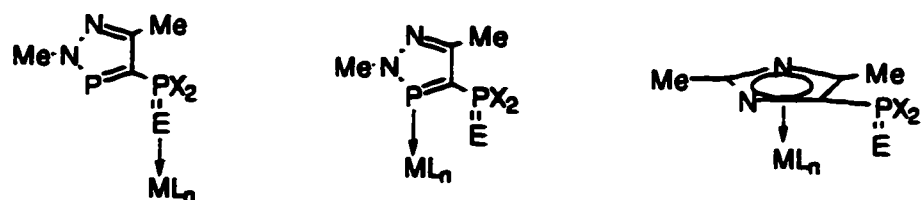


Figure 6.1 Possible coordination modes of the phosphorano-2,5-dimethyl-2H-1,2,3 σ^2 -diazaphosphole.

We did not extensively investigate coordination through the nitrogens of the amino derivatives, *via* the electron lone pairs on the nitrogen on the exo-phosphorus centre (Figure 6.2) as it was not a goal of this work. The reaction of **23** with $\text{Mo}(\text{cht})(\text{CO})_3$ did however suggest that such a complex of this type may be formed. The oxidized diaminophosphorano derivatives may also coordinate in a similar fashion. For the diaminophosphoranodiazaphospholes, it would be interesting to see the effect of the orientation of the chalcogen moiety or if there was a preferred orientation of this substituent. In all the crystal structures obtained in this thesis, the imino group and the metals point towards the two-coordinate phosphorus centre and away from the methyl group at the 5-position. This regularity of structure suggests that intramolecular interactions may yield a series of complexes with an interesting preferred conformation.

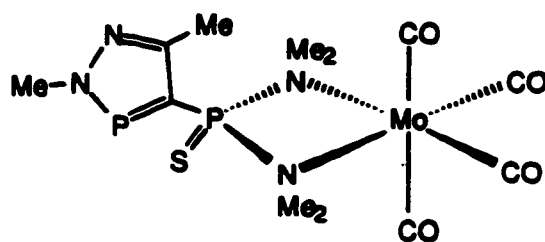


Figure 6.2 Formation of metallacycles *via* coordination of nitrogens on the exo-phosphorus centre.

Attempts have been made to use *p*-cyanotetrafluorophenylimino derivatives of other bisphosphine systems as complexation ligands. These iminophosphoranes are

reluctant to form stable metal complexes with palladium and platinum due to the electron-withdrawing nature of the tbn group on the nitrogen.⁶ Electron-rich metals may be needed in order to stabilize metal complexes of these ligands. In this work, the *p*-cyanotetrafluorophenylimino derivative **18** was reacted with the rhenium complex $\text{Re}(\text{CO})_4(\text{THF})\text{Br}$ in an attempt to coordinate the phosphoranodiazaphosphole in the desired bidentate fashion (Figure 6.3). Spectroscopic evidence suggested that the chelated complex did form however it was not possible to isolate and characterize the product.

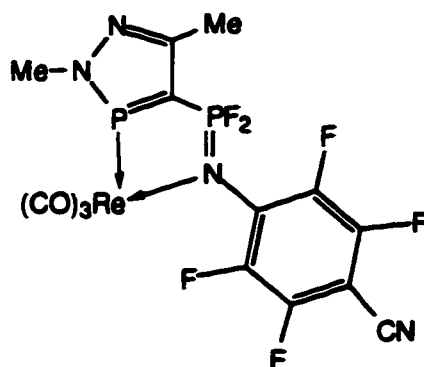


Figure 6.3 Possible reaction product of **18** with $\text{Re}(\text{CO})_4(\text{THF})\text{Br}$.

The versatility of these phosphinodiazaphospholes provides a ligand system which is easily modified and which shows a wide variety of metal complexation chemistry. There remain a number of applications that can be visualized

6.6 References

- (1) Kraaijkamp, J. G.; Van Koten, G.; Vrieze, K.; Grove, D. M.; Klop, E. A.; Spek, A. L.; Schmidpeter, A. *J. Organomet. Chem.* **1983**, *256*, 375.
- (2) Kraaijkamp, J. G.; Grove, D. M.; van Koten, G.; Schmidpeter, A. *Inorg. Chem.* **1988**, *27*, 2612.
- (3) Riera, V.; Ruiz, M. A.; Villafaña, F. *Organometallics* **1992**, *11*, 2854.
- (4) Appel, R.; Schuhn, W.; Knoch, F. *J. Organomet. Chem.* **1987**, *319*, 345.
- (5) Appel, R.; Schuhn, W. *J. Organomet. Chem.* **1987**, *329*, 179.
- (6) Mozol, V. J. M.Sc. Thesis, University of Alberta, 1993.

A.1 Compounds and Complexes Synthesized

Table A.1.1 Compounds and Complexes Synthesized.

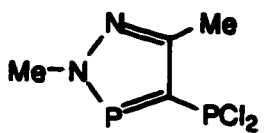
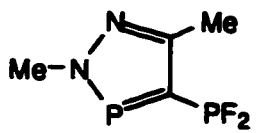
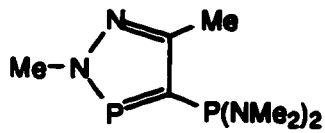
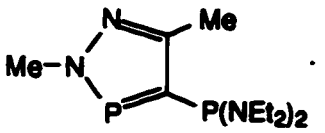
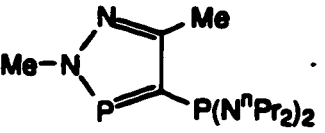
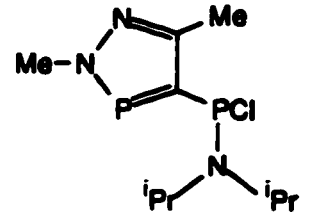
Compound or Complex	Number
	1
	2
	3
	4
	5
	6

Table A.1 continued

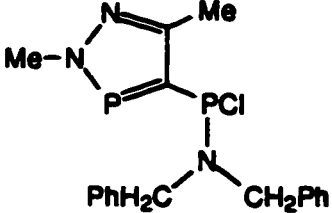
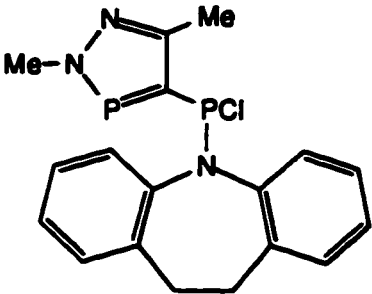
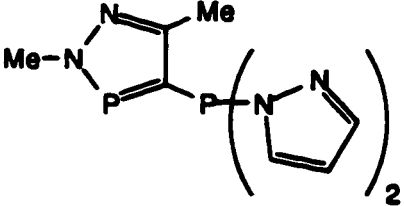
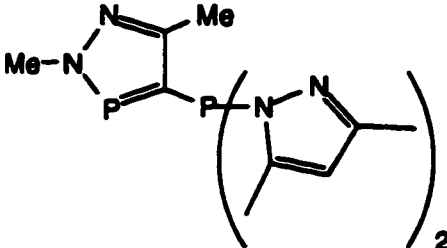
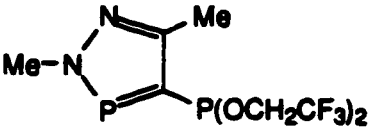
Compound or Complex	Number
	7
	8
	9
	10
	11

Table A.1 continued

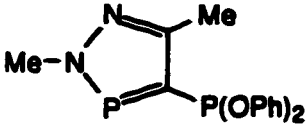
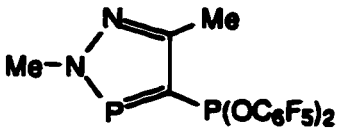
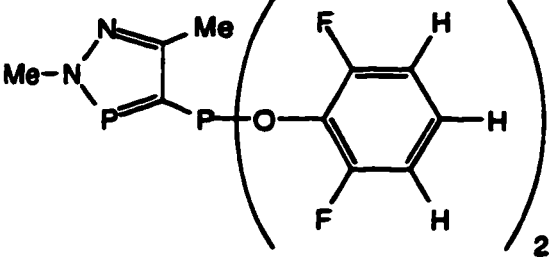
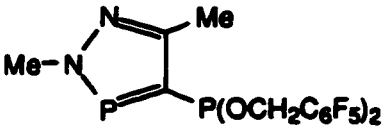
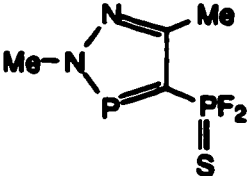
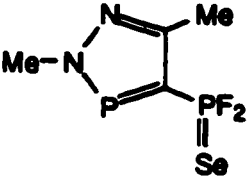
Compound or Complex	Number
	12
	13
	14
	15
	16
	17

Table A.1 continued

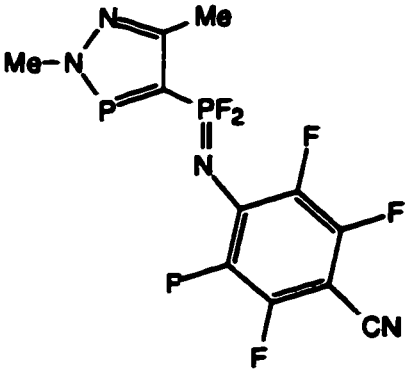
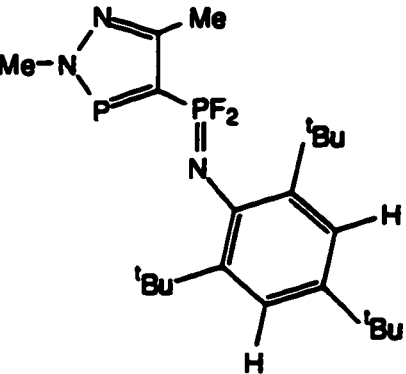
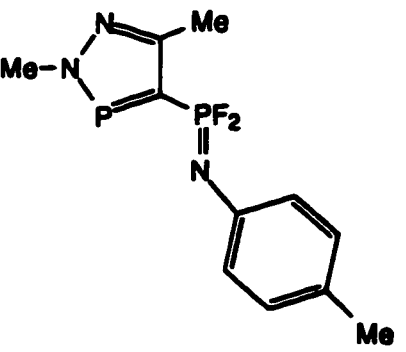
Compound or Complex	Number
	18
	19
	20

Table A.1 continued

Compound or Complex	Number
	21
	22
	23
	24
	25

Table A.1 continued

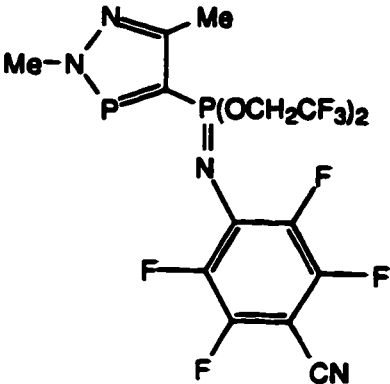
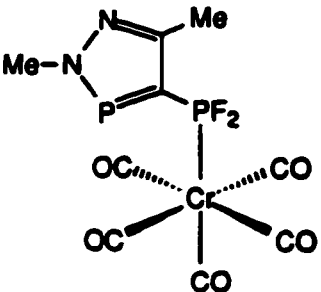
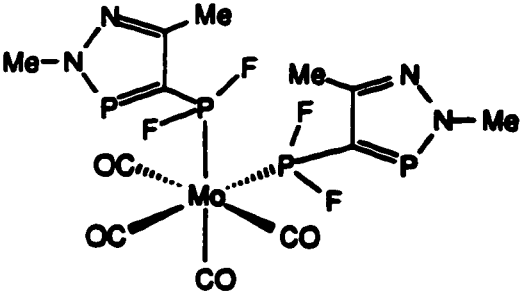
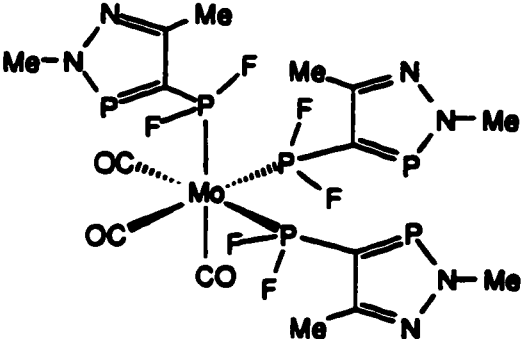
Compound or Complex	Number
	26
	27
	28
	29

Table A.1 continued

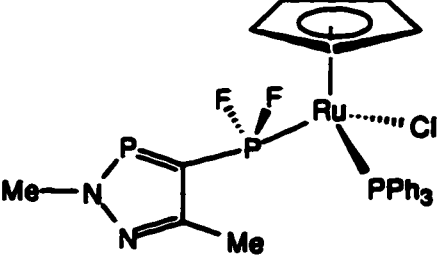
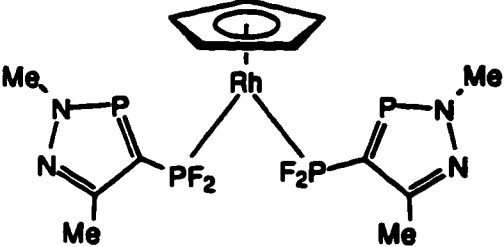
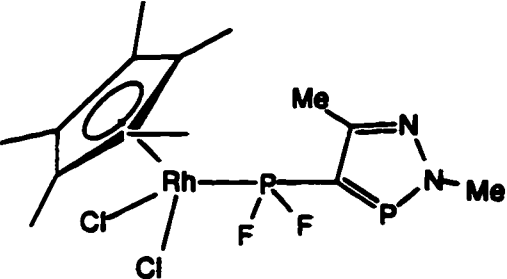
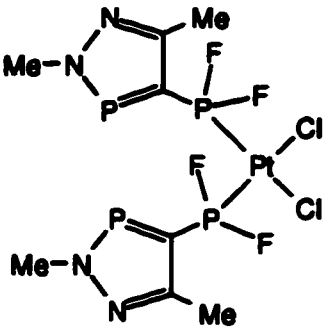
Compound or Complex	Number
	30
	31
	32
	33

Table A.1 continued

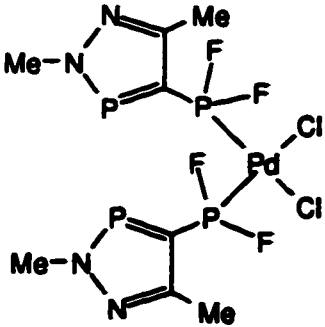
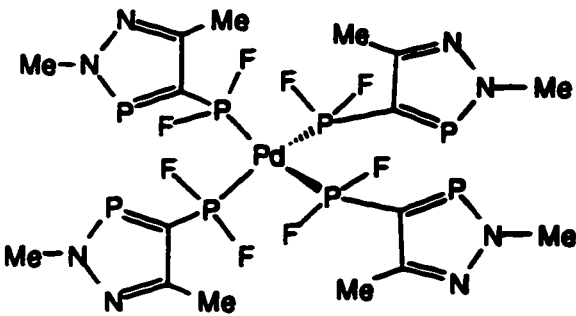
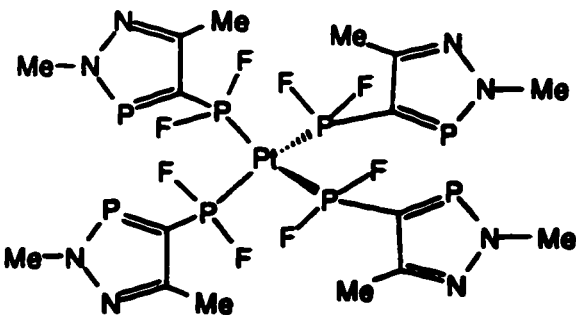
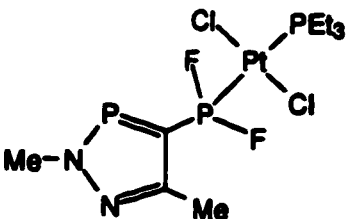
Compound or Complex	Number
 <p>Chemical structure of compound 34: A palladium complex. The central Pd atom is coordinated to two chlorine atoms (Cl) and two phosphorus atoms (P). Each phosphorus atom is part of a 1-methyl-2-methylimidazol-2-ylidene phosphorus ligand, which is coordinated to the Pd through the phosphorus atom. The ligands are also coordinated to the Pd through their respective phosphorus atoms, forming a PdCl2(PF2)2 moiety.</p>	34
 <p>Chemical structure of compound 35: A palladium complex. The central Pd atom is coordinated to four phosphorus atoms (P). Each phosphorus atom is part of a 1-methyl-2-methylimidazol-2-ylidene phosphorus ligand, which is coordinated to the Pd through the phosphorus atom. The ligands are also coordinated to the Pd through their respective phosphorus atoms, forming a Pd(PF2)4 moiety.</p>	35
 <p>Chemical structure of compound 36: A platinum complex. The central Pt atom is coordinated to four phosphorus atoms (P). Each phosphorus atom is part of a 1-methyl-2-methylimidazol-2-ylidene phosphorus ligand, which is coordinated to the Pt through the phosphorus atom. The ligands are also coordinated to the Pt through their respective phosphorus atoms, forming a Pt(PF2)4 moiety.</p>	36
 <p>Chemical structure of compound 37: A platinum complex. The central Pt atom is coordinated to one phosphorus atom (P) and two chlorine atoms (Cl). The phosphorus atom is part of a 1-methyl-2-methylimidazol-2-ylidene phosphorus ligand, which is coordinated to the Pt through the phosphorus atom. The ligand is also coordinated to the Pt through its respective phosphorus atom, forming a PtCl2(PF2) moiety.</p>	37

Table A.1 continued

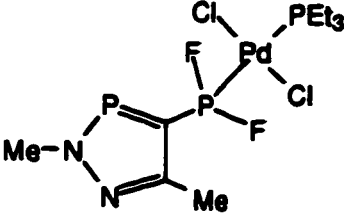
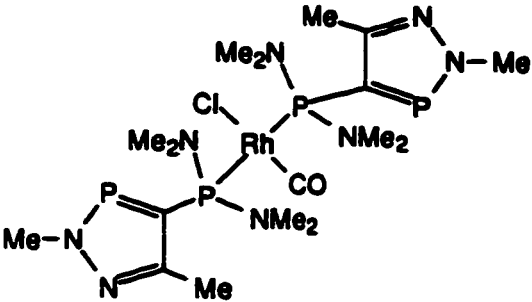
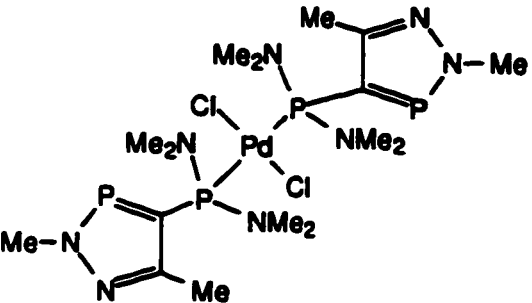
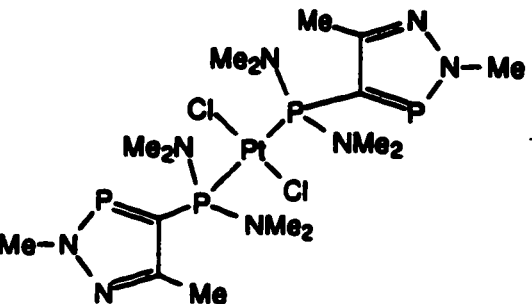
Compound or Complex	Number
	38
	39
	40
	41

Table A.1 continued

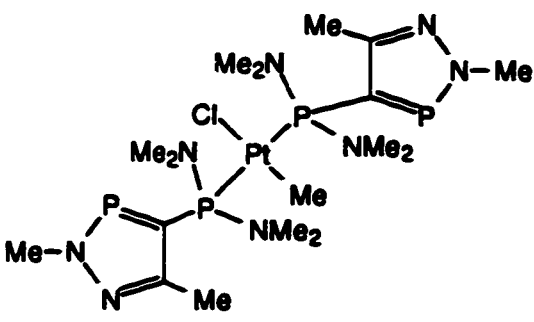
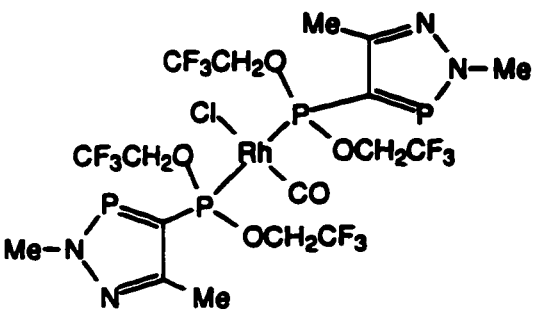
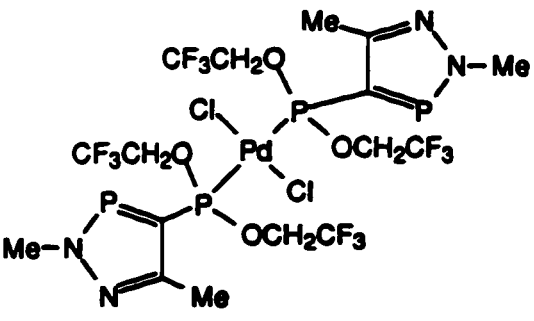
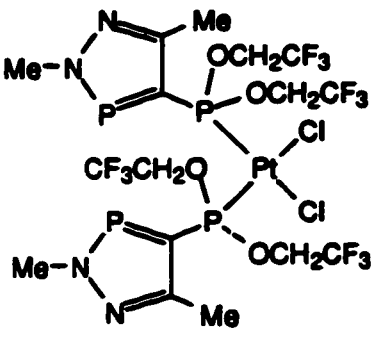
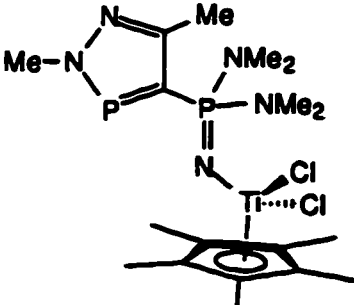
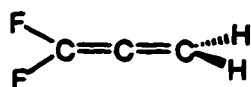
Compound or Complex	Number
	42
	43
	44
	45

Table A.1 continued

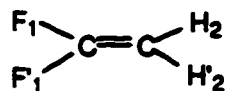
Compound or Complex	Number
	46

A.2 Analysis of an AA'XX' Spectrum^{1,2}

Nuclei are said to be chemically equivalent when they have the same chemical shift.¹ If a molecule has elements of symmetry, such as a twofold or higher axis or a mirror plane, magnetic nuclei of the same species which exchange their positions under the appropriate symmetry operation have symmetry equivalence and must have the same chemical shift.² A group of spins A_n possess complete magnetic equivalence if all n spins have the same chemical shift and are equally coupled to each of the m spins in every other magnetically equivalent spin group B_m . Thus the protons and fluorine nuclei of difluoromethane and of 1,1-difluoroallene,



are magnetically equivalent, but those of 1,1-difluoroethylene,



are not since the cis couplings J_{12} and $J_{1'2'}$ are not equal to the trans couplings $J_{12'}$ and $J_{1'2}$. Magnetic equivalence does not necessarily imply symmetry equivalence.²

Two pairs of spins, the members of each pair being equivalent in chemical shift but not magnetically equivalent, constitute an AA'XX' spin system. The entire spectrum contains 24 lines where there are 12 transitions for the A portion of the spectrum and 12 transitions for the X portion. Both portions, A and X, are identical in form. Line positions and relative intensities are given in Table A.2.1.^{1,2}

Table A.2.1

Transitions of AA'XX' System: Frequencies and Relative Intensities of the A Portion. a.1.2

Line	Frequency Relative to ν_A	Relative Intensity
1	$1/2 N$	1
2	$1/2 N$	1
3	$-1/2 N$	1
4	$-1/2 N$	1
5	$P + 1/2 K$	$1 - K/2P$
6	$P - 1/2 K$	$1 + K/2P$
7	$-P + 1/2 K$	$1 + K/2P$
8	$-P - 1/2 K$	$1 - K/2P$
9	$R + 1/2 M$	$1 - M/2R$
10	$R - 1/2 M$	$1 + M/2R$
11	$-R + 1/2 M$	$1 + M/2R$
12	$-R - 1/2 M$	$1 - M/2R$

$$a) K = J_{AA'} + J_{XX'}, L = J_{AX} - J_{AX'}, M = J_{AA'} - J_{XX'}, N = J_{AX} + J_{AX'}$$

$$2P = (K^2 + L^2)^{1/2}, 2R = (M^2 + L^2)^{1/2}.$$

Considering only the A portion of the spectrum, the 12 transitions form a group centrosymmetric about ν_A (Figure A.2.1 a)). Only ten lines are actually observed, as transitions 1 and 2 and transitions 3 and 4 are always degenerate. The line positions are given relative to ν_A . The spectrum is also characterized by the fact that the separation of lines 1,2 and 3,4 equals $N = J_{AX} + J_{AX'}$, the separation of lines 5 and 6 (and of 7 and 8) gives K, the separation of lines 9 and 10 (and of 11 and 12) gives M. Lines 5, 6, 7, and 8 form a quartet centred on ν_A , lines 9, 10, 11, and 12

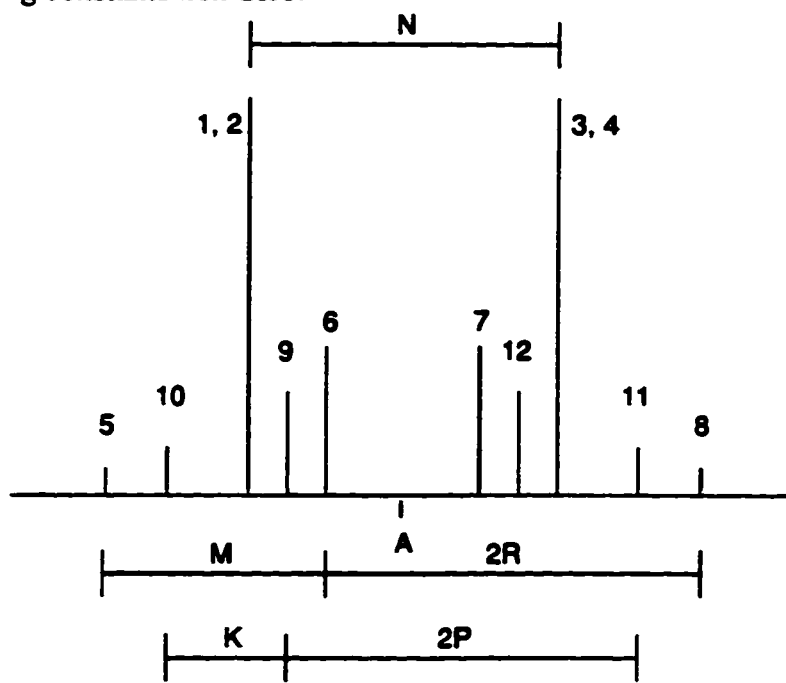
form a quartet, also centred on ν_A . The spacings of line 5 and 7 (and 6 and 8) give $2P = (K^2 + L^2)^{1/2}$ and the spacings of line 9 and 11 (and 10 and 12) give $2R = (M^2 + L^2)^{1/2}$. Figure A.2.1 shows the effect on the A portion of the AA'XX' spectrum achieved by varying the coupling constant values. In this work not all of the lines could be identified, hence the complete analysis could not be performed. Similar observations have been made by Nixon.³ All systems of this type are however characterized by the large value of $J_{AX} + J_{AX'}$ (N) which is representative. It is also notable that the A and the X spectra are identical and in principle all coupling constants operational in the system can be extracted from either the A or the X spectrum.

References

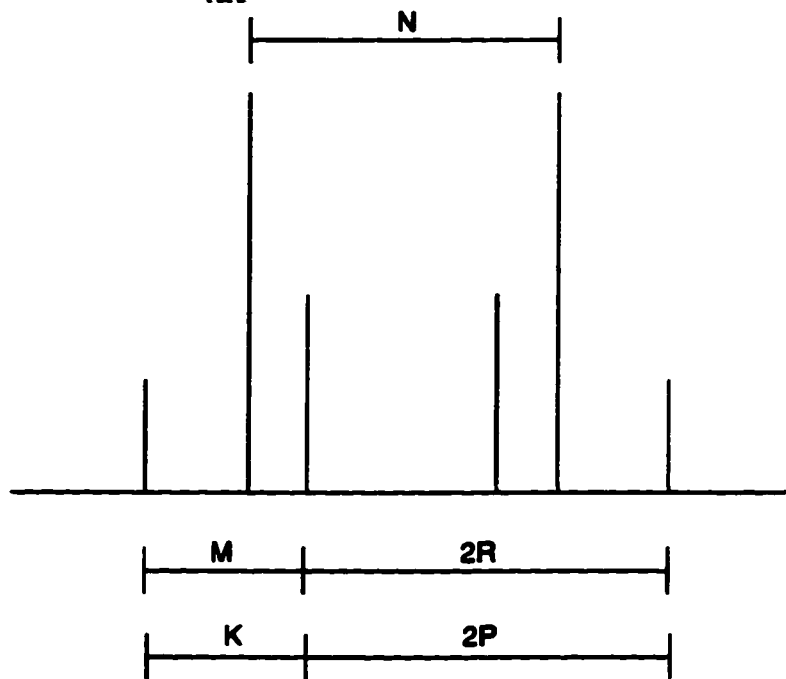
- (1) Becker, E. D. *High Resolution NMR, Theory and Chemical Applications.*; 2nd ed.; Academic Press, Inc.: New York, 1980, pp 88.
- (2) Bovey, F. A. *Nuclear Magnetic Resonance Spectroscopy*; Academic Press, Inc.: New York, 1969, pp 88.
- (3) Nixon, J.F.; Pidcock, A. In *Annual Review of NMR Spectroscopy*; Mooney, E.F., Ed.; Academic Press, New York, 1969; Vol. 2; pp 345.

Figure A.2.1 The effect on one portion of the AA'XX' spectrum due to varying the coupling constant values.

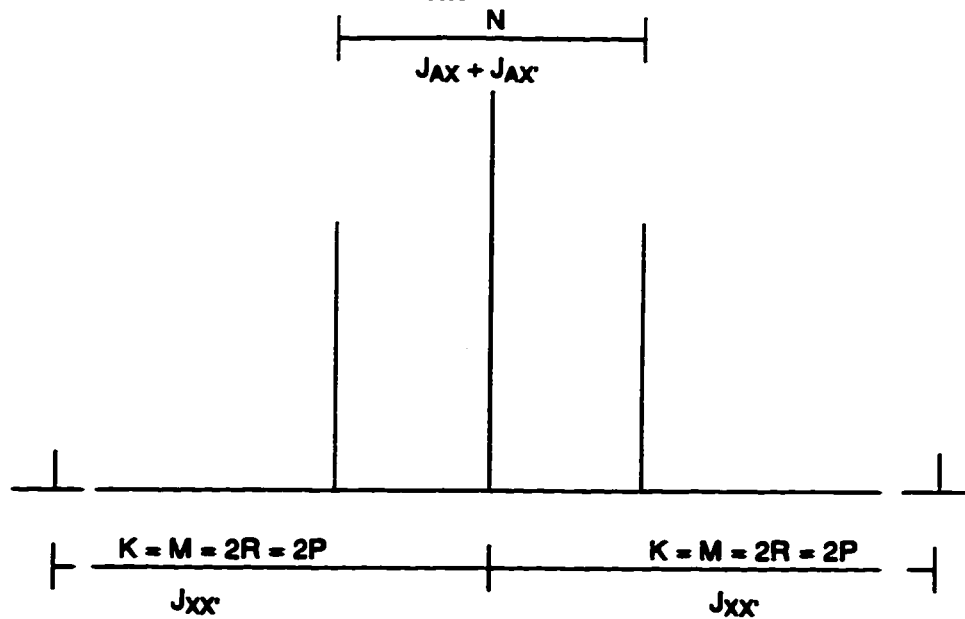
a) All coupling constants non-zero.



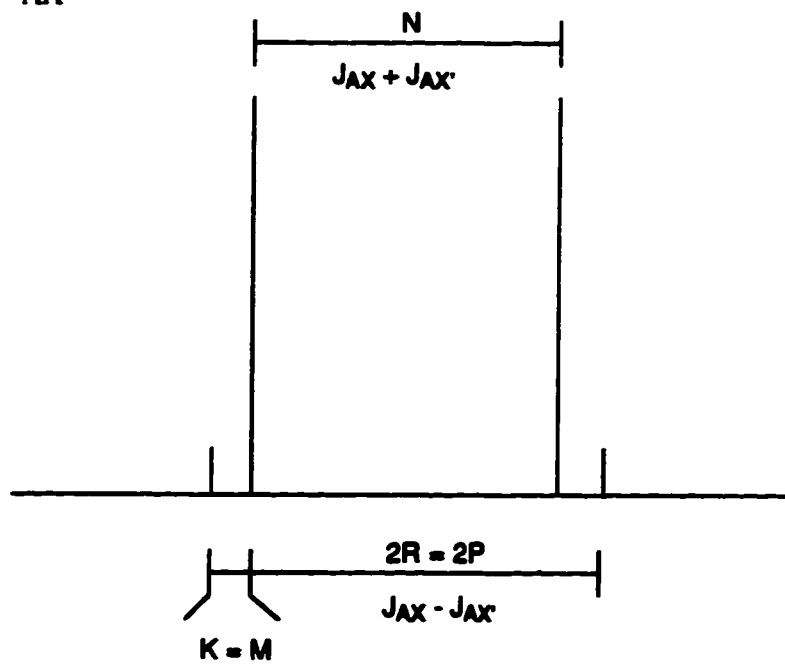
b) $J_{AA'} = 0$ HZ, $K = M = J_{XX'}$, $2P = 2R$.



c) $J_{XX'} \gg N$, $J_{AA'} = 0$ Hz, $K = M = J_{XX'} = 2P = 2R$



d) $J_{XX'} < N$, $J_{AA'} = 0$ Hz.



A.3 Solvents and Drying Agents

Acetone	Potassium carbonate
Acetonitrile	Phosphorus pentoxide then calcium hydride
Benzene	Sodium
Chloroform	Phosphorus pentoxide
Dichloromethane	Phosphorus pentoxide
Diethyl ether	Sodium/benzophenone
Hexanes	Sodium
Octane	Potassium
Pentane	Sulfuric acid then calcium hydride
Tetrahydrofuran	Potassium/benzophenone
Toluene	Sodium

A.4 Crystallographic Data

The complete structure and refinement of 4-(difluoro(*p*-cyanotetrafluorophenyl)iminophosphorano)-2,5-dimethyl-2*H*-1,2,3σ²-diazaphosphole, **18**, was carried out by Dr. R. McDonald, Structure Determination Laboratory, University of Alberta (reference file number: SDL:RGC9415).

Table A.4.1

Crystallographic Experimental Data for **18**.

A. Crystal Data

Empirical formula	$C_{11}H_6F_6N_4P_2$
Formal weight (g/mol)	370.14
Crystal dimensions (mm)	0.72 x 0.47 x 0.46
Crystal system	triclinic
Space group	$P\bar{1}$ (No. 2)
Unit cell parameters	
a (Å)	7.272 (2)
b (Å)	10.088 (4)
c (Å)	10.56 (2)
α (deg)	66.62 (2)
β (deg)	77.60 (2)
γ (deg)	78.14 (3)
V (Å ³)	688.8 (4)
Z	2
ρ _{calcd} (g cm ⁻³)	1.785
μ (cm ⁻¹)	3.79

Table A.4.1 continued

B. Data Collection and Refinement Conditions

Diffractometer	Enraf-Nonius CAD4
Radiation (λ [Å])	Mo K α (0.71073)
Monochromator	incident beam, graphite crystal
Temperature (°C)	-50
Take-off angle (deg)	3.0
Detector aperture (mm)	(3.00 + $\tan\theta$) horiz x 4.00 vert
Crystal-to-detector distance (mm)	173
Scan type	θ - 2θ
Scan rate (deg min ⁻¹)	6.7-1.7
Scan width (deg)	0.80 + 0.344tan θ
Data collection 2θ limit (deg)	50.0
Total data collected	2554 ($\pm h \pm k + l$)
Range of absorption corr. factors	0.7973-1.2405
Total unique data	2411
Number of observations (NO)	1975 ($I > 3\sigma(I)$)
Final no. parameter varied (NV)	208
R^a	0.036
R_w^b	0.049
GOF ^c	1.814

a) $R = \Sigma ||F_o| - |F_c|| / \Sigma |F_o|$.

b) $R_w = [\Sigma w(|F_o| - |F_c|)^2 / \Sigma wF_o^2]^{1/2}$.

c) $GOF = [\Sigma w(|F_o| - |F_c|)^2 / (NO - NV)]^{1/2}$.

Table A.4.2**Weighted^a Least-Squares Planes for 18.**

Plane	Coefficients ^b	Defining Atoms with Deviations ^c
1	3.9917 -2.3222 -7.3692 1.0258	N1 0.00 N2 0.00 P3 0.00 C4 0.00 C5 0.00 <u>C21</u> -0.031 <u>P41</u> -0.069 <u>N41</u> -0.087 <u>C51</u> -0.023
2	6.1665 -1.4737 -3.3268 1.3978	C41 -0.01 C42 0.00 C43 0.01 C44 -0.01 C45 0.00 C46 0.01

- a) Weights are derived from the atomic positional e. s. d.'s using the method of Hamilton (Hamilton, W.C. *Acta Crystallogr.* 1961, 14, 185).
- b) Coefficients are for the form $\{ax + by + cz - d = 0\}$ where x , y , and z are crystallographic coordinates.
- c) Deviations are in Ångstroms. Underlined atoms were not included in the definition of the plane.

Table A.4.3

Selected Torsional Angles (deg) for 4-(difluoro(*p*-cyanotetrafluorophenyl)iminophosphorano)-2,5-dimethyl-2*H*-1,2,3 σ^2 -diazaphosphole (18).

Atom1	Atom2	Atom3	Atom4	Angle
C4	P3	N2	N1	0.42 (0.23)
C4	P3	N2	C21	-178.65 (0.21)
N2	P3	C4	P41	177.22 (0.16)
N2	P3	C4	C5	-0.18 (0.33)
F41	P41	N41	C41	-37.73 (0.34)
F42	P41	N41	C41	76.15 (0.31)
C4	P41	N41	C41	-160.58 (0.25)
F41	P41	C4	P3	-127.79 (0.14)
F41	P41	C4	C5	49.10 (0.24)
F42	P41	C4	P3	128.17 (0.14)
F42	P41	C4	C5	-54.94 (0.25)
N41	P41	C4	P3	1.43 (0.19)
N41	P41	C4	C5	178.32 (0.21)
C5	N1	N2	P3	-0.54 (0.32)
C5	N1	N2	C21	178.62 (0.22)
N2	N1	C5	C4	0.37 (0.38)
N2	N1	C5	C51	-178.80 (0.22)
P3	C4	C5	N1	-0.08 (0.71)
P3	C4	C5	C51	179.00 (0.21)
P41	C4	C5	N1	-177.24 (0.18)
P41	C4	C5	C51	1.84 (0.39)

Table A.4.4

Atomic Coordinates and Equivalent Isotropic Displacement Parameters for 18.

Atom	x	y	z	B _{eq} , Å ²
P3	-0.03113(9)	0.51209(7)	-0.31767(6)	2.41(2)*
P41	0.25867(8)	0.47866(6)	-0.14049(6)	2.10(1)*
F41	0.2175(2)	0.5421(2)	-0.0252(1)	3.43(4)*
F42	0.4617(2)	0.5165(2)	-0.1975(2)	3.39(4)*
F43	0.1848(2)	0.0777(1)	-0.1294(1)	3.00(4)*
F44	0.2259(2)	-0.1871(1)	0.0685(1)	3.10(4)*
F45	0.4207(2)	0.0091(1)	0.3468(1)	2.99(4)*
F46	0.3804(2)	0.2748(1)	0.1476(1)	2.97(4)*
N1	-0.0420(3)	0.7927(2)	-0.4121(2)	2.52(5)*
N2	-0.1144(3)	0.6804(2)	-0.4152(2)	2.34(5)*
N41	0.2396(3)	0.3195(5)	-0.0983(2)	2.61(5)*
N42	0.3526(3)	-0.3495(2)	0.4065(2)	3.52(7)*
C4	0.1137(3)	0.5868(2)	-0.2624(2)	2.16(6)*
C5	0.0858(3)	0.7404(2)	-0.3259(2)	2.23(6)*
C21	-0.2614(4)	0.7187(3)	0.5030(3)	3.22(7)*
C41	0.2721(3)	0.1869(2)	0.0049(2)	2.05(6)*
C42	0.2365(3)	0.0631(2)	-0.0108(2)	2.15(6)*
C43	0.2596(3)	-0.0730(2)	0.0907(2)	2.20(6)*
C44	0.3176(3)	-0.0948(2)	0.2145(2)	2.15(6)*
C45	0.3579(3)	0.0258(2)	0.2305(2)	2.16(6)*
C46	0.3360(3)	0.1622(2)	0.1284(2)	2.15(6)*
C47	0.3381(3)	-0.2366(3)	0.3218(2)	2.49(6)*
C51	0.1814(4)	0.8451(3)	-0.3040(3)	3.46(8)*

Anisotropically-refined atoms are marked with an asterisk(*). Displacement parameters for the anisotropically refined atoms are given in the form of the equivalent isotropic Gaussian displacement parameter, B_{eq}, defined as $\frac{4}{3}[a^2\beta_{11} + b^2\beta_{22} + c^2\beta_{33} + ab(\cos\gamma)\beta_{12} + ac(\cos\beta)\beta_{13} + bc(\cos\alpha)\beta_{23}]$.

The complete structure and refinement of [CpRh(difluoro(2,5-dimethyl-2*H*-1,2,3σ²-diazaphosphol-4-yl)phosphine)₂], **31**, was carried out by Dr. R. McDonald, Structure Determination Laboratory, University of Alberta (reference file number: SDL:RGC9514).

Table A.4.5

Crystallographic Experimental Data for 31.

A. Crystal Data

Empirical formula	C₁₃H₁₇F₄N₄P₄Rh
Formal weight (g/mol)	532.10
Crystal dimensions (mm)	0.37 x 0.22 x 0.08
Crystal system	monoclinic
Space group	P₂₁/c (No. 14)
Unit cell parameters	
a (Å)	14.653 (2)
b (Å)	7.9711 (8)
c (Å)	18.010 (2)
β (deg)	105.417 (10)
V (Å ³)	2027.9 (4)
Z	4
ρ _{calcd} (g cm ⁻³)	1.743
μ (mm ⁻¹)	1.198

Table A.4.5 continued

B. Data Collection and Refinement Conditions

Diffractometer	Enraf-Nonius CAD4 ^b
Radiation (λ [Å])	Mo K α (0.71073)
Monochromator	incident beam (graphite crystal)
Temperature (°C)	-50
Scan type	θ - 2θ
Data collection 2θ limit (deg)	50.0
Total data collected	3687 ($-17 \leq h \leq 16$, $0 \leq k \leq 9$, $0 \leq l \leq 21$)
Independent reflections	3559
Number of observations (<i>NO</i>)	2579 ($F_o^2 \geq 2\sigma(F_o^2)$)
Structure solution method	direct methods (<i>SHELXSI-86</i> ^c)
Refinement method	full-matrix least-squares on F^2 (<i>SHELXSI-93</i> ^d)
Absorption correction method	<i>DIFABS</i> ^e
Range of absorption corr. factors	1.126-0.800
Data/restraints/parameters	3558 [$F_o^2 \geq 3\sigma(F_o^2)$]/0/239
Goodness-of-fit (<i>S</i>) ^f	1.002 [$F_o^2 \geq 3\sigma(F_o^2)$]
Final <i>R</i> indices ^g	
$F_o^2 > 2\sigma(F_o^2)$	$R_1 = 0.0313$, $wR_2 = 0.0649$
All data	$R_1 = 0.0688$, $wR_2 = 0.0747$
Largest difference peak and hole	0.363 and -0.464 e Å ⁻³

^aObtained from least-squares refinement of 37 reflections with $54.1^\circ < 2\theta < 57.9^\circ$.

^cSheldrick, G. M. *Acta Crystallogr.* **1990**, *A46*, 467-473.

^dSheldrick, G. M. *SHELXL-93*. Program for crystal structure determination. University of Göttingen, Germany, 1993. Refinement on F_o^2 for all reflections except for 13 having $F_o^2 < 3\sigma(F_o^2)$. Weighted *R*-factors wR_2 and all goodnesses of fit *S*

are based on F_o^2 ; conventional R -factors R_1 are based on F_o , with F_o set to zero for negative F_o^2 . The observed criterion of $F_o^2 > 2\sigma(F_o^2)$ is used only for calculating R_1 , and is not relevant to the choice of reflections for refinement. R -factors based on F_o^2 are statistically about twice as large as those based on F_o , and R -factors based on ALL data will be even larger.

^eWalker, N. *Acta Crystallogr.* 1983, A39, 158–166.

$fS = [\sum w(F_o^2 - F_c^2)^2 / (n - p)]^{1/2}$ (n = number of data; p = number of parameters varied; $w = [\sigma^2(F_o^2) + (0.0936P)^2 + 4.3804P]^{-1}$ where $P = [\text{Max}(F_o^2, 0) + 2F_c^2]/3$).

$8R_1 = \sum |F_o| - |F_c| / \sum |F_o|$; $wR_2 = [\sum w(F_o^2 - F_c^2)^2 / \sum w(F_o^4)]^{1/2}$.

Table A.4.6

Selected Torsional Angles (deg) for [CpRh(difluoro{2,5-dimethyl-2*H*-1,2,3σ²-diazaphosphol-4-yl}phosphine)₂] (31).

Atom1	Atom2	Atom3	Atom4	Angle
P21	Rh	P11	F11	124.09(15)
P21	Rh	P11	F12	10.1(2)
P21	Rh	P11	C11	-115.5(2)
P11	Rh	P21	F21	140.9(2)
P11	Rh	P21	F22	27.4(2)
P11	Rh	P21	C21	-99.1(2)
Rh	P11	C11	P21	20.8(2)
Rh	P11	C11	C15	-162.2(4)
F11	P11	C11	P12	148.7(3)
F11	P11	C11	C15	-34.(5)
F12	P11	C11	P12	-113.7(3)
F12	P11	C11	C15	63.3(4)
C11	P12	N13	N14	0.9(3)
C11	P12	N13	C17	179.9(4)
N13	P12	C11	P11	177.2(3)
N13	P12	C11	C15	-0.3(3)
Rh	P21	C21	P22	-1.1(3)
Rh	P21	C21	C25	-176.5(3)
F21	P21	C21	P22	126.2(3)
F21	P21	C21	C25	-49.2(4)
F22	P21	C21	P22	136.1(3)
F22	P21	C21	C25	48.5(4)
C21	P22	N23	N24	-0.7(3)
C21	P22	N23	C27	179.4(4)
N23	P22	C21	P21	-175.5(3)
N23	P22	C21	C25	0.8(3)
P12	N13	N14	C15	-1.2(5)
C17	N13	N14	C15	179.7(4)
N13	N14	C15	C11	0.9(6)
N13	N14	C15	C16	179.1(4)

Table A.4.6 continued

Atom1	Atom2	Atom3	Atom4	Angle
C27	N23	N24	C25	179.2(4)
P22	N23	N24	C25	0.4(4)
N23	N24	C25	C21	0.3(5)
N23	N24	C25	C26	-177.8(3)
P11	C11	C15	N14	-177.(5)
P12	C11	C15	N14	-0.3(5)
P11	C11	C15	C16	2.5(7)
P12	C11	C15	C16	179.7(4)
P21	C21	C25	N24	175.1(3)
P22	C21	C25	N24	-0.8(5)
P21	C21	C25	C26	-7.1(6)
P22	C21	C25	C26	177.0(3)

Table A.4.7

Atomic Coordinates and Equivalent Isotropic Displacement Parameters for 31.

Atom	x	y	z	B _{eq} , Å ²
Rh	0.26289(2)	0.02529(4)	-0.12456(2)	0.03164(10)*
P11	0.12070(8)	0.1150(2)	-0.15976(6)	0.0382(3)*
P12	0.13175(8)	0.2282(2)	-0.00192(7)	0.0451(3)*
P21	0.31954(9)	0.22788(15)	-0.17584(6)	0.0403(3)*
P22	0.32560(8)	0.02734(15)	-0.31810(6)	0.0385(3)*
F11	0.0453(2)	-0.0108(4)	-0.2083(2)	0.0721(9)*
F12	0.0934(2)	0.2634(4)	-0.2180(2)	0.0709(9)*
F21	0.4187(2)	0.2943(4)	-0.12710(15)	0.0782(11)*
F22	0.2690(2)	0.4023(3)	-0.1862(2)	0.0757(10)*
N13	0.0320(3)	0.2750(5)	-0.0255(2)	0.0480(10)*
N14	-0.0508(3)	0.2533(5)	-0.0292(2)	0.0494(10)*
N23	0.3732(2)	0.1174(4)	-0.3829(2)	0.0354(8)*
N24	0.4023(2)	0.2787(4)	-0.3700(2)	0.0375(8)*
C1	0.2562(4)	-0.2525(6)	-0.1023(3)	0.0595(15)*
C2	0.3398(4)	-0.2276(7)	-0.1195(3)	0.0619(15)*
C3	0.3924(3)	-0.1185(7)	-0.0652(3)	0.0590(14)*
C4	0.3437(4)	-0.0841(6)	-0.0098(3)	0.0550(14)*
C5	0.2564(4)	-0.1658(6)	-0.0352(3)	0.0533(14)*
C11	0.0642(3)	0.1768(5)	0.0884(2)	0.0361(10)*
C15	-0.0333(3)	0.1998(6)	-0.0931(3)	0.0443(11)*
C16	-0.1154(3)	0.1697(7)	-0.1621(3)	0.0640(15)*
C17	0.0246(4)	0.3354(7)	0.1005(3)	0.0642(15)*
C21	0.3442(3)	0.2106(5)	-0.3666(2)	0.0327(9)*
C25	0.3857(5)	0.3303(5)	-0.3051(2)	0.0329(9)*
C26	0.4095(3)	0.5094(5)	-0.2815(2)	0.0455(11)*
C27	0.3858(4)	0.0423(6)	-0.4539(2)	0.0544(13)*

Anisotropically-refined atoms are marked with an asterisk(*). Displacement parameters for the anisotropically refined atoms are given in the form of the equivalent isotropic Gaussian displacement parameter, B_{eq}, defined as $\exp[-2\pi^2(h^2a^2U_{11} + k^2b^2U_{22} + l^2c^2U_{33} + 2klb^*c^*U_{23} + 2hla^*c^*U_{13} + 2hka^*b^*U_{12})]$.

The complete structure and refinement of tetrakis(difluoro{2,5-dimethyl-2*H*-1,2,3σ²-diazaphosphol-4-yl}phosphine)platinum(0) dihydrate, **36**, was carried out by Dr. R. McDonald, Structure Determination Laboratory, University of Alberta (reference file number: SDL:RGC9605).

Table A.4.8

Crystallographic Experimental Data for **36.**

A. Crystal Data

Empirical formula	$C_{16}H_{28}F_8N_6O_2P_8Pt$
Formal weight (g/mol)	959.31
Crystal dimensions (mm)	0.33 x 0.26 x 0.26
Crystal system	tetragonal
Space group	$I\bar{4}2m$ (No. 121)
Unit cell parameters	
a (Å)	11.961 (2)
c (Å)	15.034 (3)
V (Å ³)	2250.8 (6)
Z	2
ρ_{calcd} (g cm ⁻³)	1.481
μ (mm ⁻¹)	3.619

Table A.4.8 continued

B. Data Collection and Refinement Conditions

Diffractometer	Enraf-Nonius CAD4 ^b
Radiation (λ [Å])	Mo K α (0.71073)
Monochromator	incident beam (graphite crystal)
Temperature (°C)	-50
Scan type	θ - 2θ
Data collection 2θ limit (deg)	50.0
Total data collected	4256 ($-14 \leq h \leq 14, -14 \leq k \leq 14, -17 \leq l \leq 17$)
Independent reflections	1021
Number of observations (NO)	1009 ($F_o^2 \geq 2\sigma(F_o^2)$)
Structure solution method	direct methods (<i>SHELXSI-86</i> ^c)
Refinement method	full-matrix least-squares on F^2 (<i>SHELXSI-93</i> ^d)
Absorption correction method	<i>DIFABS</i> ^e
Range of absorption corr. factors	1.157-0.815
Data/restraints/parameters	1021 [$F_o^2 \geq 3\sigma(F_o^2)$]/0/61
Goodness-of-fit (S) ^f	1.299 [$F_o^2 \geq 3\sigma(F_o^2)$]
Final R indices ^g	
$F_o^2 > 2\sigma(F_o^2)$	$R_1 = 0.0381 \cdot wR_2 = 0.1180$
All data	$R_1 = 0.0395 \cdot wR_2 = 0.1188$
Largest difference peak and hole	1.570 and -1.160 e Å ⁻³

^aObtained from least-squares refinement of 37 reflections with $54.1^\circ < 2\theta < 57.9^\circ$.

^bSheldrick, G. M. *Acta Crystallogr.* 1990, A46, 467-473.

^dSheldrick, G. M. *SHELXL-93*. Program for crystal structure determination. University of Göttingen, Germany, 1993. Refinement on F_o^2 for all reflections except for 13 having $F_o^2 < 3\sigma(F_o^2)$. Weighted R -factors wR_2 and all goodnesses of fit S

are based on F_o^2 ; conventional R -factors R_1 are based on F_o , with F_o set to zero for negative F_o^2 . The observed criterion of $F_o^2 > 2\sigma(F_o^2)$ is used only for calculating R_1 , and is not relevant to the choice of reflections for refinement. R -factors based on F_o^2 are statistically about twice as large as those based on F_o , and R -factors based on ALL data will be even larger.

⁶Walker, N. *Acta Crystallogr.* **1983**, *A39*, 158–166.

$fS = [\sum w(F_o^2 - F_c^2)^2 / (n - p)]^{1/2}$ (n = number of data; p = number of parameters varied; $w = [\sigma^2(F_o^2) + (0.0936P)^2 + 4.3804P]^{-1}$ where $P = [\text{Max}(F_o^2, 0) + 2F_c^2]/3$).

$^8R_1 = \sum |F_o| - |F_c| / \sum |F_o|$; $wR_2 = [\sum w(F_o^2 - F_c^2)^2 / \sum w(F_o^4)]^{1/2}$.

Table A.4.9

Selected Torsional Angles (deg) for tetrakis(difluoro{2,5-dimethyl-2*H*-1,2,3σ²-diazaphosphol-4-yl}phosphine)platinum(0) dihydrate (36).

Atom1	Atom2	Atom3	Atom4	Angle
P1A	Pt	P1	F	-66.1(3)
P1B	Pt	P1	F	55.2(3)
P1C	Pt	P1	F	176.6(3)
P1A	Pt	P1	C1	58.69(4)
P1B	Pt	P1	C1	180.0
Pt	P1	C1	P2	0.0
Pt	P1	C1	C2	180.0
F	P1	C1	P2	179.7(4)
F	P1	C1	C2	131.5(3)
C1	P2	N2	N1	-48.5(3)
C1	P2	N2	C3	0.0
N2	P2	C1	P1	180.0
N2	P2	C1	C2	0.0
C2	N1	N2	P2	0.0
C2	N1	N2	C3	180.0
N2	N1	C2	C1	0.0
N2	N1	C2	C4	180.0
P1	C1	C2	N1	180.0
P1	C1	C2	C4	0.0
P2	C1	C2	N1	0.0
P2	C1	C2	C4	180.0

The phosphorus atom P1 is located at the crystallographic mirror-symmetry special position (x, y, z) . thus the symmetry-generated phosphorus atoms P1^A $(x, \bar{x}, 1-z)$, P1^B (\bar{x}, \bar{x}, z) and P1^C $(x, \bar{x}, 1-z)$ are at the related special positions. No estimated standard deviation is given for angles in which all atoms involved lie in a crystallographic mirror plane.

Table A.4.10

Atomic Coordinates and Equivalent Isotropic Displacement Parameters for 36.

Atom	x	y	z	$U_{eq}, \text{\AA}^2$
Pt	0.00	0.00	0.50	0.0309(3)*
P1	0.1050(2)	0.1050(2)	0.5905(2)	0.0364(7)*
P2	0.2192(3)	0.2192(3)	0.4369(3)	0.0449(11)*
F	0.1773(6)	0.0416(5)	0.6611(3)	0.053(2)*
N1	0.3403(9)	0.3403(9)	0.5442(11)	0.060(5)*
N2	0.3176(9)	0.3176(9)	0.4560(9)	0.048(4)*
C1	0.1988(11)	0.1988(11)	0.5492(12)	0.044(4)*
C2	0.2750(10)	0.2750(10)	0.5932(9)	0.056(4)*
C3	0.3795(9)	0.3795(9)	0.3924(9)	0.060(4)*
C4	0.2904(10)	0.2904(10)	0.6915(8)	0.071(5)*
O	0.00	0.50	0.50	0.256(20)

Anisotropically-refined atoms are marked with an asterisk(*). The form of the anisotropic displacement parameter, U_{eq} , is: $\exp[-2\pi^2(h^2a^*2U_{11} + k^2b^*2U_{22} + l^2c^*2U_{33} + 2klb^*c^*U_{23} + 2hla^*c^*U_{13} + 2hka^*b^*U_{12})]$. Those parameters without an estimated standard deviation are not refined.

The complete structure and refinement of *trans*-[RhCl(CO)-(bis(dimethylamino){2,5-dimethyl-2*H*-1,2,3σ²-diazaphosphol-4-yl}phosphine)₂], **39**, was carried out by Dr. R. McDonald, Structure Determination Laboratory, University of Alberta (reference file number: SDL:RGC9615).

Table A.4.11

Crystallographic Experimental Data.

A. Crystal Data

Empirical formula	C ₁₇ H ₃₆ ClN ₈ OP ₄ Rh
Formal weight (g/mol)	630.78
Crystal dimensions (mm)	0.35 x 0.18 x 0.07
Crystal system	triclinic
Space group	P $\bar{1}$ (No. 2)
Unit cell parameters ^a	
a (Å)	9.4866 (9)
b (Å)	11.7338 (13)
c (Å)	14.9972 (15)
α (deg)	68.686 (8)
β (deg)	73.004 (8)
γ (deg)	66.764 (7)
V (Å ³)	1407.2 (2)
Z	2
ρ _{calcd} (g cm ⁻³)	1.489
μ (mm ⁻¹)	0.954

Table A.4.11 continued

B. Data Collection and Refinement Conditions

Diffractometer	Siemens P4/RA ^b
Radiation (λ [Å])	Mo K α (0.71073)
Monochromator	incident beam, graphite crystal
Temperature (°C)	-60
Scan type	θ - 2θ
Data collection 2θ limit (deg)	50.0
Total data collected	5245 ($0 \leq h \leq 11, -12 \leq k \leq 13, -17 \leq l \leq 17$)
Independent reflections	4916
Number of observations (NO)	2918 ($F_o^2 \geq 2\sigma(F_o^2)$)
Structure solution method	direct methods (<i>SHELXSI-86</i> ^c)
Refinement method	full-matrix least-squares on F^2 (<i>SHELXSI-93</i> ^d)
Absorption correction method	semiempirical (Ψ scans)
Range of absorption corr. factors	0.9965-0.8630
Data/restraints/parameters	4916 [$F_o^2 \geq 3\sigma(F_o^2)$]/2°/305
Goodness-of-fit (S) ^f	1.037 [$F_o^2 \geq 3\sigma(F_o^2)$]
Final R indices ^g	
$F_o^2 > 2\sigma(F_o^2)$	$R_1 = 0.0623 \cdot wR_2 = 0.0776$
All data	$R_1 = 0.1345 \cdot wR_2 = 0.0964$
Largest difference peak and hole	0.521 and -0.521 e Å ⁻³

^aObtained from least-squares refinement of 32 reflections with $25.5^\circ < 2\theta < 28.0^\circ$.

^bPrograms for diffractometer operation and data collection were those of the XSCANS system supplied by Siemens.

^cSheldrick, G. M. *Acta Crystallogr.* 1990, A46, 467-473.

^dSheldrick, G. M. *SHELXL-93*. Program for crystal structure determination. University of Göttingen, Germany, 1993. Refinement on F_o^2 for all reflections except for 13 having $F_o^2 < -3\sigma(F_o^2)$. Weighted R -factors wR_2 and all goodnesses of fit S are based on F_o^2 ; conventional R -factors R_1 are based on F_o , with F_o set to zero for negative F_o^2 . The observed criterion of $F_o^2 > 2\sigma(F_o^2)$ is used only for calculating R_1 , and is not relevant to the choice of reflections for refinement. R -factors based on F_o^2 are statistically about twice as large as those based on F_o , and R -factors based on ALL data will be even larger.

^fDistances involving the carbonyl group C(2)O(2) of the minor isomer were fixed as follows: d(Rh-C(2)) = 1.78(1)Å; c(C(2)-O(2)) = 1.12(1)..

^f $S = [\sum w(F_o^2 - F_c^2)^2 / (n - p)]^{1/2}$ (n = number of data; p = number of parameters varied; $w = [\sigma^2(F_o^2) + (0.0936P)^2 + 4.3804P]^{-1}$ where $P = [\text{Max}(F_o^2, 0) + 2F_c^2]/3$).

^g $R_1 = \sum |F_o| - |F_c| / \sum |F_o|$; $wR_2 = [\sum w(F_o^2 - F_c^2)^2 / \sum w(F_o^4)]^{1/2}$.

Table A.4.12

Selected Torsional Angles (deg) for *trans*-[RhCl(CO)(bis{dimethylamino}{2,5-dimethyl-2*H*-1,2,3 σ^2 -diazaphosphol-4-yl}phosphine)₂] (39).

Atom1	Atom2	Atom3	Atom4	Angle
C11	Rh	P11	N11	-173.9(3)
C11	Rh	P11	N12	58.6(3)
C11	Rh	P11	C11	-55.0(3)
C12	Rh	P11	N11	-4.5(6)
C12	Rh	P11	N12	132.0(6)
C12	Rh	P11	C11	114.4(6)
P21	Rh	P11	N11	-150.4(8)
P21	Rh	P11	N12	82.1(9)
P21	Rh	P11	C11	-31.4(9)
C1	Rh	P11	N11	-0.4(5)
C1	Rh	P11	N12	-127.9(5)
C1	Rh	P11	C11	118.6(5)
C2	Rh	P11	N11	-176.9(13)
C2	Rh	P11	N12	55.6(13)
C2	Rh	P11	C11	-58.0(13)
C11	Rh	P21	N21	-179.7(3)
C11	Rh	P21	N22	-52.5(3)
C11	Rh	P21	C21	65.1(3)
C12	Rh	P21	N21	10.9(6)
C12	Rh	P21	N22	138.0(6)
C12	Rh	P21	C21	-104.3(6)
P11	Rh	P21	N21	156.8(8)
P11	Rh	P21	N22	-76.1(9)
P11	Rh	P21	C21	41.6(9)
C1	Rh	P21	N21	6.7(5)
C1	Rh	P21	N22	133.9(5)
C1	Rh	P21	C21	-108.5(5)
C2	Rh	P21	N21	-176.6(13)
C2	Rh	P21	N22	-49.5(13)

Table A.4.12 continued

Atom1	Atom2	Atom3	Atom4	Angle
C2	Rh	P21	C21	68.2(13)
C11	Rh	C1	O1	5.5(166)
P11	Rh	C1	O1	-87.4(141)
P21	Rh	C1	O1	89.3(141)
C12	Rh	C2	O2	-25.6(1000)
P11	Rh	C2	O2	71.9(1000)
P21	Rh	C2	O2	-105.1(1000)
Rh	P11	N11	C15	151.0(5)
Rh	P11	N11	C16	-61.7(5)
N12	P11	N11	C15	-80.4(7)
N12	P11	N11	C16	67.0(6)
C11	P11	N11	C15	28.4(7)
C11	P11	N11	C16	175.8(5)
Rh	P11	N12	C17	26.8(6)
Rh	P11	N12	C18	174.6(5)
N11	P11	N12	C17	-104.9(6)
N11	P11	N12	C18	42.9(6)
C11	P11	N12	C17	145.4(5)
C11	P11	N12	C18	-66.8(6)
Rh	P11	C11	P12	102.8(4)
Rh	P11	C11	C12	-65.6(78)
N11	P11	C11	P12	-130.3(4)
N11	P11	C11	C12	61.3(7)
N12	P11	C11	P12	-16.4(5)
N12	P11	C11	C12	175.1(6)
C11	P12	N13	N14	1.0(5)
C11	P12	N13	C14	178.1(6)
N13	P12	C11	P11	-171.1(4)
N13	P12	C11	C12	-0.9(5)
Rh	P21	N21	C25	62.8(6)
Rh	P21	N21	C26	-155.8(5)
N22	P21	N21	C25	-65.8(6)

Table A.4.12 continued

Atom1	Atom2	Atom3	Atom4	Angle
N22	P21	N21	C26	75.6(7)
C21	P21	N21	C25	-177.6(5)
C21	P21	N21	C26	-36.2(7)
Rh	P21	N22	C27	177.9(6)
Rh	P21	N22	C28	-25.7(7)
N21	P21	N22	C27	-50.5(7)
N21	P21	N22	C28	105.9(6)
C21	P21	N22	C27	58.1(7)
C21	P21	N22	C28	-145.4(6)
Rh	P21	C21	P22	-109.9(4)
Rh	P21	C21	C22	60.2(7)
N21	P21	C21	P22	125.1(5)
N21	P21	C21	C22	-64.8(7)
N22	P21	C21	P22	11.3(6)
N22	P21	C21	C22	-178.6(6)
C21	P22	N23	N24	-0.1(6)
C21	P22	N23	C24	179.0(7)
N23	P22	C21	P21	172.6(5)
N23	P22	C21	C22	1.3(5)
P12	N13	N14	C12	-0.7(7)
C14	N13	N14	C12	-178.1(6)
N13	N14	C12	C11	-0.1(9)
N13	N14	C12	C13	176.8(6)
P22	N23	N24	C22	-1.2(8)
C24	N23	N24	C22	179.6(6)
N23	N24	C22	C21	2.2(9)
N23	N24	C22	C23	-179.6(6)
P11	C11	C12	N14	170.5(5)
P11	C11	C12	C13	-6.0(11)
P12	C11	C12	N14	0.8(8)
P12	C11	C12	C13	175.7(6)
P21	C21	C22	N24	-173.9(5)

Table A.4.12 continued

Atom1	Atom2	Atom3	Atom4	Angle
P21	C21	C22	C23	8.1(11)
P22	C21	C22	N24	-2.3(8)
P22	C21	C22	C23	179.7(6)

Table A.4.13

Atomic Coordinates and Equivalent Isotropic Displacement Parameters of 39.

Atom	<i>x</i>	<i>y</i>	<i>z</i>	<i>U</i> _{eq} , Å ²
Rh	0.32975(8)	0.28552(6)	-0.29259(5)	0.0221(2)*
Cl1 ^a	0.2916(5)	0.2602(3)	-0.1223(3)	0.0352(8)*
Cl2 ^b	0.3227(31)	0.3044(29)	-0.4605(17)	0.049(5)*
P11	0.1894(2)	0.5039(2)	-0.30903(14)	0.0243(5)*
P12	-0.0350(2)	0.5597(2)	-0.12455(15)	0.0305(5)*
P21	0.4549(2)	0.0633(2)	-0.25749(14)	0.0257(5)*
P22	0.3155(3)	-0.1056(2)	-0.0636(2)	0.0493(7)*
O1 ^a	0.3364(21)	0.3071(17)	-0.4926(10)	0.065(5)*
O2 ^b	0.2984(50)	0.2517(39)	-0.0882(11)	0.077(16)*
N11	0.1454(7)	0.5980(5)	-0.4201(4)	0.030(2)*
N12	0.2738(7)	0.5734(5)	-0.2685(4)	0.031(2)*
N13	-0.2056(7)	0.5327(5)	-0.0978(4)	0.030(2)*
N14	-0.2380(7)	0.4952(5)	-0.1626(4)	0.035(2)*
N21	0.5255(7)	-0.0021(5)	-0.3512(4)	0.034(2)*
N22	0.5959(7)	0.0149(6)	-0.1936(4)	0.038(2)*
N23	0.1461(8)	-0.1210(6)	-0.0619(5)	0.048(2)*
N24	0.0867(8)	-0.0662(6)	-0.1454(5)	0.046(2)*
C1 ^a	0.3389(16)	0.2995(12)	-0.4160(9)	0.038(4)*
C2 ^b	0.3133(45)	0.2645(36)	-0.1674(9)	0.024(11)*
C11	0.0042(8)	0.5230(6)	-0.2311(5)	0.023(2)*
C12	-0.1189(8)	0.4898(7)	-0.2379(5)	0.031(2)*
C13	-0.1276(9)	0.4431(7)	-0.3160(5)	0.043(2)*
C14	-0.3198(8)	0.5404(7)	-0.0083(5)	0.044(2)*
C15	0.0089(9)	0.7127(7)	-0.4362(5)	0.054(3)*
C16	0.2783(9)	0.6078(7)	-0.4978(5)	0.045(2)*
C17	0.4417(9)	0.5214(7)	-0.2694(5)	0.043(2)*
C18	0.2116(9)	0.7119(7)	-0.2803(6)	0.051(2)*
C21	0.3185(8)	-0.0196(6)	-0.1836(5)	0.029(2)*
C22	0.1826(9)	-0.0078(6)	-0.2119(6)	0.034(2)*
C23	0.1385(9)	0.0608(7)	-0.3107(5)	0.049(2)*
C24	0.0539(10)	-0.1903(7)	0.0213(6)	0.071(3)*

Table A.4.13

Atomic Coordinates and Equivalent Isotropic Displacement Parameters of 39.

Atom	x	y	z	$U_{eq}, \text{\AA}^2$
C25	0.6468(10)	0.0430(7)	-0.4236(5)	0.058(3)*
C26	0.5516(10)	-0.1394(6)	-0.3394(6)	0.059(3)*
C27	0.6888(10)	-0.1201(8)	-0.1593(6)	0.076(3)*
C28	0.6738(10)	0.1042(8)	-0.1966(6)	0.065(3)*

Anisotropically-refined atoms are marked with an asterisk(*). The form of the anisotropic displacement parameter, U_{eq} , is: $\exp[-2\pi^2(h^2a^{*2}U_{11} + k^2b^{*2}U_{22} + l^2c^{*2}U_{33} + 2klb^{*c^*}U_{23} + 2hla^{*c^*}U_{13} + 2hka^{*b^*}U_{12})]$. ^a Refined with an occupancy factor of 0.75. ^b Refined with an occupancy factor of 0.25.

The complete structure and refinement of $[(\eta^5\text{-C}_5\text{Me}_5)\text{TiCl}_2(\text{N}=\text{P}(\text{NMe}_2)_2)\text{-}(2,5\text{-dimethyl-}2H\text{-}1,2,3\sigma^2\text{-diazaphosphol-4-yl})]$ (**46**) was carried out by Dr. R. McDonald, Structure Determination Laboratory, University of Alberta (reference file number: SDL:RGC9703).

Table A.4.14

Crystallographic Experimental Data for **46**.

A. Crystal Data

Empirical formula	$\text{C}_{18}\text{H}_{33}\text{Cl}_2\text{N}_5\text{P}_2\text{Ti}$
Formal weight (g/mol)	500.23
Crystal dimensions (mm)	0.41 x 0.34 x 0.12
Crystal system	monoclinic
Space group	$\text{P}2_1$ (No. 4)
Unit cell parameters ^a	
a (Å)	11.9477 (11)
b (Å)	8.4757 (6)
c (Å)	12.7567 (11)
β (deg)	108.824 (8)
V (Å ³)	1222.7 (2)
Z	2
ρ_{calcd} (g cm ⁻³)	1.359
μ (mm ⁻¹)	6.321

Table A.4.14 continued

B. Data Collection and Refinement Conditions

Diffractometer	Siemens P4/RA ^b
Radiation (λ [Å])	graphite-monochromated Cu K α (0.1.54178)
Temperature (°C)	-60
Scan type	θ - 2θ
Data collection 2θ limit (deg)	113.5
Total data collected	3646 ($-12 \leq h \leq 12, -9 \leq k \leq 9, -13 \leq l \leq 13$)
Independent reflections	3231
Number of observations (<i>NO</i>)	2891 ($F_o^2 \geq 2\sigma(F_o^2)$)
Structure solution method	direct methods (<i>SHELXSI-86</i> ^c)
Refinement method	full-matrix least-squares on F^2 (<i>SHELXSI-93</i> ^d)
Absorption correction method	semiempirical (Ψ scans)
Range of transmission factors	0.6907-0.2434
Data/restraints/parameters	3218 [$F_o^2 \geq 3\sigma(F_o^2)$]/0/260
Extinction coefficient	0.0037 (6)
Flack absolute structure parameter ^g	-0.02 (2)
Goodness-of-fit (<i>S</i>) ^f	1.081 [$F_o^2 \geq 3\sigma(F_o^2)$]
Final <i>R</i> indices ^g	
$F_o^2 > 2\sigma(F_o^2)$	$R_1 = 0.0630 \cdot wR_2 = 0.1593$
All data	$R_1 = 0.0768 \cdot wR_2 = 0.1973$
Largest difference peak and hole	0.406 and -0.429 e Å ⁻³

^aObtained from least-squares refinement of 37 reflections with $54.1^\circ < 2\theta < 57.9^\circ$.

^bPrograms for diffractometer operation and data collection were those of the XSCANS system supplied by Siemens.

^cData were collected with indices of the form $+h +k \pm l$ and $-h -k \pm l$.

^dSheldrick, G. M. *Acta Crystallogr.* 1990, A46, 467–473.

^eSheldrick, G. M. *SHELXL-93*. Program for crystal structure determination. University of Göttingen, Germany, 1993. Refinement on F_o^2 for all reflections except for 13 having $F_o^2 < 3\sigma(F_o^2)$. Weighted R -factors wR_2 and all goodnesses of fit S are based on F_o^2 ; conventional R -factors R_1 are based on F_o , with F_o set to zero for negative F_o^2 . The observed criterion of $F_o^2 > 2\sigma(F_o^2)$ is used only for calculating R_1 , and is not relevant to the choice of reflections for refinement. R -factors based on F_o^2 are statistically about twice as large as those based on F_o , and R -factors based on ALL data will be even larger.

^f $F_c^* = kF_c[1 + x(0.001F_c^2\lambda^3/\sin(2\theta))]^{-1/4}$ where k is the overall scale factor.

^gFlack, H. D. *Acta Crystallogr.* 1983, A39, 876–881. The Flack parameter will refine to a value near zero if the structure is in the correct configuration and will refine to a value near one for the inverted configuration.

^h $S = [\sum w(F_o^2 - F_c^2)^2 / (n - p)]^{1/2}$ (n = number of data; p = number of parameters varied; $w = [\sigma^2(F_o^2) + (0.0936P)^2 + 4.3804P]^{-1}$ where $P = [\text{Max}(F_o^2, 0) + 2F_c^2]/3$).

ⁱ $R_1 = \sum ||F_o| - |F_c|| / \sum |F_o|$; $wR_2 = [\sum w(F_o^2 - F_c^2)^2 / \sum w(F_o^4)]^{1/2}$.

Table A.4.15

Selected Torsional Angles (deg) for $[(\eta^5\text{-C}_5\text{Me}_5)\text{TiCl}_2(\text{N}=\text{P}(\text{NMe}_2)_2)(2,5\text{-dimethyl-}2H\text{-}1,2,3\sigma^2\text{-diazaphosphol-4-yl})]$ (46).

Atom1	Atom2	Atom3	Atom4	Angle
C5	P1	N2	N3	-1.1(8)
C5	P1	N2	C6	-177.9(10)
N2	P1	C5	P2	173.3(6)
N2	P1	C5	C4	1.0(8)
N11	P2	N1	Ti	87.2(17)
N12	P2	N1	Ti	-28.7(17)
C5	P2	N1	Ti	-151.2(16)
N1	P2	N11	C11	-60.8(8)
N1	P2	N11	C12	80.5(8)
N12	P2	N11	C11	59.8(7)
N12	P2	N11	C12	-158.9(8)
C5	P2	N11	C11	178.3(6)
C5	P2	N11	C12	-40.4(9)
N1	P2	N12	C13	-40.9(8)
N1	P2	N12	C14	165.2(7)
N11	P2	N12	C13	-165.6(7)
N11	P2	N12	C14	40.5(8)
C5	P2	N12	C13	78.6(7)
C5	P2	N12	C14	-75.3(8)
N1	P2	C5	P1	9.2(7)
N1	P2	C5	C4	179.4(10)
N11	P2	C5	P1	135.8(5)
N11	P2	C5	C4	-54.0(11)
N12	P2	C5	P1	-112.3(6)
N12	P2	C5	C4	57.8(11)
P1	N2	N3	C4	0.8(12)
C6	N2	N3	C4	178.0(10)
N2	N3	C4	C5	0.1(14)
N2	N3	C4	C7	177.5(12)

Table A.4.15 continued

Atom1	Atom2	Atom3	Atom4	Angle
N3	C4	C5	P1	-0.8(13)
N3	C4	C5	P2	-171.7(8)
C7	C4	C5	P1	-177.9(12)
C7	C4	C5	P2	11.2(20)

Table A.4.16

Atomic Coordinates and Equivalent Isotropic Displacement Parameters of
 $[(\eta^5\text{-C}_5\text{Me}_5)\text{TiCl}_2(\text{N}=\text{P}(\text{NMe}_2)_2)\text{-(2,5-dimethyl-2H--1,2,3}\sigma^2\text{-diazaphosphol-4-yl)}]$

(46).

Atom	x	y	z	$U_{\text{eq}}, \text{\AA}^2$
Ti	0.36228(11)	0.0101(2)	-0.30073(10)	0.0221(4)*
C11	0.4609(2)	0.2392(3)	-0.2275(3)	0.0491(7)*
C12	0.2619(2)	0.0805(3)	-0.4821(2)	0.0459(7)*
P1	0.2887(2)	-0.0027(3)	0.0081(2)	0.0345(6)*
P2	0.1213(2)	0.0295(3)	-0.22417(15)	0.0228(5)*
N1	0.2452(5)	0.0007(10)	-0.2429(5)	0.028(2)*
N2	0.2388(6)	0.0078(11)	0.1159(5)	0.033(2)*
N3	0.1198(6)	0.0239(11)	0.0932(5)	0.039(2)*
N11	0.0122(7)	-0.0896(8)	-0.2908(6)	0.031(2)*
N12	0.0676(6)	0.2034(9)	-0.2721(6)	0.032(2)*
C4	0.0688(7)	0.0256(14)	-0.0161(6)	0.039(2)*
C5	0.1454(6)	0.0110(11)	-0.0797(6)	0.025(2)*
C6	0.3093(7)	0.0091(16)	0.2335(6)	0.042(2)*
C7	-0.0642(8)	0.0356(25)	-0.0598(8)	0.085(5)*
C11	-0.0233(9)	-0.0874(12)	-0.4125(7)	0.045(3)*
C12	0.0052(10)	-0.2463(13)	-0.2462(9)	0.054(3)*
C13	0.1501(9)	0.3377(11)	-0.2524(10)	0.046(3)*
C14	-0.0538(9)	0.2521(13)	-0.2915(9)	0.049(3)*
C20	0.3910(7)	-0.2559(9)	-0.3427(6)	0.023(2)*
C21	0.4736(7)	-0.1666(9)	-0.3808(6)	0.022(2)*
C22	0.5565(7)	-0.0958(10)	-0.2891(7)	0.026(2)*
C23	0.5281(8)	-0.1394(10)	-0.1925(7)	0.031(2)*
C24	0.4302(8)	-0.2378(10)	-0.2248(7)	0.029(2)*
C25	0.2912(8)	-0.3551(12)	-0.4108(8)	0.044(2)*
C26	0.4745(9)	-0.1595(12)	-0.4970(8)	0.040(2)*
C27	0.6607(7)	-0.0015(14)	-0.2888(8)	0.045(2)*
C28	0.5979(9)	-0.0922(12)	-0.0766(8)	0.046(3)*
C29	0.3761(9)	-0.3278(11)	-0.1513(7)	0.042(2)*

Anisotropically-refined atoms are marked with an asterisk(*). The form of the anisotropic displacement parameter, U_{eq} , is: $\exp[-2\pi^2(h^2a^{*2}U_{11} + k^2b^{*2}U_{22} + l^2c^{*2}U_{33} + 2klb^*c^*U_{23} + 2hla^*c^*U_{13} + 2hka^*b^*U_{12})]$. ^a Refined with an occupancy factor of 0.75. ^b Refined with an occupancy factor of 0.25.